PROCEEDINGS OF
THE GHRSST XX SCIENCE TEAM MEETING

FRASCATI, ITALY
3RD – 7TH JUNE 2019

ISSN 2049–2529
VERSION 1.0

Edited by the GHRSST Project Office

Meeting hosted by:

GHRSST International Project Office

Karen Veal, Project Co-ordinator
gpc@ghrsst.org

Silvia Bragaglia-Pike, Project Administrator
gpa@ghrsst.org

www.ghrsst.org

The GHRSST Project Office is funded by the European Union

Table of Contents

SECTION 1: AGENDA

Agenda with links to individual presentations available on the GHRSST website under 'Resources' of the G-XX meeting page (https://www.ghrsst.org/agenda/g-xx/).

MONDAY, 3RD JUNE 2019

Plenary Session I: Introduction

Chair: Anne O'Carroll - Rapporteur: Gary Corlett

09:00-09:10	Welcome to G-XIX from ESA	Olivier Arino
09:10-09:40	SST related activities at ESA	Craig Donlon
09:40-10:00	SST activities at CNR	Rosalia Santoleri
10:00-10:15	GHRSST Connection with CEOS: SST-VC	Kenneth Casey
10:15-10:30	G-XX: Logistics	Gary Corlett

10:30-11:00	Tea/Coffee Break

Plenary Session II (Part 1): Review of activities since G-XIX

Chair: Eileen Maturi - Rapporteur: Marouan Bouali

11:00-11:10	GHRSST system Components: GDAC	Ed Armstrong
11:10-11:20	GHRSST system Components: EU GDAC	Jean-François Piollé
11:20-11:30	GHRSST system Components: LTSRF	Kenneth Casey
11:30-11:40	GHRSST system Components: SQUAM and iQUAM	Alexander Ignatov
11:40-11:50	RDAC Update: ABoM	Helen Beggs
11:50-12:00	RDAC Update: CMC	Dorina Surcel Colan
12:00-12:10	RDAC Update: CMEMS	Bruno Buongiorno Nardelli
12:10-12:20	RDAC Update: EUMETSAT	Anne O'Carroll
12:20-12:30	RDAC Update: JAXA	Misako Kachi
12:30-12:40	RDAC Update: JMA	Toshiyuki Sakurai
12:40-12:50	RDAC Update: Met Office	Chongyuang Mao

MONDAY, 3RD JUNE 2019		
12:50-13:00	RDAC Update: NASA	Ed Armstrong
13:00-14:30	Lunch	
Plenary Session II (Part 2): Review of activities since G-XIX ***Chair: Charlie Barron - Rapporteur: Ioanna Karagali***		
14:30-14:40	RDAC Update: NAVO	Bruce McKenzie
14:40-14:50	RDAC Update: NOAA/NESDIS/STAR 1	Alexander Ignatov
14:50-15:00	RDAC Update: NOAA/NESDIS/STAR 2	Eileen Maturi
15:00-15:10	RDAC Update: NOAA/NCEI	Kenneth Casey
15:10-15:20	RDAC Update: OSI-SAF	Stéphane Saux Picart
15:20-15:40	RDAC Update: RSS & Report from MISST	Chelle Gentemann
15:50-16:00	Report from NSOAS	Qimao Wang

16:00-16:30	Tea/Coffee Break

16:30-18:30	**Interactive Presentations Session I**
See Section 3 for List	

18:30-19:30	**Icebreaker**

TUESDAY 4TH JUNE 2019

Plenary Session III: Passive Microwave Measurements

Chair: Chelle Gentemann - Rapporteur: Craig Donlon

09:00-09:20	Recent Improvements in AMSR2 Sea Surface Temperature Products	Misako Kachi
09:20-09:40	Determining the AMSR-E SST Footprint from Co-Located MODIS SSTs	Brahim Boussidi
09:40-10:00	Impact of CIMR Microwave observations on the CMEMS SST product in the North Sea/Baltic Sea	Jacob Hoeyer
10:00-10:30	Open discussion led by session chair	

10:30-11:00	Tea/Coffee Break

Plenary Session IV: Feature resolution

Chair: Alexander Ignatov - Rapporteur: Dorina Surcel Colan

11:00-11:20	On the Importance of the Spectral Phase for Upper Ocean Studies: from Geophysical Fluid Dynamics to Statistical Mechanics	Jordi Isern-Fontanet
11:20-11:40	Towards High-Resolution Multi-Sensor Gridded ACSPO SST Product at NOAA	Irina Gladkova
11:40-12:00	A Comparative Study of Ocean Thermal Gradients from GHRSST Level 4 SST Products	Marouan Bouali
12:00-12:30	Open discussion led by session chair	
12:30-13:00	Task Teams I – Spatial Precision; SSES; Ocean Obs	

13:00-14:30	Lunch

TUESDAY 4TH JUNE 2019

Plenary Session V: Applications Chair: Prasanjit Dash - Rapporteur: Rosalia Santoleri		
14:30-14:50	Satellite-observed Spatial and Temporal Evolution of The East Australian Current Encroachment from Himawari-8 SST Data: Implications for Upwelling and Shelf Circulation	Senyang Xie
14:50-15:10	From SST Measurements to Actionable Information for Public and Private Users: Rheticus© Services	Daniela Drimaco
15:10-15:30	SSTs Over and Around Reefs (SOAR) Workshop Outcomes	Craig Steinberg
15:30-16:00	Open discussion led by session chair	

16:00-16:30	Tea/Coffee Break

16:30-18:30	Interactive Presentations Session II
See Section 3 for List	

WEDNESDAY 5TH JUNE 2019

09:00-10:30	Round Table on the future of GHRSST

10:30-11:00	Tea/Coffee Break

11:00-12:00	Task Teams II – Evolution of the R/GTS

12:00-13:00	Lunch

14:00-19:00	GHRSST Team Building
19:30-22:00	GHRSST Dinner

THURSDAY 6TH JUNE 2019

Plenary Session VI: Retrieval

Chair: Peter Cornillon - Rapporteur: Misako Kachi

09:00-09:20	Exploration of Retrieval Approaches For SLSTR	Andrew Harris
09:20-09:40	Satellite Infrared Retrievals Of Sea-surface Temperature At High Latitudes	Peter Minnett
09:40-10:00	Determining Covariance Parameters for Optimal Estimation of Sea Surface Temperature by Exploiting Matched In-situ References	Christopher Merchant
10:00-10:30	Open discussion led by session chair	

10:30-11:00	Tea/Coffee Break

Plenary Session VII: In situ measurements

Chair: Lei Guan - Rapporteur: Werenfrid Wimmer

11:00-11:20	Accurate Temperature Measurements of GHRSST Quality from Global Drifter Program Drifters	Luca Centurioni
11:20-11:40	Evaluation and Initial Results from the 2018 San Francisco to Baja Cruise of the Saildrone Unmanned Surface Vehicle	Chelle Gentemann
11:40-12:00	Sea Surface Temperature and Air-Sea Interaction in the Mediterranean Region	Salvatore Marullo
12:00-12:30	Open discussion led by session chair	
12:30-13:00	Task Teams III – SST Climatology; High-latitude; Cloud Masking	

13:00-14:30	Lunch

THURSDAY 6TH JUNE 2019		
Plenary Session VIII: Diurnal variability *Chair: Andrew Harris - Rapporteur: Sandra Castro*		
14:30-14:50	Results from the SOSSTA Project on Developing a Statistical-Dynamical Observation Operator for SST Data Assimilation	Sam Pimentel
14:50-15:10		
15:10-15:30	The "Improved Diurnal Variability Forecast of Ocean Surface Temperature through Community Model development" Project Results	Ioanna Karagali
15:30-16:00	Open discussion led by session chair	

16:00-16:30	Tea/Coffee Break

16:30-18:30	Interactive Presentations Session III
See Section 3 for List	

18:30-21:00	Advisory Council

FRIDAY 7TH JUNE 2019

Plenary Session IX: Climate Data Records

Chair: Helen Beggs - Rapporteur: Christopher Merchant

09:00-09:20	A 35 year Sea Surface Temperature Climate Data Record from the ESA Climate Change Initiative	Owen Embury
09:20-09:40	CCI OSTIA as the Standard of Truth: Detailed Error Models for in Situ SST Data From Ships and Other Platforms	Alexey Kaplan
09:40-10:00	Use Of SST For Monitoring Coral Stress: Looking Forward While Keeping An Eye On The Past	William Skirving
10:00-10:30	Open discussion led by session chair	

10:30-11:00	Tea/Coffee Break

Closing Session

Chair: Anne O'Carroll - Rapporteur: Karen Veal

11:00-11:15	Report from AC Meeting	Jean-François Piollé
11:15-12:00	Task Team planning for next year	
12:00-12:45	Review of action items/AOB	
12:45-13:00	Wrap-up/closing remarks	

Close of GHRSST XX

13:00-14:00	Lunch

14:00-17:00	CEOS SST-VC

Meeting of the CEOS SST Virtual Constellation

For further information please contact: Kenneth Casey (NOAA) or Anne O'Carroll (EUMETSAT)

SECTION 2: PLENARY SESSION SUMMARY REPORTS

PLENARY SESSION I: INTRODUCTION

SESSION I REPORT

Anne O'Carroll[(1)], Gary Corlett[(2)]

(1) EUMESAT, Darmstadt, Germany, Email: anne.ocaroll@eumetsat.int
(2) EUMESAT, Darmstadt, Germany, Email: gary.corlett@eumetsat.int

Olivier Arino (OA) welcomed everyone to the 20th GHRSST Science Team meeting on behalf of Josef Aschbacher, the Director of Earth Observation at ESA, who unfortunately was not able to attend. ESA supports three main EO activities (1) Science, (2) Copernicus and (3) Meteorology. OA noted that EO is now undergoing a big data revolution where 15 TB of data generates 150 TB of usage. A new programme, EO4Society, will pioneer excellent innovative applications of EO data, with a work cycle based on user requirements. OA concluded with a review of Sentinel-3 SLSTR, which is performing exceedingly well and providing additional coverage owing to a wider swath than its predecessors (ATSRs).

Craig Donlon presented an overview of SST and oceanography at ESA. ESA are currently continuing activities on Sentinel 3, in particular preparing for the C and D satellites, as well as analysis of the S3A and S3B tandem project, where both satellites were flown 30 s apart in orbit. ESA are starting working on new concepts that may in future join the Sentinel series. Two missions of particular interest to GHRSST are LSTM (mainly land focussed but with coverage of coastal zones) and CIMR (passive microwave imager) focussing on the Arctic. EO4society has a large range of oceanographic projects and there are six ocean related projects in the ESA Climate Change Initiative (CCI) programme. Other projects of note for GHRSST are ocean surface winds from SMOS – useful for DV studies – and the ships4SST project.

Lia Santoleri summarised SST related activities at CNR (who were co-hosting the meeting with ESA). These activities are funded under Copernicus under both the marine and climate services. Several products are generated – regional and global – and also covering reprocessing. S3A is now operational in CMEMS and S3B under testing; activities related to reprocessing will move to C3S. Initial SLSTR SST results are quite promising and SLSTR SSTs are now used to generate high resolution sea surface salinity products. SST is also used for optimising altimeter derived currents. CNR will be starting a climate product assessment, which will cover many long term data records generated by the GHRSST community.

Ken Casey (KC) concluded the session with an overview of the CEOS SST Virtual Constellation, highlighting the connections between CEOS and GHRSST (top down and bottom up approaches). KC summarised two key targets that the SST-VC was involved with, a community white paper and PMW continuity. Finally, he noted a key challenge for the SST-VC, where it has been suggested that all ocean related VCs should merge into one single entity.

SST RELATED ACTIVITIES AT ESA

Craig Donlon

SST ACTIVITIES AT CNR

Rosalia Santoleri

CEOS SST-VC REPORT TO GHRSST XX

Anne O'Carroll[1], Kenneth S. Casey[2] and SST-VC members

(1) EUMETSAT, Darmstadt, Germany, Email: Anne.Ocarroll@eumetsat.int
(2) NOAA NCEI, USA, Email: Kenneth.Casey@noaa.gov

1. ABSTRACT

The Committee on Earth Observing Satellites (CEOS) SST Virtual Constellation (SST-VC) serves as the bridge between the international SST community, GHRSST, and the coalition of national space agencies, CEOS. During the GHRSST-XX meeting, the SST-VC presented an overview to the GHRSST Science Team, then met at the end of the week to discuss updates from the member agencies, the Constellation White Paper, Passive Microwave Radiometer Continuity, SST-VC Data, and the CEOS COVERAGE project. In addition, the SST-VC discussed the CEOS proposal to merge the four ocean virtual constellations into one, began documenting possible future key activities, and discussed the need to find a new co-chair. This report contains a summary of all the information presented to the Science Team and includes the results of the 8th Meeting of the SST-VC on Friday, June 7, 2019 as well.

2. COVERAGE

Jorge Vazquez gave an update of COVERAGE activities to kick off the SST-VC meeting. The product inventory has been completed for all 4 VC's and now the next steps are in progress including waiting for funds. Then the implementation of the demo phase will begin this summer. This phase includes all 4 VCs and specific in situ datasets. Blue Planet was identified as a possible stakeholder of the project, which is now looking forward to sustainability through activities like integration of ocean colour and SST datasets. The ocean colour product will be a major part of phase B, including a focus on validation. COVERAGE is working closely with the Ocean Colour Radiometry Virtual Constellation to complete this activity.

3. MAIN ACTIVITIES IN 2018/2019

The SST-VC spent the last year focused on its CEOS Work Plan elements, including the Constellation White Paper, Passive Microwave Continuity, and Data. More details are provided in separate sections below. In addition, the SST-VC participated in inter-sessional teleconference with the CEOS Strategic Implementation Team (SIT) chair. Other activities included:

- CEOS COVERAGE Teleconference, 19 Jul 2018
- CEOS SIT Chair Tag-Up with Ocean VCs, 02 Aug 2018
- CEOS SIT Technical Workshop, Darmstadt, 10-14 Sep 2018
- CEOS SIT-34 Meeting, Miami, 02-05 April 2019

4. UPDATES FROM MEMBERS

An extensive set of updates were collected in advance of the meeting from each VC member and included in the Meeting Minutes and Agenda document. Each VC member was able to highlight to the team the key points from their agencies during the VC meeting.

5. PROGRESS ON DATA

As of this week, 96 standardized GHRSST products now can be found in the GHRSST LTSRF archive, consisting of 7.21 million CF/ACDD netCDF data files and 161 TB. Their temporal coverage spans Sep 1981 – May 2019. These and other details on the data sharing were presented to the GHRSST Science Team.

During the Friday SST-VC meeting, ISRO, CMA, and KMA all reported that they are considering creating GDS2 products and JMA is considering an L4 GDS2.

The group also held a discussion on possibly developing a tailored user interface to focus users on specific datasets for their needs.

6. PROGRESS ON CONSTELLATION WHITE PAPER

The SST-VC is developing a whitepaper on the next generation SST Virtual Constellation, including necessary on-orbit assets, measurement method (microwave and infrared, geostationary and polar), Fiducial Reference Measurements, and the required data management system. A draft of the white paper is in preparation with publication targeted for later in 2019. This information was presented and the team discussed during the VC meeting the reasons for slow progress lately, including the physical move of the lead author Gary Corlett to Darmstadt and the time spent by many of the authors on the OceanObs '19 community white papers. The team revitalized the activity, and established new due dates in July for Gary to assign the figures to the authors. The text remains complete, but may need a very few updates to make sure it is still up to date.

7. PROGRESS ON PASSIVE MICROWAVE RADIOMETER CONTINUITY

The team closed out its CEOS actions and focus on PMW radiometer continuity with a brief wrap up session during the meeting, and also reported this information to the Science Team earlier in the week. Successes in JAXA and ESA were discussed, noting the important contributions of the SST-VC advocacy efforts of the last few years. Misako Kachi also shared that there may be some discussion about a possible WindSat follow-on mission, known as the "Weather System Follow-on Microwave" mission, with a target launch date in 2022. The X-CAL team presented this information at the US Precipitation Measurement Mission (PMM) science team meeting held by NASA/GSFC in Oct. 2018 in Phoenix.

8. DISCUSSION ON THE PROPOSED CEOS MERGER OF THE FOUR OCEAN VCS INTO ONE

The SST-VC spent much of the VC meeting discussing the proposed merger of the four ocean VCs into one Ocean VC, noting that both Kenneth Casey and Misako Kachi are serving on the newly formed ocean merger study team. The meeting minutes captures the details of the conversation, with all agencies providing examples of the importance of having a focused SST-VC. Alternative ideas were discussed and developed the following consensus statement: A merged ocean VC would not be suitable for the SST-VC. Alternative options were discussed and these will be presented in the working group study team meetings. The proposed merger was also presented to the GHRSST Science Team and the GHRSST Advisory Council, and both groups expressed concerns.

9. OTHER BUSINESS

The SST-VC discussed three other items during the VC meeting.

Radio Frequency Interference (RFI): The team discussed this issue, which had been raised repeatedly at the GHRSST Science Team meeting. An agreement was reached to present the issue at the next CEOS meeting. While it is known that the space agencies are aware of the issue, having a more consolidated statement of impacts from the SST community may prove useful. To start, a few examples will be assembled and presented to the CEOS principals before any detailed analysis is performed.

GTS Problems: The team discussed the problem of the change in the length of platform identifiers for drifting buoys on the GTS, and how many agencies are still struggling to update their systems. This conversation led to the point that the SST community needs to more completely free itself from reliance on in situ data for calibration, and toward using it solely for validation. The team agreed to convey this message back to the GHRSST Science Team through this report, noting the need for better communication and to facilitate independent SST retrievals using, for example, systems like the Global Space-based Inter-Calibration System (GSICS).

SST-VC Co-Chair Rotation: Following the SST-VC charter, it is time for Kenneth Casey to step down as co-chair of the VC. The team discussed roles and responsibilities and the level of effort required. Interested VC members will consult with their agencies and once they feel they can commit to the position, will nominate themselves for consideration by mid-July. Ideally, the team would like to rotate the co-chair position at the September CEOS SIT Technical Workshop.

PLENARY SESSION II: REVIEW OF ACTIVITIES SINCE G-XIX

SESSION II REPORT (PART 1)

Eileen Maturi [(1)], Marouan Bouali [(2)]

(1) National Oceanic and Atmospheric Administration (NOAA), email: eileen.maturi@noaa.gov
(2) Institute of Oceanography of the University of São Paulo (IOUSP), email: marouan.bouali@usp.br

ABSTRACT

The plenary session II (morning of June 3rd 2019) covered a review of the main activities of several agencies and organizations since the 19th GHRSST meeting. Following is a brief summary of the session presentations.

1. GHRSST SYSTEM COMPONENTS: GDAC

Edward Armstrong

- Included datasets from NPP and NOAA-20 VIIRS (L2P/L3U ACSPO and L2P NAVO), NPP GOES-16 (L2P/L3C ABI ACSPO), Level 4 K10 (NAVO)
- Included in situ datasets from Saildrone and SPURS-2
- Retired FTP and replaced it with PODAAC Earthdata Drive
- Updated SOTO to version 5 with server side analytics and visualization (Oceanworks)
- Improved PODAAC's data discovery

2. GHRSST SYSTEM COMPONENTS: EU GDAC

Jean-François Piollé

- Extended the North West Shelf (NWS) to West Europe Area (ATL) (includes the Iberian-Biscay-Irish areas)
- Conducted reprocessing for CMEMS (1982-2018),
- Real time product will replace AVHRR 18-19G with CCI SST
- Introduced experimental remote processing capabilities (JupyterHub on HPC)
- Discussed the issue of traceability and reproducibility due to increasing satellite datasets and reprocessing versions, as well as the impact of emerging cloud technologies in GHRSST's future

3. GHRSST SYSTEM COMPONENTS: LTSRF

Kenneth Casey

- New products since last GHRSST include L3C GOES 16 (OSISAF), L2P and L3U ACSPO from NPP and N20, and L4 K10 (NAVO)
- Indexation of granules in the CEOS CWIC integration is beyond half way (4 out of 7 millions)
- Significant increase in the number of products and files served by day for 2018 (~400GB)
- Discussed need to redesign data archival and access of NCEI and mitigate differences with PODAAC system

4. GHRSST SYSTEM COMPONENTS: SQUAM AND IQUAM

Alexander Ignatov

- Provided summary of iQUAM functionalities
- iQUAM updated to version 2.1 in November 2018
- Main updates include merging RT GTS from NCEP, FNMOC and ICOADS, enhanced interactivity/visualization for individual platforms and only one update/day of files
- 7-Digit WMO ID`s now included in iQUAM v2.1
- GPS clock issue on Hi Frequency drifters in April 2019 had major impact on SST validation statistics.
- Provided summary of SQUAM functionalities
- Started redesign of SQUAM back end. Replacing IDL and bash with a combination of python, C++ and SQL
- Current version of SQUAM includes a new colour scheme for improved visualization of data in maps
- Future work includes redesign of back end for iQUAM and SQUAM

5. RDAC UPDATE: ABOM

Helen Beggs

- Provided summary of ABoM GHRSST operational products
- Experimental products GDS2.0 include
- Real-time IMOS fv01 Metop-B AVHRR (L3U, L3C), N20 VIIRS(L3U, L3C), 4h and daily L3C Himawari-8
- Reprocessed IMOS VIIRS+AVHRR L3C and L3S for 2012-2016
- Removed N19 SST from ocean models, daily L4 and IMOS L3 due to calibration deterioration of AVHRR
- Ongoing ingestion of N18 AVHRR SST
- Started ingestion of 7-digit ID drifting buoys in IMOS SST systems (Dec 2016) and SST analysis (Jul 2018)
- Ingestion of VIIRS SST data in optimal interpolation scheme is a major issue to be investigated

6. RDAC UPDATE: CMC

Dorina Surcel Colan

- L4 CMC SST v.3.0 will include new ice analysis
- Improved performance of CMC 0.1˚
- New ice analysis leads to reduction in total error (against Multisensor Snow and Ice Mapping System)
- Discussed ocean modelling at CMC. Global , regional (North Atlantic and Arctic) and costal Ice-Ocean Prediction Systems
- Future work include ingestion of Sentinel 3A, N20 VIIRS and update assimilation scheme of SST.

7. RDAC UPDATE: CMEMS

Bruno Buongiorno Nardelli

- Provided summary of Copernicus Marine Services
- Overview of current SST-TAC products (Main update is upcoming retirement of IFREMER L4 for North Atlantic Shelf region)
- New products include Ifremer NRT and reprocessed L4 (North Eastern Atlantic Ocean) and DMI NRT L3S (Baltic Sea)
- Completed ingestion of S3A, improved interpolation methods and implemented new Ocean Monitoring Indicators (Global/Regional SST anomalies and trends)
- Update global and regional REP products using ESA CCI/C3S
- Continuing contribution to the Ocean State Report (OSR 3 under revision)

8. RDAC UPDATE: EUMETSAT

Anne O'Carroll

- Provided overview of EUMETSAT activities in oceanography
- Completed reprocessing of SLSTR-A SST (Apr 2016-Apr 2018)
- SST projects for SLSTR-B operational since March 2019
- Extensive 2 days coverage from SLSTR-A and SLSTR-B
- OSI SAF IASI SST to be updated to v6.5
- SST MDB gradually including Trusted drifter data
- SLSTR-B SST to be included in METIS system
- New GHRSST Project Office Coordinator: Karen Veal
- Encouraged participation of new countries, interaction with users and involvement of early career researchers

9. RDAC UPDATE: JAXA

Misako Kachi

- Provided overview of JAXA GHRSST datasets
- Future products include update of AMSRE-E and AMSRE-2 SST, and production of L2P or higher level SST from GCOM-C/SGLI and NPP/VIIRS
- L2 v.8 AMSRE-E (GDS2.0) and L2 v.4 AMSRE-2 SST to be released in 2019
- Thin ice detection and Total precipitable water over land now available
- Ongoing update algorithm for Himawari-8/AHI for consistency with SGL
- Near Phase-B of the AMSRE-2 follow mission
- Regional assimilated SST and 2-week forecast around Japan available (JAXA and JAMSTEC)

10. RDAC UPDATE: JMA

Toshiyuki Sakurai

- Increased time frequency of Himawari SST products from 1h to 10 min
- Ingestion of ACSPO VIIRS L3U SST decreases MGDSST REMSE by 0.02K.
- MGDSST and HINSST to include
- ACSPO NPP/N20 L3U SST and GCOM/SGLI JAXA/EORC L2P SST (Polar)
- ACSPO GOES-16/ABI L3C/L3U SST (Geo)
- Plans to increase resolution of ocean data assimilation system (using L2P/L3 instead of L4)

11. RDAC UPDATE: MET OFFICE

Chongyuang Mao

- Provided overview of Met Office GHRSST NRT and Reprocessed products (OSTIA, GMPE, Diurnal skin, Climate datasets)
- Improved feature resolution (new variational data assimilation scheme) and ingestion of SLSTR-A in OSTIA
- On-going testing of SLSTR-B and N20 VIIRS ingested in OSTIA
- Discussed challenges related to use of radiances instead of SST in coupled NWP and needs of climate users for different format of SST uncertainties

12. RDAC UPDATE: NASA

Edward Armstrong

- Provided overview of NASA RDAC components
- G1SST 2DVar to account for time differences + GDS2 format for data
- MUR will have a downsampled (25km) by-product SST and include VIIRS and N17 L2P in v.5
- Ongoing effort with COVERAGE (CEOS Ocean Variables Enabling Research and Application for GEO) and entering Phase B (initial prototype of COVERAGE system)
- Continue collaboration with Saildrone Project and support for CEOS SST VC

GLOBAL DATA ASSEMBLY CENTER (GDAC) REPORT TO THE GHRSST SCIENCE TEAM

Edward Armstrong[(1)], Jorge Vazquez[(1)], Wen-Hao Li[(2)], Chris Finch[(1)]

Jet Propulsion Laboratory, California Institute of Technology, Pasadena, CA, 91109 USA
Raytheon Corp., Pasadena, CA 91101
Email: edward.m.armstrong@jpl.nasa.gov

ABSTRACT

In 2018-2019 the Global Data Assembly Center (GDAC) at NASA's Physical Oceanography Distributed Active Archive Center (PO.DAAC) provided ingest, archive, distribution and user services for GHRSST operational data streams with improved and evolved tools, services, and tutorials, and interfaced with the user community to address technical inquiries. Several new GHRSST datasets including novel supporting *in situ* datasets were made available. The PO.DAAC participated in the evolving GHRSST data management re architecture and development activities. The following sections summarize and document the specific achievements of the GDAC to the GHRSST community.

1. INTRODUCTION

The primary contributions to GHRSST for this period are in three categories: Data Management and User Services, Tools and Services, and R/G TS evolution. For data management, the GDAC ingested twelve new or updated GHRSST datasets from multiple data providers (See Appendix A). The GDAC continued to support operational data streams for L2P/L3/L4 data from 15 unique RDACs and maintain linkages to the NASA Common Metadata Repository (CMR; https://search.earthdata.nasa.gov/search) and LTSRF archive. For user community engagement the PO.DAAC responded to GHRSST user queries through its help desk and user forum, and improved data recipes with data and tutorials (also promulgated on the PO.DAAC user forum)

The PO.DAAC FTP server was officially retired in early June 2019 and the PO.DAAC provided many tutorial, recipes and hands on training to transition the oceanographic community to the new PO.DAAC Drive HTTPS based interface and protocol presented in the previous two meetings.

Members of the PO.DAAC also collaborated on the development to re-architect the Regional Global Task Sharing (R/G TS) framework to decentralize the GHRSST data ingest and distribution nodes approved by the science team at the last meeting.

2. DISTRIBUTION METRICS

The following figures show distribution metrics and relative popularity of GHRSST datasets. On a typical monthly basis GHRSST datasets are consistently among the most popular products in the entire PO.DAAC catalogue. Users, data volumes and number of files are all steady or have slightly increased. Users are continuing to leverage services such as OPeNDAP, THREDDS and LAS more so than in the past.

Top 10 Datasets for FTP by users during 2019					
Rank	Name	Tool	Files	Volume (GB)	Users
1	PODAAC-GMSLM-TJ142 Global Mean Sea Level Trend from Integrated Multi-Mission Ocean Altimeters TOPEX/Poseidon Jason-1 and OSTM/Jason-2 Version 4.2	FTP	9473	1.01	5187
2	PODAAC-TEMSC-ANTS1 Antarctica Mass Variability Time Series Version 1 from JPL GRACE Mascon CRI Filtered	FTP	1392	0.01	724
3	PODAAC-OSCAR-03D01 OSCAR third degree resolution ocean surface currents	FTP	34600	829.19	597
4	PODAAC-GHOST-4FK01 GHRSST Level 4 OSTIA Global Foundation Sea Surface Temperature Analysis	FTP	164196	516.29	482
5	PODAAC-TEMSC-GRTS1 Greenland Mass Variability Time Series Version 1 from JPL GRACE Mascon CRI Filtered	FTP	1064	0.01	449
6	PODAAC-GHGMR-4FJ01 GHRSST Level 4 MUR Global Foundation Sea Surface Temperature Analysis	FTP	246371	141.47	378
7	PODAAC-GHG1S-4FP01 GHRSST Level 4 G1SST Global Foundation Sea Surface Temperature Analysis	FTP	56686	2400.00	299
8	PODAAC-GHGMR-4FJ04 GHRSST Level 4 MUR Global Foundation Sea Surface Temperature Analysis (v4.1)	FTP	100247	22544.18	267
9	PODAAC-GOSTA-HDF01 Global Ocean Surface Temperature Atlas Plus (MIT,UKMO,JPL)	FTP	2961	0.09	184

Figure 1. Top 10 Datasets for FTP by users during 2019 showing the relative popularity (by Users) of the GHRSST OSTIA, MUR and G1SST L4 datasets.

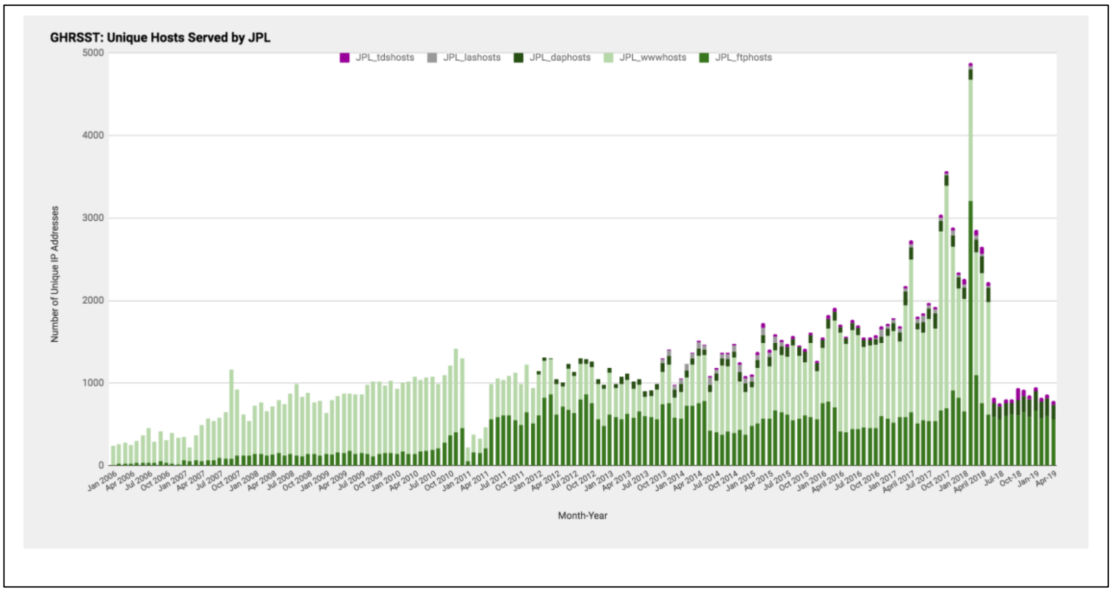

Figure 2. Monthly unique users by FTP, OPeNDAP, THREDDS, LAS or WWW since 2006 to April 2019. In the last few months WWW users were not recorded.

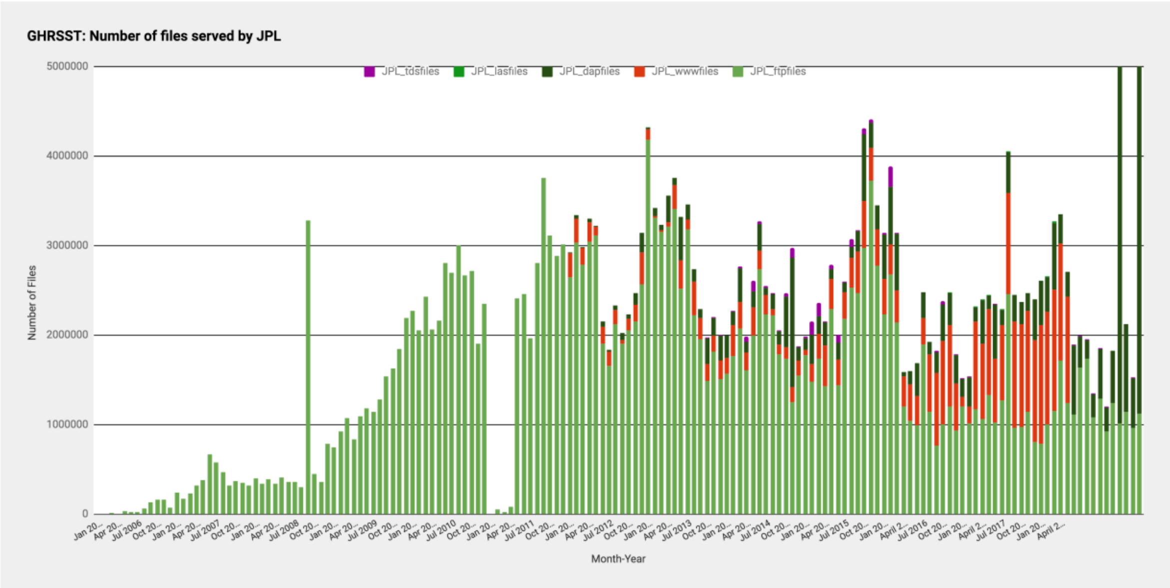

Figure 3. Number of monthly files distributed. OPeNDAP requests have recently dramatically increased.

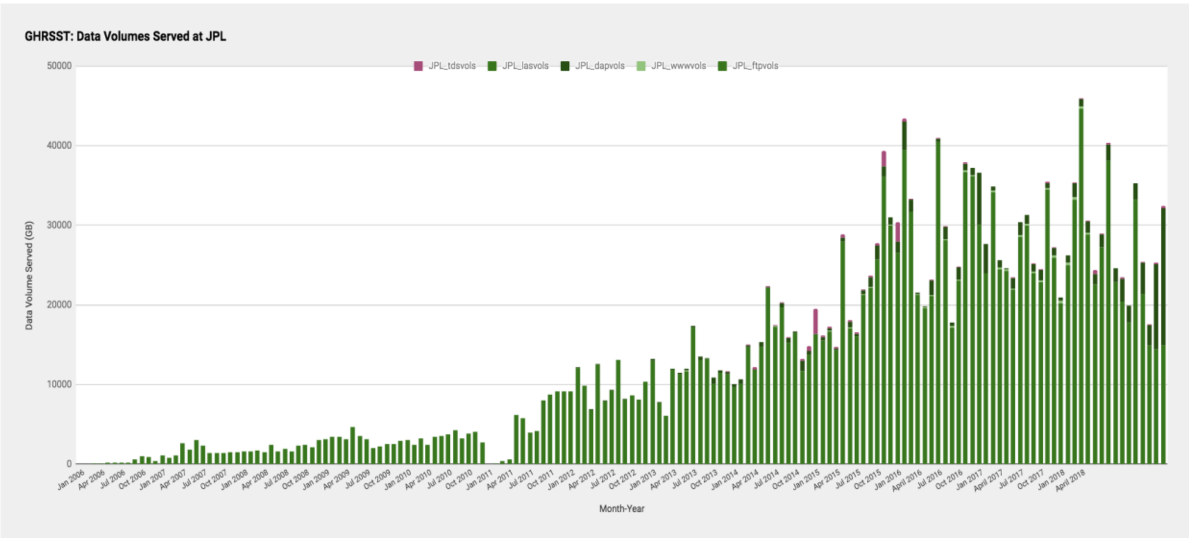

Figure 4. Volume of monthly files (GBs) distributed.

3. TOOLS AND SERVICES

The following list summarizes the improvements and availability of various tools and services for GHRSST data.

- PO.DAAC Earthdata Drive (PO.DAAC Drive)

    - Designated FTP replacement using HTTPS
- State Of The Ocean (SOTO) version 5 (in development)
    - Analytics capability from Oceanworks (NEXUS) presented at GHRSST-19 meeting
    - Includes MUR L4 and MODIS L2
- HiTIDE
    - GUI based L2 subsetting
- OPeNDAP, THREDDS, LAS, Webification-sci, Metadata Compliance Checker
- Improved discovery of GHRSST datasets
    - PO.DAAC dataset landing page markups using schema.org
- See poster by Wen-Hao Li documenting many of these enhancements

4. NEW IN SITU DATASETS

PO.DAAC released several new *in situ* datasets containing a wealth of oceanographic observations. These datasets included results from a Saildrone cruise in Alta California/Baja California in 2018 (https://podaac.jpl.nasa.gov/saildrone). Future Saildrone datasets will include results from the ongoing NOPP MISST Arctic cruises. Additionally, 7 datasets were released from the SPURS-2 Eastern Tropical Pacific field campaign with more expected in the near future (https://podaac.jpl.nasa.gov/spurs). The SPURS-2 datasets contain observations from CTD, XBT, ARGO, ADCP, WAMOS, and SEA-POL instruments.

PO.DAAC is investigating future infusion strategies for accessing and visualizing global *in situ* data in its tools and service suite.

See posters by Armstrong and Vazquez-Cuervo for more specific summaries.

Acknowledgements

This work was carried out at the NASA Jet Propulsion Laboratory, California Institute of Technology. Government sponsorship acknowledged. Copyright 2019 California Institute of Technology. Government sponsorship acknowledged. URS284476.

Appendix A. New or updated GHRSST datasets ingested in the last 12 months

Process Level	Sensors	RDAC	Resolution	Short Name	Persistent ID
Level2	VIIRS/NPP	OSPO	0.75 km	VIIRS_NPP-OSPO-L2P-v2.60	10.5067/GHVRS-2PO60
Level3	VIIRS/NPP	OSPO	2 km	VIIRS_NPP-OSPO-L3U-v2.60	10.5067/GHVRS-3UO60
Level2	VIIRS/N-20	OSPO	0.75 km	VIIRS_N20-OSPO-L2P-v2.60	10.5067/GHV20-2PO60
Level3	VIIRS/N-20	OSPO	2 km	VIIRS_N20-OSPO-L3U-v2.60	10.5067/GHV20-3UO60
Level2	VIIRS/NPP	OSPO	0.75 km	VIIRS_NPP-OSPO-L2P-v2.61	10.5067/GHVRS-2PO61
Level3	VIIRS/NPP	OSPO	2 km	VIIRS_NPP-OSPO-L3U-v2.61	10.5067/GHVRS-3UO61
Level2	VIIRS/N-20	OSPO	0.75 km	VIIRS_N20-OSPO-L2P-v2.61	10.5067/GHV20-2PO61
Level3	VIIRS/N-20	OSPO	2 km	VIIRS_N20-OSPO-L3U-v2.61	10.5067/GHV20-3UO61

Process Level	Sensors	RDAC	Resolution	Short Name	Persistent ID
Level2	VIIRS	NAVO	0.75 km	VIIRS_NPP-NAVO-L2P-v3.0	10.5067/GHVRS-2PN30
Level4	K10_SST	NAVO	11 km	K10_SST-NAVO-L4-GLOB-v01	10.5067/GHK10-L4N01
Level3	GOES-16/ABI	OSPO	2 km	ABI_G16-STAR-L3C-v2.70	10.5067/GHG16-3UO27
Level2	GOES-16/ABI	OSPO	2 km	ABI_G16-STAR-L2P-v2.70	10.5067/GHG16-2PO27

THE EU GDAC AND IFREMER RELATED ACTIVITIES

Jean-François Piollé[(1)], Emmanuelle Autret[(1)], Cédric Prevost[(1)]

(1) Institut Français de Recherche pour l'Exploitation de la Mer (Ifremer), Brest, France, Email: jfpiolle@ifremer.fr

1. INTRODUCTION

Ifremer's Satellite Data Centre (CERSAT) operates as a GHRSST producer and Global Data Assembly Center (G-DAC) for Europe since Medspiration (2005). It delivers a wide range of L2P, L3 and L4 products together with different access services. It also maintains the Felyx system for match-up production, in particular in the context of Sentinel-3 cal/val.

2. PRODUCTS

2.1. DISTRIBUTED PRODUCTS

As a DAC, Ifremer distributes the L2P and L3 products from OSI SAF, pushed to US-GDAC, and also mirrors several products from US-GDAC for European users. All these data are used as input to multi-sensor products processed at Ifremer.

Since 2018, Ifremer is also the main DAC for all in situ radiometer data from the shipborne radiometer network (http://www.ships4sst.org/).

The distribution statistics of these products show a steady number of users and distributed volume over the last few years. The equally steady number of newly registered users compared to the two previous numbers also seems to demonstrate that most usages are still occasional rather than continuous operational applications. The non-European products represent less than 10% of distributed data pointing out that mirroring of data is no longer required.

Ifremer also now offers to registered users (request to cersat@ifremer.fr) remote processing capabilities on its HPC, in particular through Jupyter notebooks. Predefined and customizable conda environments are provided together with Jupyter.

2.2. GENERATED PRODUCTS

Ifremer processes and delivers several global and regional multi-sensor products, including:

- the continuation of Medspiration project time series for regional L4 products over Mediterranean Sea, South Africa, and Brazil/Tropical Atlantic
- an operational global multi-sensor L3S and a L4 over the Eastern Atlantic (including Europe North Western Shelves, Iberian sea and canary islands) in the context of Copernicus Marine Service (CMEMS). These products are exclusively distributed at CMEMS (http://marine.copernicus.eu/). The former NWS product restricted to North Western Shelves is now superseded by this new ATL product.

In the last year, we have focused on two main activities:

- The reprocessing of a long time series (1982-2018) of the multi-sensor daily 2km resolution L4 over the East Atlantic (ATL) for Copernicus Marine Environment Monitoring Service (CMEMS), using the AVHRR Pathfinder v5.3 (PFv53) archive extended to 2018 with AVHRR GAC data (Figure 1).
- A new analysis methodology was used for this product based on a Kalman smoother (Tandéo et al., 2011). This product is available on CMEMS portal and used to derive the annual CMEMS State of the Ocean report.

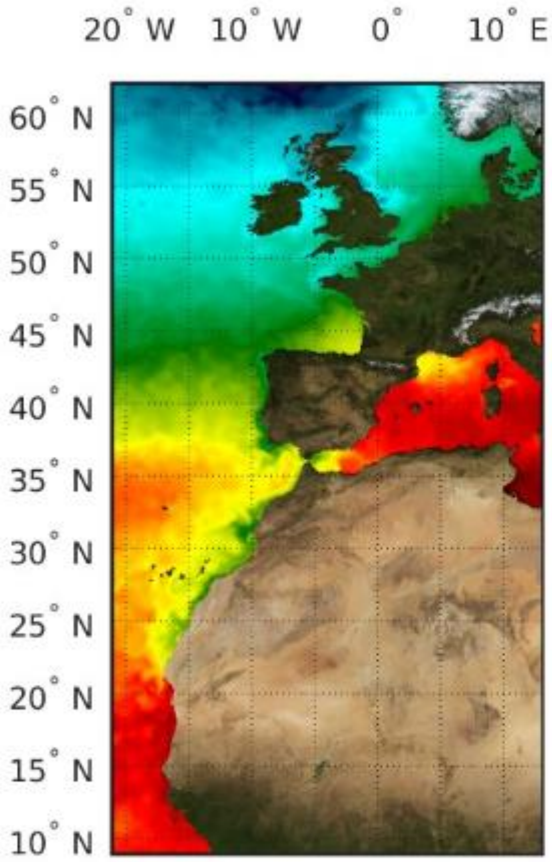
20° W
10° W
0°
10° E
60° N
55° N
50° N
45° N
40° N
35° N
30° N
25° N
20° N
15° N
10° N

GHRSST SYSTEM COMPONENTS: LTSRF

Kenneth S. Casey, Yongsheng Zhang, John Relph, Yuanjie Li, Korak Saha, Xuepeng Zhao, and Huai-min Zhang

NOAA National Centers for Environmental Information, Email: kenneth.casey@noaa.gov

ABSTRACT

The GHRSST Long Term Stewardship and Reanalysis Facility (LTSRF) at the NOAA National Centers for Environmental Information (NCEI) had another successful year maintaining GHRSST archive and access operations. New products were included in the archive, the Dynamic Data Table was maintained, substantial progress was made integrating GHRSST data in to the new NOAA OneStop system, and advances in CEOS CWIC Integration were achieved. Archive and access Statistics are also presented showing continued use of the GHRSST data by the broader community.

1. INTRODUCTION

The GHRSST Long Term Stewardship and Reanalysis Facility (LTSRF) at the NOAA National Centers for Environmental Information (NCEI) had another successful year maintaining GHRSST archive and access operations. New products were included in the archive, the Dynamic Data Table was maintained, substantial progress was made integrating GHRSST data in to the new NOAA OneStop system, and advances in CEOS CWIC Integration were achieved. Archive and access Statistics are also presented showing continued growth in user uptake of GHRSST data. The remaining sections of this document provide details in these areas.

2. NEW PRODUCTS

New products this past year brought into the LTSRF are shown below:

- GHRSST-GOES16-OSISAF-L3C-v1.0
- GHRSST-K10_SST-NAVO-L4-GLOB-v01
- GHRSST-VIIRS_N20-OSPO-L2P-v2.60, GHRSST-VIIRS_N20-OSPO-L2P-v2.61
- GHRSST-VIIRS_N20-OSPO-L3U-v2.60, GHRSST-VIIRS_N20-OSPO-L3U-v2.61
- GHRSST-VIIRS_NPP-OSPO-L2P-v2.60, GHRSST-VIIRS_NPP-OSPO-L2P-v2.61
- GHRSST-VIIRS_NPP-OSPO-L3U-v2.60, GHRSST-VIIRS_NPP-OSPO-L3U-v2.61

3. DYNAMIC DATA TABLE

The dynamic data table was maintained at: http://ghrsst.nodc.noaa.gov/accessdata.html. The table:

- Is built automatically and dynamically from metadata and archive metrics
- Includes key summary information for each product
- Includes data access and metadata links
- Displays Summary stats for all products at bottom

4. GHRSST IN NOAA ONESTOP

One of the featured datasets in the NOAA OneStop system at https://data.noaa.gov/onestop is the collection of GHRSST products. All of the products (and others that reference or use GHRSST in some way) can be searched there by typing "GHRSST" in the search bar, or clicking on https://data.noaa.gov/onestop/#/collections?q=GHRSST. NOAA OneStop supports the two-step discovery process, of first finding the relevant collection, and then finding the relevant data granules within that collection. This two-step process is illustrated in Figure 1 below.

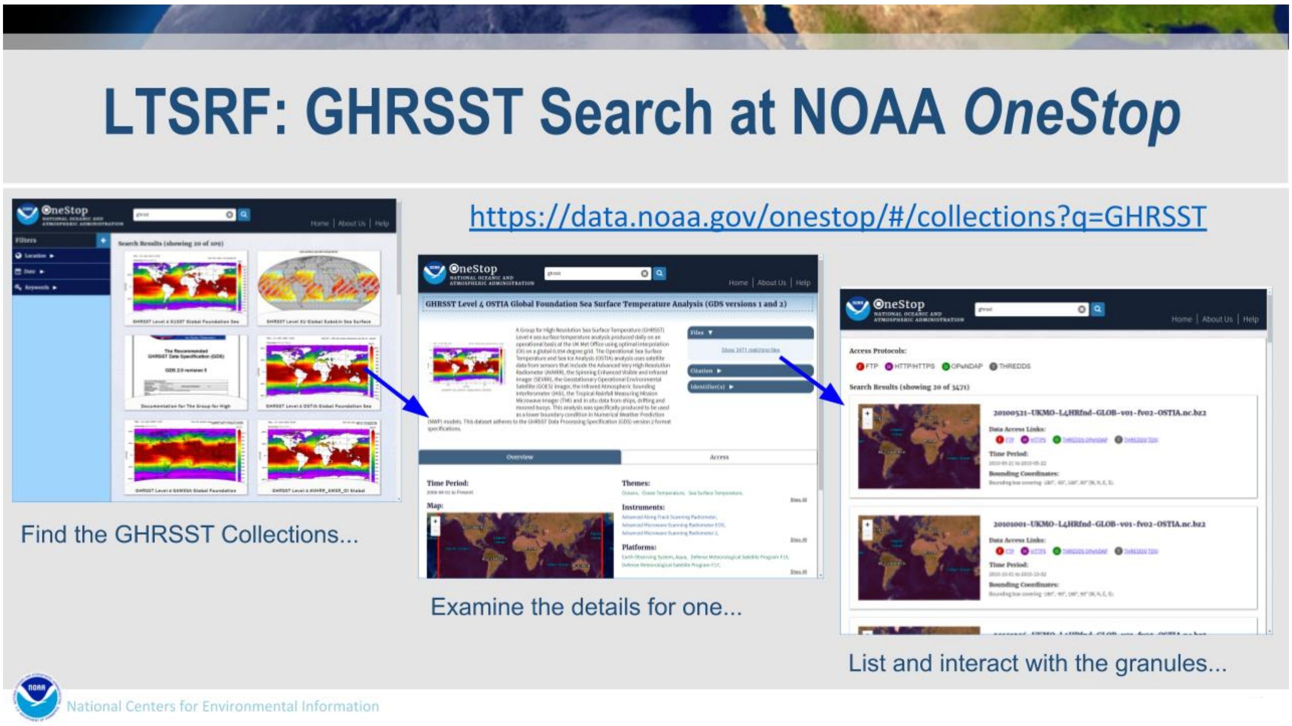

Figure 1: Discovery GHRSST data in NOAA OneStop

5. CEOS CWIC INTEGRATION UPDATE

Connections to the CEOS WGISS Integrated Catalog (CWIC) were improved at the LTSRF this year on behalf of the GHRSST community. These updates were initiated to ensure that the GHRSST connection to the CWIC catalog can take advantage of the new NOAA OneStop API capabilities. Updates since the last GHRSST meeting include:

- Established the test connection to the OneStop granule search API
- Granule inventories 90 out of 99 GHRSST data sets are discoverable
- Over 4 million granules indexed, on way to 7 million

6. ARCHIVE AND ACCESS STATISTICS

Figures 2 through 4 highlight the various access statistics at the LTSRF over time.

LTSRF: Daily Access Statistics

	2006	2007	2008	2009	2010	2011	2012	2013	2014	2015	2016	2017	2018	2019*
Files served per day	85	1130	1734	3413	21,956	14,896	28,807	20,056	21,196	12,979	15,020	18,041	32,850	9612
GB served per day	0.2	1.8	3.9	18.8	66.3	115	73	145	156	122	202	153	407	204
Users served per day	3	7	8	8	11	19	19	24	36	38	63	39	33	19

* Estimated based on January 1 - April 30, 2019
* Statistics only cover ftp and http access since July 1, 2018

National Centers for Environmental Information

Figure 2: Daily Average access statistics since 2006 at the LTSRF.

LTSRF: Total Archive Holdings

	2008	2009	2010	2011	2012	2013	2014	2015	2016	2017	2018	2019*
Products	22	26	27	40	59	60	62	77	81	89	97	99
# of AIPs (K)	39	50	60	68	92	105	112	132	148	158	169	174
Files (M)	0.68	0.99	1.35	1.66	2.46	3.29	3.97	4.89	5.89	6.44	6.67	7.21
Volume (TB)	13	20	28	34	57	69	81	99	124	139	154	161

* As of May 20, 2019

National Centers for Environmental Information

Figure 3: Number of GHRSST products, archival information packages (accessions), files, and data volumes for GHRSST data at the LTSRF.

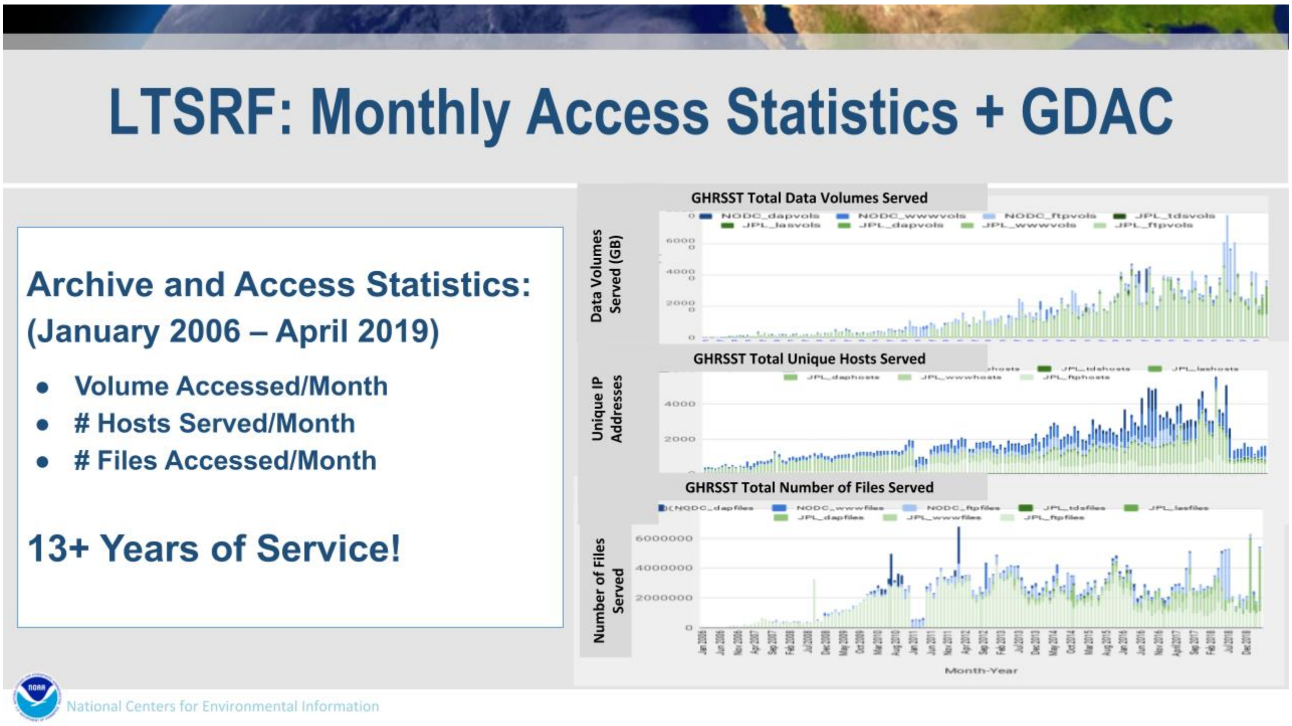

Figure 4: Combined access statistics between the LTSRF and PO.DAAC GDAC going back to 2006.

7. CONCLUSION

The last year marked another successful year of operations at the GHRSST LTSRF.

8. REFERENCES

None.

NOAA *i*QUAM AND SQUAM: UPDATE FOR GHRSST-XX

Alexander Ignatov[(1)], Matthew Pennybacker[(2)], Olafur Jonasson[(3)], Yury Kihai[(4)]

(1) NOAA STAR, NCWCP, USA Email: Alex.Ignatov@noaa.gov
(2) NOAA STAR & GST Inc., NCWCP, USA Email: Matthew.Pennybacker@noaa.gov
(3) NOAA STAR & GST Inc., NCWCP, USA Email: Olafur.Jonasson@noaa.gov
(4) NOAA STAR & GST Inc., NCWCP, USA Email: Yury.Kihai@noaa.gov

1. INTRODUCTION

Progress between GHRSST-XIX and -XX summarized with two SST Monitoring systems at NOAA, considered GHRSST resources: the *in situ* SST Quality Monitor (*i*Quam; www.star.nesdis.noaa.gov/sod/sst/iquam/) and SST Quality Monitor, SQUAM; www.star.nesdis.noaa.gov/sod/sst/squam/).

2. IQUAM

The *i*Quam system was introduced at NOAA in 2010 (Xu and Ignatov, 2010; 2014). It serves the following main functions: (1) collects *in situ* data (with its own QC, if available) from various sources; (2) Performs a uniform QC and sets *i*Quam QFs; (3) Serves data online in monthly GDS*i* netCDF files, updated daily; and (4) Monitors QC'ed in situ data online. Development has been going on to upgrade to iQuam v2.1, which is still a work in progress. We recommend that users use the following temporary URL, until further notice: www.star.nesdis.noaa.gov/sod/sst/iquam2/. This "*i*Quam2" reports data of v2.1 which includes the following major updates from v2.0: (1) Merged RT GTS data from NCEP, FNMOC, ICOADS (to improve data stability, and to address the 5-to-7 digit ID WMO transition which is still not addressed in NCEP GTS, the major feed in v2.0 – cf. Figures 1 and 2); (2) Added Argo floats from 2 more sources (in addition to IFREMER), USGODAE & NOAA NODC; (3) Replaced ICOADS R2.5 with R3.0 (also netCDF data are used instead of IMMA1); (4) Added interactive plots for individual platforms; (5) Added time series of mean/SD/NOBS for individual platforms (all are now interactive); (6) Added hourly maps (useful to analyse & fill data gaps); (7) Added permalink feature (useful to share the page content with partners); (8) Last-month file is now updated once daily (vs. twice daily before, because increased data volumes started creating job run conflicts).

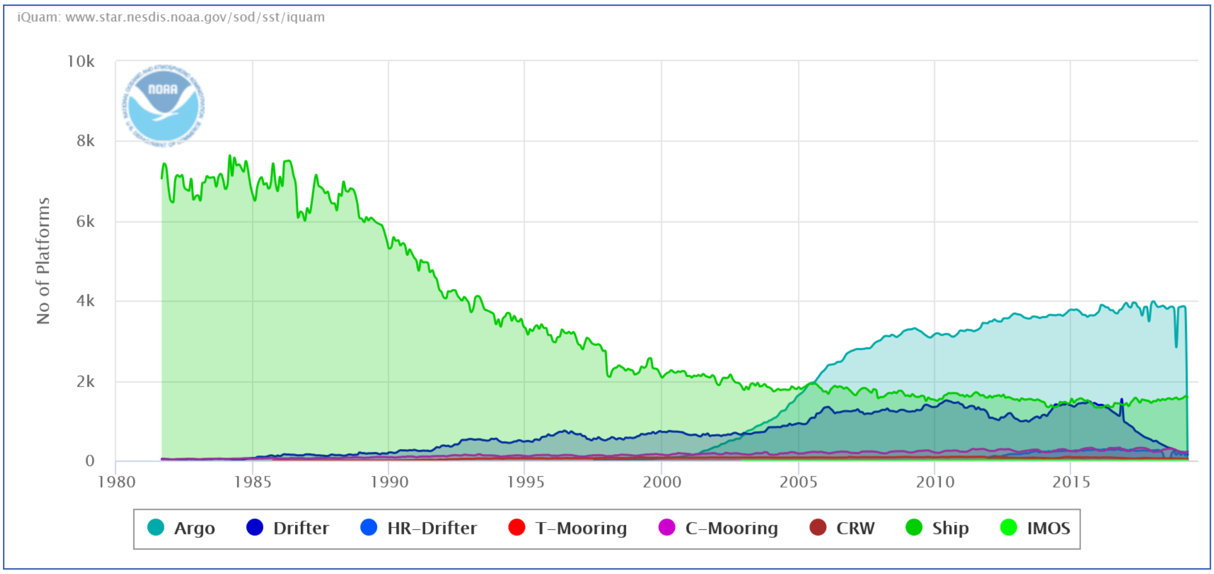

Figure 1: Time series of number of IDs in iQuam v2.0 (reported at www.star.nesdis.noaa.gov/sod/sst/iquam/). Note a declining trend in number of drifters after 1st November 2016 due to missing 7-digit ID's in NCEP GTS data.

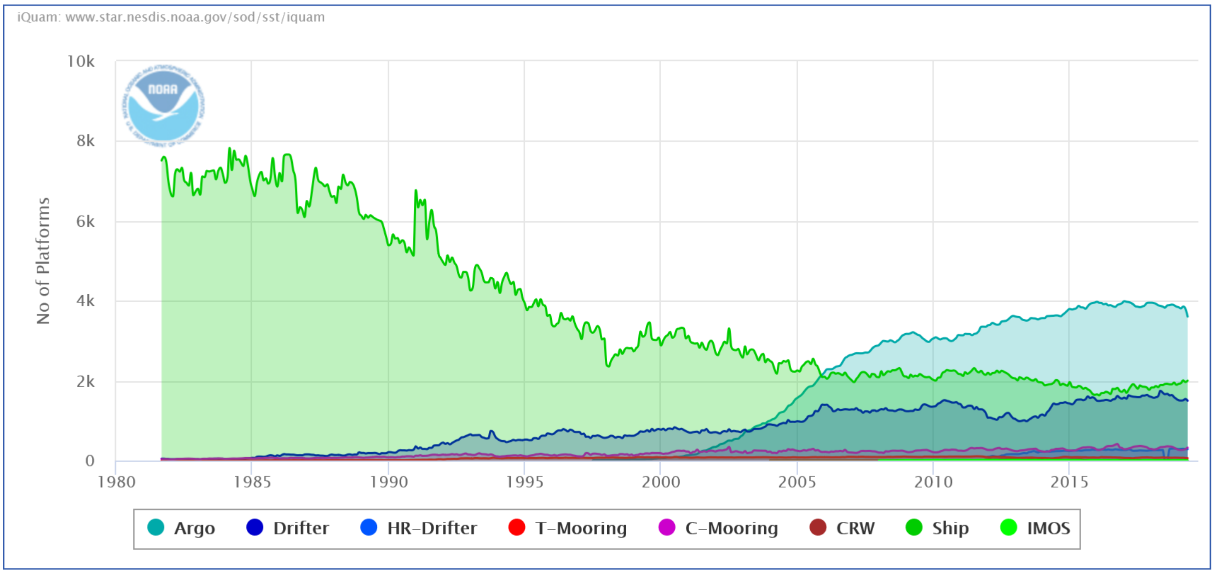

Figure 2: Time series of number of IDs in iQuam v2.1 (reported at www.star.nesdis.noaa.gov/sod/sst/iquam2/). Note that the number of drifter ID's after 1st November 2016 is now flat, due to inclusion of 7-digit ID's from FNMOC and ICOADS.

3. SQUAM

SQUAM was introduced at NOAA in 2009 (Dash et al., 2010). It monitors satellite L2/3/4 SST products with respect to two references: (1) QC'ed *in situ* SSTs from *i*Quam; and (2) several selected gap-free L4 analyses. It checks if the distributions of the corresponding deltas are near-Gaussian, centred at approximately zero, with the width of the distribution measuring the relative noise in the product being evaluated, and the reference. Results are presented in the form of maps, histograms, time series, dependencies, and Hovmöller plots.

SQUAM was updated to v2 in 2017. The v2 release focused on NOAA and NOAA partners' products, due to prohibitive data volumes. It added interactive / user-controlled graphics, a permalink feature, an option to display SSES-bias corrected SSTs (with a turn on/off radio button), and monthly and yearly aggregations of performance metrics. The geostationary SST page was introduced in v2.

SQUAM was updated to v2.1 in 2018. The v2.1 release provisioned for newly launched or planned to be launched satellites (NOAA-20, GOES-17, and Metop-C). It also added monitoring of the full suite of the ACSPO L3U products, from all polar and geo sensors and moved all NOAA developmental and many partners' products to NOAA SQUAM internal pages, to minimize the stress on the public SQUAM and make its results more transparent.

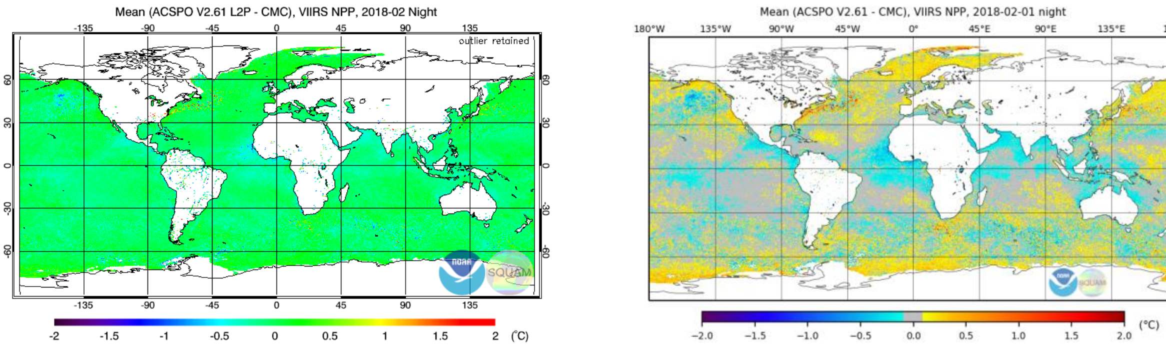

Figure 3: Currently used colour scheme for SST deltas (on the left) vs currently implemented in SQUAM.

Since GHRSST-XIX, the focus has been on the redesign of the backend. The SQUAM backend was initially designed for much smaller data volumes (such as AVHRR GAC), and had difficulties handling multiple new hi-res data streams produced by the NOAA ACSPO system, including JPSS VIIRS, GOES-R ABI, Himawari-8 AHI, AVHRR FRAC, and EOS MODIS. Oftentimes, the same sensor is placed on board multiple platforms (*e.g.*, NPP and NOAA-20 VIIRSs; GOES-16 and -17 ABIs; Metop-A, -B, and -C AVHRR FRACs; Terra and Aqua MODISs; *etc.*). The old back-end based on a combination of IDL and bash scripts, cannot keep up with new data volumes. A more robust design based on Python, C++, and an SQL database is underway.

Changes in the front end are relatively minor, and mainly include adjusting the colour scale of the maps and Hovmöller plots of the delta-SSTs. An example in Fig.3 shows an example of the currently used colour scheme, and the one being explored. Comparison shows that the current scheme is not well suited to distinguish the anomalies in a 0.5K range, whereas the newly proposed scheme is capable to differentiate and emphasize subtler shades of SST differences, which is the objective of the SST quality monitoring in SQUAM.

4. CONCLUSION AND FUTURE WORK

Upon testing, iQuam v2.1 will be promoted to the main URL www.star.nesdis.noaa.gov/sod/sst/iquam/ (from the current temporary URL www.star.nesdis.noaa.gov/sod/sst/iquam2/). Until further notice, users are advised to use the "iquam2" URL. The other priority is to identify *in situ* data for the early 1980s, to support the ongoing AVHRR GAC reanalysis 2 (RAN2).

SQUAM is being tweaked to add new GOES-17 data, and newly developed reanalyses (VIIRS, ABI, AHI, AVHRR, and MODIS). The front end is being tweaked to accommodate the new colour scheme presented in Fig.3.

Work is underway to redesign the back ends of both *i*Quam and SQUAM, based on new and more robust IT technologies and programming languages, to make both systems more stable and scalable.

5. REFERENCES

Xu, F., and A. Ignatov, Evaluation of in situ sea surface temperatures for use in the calibration and validation of satellite retrievals, *JGR*, 115, C09022, doi: 10.1029/2010JC006129, 2010.

Xu, F., and A. Ignatov, *In situ* SST Quality Monitor (*i*Quam), *JTech*, 31, 164-180, doi:10.1175/JTECH-D-13-00121.1, 2014.

Dash, P., A. Ignatov, Y. Kihai, and J. Sapper, The SST Quality Monitor (SQUAM), *JTech*, 27, 1899-1917, doi:10.1175/2010JTECHO756.1, 2010.

REPORT FROM THE AUSTRALIAN RDAC TO GHRSST-XX

Helen Beggs[(1)], Pallavi Govekar[(2)], Christopher Griffin[(3)], Leon Majewski[(4)], Lixin Qi[(5)], Aihong Zhong[(6)] and Pavel Sakov[(7)]

(1) Bureau of Meteorology, Melbourne, Australia, Email: helen.beggs@bom.gov.au
(2) Bureau of Meteorology, Melbourne, Australia, Email: pallavi.govekar@bom.gov.au
(3) Bureau of Meteorology, Melbourne, Australia, Email: christopher.griffin@bom.gov.au
(4) Bureau of Meteorology, Melbourne, Australia, Email: leon.majewski@bom.gov.au
(5) Bureau of Meteorology, Melbourne, Australia, Email: lixin.qi@bom.gov.au
(6) Bureau of Meteorology, Melbourne, Australia, Email: aihong.zhong@bom.gov.au
(7) Bureau of Meteorology, Melbourne, Australia, Email: pavel.sakov@bom.gov.au

ABSTRACT

This is a report of progress during the past 12 months in the Australian Regional Data Assembly Centre at the Bureau of Meteorology (BoM), relating to the provision and validation of Group for High Resolution Sea Surface Temperature (GHRSST) products, and related SST research.

1. OVERVIEW

As a contribution to the Integrated Marine Observing System (IMOS), the Australian Bureau of Meteorology produces several real-time and delayed mode (reprocessed), GHRSST format products (GHRSST Science Team, 2012) for a range of operational and research applications, using locally received and overseas sea surface temperature (SST) data sets obtained from polar-orbiting and geostationary satellites (Beggs, 2019). In summary, they are:

1.1. OPERATIONAL REAL-TIME GDS1.6

- Daily Regional 1/12º SST_{fnd} L4 ("RAMSSA") over 60ºE to 190ºE, 70ºS to 20ºN (Figure 1(a))
- Daily Global 0.25º SST_{fnd} L4 ("GAMSSA") (Figure 2(b))

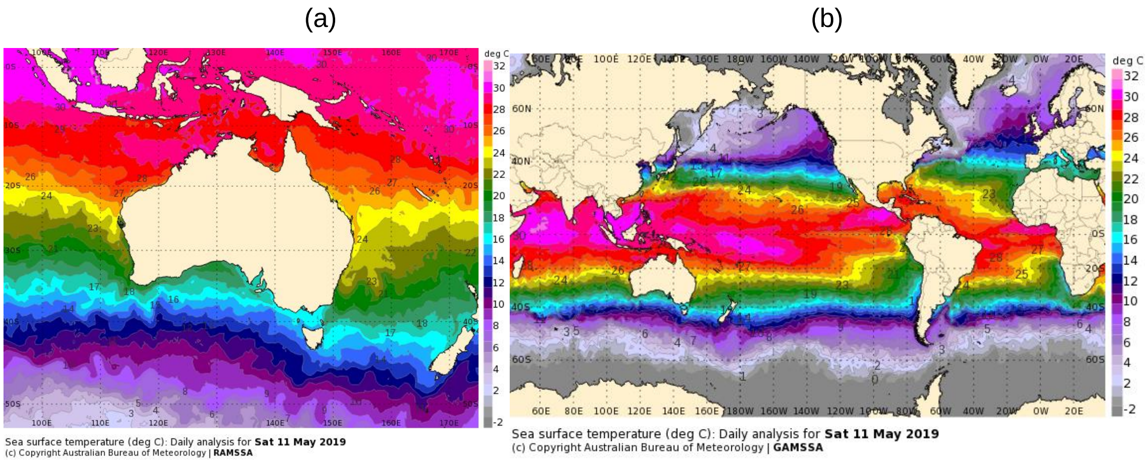

Figure 1: Example of foundation SST for 11th May 2019 from BoM Daily L4 analyses (a) RAMSSA and (b) GAMSSA, formed from NAVOCEANO GAC AVHRR L2P (Metop-A, Metop-B), JAXA AMSR-2 and in situ SST (ships, buoys).

1.2. OPERATIONAL REAL-TIME GDS2.0

- Daily Regional 1/12º SST_{fnd} L4 ("RAMSSA") over 60ºE to 190ºE, 70ºS to 20ºN

- Daily Global 0.25º SST_{fnd} L4 ("GAMSSA")
- 1 km SST_{skin} L2P from High Resolution Picture Transmission (HRPT) Advanced Very High Resolution Radiometer (AVHRR) data (NOAA-15, NOAA18, NOAA-19)
- 0.02º SST_{skin} L3U and day/night L3C over Australia (70ºE to 190ºE, 70ºS to 20ºN) and Southern Ocean (2.5°E to 202.5°E, 77.5°S to 27.5°S) from HRPT AVHRR data (NOAA15, NOAA-18, NOAA-19) and ACSPO Visible Infrared Imaging Radiometer Suite (VIIRS) L3U data (Suomi-NPP)
- 0.02º day/night SST_{skin} and day+night SST_{fnd} L3S over Australia (70ºE to 190ºE, 70ºS to 20ºN) and Southern Ocean (2.5°E to 202.5°E, 77.5°S to 27.5°S) from
    - AVHRR-only: HRPT AVHRR data (NOAA-18, NOAA-19)
    - Multi-sensor: HRPT AVHRR data (NOAA-18) and VIIRS data (Suomi-NPP) (Figure 3(a))
    - 2 km 10-minute Himawari-8 AHI SST_{skin} L2P

1.3. EXPERIMENTAL REAL-TIME GDS2.0

- 0.02º SST_{skin} L3U and day/night L3C over Australia (70ºE to 190ºE, 70ºS to 20ºN) and Southern Ocean (2.5°E to 202.5°E, 77.5°S to 27.5°S) from OSI-SAF Full Resolution Area Coverage (FRAC) AVHRR L2P (Metop-B) and ACSPO VIIRS L3U data (NOAA-20)
- 0.02º day/night SST_{skin} and day+night SST_{fnd} L3S over Australia (70ºE to 190ºE, 70ºS to 20ºN) and Southern Ocean (2.5°E to 202.5°E, 77.5°S to 27.5°S) from
    - Multi-sensor: HRPT AVHRR data (NOAA-18), FRAC AVHRR data (Metop-B) and VIIRS data (Suomi-NPP, NOAA-20) (Figure 3(b))
    - 0.02º Hourly, 4-hourly and Daily night-only SST_{skin} L3C over Australia (70ºE to 190ºE, 70ºS to 20ºN) from Himawari-8 AHI

1.4. REPROCESSED GDS2.0

- HRPT AVHRR L2P/L3U/L3C/L3S from 1992 to 2016 (NOAA-11 to NOAA-19 satellites)
- AVHRR and VIIRS L3U/L3C/L3S from 2012 to 2016 (NOAA-18, NOAA-19, Metop-A, Metop-B, Suomi-NPP)
- MTSAT-1R Hourly 0.05º L3U (2006 to 2010)

2. DATA AVAILABILITY

2.1. REAL-TIME GDS1.6

Operational daily L4 (RAMSSA/GAMSSA) are available within 6 hours of final observation back to 2008 from JPL PO.DAAC (http://podaac.jpl.nasa.gov/dataset/ABOM-L4HRfnd-AUS-RAMSSA_09km and http://podaac.jpl.nasa.gov/dataset/ABOM-L4LRfnd-GLOB-GAMSSA_28km), NOAA/NCEI (https://www.nodc.noaa.gov/SatelliteData/ghrsst/accessdata.html) and Bureau OPeNDAP server.

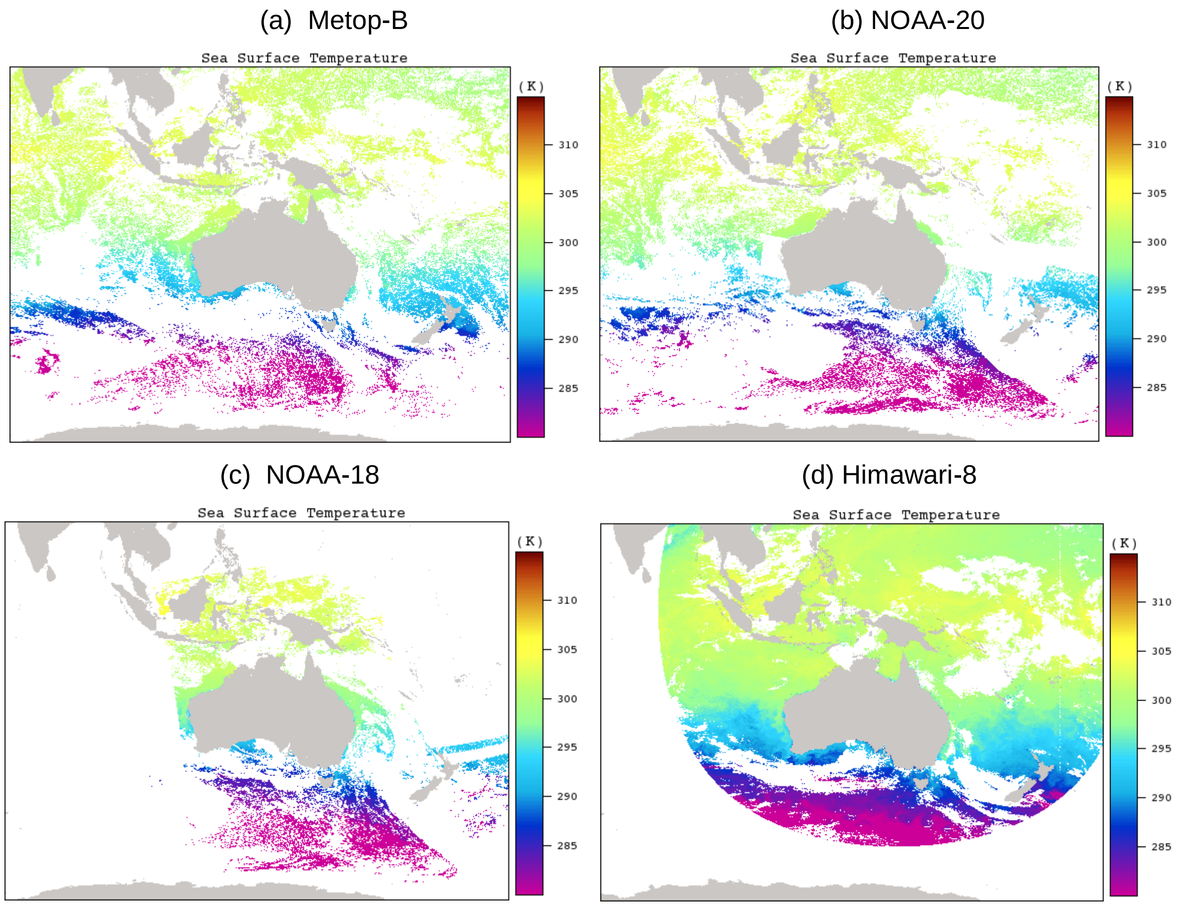

Figure 2: Example of skin SST for 11th May 2019 from IMOS 1-day L3C products formed from (a) daytime Metop-B FRAC AVHRR, (b) night-time NOAA-20 VIIRS, (c) night-time NOAA-18 HRPT AVHRR and (d) night-time Himawari-8 AHI L3U SST.

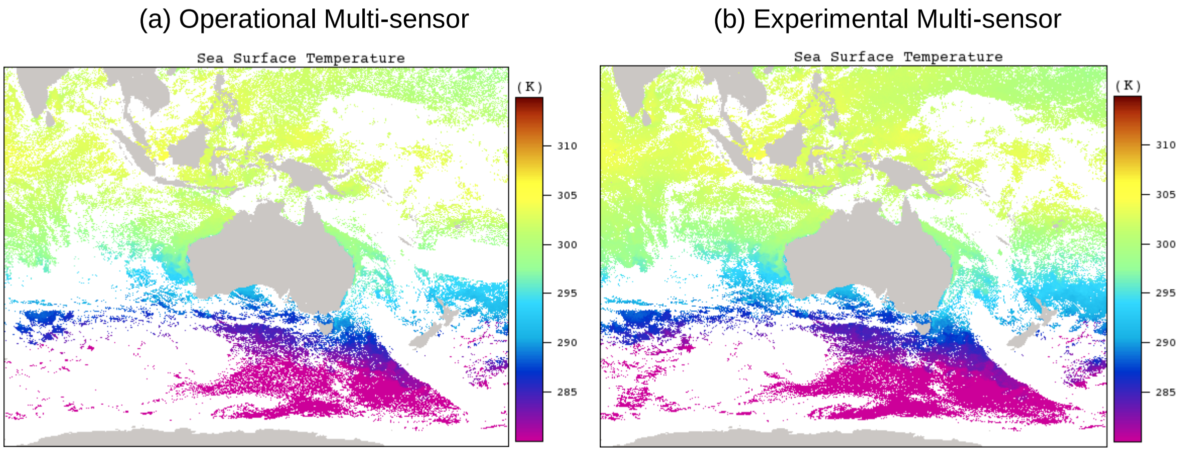

Figure 3: Example of skin SST for 11th May 2019 from IMOS 1-day night-time Multi-sensor L3S products formed from (a) NOAA-18/AVHRR and Suomi-NPP/VIIRS and (b) NOAA-18/AVHRR, Metop-B/AVHRR, Suomi-NPP/VIIRS and NOAA-20/VIIRS L3C SST.

2.2. REAL-TIME GDS2.0

- Operational daily l4 (ramssa/gamssa) are available within 6 hours of final observation back to 2006/2008 from the Australian Ocean Data Network (AODN) THREDDS server at http://thredds.aodn.org.au/thredds/catalog/imos/srs/sst/ghrsst/l4/catalog.html
- Operational IMOS fv01 HRPT AVHRR (available 2015 to present)
    - L2P: OPeNDAP server (contact ghrsst@bom.gov.au)
- Operational IMOS fv01 HRPT AVHRR L3U/L3C/L3S (available 2015 to present): http://thredds.aodn.org.au/thredds/catalog/IMOS/SRS/SST/ghrsst/catalog.html
- Experimental IMOS fv01 Metop-B, NOAA-20 L3C and Multi-sensor L3S: OPeNDAP servers (contact ghrsst@bom.gov.au)
- BoM AHI Himawari-8
    - L2P: (available 24 March 2016 to present) Contact ghrsst@bom.gov.au
    - L3C: (available 1 October 2017 to present) Contact ghrsst@bom.gov.au

2.3. REPROCESSED GDS2.0

- IMOS fv02 HRPT AVHRR (available 1992 to 2016)
    - L2P: http://dapds00.nci.org.au/thredds/catalog/rr5/satellite/GHRSST/v02.0fv02/L2P/catalog.html
    - L3U/L3C/L3S: http://portal.aodn.org.au and http://dapds00.nci.org.au/thredds/catalog/rr5/satellite/GHRSST/v02.0fv02/Continental/catalog.html
- IMOS AVHRR and VIIRS L3U/L3C/L3S (available 2012 to 2016): Contact ghrsst@bom.gov.au
- IMOS MTSAT-1R L3U (available Jun 2006 to Jun 2010): IMOS THREDDS server at http://rs-data1-mel.csiro.au/thredds/catalog/imos-srs/sst/ghrsst/L3U/mtsat1r/catalog.html

3. PROGRESS SINCE GHRSST-XIX

3.1. ISSUES WITH NOAA-18 AND NOAA-19 AVHRR SST

Orbital decay of NOAA-18 and NOAA-19 in recent years has affected the accuracy of real-time AVHRR SST products during some months, particularly since April 2017 for NOAA-18 and November 2017 for NOAA-19 (NOAA NESDIS, 2019). From 22 May 2018, Global Area Coverage (GAC) AVHRR NOAA-18 L2P SST data has no longer been ingested into BoM ocean models and SST analyses. IMOS NOAA-18 L3C SSTs are still ingested into IMOS L3S as errors are relatively small since August 2018 (BoM, 2019). BoM removed NOAA-19 SST data from ocean models (7 August 2018), Daily L4 (24 October 2018), IMOS Multi-sensor L3S (7 September 2018) and IMOS AVHRR L3S (1 October 2018).

3.2. ISSUES WITH CHANGE IN GTS FORMAT OF DRIFTING BUOY SST

Since 2nd November 2016 the number of 5-digit WMO ID drifting buoys providing SST data to GTS has steadily decreased, with new drifting buoys all having 7-digit IDs. BoM started ingesting 7-digit ID drifting buoy SSTs into IMOS SST systems from 9th December 2016 and SST analyses from 1st July 2018. The decrease in drifting buoy SST ingested from 2nd November 2016 to 30th June 2018 has had no noticeable impact on RAMSSA or GAMSSA SST analysis accuracy compared with independent Argo SST (5m) data (https://www.star.nesdis.noaa.gov/sod/sst/squam/analysis/l4/)

3.3. OPERATIONAL SST ANALYSES

3.3.1. Overview

BoM produces regional 1/12º ("RAMSSA") and global 1/4º ("GAMSSA") operational daily foundation L4 SST analyses in near real-time based on an optimal interpolation method. For more information on RAMSSA see Beggs et al (2011) and for GAMSSA see Zhong and Beggs (2009) and Beggs et al (2011). RAMSSA and GAMSSA are available in both GDS1.6 (Beggs and Pugh, 2009) and GDS2.0 L4 format (GHRSST Science Team, 2012) (Section 2).

SST inputs:

- 1 km IMOS fv01 HRPT AVHRR (NOAA-18, -19) L2P SST_{skin} (Paltoglou et al., 2010) (Stopped 21st October, 2018)
- 9 km NAVOCEANO GAC AVHRR GHRSST-L2P SST1m (NOAA-18, NOAA-19, Metop-A, Metop-B) (NOAA-18 stopped 22 May 2018, NOAA-19 stopped 24 October 2018)
- ~50 km AMSR-2 (GCOM-W) L2P $SST_{subskin}$ (since 1 December 2014)
- GTS Buoy and ship in situ SST_{depth} (Argo and CTD SST_{depth} ingested only into RAMSSA)

Sea Ice inputs: NOAA/NCEP Daily 1/12º sea-ice concentration analysis (Grumbine, 1996)

Background:

- RAMSSA: Formed from a combination of previous day's RAMSSA analysis and BoM Global Weekly 1º SST analysis (Smith et al., 1999).
- GAMSSA: Formed from a combination of previous day's GAMSSA analysis and Reynolds and Smith (1994) Monthly 1º 1961 – 1990 SST climatology.

Applications: Boundary condition for NWP models, validating ocean forecasts and MetEye. In addition, GAMSSA contributes to the GHRSST Multi-Product Ensemble.

3.3.2. Progress

ACSPO 0.02º Suomi-NPP VIIRS L3U SST data is being ingested into experimental, near real-time daily SST analyses (1/4º GAMSSA and 1/12º RAMSSA). Night-only ACSPO VIIRS L3U (quality level 5) data are collated to daily 1/4º and 1/12º L3C SST_{fnd}. Data are then further thinned by striding to 1/2º (GAMSSA) and 1/3º (RAMSSA). The thinned VIIRS SSTs are ingested along with NAVOCEANO GAC AVHRR, JAXA AMSR-2 and in situ SST_{fnd} into test RAMSSA and GAMSSA analyses. In order to reduce innovation STD compared with drifting and tropical moored buoy SST_{fnd}, the background correlation length scales have been increased from 12 km to 20 km (RAMSSA) and from 50 km to 80 km (GAMSSA). An additional change to experimental GAMSSA is that the background field is now formed from a weighted combination of the previous day's GAMSSA analysis and the BoM Global Weekly 1º SST_{blend} analysis.

Examples of the operational and test RAMSSA and GAMSSA SST maps are shown in Figure 4(a)-(d). For comparison, the Canadian Meteorological Centre (CMC) 0.1º daily foundation SST analysis (Brasnett and Surcel Colan, 2016) is also shown (Figure 4(e)).

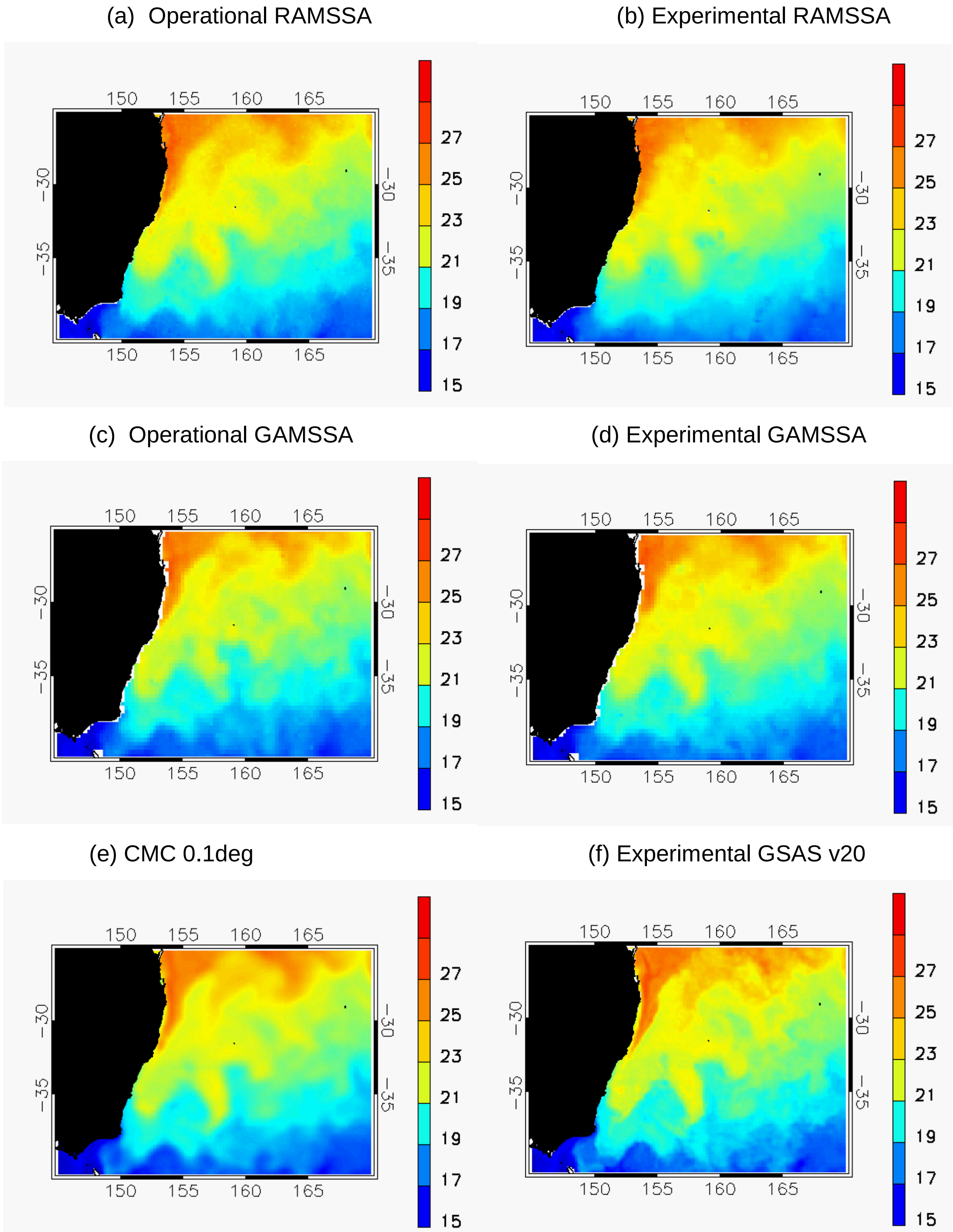

Figure 4: Example of foundation SST in the East Australian Current for 11th May 2019 from daily Multi-sensor L4 analyses (a) operational RAMSSA, (b) experimental RAMSSA (ingesting VIIRS L3U SST), (c) operational GAMSSA, (d) experimental GAMSSA (ingesting VIIRS L3U SST), (e) CMC0.1deg (ingesting VIIRS L3U SST) (Brasnett and Surcel Colan, 2016), and (f) experimental GSAS version 20 (ingesting VIIRS L3U SST).

3.4. EXPERIMENTAL ENSEMBLE OPTIMAL INTERPOLATION SST ANALYSIS (GSAS)

3.4.1. Overview

The BoM operational optimal interpolation SST analysis systems (GAMSSA, RAMSSA and Global Weekly) are based on Fortran code developed in the 1980s. Ensemble Kalman Filter data assimilation C code (EnKF-C; Sakov, 2014) is currently used for data assimilation into the BoM operational ocean model (OceanMAPS v3.2; BoM, 2017). Based on EnKF-C, an Ensemble Optimal Interpolation (EnOI) Global SST Analysis System (GSAS) has been developed, and is currently being tested and modified to eventually replace RAMSSA and GAMSSA. GSAS is a daily near-global (±75ºN) foundation SST analysis on a 0.1º x 0.1º grid. It ingests similar satellite SST inputs as operational GAMSSA (GAC AVHRR L2P and AMSR-2 L2P), with the addition of ACSPO VIIRS L3U night-only SST, strided to 0.04º. Unlike RAMSSA and GAMSSA, no in situ SST or sea ice data are currently ingested. The EnOI system uses background ensemble error covariances formed from the OFAM3 ocean model, with a support localisation radius (LOCRAD) of 100 km, RFACTOR to 0.33, and KFACTOR to 1 (Sakov, 2014). In addition, the latest GSAS test version (v20) uses a relaxation to CSIRO Atlas of Regional Seas (CARS) 2009 climatology (https://researchdata.ands.org.au/csiro-atlas-regional-cars-2009/15210) with e-folding time of 60 days. An example of the GSAS v20 SST is shown in Figure 4(f). Spectral analysis of GSAS v19 (without AMSR-2 data ingested) performed by the UK Met Office indicates that GSAS has slightly lower spectral density in boundary current regions to the current operational OSTIA but higher spectral density than CMC0.1deg (*Simon Good, pers. com.*). Globally, it has 0.02K higher RMS error compared with independent Argo SST(5m) observations than CMC0.1deg (*Simon Good, pers. com.*).

Future work in 2019/20 will concentrate on developing GSAS regional 0.1º SST analysis to replace RAMSSA, involving ingesting a sea-ice analysis, and improving the climatology and land mask.

3.5. IMOS GHRSST AVHRR AND VIIRS COMPOSITE PRODUCTS

3.5.1. Overview

As part of the Integrated Marine Observing System (IMOS: www.imos.org), BoM in collaboration with CSIRO, produces a range of HRPT AVHRR GDS2.0 L2P, L3U, L3C and L3S products from the series of NOAA Polar Orbiting Environmental Satellites (NOAA-11 to NOAA-19). Following methods documented in Griffin et al. (2017), SST values are derived by regressing brightness temperatures against regional drifting buoy SST observations at ~0.2 m depth, error estimates obtained using matchups with buoy data, and quality levels defined from proximity to detected cloud. The 0.02º resolution level 3 products are available in a range of averaging periods from single orbit to 1 month to suit different applications (Beggs, 2019). All products are available in real-time (within 3 to 24 hours of final observation) (Paltoglou et al., 2010) and have also been reprocessed to cover the period from 1992 to 2016 (Griffin et al., 2017). For more information see IMOS (2018) and AODN (2019).

Applications: BoM operational coral bleaching nowcasting service (ReefTemp NextGen: http://www.bom.gov.au/environment/activities/reeftemp/reeftemp.shtml), regional maps of ocean currents and SST (http://oceancurrent.imos.org.au/), SST climatologies (Wijfells et al., 2018), and research/monitoring SST diurnal variation, Marine Heat Waves and coastal upwelling (Beggs, 2019).

3.5.2. Progress

From 2018, NOAA officially replaced the AVHRR sensor program with the Visible Infrared Imaging Radiometer Suite (VIIRS) sensor program, after a long trial which began with the first VIIRS sensor launched in 2012 aboard the Suomi National Polar-Orbiting Partnership (NPP) platform. The VIIRS sensor provides higher spatial resolution (0.75 km at nadir) and lower noise than AVHRR, and has better orbital stability, with daily global SST coverage in cloud-free conditions at around 01:20 and 13:20 local time. The NOAA Office of Satellite and Product Operations (OSPO) produce real-time VIIRS L3U SST on the IMOS 0.02º x 0.02º grid (NOAA CoastWatch, 2018). The Bureau of Meteorology (BoM) have composited the OSPO VIIRS L3U data, following the method in Griffin et al. (2017), to produce daily day/night L3C composites of VIIRS data on the

IMOS grid and domain. The NPP VIIRS L3U data are composited based on quality and uncertainty estimates with AVHRR SST data from NOAA-18 and NOAA-19 to construct the new IMOS "Multi-sensor L3S" product suite (Griffin et al., 2017), resulting in improvements to overall quality, accuracy and coverage (Beggs et al., 2019a). These new products, produced operationally at BoM since 16 November 2018 (*e.g.* Figure 3(a)), are intended to be drop-in replacements for the existing AVHRR-only L3S product set, with similar file format. Validation of the night-time 1-day Multi-sensor L3S SST against *in situ* SST indicates incorporating VIIRS data significantly reduces the standard deviation of the 30-day differences from typically 0.4-0.7°C to 0.2-0.5°C for highest quality level L3S SSTs (BoM, 2019).

Real-time, operational, Multi-Sensor L3S netCDF files containing average SSTs over periods of 1, 3, 6 days and 1 month are available back to 1st January 2018 from the AODN THREDDS server at http://thredds.aodn.org.au/thredds/catalog/IMOS/SRS/SST/ghrsst/catalog.html in the L3SM-1d, L3SM-3d, L3SM-6d and L3SM-1m sub-directories, and from the AODN portal (http://portal.aodn.org.au). Maps of these Multi-sensor composite SSTs are available for various Australian regions from IMOS OceanCurrent (http://oceancurrent.imos.org.au/index.php) back to 1st January 2018. Since 21st November 2018, the IMOS Multi-sensor 1-day nighttime L3S SSTs have been ingested into the Bureau of Meteorology's ReefTemp NextGen coral bleaching nowcasting system (http://www.bom.gov.au/environment/activities/reeftemp/reeftemp.shtml).

Experimental real-time Multi-sensor L3S products (*e.g.* Figure 3(b)) have also been developed that ingest additional SST data from OSI-SAF Metop-B Full Resolution Area Coverage (FRAC) AVHRR L2P and ACSPO NOAA-20 VIIRS L3U. The Multi-sensor L3S products are also being reprocessed from 2012 to 2018 to incorporate all available Metop-A and Metop-B FRAC AVHRR L2P, NOAA-18 and NOAA-19 HRPT AVHRR L2P and NPP and NOAA-20 VIIRS L3U data. Example plots of the experimental 1-day night-only Multi-sensor L3S SSTskin can be viewed in the NOAA/NESDIS ACSPO Regional Monitor (*e.g.* https://www.star.nesdis.noaa.gov/sod/sst/arms/?datatype=none&data_lev=L3U&satt=VIIRS_NPP&daynight=night&variable=sst&date=2019-08-11&region-selected=AU&curr_slide=0&last_slide=0&masked=true&sses=true&front=false&cmp=true&cmp_to=MultiSensor&polar_slide=0).

3.6. HIMAWARI-8 L3C SST

3.6.1. Overview

BoM, in collaboration with JMA and NOAA/NESDIS/STAR, have since 24 March 2016 produced operational real-time Himawari-8 L2P skin SSTs on the GEOS grid, by regressing against ACSPO VIIRS L3U $SST_{subskin}$ measurements for a single date (21 July 2015), followed by subtracting 0.17 K to convert from subskin to skin SST. Currently, the Sensor Specific Error Statistics (SSES) values are estimated using a function based on AHI brightness temperature variability on 21 July 2015, and require further work to correct for sensor changes over time. Quality level values are derived for each SST value based on the Griffin et al. (2017) method, using a combination of proximity to cloud, identified using the GEOCAT method (http://cimss.ssec.wisc.edu/csppgeo/geocat.html), and size of the estimated error, estimated on "local SST variability". Possible quality levels are 0 to 5, with 5 identifying the most cloud-free pixels.

The 10-minute Himawari-8 L2P SST values are composited to hourly L3C files on the GEO projection by selecting the best quality spatially and temporally consistent SST. For the daily, night-time L3C composition, the retrieval is selected from the hourly retrievals, such that it is the best quality, closest in time to local sunrise. The hourly, 4-hourly or daily L3C data on the GEO projection is further mapped to the IMOS 0.02º x 0.02º grid using sub-pixel area weighted averaging of any overlapping pixels. An example of the Himawari-8 daily night-time L3C SST_{skin} over the IMOS domain (70ºS to 20ºN, 70ºE to 190ºE) is shown in Figure 2(d). The Himawari-8 SST composition method involves no smoothing or interpolation.

Experimental Himawari-8 L3C GDS2.0 files from 1st October 2017 to present are available via OPeNDAP on request. Near real-time validation plots of hourly and Daily L3C against drifting and tropical moored buoy SSTs are available at BoM (2019).

Applications: Himawari-8 L2P files are ingested into IMOS 4-hourly SST composite maps (http://oceancurrent.imos.org.au/product.php?product=fourhour), L3C files are used for research into coastal upwelling (Beggs et al., 2019b).

4. PLANS FOR 2019/2020

During the coming 12 months, the Bureau of Meteorology plans to:

- Tune optimal interpolation of ACSPO VIIRS L3U SSTs into RAMSSA and GAMSSA daily SST analyses before operational release
- Continue to develop new "GSAS" L4 product in order to replace RAMSSA and GAMSSA as operational SST analyses
- Add NAVOCEANO Metop-C GAC AVHRR L2P and ACSPO NOAA-20 VIIRS L3U data to BoM L4 and ocean models
- Investigate ingesting EUMETSAT Sentinel-3A/B SLSTR L2P and L3C SST to IMOS Multi-sensor L3S, GSAS L4 and BoM ocean models
- In collaboration with Jon Mittaz (Uni Reading), improve cloud-clearing and SSES of BoM Himawari-8 SST prior to ingesting into IMOS Multi-sensor L3S

5. REFERENCES

AODN (2019). Australian Ocean Data Network Satellite SST Products Help Page: https://help.aodn.org.au/satellite-sst-data/

Beggs, H. and Pugh T. (2009) Format Specification for the Australian Bureau of Meteorology's SST Analysis L4 files. *Bureau of Meteorology Technical Document*, 12 March 2009, Version 7, 12 pp.

Beggs H., A. Zhong, G. Warren, O. Alves, G. Brassington and T. Pugh (2011). RAMSSA – An Operational, High-Resolution, Multi-Sensor Sea Surface Temperature Analysis over the Australian Region, *Australian Meteorological and Oceanographic Journal*, **61**, 1-22, 2011 http://www.bom.gov.au/jshess/papers.php?year=2011

Beggs, H., Griffin, C. and Govekar, P. (2019a). New IMOS multi-sensor sea surface temperature composites provide better coverage and accuracy, *IMOS web article, 21 February 2019,* http://imos.org.au/fileadmin/user_upload/shared/SRS/SST/Beggs_2019_IMOS_Multi-sensor_L3S_article_21Feb2018.pdf

Beggs, Helen, Christopher Griffin, Gary Brassington and Pallavi Govekar (2019b) Measuring coastal upwelling using IMOS Himawari-8 and Multi-Sensor SST. *Presented as a poster presentation at the 20th GHRSST Science Team Meeting, Frascati, Italy, 3rd – 7th June, 2019.* DOI: 10.13140/RG.2.2.22966.45129

Beggs, Helen (2019). Temperature. Ch 12 in Earth Observation: Data, Processing and Applications. Volume 3B: Applications – Surface Waters (Eds. Harrison, B.A., Anstee, J.A., Dekker, A., Phinn, S., Mueller, N., and Byrne, G.) CRCSI, Melbourne. (in press)

BoM (2017) Bluelink> Ocean Model, Analysis and Prediction System version 3 (OceanMAPSv3) Technical Specification. http://www.bom.gov.au/oceanography/forecasts/technical_specification.v2.pdf.

BoM (2019). BoM IMOS near real-time fv01 SST Validation Web Page: http://opendap.bom.gov.au:8080/thredds/fileServer/abom_imos_ghrsst_archive-1/staticweb/sst-nrt-batch/index01.html

Brasnett, B. and Surcel Colan, D. (2016). Assimilating Retrievals of Sea Surface Temperature from VIIRS and AMSR2, *J. Atmospheric and Oceanic Tech*., https://doi.org/10.1175/JTECH-D-15-0093.1

GHRSST Science Team (2012). The Recommended GHRSST Data Specification (GDS) 2.0, document revision 5, available from the GHRSST International Project Office, 2012, pp 123. https://www.ghrsst.org/wp-content/uploads/2016/10/GDS20r5.pdf

Griffin, C., H. Beggs and L. Majewski (2017). GHRSST compliant AVHRR SST products over the Australian region – Version 1, *Technical Report, Bureau of Meteorology, Melbourne, Australia, 151 pp.* http://imos.org.au/fileadmin/user_upload/shared/SRS/SST/GHRSST-DOC-basic-v1.0r1.pdf

Grumbine, R.W. 1996. Automated Passive Microwave Sea Ice Concentration Analysis at NCEP. *Tech. Note,* NOAA/NCEP, 13 pp.

IMOS (2018). IMOS Satellite Remote Sensing SST Data Web Page: http://imos.org.au/facilities/srs/sstproducts/sstdata0/

NOAA CoastWatch (2018). ACSPO Global SST from VIIRS Web Page: https://coastwatch.noaa.gov/cw/satellite-data-products/sea-surface-temperature/acspo-viirs.html

NOAA NESDIS (2019). National Oceanographic and Atmospheric Administration NESDIS 3S Sensor Stability for SST web site, showing night duration plots for NPOES and METOP satellites, see "N Dur" tab at https://www.star.nesdis.noaa.gov/sod/sst/3s/

Paltoglou, G, H. Beggs and L. Majewski (2010) New Australian High Resolution AVHRR SST Products from the Integrated Marine Observing System, *In: Extended Abstracts of the 15th Australian Remote Sensing and Photogrammetry Conference, Alice Springs, 13-17 September, 2010.* http://imos.org.au/sstdata_references.html

Reynolds, R. W. and T. H. Smith, 1994: Improved global sea surface temperature analyses using optimum interpolation, *j. Climate*, **7**, 929-948.

Sakov, P. (2014) EnKF-C user guide. arXiv:1410.1233 http://github.com/sakov/enkf-c

Smith, N.S., Ebert, B. and Warren, G. 1999. The Bureau of Meteorology SST Analysis System. An informal paper produced as background for the OOPC/AOPC Workshop on SST Analyses for Climate, International Research Institute, LDEO, Palisades NY USA, Nov 10–12, 1998.

Wijffels, Susan E., Helen Beggs, Christopher Griffin, John F. Middleton, Madeleine Cahill, Edward King, Emlyn Jones, Ming Feng, Jessica A. Benthuysen, Craig R. Steinberg and Phil Sutton (2018). A fine spatial scale sea surface temperature atlas of the Australian regional seas (SSTAARS): seasonal variability and trends around Australasia and New Zealand revisited, *J. Marine Systems*, **187**, 156-196. https://doi.org/10.1016/j.jmarsys.2018.07.005

Zhong, Aihong and Helen Beggs (2008). Analysis and Prediction Operations Bulletin No. 77 - Operational Implementation of Global Australian Multi-Sensor Sea Surface Temperature Analysis, *Bureau of Meteorology Web Document*. http://www.bom.gov.au/australia/charts/bulletins/apob77.pdf

RDAC UPDATE: CMC

Dorina Surcel Colan

UPDATE ON THE COPERNICUS MARINE ENVIRONMENT MONITORING SERVICE (CMEMS) SEA SURFACE TEMPERATURE THEMATIC ASSEMBLY CENTRE (SST-TAC)

Bruno Buongiorno Nardelli[(1)], Andrea Pisano[(2)], Rosalia Santoleri[(3)], Jacob Hoyer[(4)], Jean-François Piollé[(5)], Emmanuelle Autret[(6)], Emma Saux-Picard[(7)], Simon Good[(8)]

(1) Consiglio Nazionale delle Ricerche, Napoli, Italy, Email: bruno.buongiornonardelli@cnr.it
(2) Consiglio Nazionale delle Ricerche, Roma, Italy, Email: andrea.pisano@cnr.it
(3) Consiglio Nazionale delle Ricerche, Roma, Italy, Email: rosalia.santoleri@cnr.it
(4) Danish Meteorological Institute, Copenhagen, Denmark, Email: jlh@dmi.dk
(5) French Research Institute for Exploitation of the Sea, Brest, France, Email: jfpiolle@ifremer.fr
(6) French Research Institute for Exploitation of the Sea, Brest, France, Email: emmanuelle.autret@ifremer.fr
(4) Met Office, Exeter, United Kingdom, Email: Simon.Good@metoffice.gov.uk
(5) Météo-France, Lannion, France, Email: emma.sauxpicart@meteo.fr

1. INTRODUCTION

The European Copernicus Marine Environment Monitoring Service (CMEMS) Sea Surface Temperature Thematic Assembly Centre (SST-TAC) provides state of the art level 3 (L3) and 4 (L4) products based primarily on satellite observational data, both for dissemination to external users and for use internally within CMEMS. CMEMS users require both global products and products designed for specific European regions (Le Traon et al., 2019). Both are provided operationally as near real time products (NRT) and multi-year reprocessed products (MYP/REP). The SST-TAC is responsible for ensuring the quality of CMEMS products by planning and carrying out preliminary validation activities, quality control of incoming data streams and then monitoring the quality of the data produced in near real time.

Ocean Monitoring Indicators (OMI) derived from the MYPs are also produced, providing consistent descriptions of the ocean state over the past decades. OMIs were produced from MYP SST products following a common strategy among the different CMEMS elements. The first SST-TAC OMIs are the monthly SST spatially averaged anomalies with respect to the reference 1993 - 2014 climatologies and the related map of trends, plus supplementary yearly mean anomaly maps, which were used also for the preparation of the Copernicus Ocean State Reports (von Schuckmann et al., 2016; 2018).

The SST-TAC was set up in the second phase of CMEMS (2018 - 2021) by the European team which delivered the operational service for the SST products in the framework of the “Wind, Ice and Temperature at the Sea Surface (WITS)” service (see Table 1), operating as the Ocean and Sea Ice Thematic Assembly Centre (OSI TAC) during the first phase of CMEMS (2015 - 2018).

No.	Acronym	Name	Country	Resp.
1	CNR	National Research Council	Italy	Overall Coord. PU
2	DMI	Danish Meteorological Institute	Denmark	PU
3	IFREMER	French Research Institute for Exploitation of the Sea	France	PU
4	MET (subcontractor)	Norway Norwegian Meteorological Institute	Norway	Service Desk
5	METO	Met Office	UK	PU
6	MF	Météo-France	France	PU

Table 1. SST-TAC Consortium and main roles/responsibilities

The SST-TAC is led by CNR, which manages and coordinates all activities, and includes CNR, DMI, IFREMER, METO and MF as Production Units (PUs) for the regional and global SST products, and MET as a subcontractor responsible for the SST-TAC service desk.

2. A CONTINUOUSLY EVOLVING SYSTEM

The CMEMS SST-TAC products released at the Phase 2 entry into service were initially those produced and distributed in the framework of the OSI TAC, which covered the operational production until April 2018. Since then, the product portfolio has been continuously evolving (with new releases occurring up to three times per year) thanks to the update of existing products, the development of new products and datasets, and the removal of products which displayed degraded performances and/or were superseded by new products.

The SST-TAC products are listed in Table 2 and Table 3 and fully documented in the CMEMS online catalogue (http://marine.copernicus.eu/services-portfolio/access-to-products/). Main product evolutions are briefly described in the following subsections.

Product reference	Description	PU
SST_BS_SST_L3S_NRT_OBSERVATIONS_010_013	Black Sea - High Resolution and Ultra High Resolution L3S Sea Surface Temperature	CNR
SST_BS_SST_L4_NRT_OBSERVATIONS_010_006	Black Sea High Resolution and Ultra High Resolution Sea Surface Temperature Analysis	CNR
SST_BS_SST_L4_REP_OBSERVATIONS_010_022	Black Sea - High Resolution L4 Sea Surface Temperature Reprocessed	CNR
SST_MED_SST_L3S_NRT_OBSERVATIONS_010_012	Mediterranean Sea - High Resolution and Ultra High Resolution L3S Sea Surface Temperature	CNR
SST_MED_SST_L4_NRT_OBSERVATIONS_010_004	Mediterranean Sea High Resolution and Ultra High Resolution Sea Surface Temperature Analysis	CNR
SST_MED_SST_L4_REP_OBSERVATIONS_010_021	Mediterranean Sea - High Resolution L4 Sea Surface Temperature Reprocessed	CNR
SST_BAL_SST_L4_NRT_OBSERVATIONS_010_007_b	Baltic Sea- Sea Surface Temperature Analysis	DMI
SST_BAL_SST_L4_REP_OBSERVATIONS_010_016	Baltic Sea- Sea Surface Temperature Reprocessed	DMI
SST_GLO_SST_L3S_NRT_OBSERVATIONS_010_010	Global Ocean Sea Surface Temperature L3 Observations	IFREMER
SST_NWS_SST_L4_NRT_OBSERVATIONS_010_003	Atlantic European North West Shelf Ocean - ODYSSEA Sea Surface Temperature Analysis	IFREMER
SST_NWS_SST_L4_REP_OBSERVATIONS_010_023	Atlantic European North West Shelf Seas - High Resolution L4 Sea Surface Temperature Reprocessed (1982-2012)	IFREMER
SST_GLO_SST_L4_NRT_OBSERVATIONS_010_001	Global Ocean OSTIA Sea Surface Temperature and Sea Ice Analysis	METO
SST_GLO_SST_L4_NRT_OBSERVATIONS_010_005	Global Ocean Sea Surface Temperature Multi Product Ensemble (GMPE)	METO
SST_GLO_SST_L4_NRT_OBSERVATIONS_010_014	Global Ocean OSTIA Diurnal Skin Sea Surface Temperature	METO
SST_GLO_SST_L4_REP_OBSERVATIONS_010_011	Global Ocean OSTIA Sea Surface Temperature and Sea Ice Reprocessed	METO

SST_GLO_SST_L4_REP_OBSERVATIONS_010_024	ESA SST CCI reprocessed sea surface temperature analyses	METO
SST_EUR_SST_L3C_NRT_OBSERVATIONS_010_009_b	European Ocean- Sea Surface Temperature Mono-Sensor L3 Observations	MF
SST_EUR_SST_L3S_NRT_OBSERVATIONS_010_009_a	European Ocean- Sea Surface Temperature Multi-Sensor L3 Observations	MF

Table 2. SST-TAC Product summary and associated PU at the start of phase-2 service

Product reference	Description	PU
SST_ATL_SST_L4_NRT_OBSERVATIONS_010_025	New daily L4 NRT over the NWS+IBI area (substitutes NWS-NRT-L4)	IFREMER
SST_ATL_SST_L4_NRT_OBSERVATIONS_010_026	New daily L4 REP over the NWS+IBI area (substitutes NWS-REP-L4)	IFREMER
SST_EUR_SST_L4_NRT_OBSERVATIONS_010_031	New daily L4 NRT EUR product	MF
SST_MED_SST_L4_NRT_OBSERVATIONS_010_033	New diurnal NRT L4 over the MED	CNR
SST_BS_SST_L4_NRT_OBSERVATIONS_010_034	New diurnal NRT L4 over the BS	CNR
SST_BAL_SST_L4_NRT_OBSERVATIONS_010_035	New diurnal NRT L4 over the Baltic Sea	DMI
SST_EUR_SST_L4_REP_OBSERVATIONS_010_036	New daily L4 EUR REP product	MF
SST_BAL_SST_L3S_NRT_OBSERVATIONS_010_032	New daily L3S BAL NRT product	DMI

Table 3. List of new/future SST-TAC products.

2.1. EVOLUTION OF REAL TIME PRODUCTS

One of the most important objectives of the SST-TAC covers the evolution of global and regional algorithms to guarantee that CMEMS will provide state-of-the-art products in terms of scientific quality and to provide consistent L3/L4 products for each target area and consolidated set of users. Different priorities have been identified within each PU concerning the type of evolution to be carried out during CMEMS phase 2. This is related to the different status of each production line, as regional and global products have been developed following different approaches and configurations, in order to account for each region specifically. As a general rule, the improvements lead to product evolutions in terms of timeliness, effective spatial resolution, output frequency, update cycle and accuracy. Three main lines can however be identified: the modification and tuning of the interpolation algorithms to better resolve the small scales (leading to the improvement of existing products), the implementation of new processing chains to resolve the diurnal cycle, and the development of L4 products consistent with existing L3 products for regional areas where they are presently not available. Moreover, a new L4 product has been introduced covering the North-Western Shelf and Iberia Biscay Irish (ATL) area, with specific regional tuning of the interpolation algorithms. The proposed changes thus aim at providing a consistent portfolio, responding to the specific requirements of the vast range of existing users of present global, European and regional products, but also attracting new users.

2.2. EVOLUTION OF MULTI YEAR PRODUCTS

During CMEMS-phase 2, a strong effort is dedicated to provide more homogeneous and accurate regional and global MYP products and information on the ocean state with respect to CMEMS-phase 1, taking advantage of the planned regular release schedule of upstream high quality climatic records by ESA CCI/C3S initiatives. Indeed, CNR, DMI and IFREMER MYP products have been based until now on the U.S. NASA Pathfinder programme, which will not guarantee the necessary level of commitment in terms of update of the input data time series, and will consequently need to be superseded by upcoming ESA CCI data, which covers the entire period back to 1982. The close interactions between the SST-TAC partners and the ESA CCI data producers ensures prompt access to the data to allow consistent reprocessing among all PU. Upgraded MYP products will then be used to provide both updated and new CMEMS Ocean Monitoring Indicators (OMIs). The next OMIs will be global time series, anomaly maps and trend maps based on ESA SST CCI and C3S data.

The original schedule for SST TAC multi-year product development anticipated the release of ESA CCI/C3S data much earlier than occurred in reality. The new climate data record from the ESA SST CCI project covering late 1981 to 2016 became available in the first half of 2019. However, the interim climate data record from C3S, which is intended to extend the ESA CCI dataset and will eventually cover 2017 to approx. 10 days delay to real time, is not yet publicly available. The expectation is that the public release of C3S data will happen during this year, and that it will reach its target of 10 day delay to real time by early next year.

2.3. EVOLUTIONS LINKED TO THE SPACE COMPONENT

During the entire CMEMS-phase 2, the SST-TAC PUs put in a continuous effort to include relevant new sources of data in the processing systems. This required the processing chains to be adapted for the ingestion and specific tests to ensure that the new sources do not degrade the quality of CMEMS output products. The main novelties concerned specifically the transition from MSG-10 to MSG-11 platform for SEVIRI data and, more noticeably, the ingestion of SLSTR data acquired by ESA Sentinel 3A mission, which have been included in the majority of regional and global products, and Sentinel 3B mission (ongoing development), carried out at different system update releases (Figure 1). The preliminary qualification of SLSTR data took advantage of the participation of CMEMS-SST-TAC partners to the Sentinel-3 Scientific Validation Team, providing fundamental feedback on the improvements that had to be implemented by the data producers to make L2 products usable for operational L3/L4 data upgrades. Demonstration and quantification of the added value on the resulting SST-TAC products has been part of the work done within CMEMS before product upgrades, and publications describing related results are in preparation.

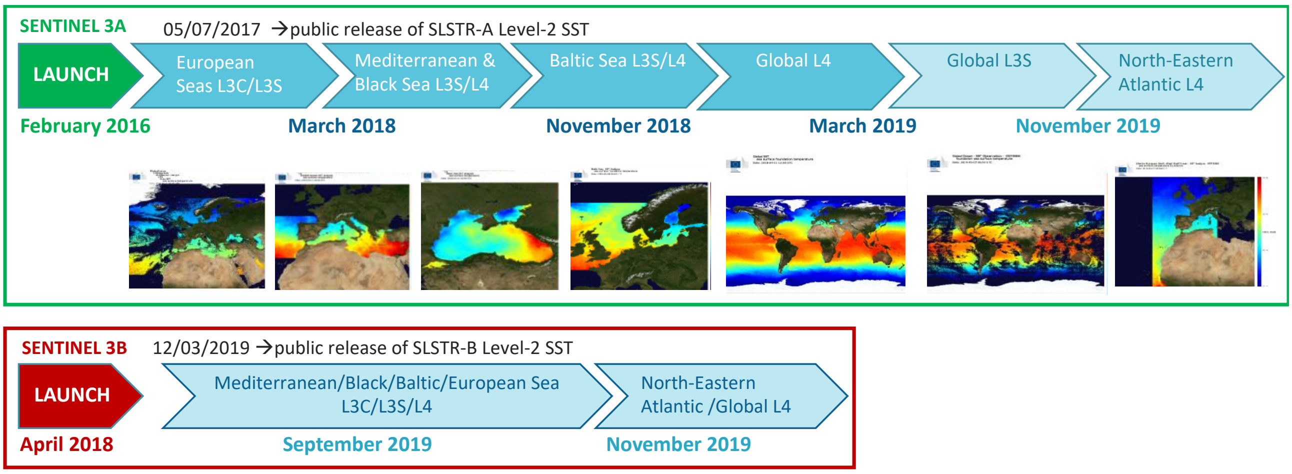

Figure 1. Scheduling of the SLSTR data ingestion in the SST-TAC production chains

3. CONCLUSION

During the first one year and a half of CMEMS phase 2, the SST-TAC activities progressed smoothly, with only minor deviations to what had been initially planned. Several further evolutions will enter into service before the end of the contract and will be reported in future communications.

4. REFERENCES

Le Traon, P. Y., and Coauthors, 2019: From Observation to Information and Users: The Copernicus Marine Service Perspective. *Front. Mar. Sci*., **6**, https://doi.org/10.3389/fmars.2019.00234.

von Schuckmann, K., and Coauthors, 2016: The Copernicus Marine Environment Monitoring Service Ocean State Report. *J. Oper. Oceanogr*., **9**, s235–s320, https://doi.org/10.1080/1755876X.2016.1273446.

von Schuckmann, K., and Coauthors, 2018: Copernicus Marine Service Ocean State Report. *J. Oper. Oceanogr.,* **11**, S1–S142, https://doi.org/10.1080/1755876X.2018.1489208.

EUMETSAT SUPPORT TO GHRSST

Anne O'Carroll, G. Corlett, I. Tomazic

EUMETSAT, Eumetsat-allee 1, 64295 Darmstadt (Germany), Email: Anne.Ocarroll@eumetsat.int

ABSTRACT

The European Organisation for the Exploitation of Meteorological Satellites (EUMETSAT) delivers operational weather and climate-related satellite data, images and products throughout all day and year. EUMETSAT also has commitments to operational oceanography and atmospheric composition monitoring. Activities over the next twenty years include the continuation of the Mandatory Programmes (MSG, EPS) and future programmes (MTG, EPS-SG), which all include ocean observations of SST and sea surface winds.

EUMETSAT supervises and coordinates its Satellite Application Facility (SAF) network. The EUMETSAT Ocean and Sea-ice SAF (OSI SAF) is led by Meteo-France with a consortium of institutes from EUMETSAT member states, and provides reliable and timely operational services related to meteorology, oceanography and the marine environment.

EUMETSAT operational services from Metop-B (AVHRR, IASI) and Meteosat (SEVIRI) continue, with Metop-C launched on 7th November 2018 and Meteosat-11 launched on 15th July 2015. The OSI-SAF produces IASI L2P in full GDS2 format (including auxiliary data). IASI SST in L2Pcore format continues to be available from the EUMETSAT data centre via ftp. Meteosat-8 Indian Ocean Data Coverage (IODC) services are available from January 2017 onwards.

EUMETSAT continues to participate in the European Commission's Copernicus Sentinel-3 programme in partnership with ESA, where EUMETSAT operates the satellite and serves the marine user community. Sentinel-3A was launched on 16th February 2016 and Sentinel-3B was launched on 25th April 2018. ESA is responsible for the development of the Sentinel-3 space and ground components and serves the land user community. The fifth meeting of the ESA-EUMETSAT Sentinel-3 Validation team (S3VT) meeting took place in May 2019.

Sentinel-3A SLSTR Sea Surface Temperature

The operational release of SST products from SLSTR-A took place on 5th July 2017. A major version update was released on 4th April 2018 to include Bayesian cloud implementation and revised Quality Levels. SLSTR-A SST has been fully reprocessed from April 2016 to April 2018. More information can be found from: *https://www.eumetsat.int/website/home/Data/CopernicusServices/Sentinel3Services/SeaSurfaceTemperature/index.html*.

Sentinel-3B SLSTR Sea Surface Temperature

SST products from SLSTR-B have been available operationally since 12th March 2019, with preliminary products provided to the S3VT from 8th November 2018. Participation to the S3VT is still possible with application via (https://earth.esa.int/aos/S3VT). Figure 1 shows the combined SST coverage for two days from both Sentinel-3A and Sentinel-3B SST.

Compilation of a satellite in situ matchup dataset (MDB) is a core part of Sentinel-3 validation activities at EUMETSAT. Currently five MDB's are compiled using the Felyx system: Sentinel-3A SLSTR, Sentinel-3B SLSTR, IASI-B, AVHRR-B and VIIRS experimental. A reprocessed SLSTR-A MDB is now available. Both for Sentinel-3 MDB's are available to the S3VT. Current improvements include adding additional in situ data including from radiometer experiments and new drifter SST.

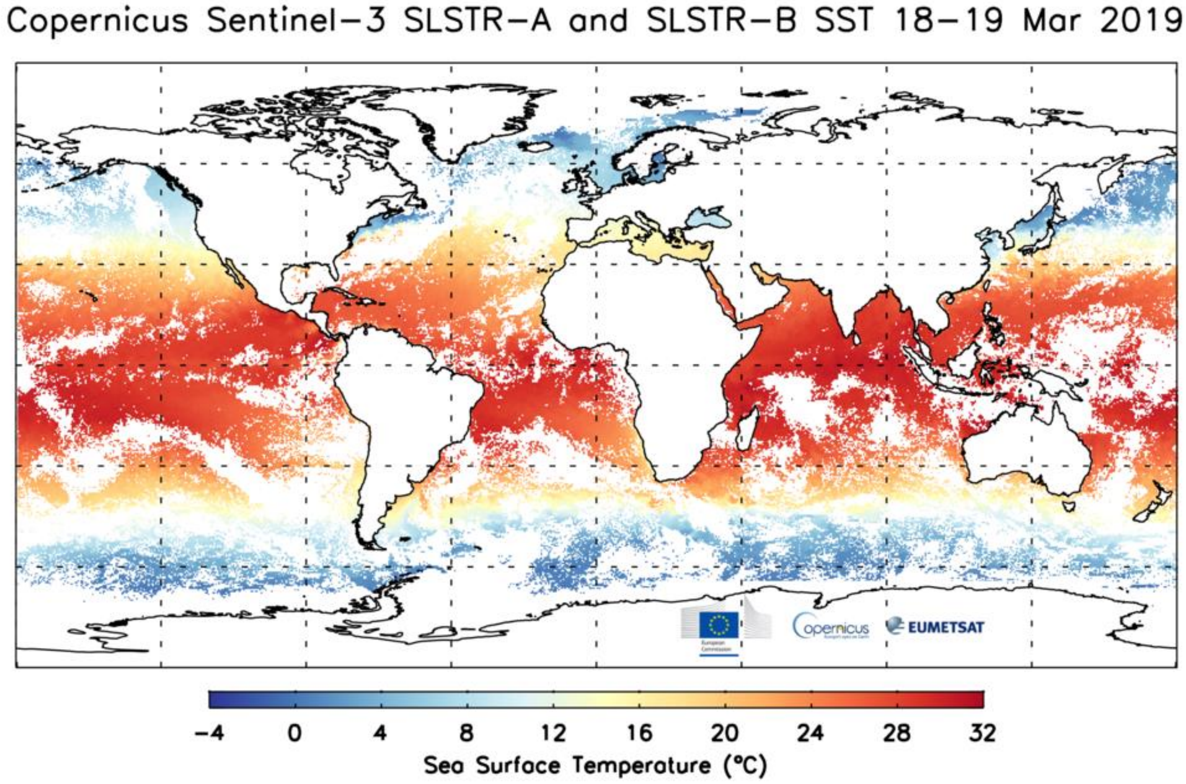

Figure 1: Combined coverage of Sentinel-3A and Sentinel-3B Sea Surface Temperature for 18 - 19 March 2019.

Metop IASI Sea Surface Temperature

Sea Surface Temperature from Metop IASI continues to be operational, with L2Pcore available from EUMETSAT and the full L2P from the EUMETSAT OSI SAF. Recent updates to the processor include: v6.2 in June 2016 (no SST impact); v6.3 20th June 2017 to include an SST retrieval update (greater number of clear obs; aerosol flagging / correction; uncertainties); and v6.4 on 7th March 2018. The next version v6.5 is under preparation. Metop-C was launched on 7th November 2018 and SST products are under preparation. The reprocessing of Metop-A/B IASI is underway with a target for preliminary products for evaluation at the end of 2018.

Current and upcoming projects

Recent projects (now completed) include: SLSTR sea-ice cloud-screening (completed in 2017 with CNR); IASI ice surface temperature validation (completed in 2017 with DMI); and SLSTR cloud validation processor (completed in 2018 with Deimos).

Ongoing projects include: GHRSST project office (now extended till 2021); TRUSTED drifting buoys (2018 - 2022 with CLS); SLSTR sea-ice surface temperature (2018 - 2020 with DMI); and SLSTR level-1 uncertainties and monitoring (2018/2019 with RAL).

Further and upcoming projects include: thermal infrared product inter-comparison and validation with FRM radiometers; further SST studies; and further Fiducial Reference Measurement studies.

More information is available from:
https://www.eumetsat.int/website/home/Data/ScienceActivities/ScienceStudies/index.html.

TRUSTED drifting buoys

The Copernicus project "Towards fiducial Reference measUrements of SST from European drifters" aims to deliver improved high resolution SST drifter measurements with additional fields (near surface water pressure), both analogue and high resolution digital SST sensors, plus high-frequency data on some drifters for 100 - 150 drifters, for Sentinel-3 SST validation. Nearly 50 have already been deployed worldwide and are providing data to the GTS. Access to the high frequency data is possible to interested users.

More information can be found from: https://www.eumetsat.int/website/home/Data/ScienceActivities/ScienceStudies/TowardsfiducialReferencemeasUrementsofSeaSurfaceTemperaturebyEuropeanDriftersTRUSTED/index.html and www.jcommops.org.

REPORT TO GHRSST XX FROM JAXA

Misako Kachi [(1)]

(1) Japan Aerospace Exploration Agency (JAXA), Tsukuba (Japan), Email: kachi.misako@jaxa.jp

1. INTRODUCTION

JAXA has operated the GHRSST server (Japanese RDAC) to distribute JAXA-produced Sea Surface Temperature (SST) products in GDS 2.0 format (https://www.eorc.jaxa.jp/ptree/ for Himawari-related products and https://suzaku.eorc.jaxa.jp/GHRSST/ for others). Those products include SST from non-JAXA satellites as well as JAXA satellites.

JAXA has developed several instruments that measure SST. Especially, a series of conical scanning passive microwave imagers that have C-band channels and provide invaluable information of SST under clouds, which cannot be obtained by infrared (IR) imagers.

The latest and currently operational passive microwave imager is the Advanced Microwave Scanning Radiometer 2 (AMSR2) on board the Global Change Observation Mission (GCOM) – Water (GCOM-W, also known as "SHIZUKU"), which was launched in May 2012 and has been in post-mission phase since 2017. AMSR2 has succeeded the observation by AMSR for EOS (AMSR-E) on board the NASA's EOS Aqua satellite in the A-train orbit. Its big antenna size of 2-m diameter and C-band (6.9-/7.3 GHz) channels with all-weather capability enable frequent measurements of SST and other water-related parameters for various applications.

JAXA also developed the optical and infrared radiometer, the Second-generation Global Imager (SGLI), which is carried by the GCOM - Climate (GCOM-C) launched in December 2017. SGLI data is already open to the public since December 2018.

The Global Precipitation Measurement (GPM) Core Observatory, which is a JAXA-NASA joint mission launched in February 2014 and has been in post-mission phase since 2017, also carries a conical scanning passive microwave imager provided by NASA. The GPM Microwave Imager (GMI) has 10 GHz channels that can measure SST higher than around 10 °C.

JAXA has collaborated with the Japan Meteorological Agency (JMA) to distribute Level 1 data of the geostationary satellites Himawari-8 and -9 (backup), which were launched in October 2014 and November 2016 respectively, from the JAXA server to non-profit purposes in near-real-time basis. JAXA Himawari Monitor web site has been operated since August 2015 (https://www.eorc.jaxa.jp/ptree/), and JAXA-produced Level 2, 3 and 4 products, including SST are also available from the server.

2. CURRENT STATUS OF JAXA MISSIONS

2.1. AMSR-E

AMSR-E on board the Aqua satellite was launched on 4th May 2002 and halted its observation on 4th October 2011. AMSR-E has restarted observations in slow rotation mode at 2 rpm (2 rotations per minute) since 4th December 2012 to implement cross-calibration with AMSR2. It completed its operation on 4th December 2015, archiving 3 year overlapping observation data with AMSR2. AMSR-E L1B data in 2 rpm mode is distributed to public through the GCOM-W Research Product Distribution Service (https://suzaku.eorc.jaxa.jp/GCOM_W/research/resdist.html).

One of GCOM-W mission targets is to implement long-term and continuous global observation of Essential Climate Variables that are important to understand global change and water cycle mechanisms. Although there is 9 month gap between AMSR-E & AMSR2 (October 2011 – June 2012), almost 17 years of data has been archived since June 2002.

Since the AMSR-E L2 V7 products used a different retrieval algorithm or an older version, they are not consist with the current AMSR2 L2 products. To develop a continuous dataset between AMSR-E and AMSR2, we applied the latest AMSR2 L1/L2 algorithms to AMSR-E data. New AMSR-E L1 V4 and L2 V8 products are available via the JAXA G-Portal (https://www.gportal.jaxa.jp/gp/). New AMSR-E V8 SST in GDS 2.0 is in preparation. In new AMSR-E L1 V4 products, brightness temperatures (TB) are not adjusted between AMSR-E and AMSR2. The swath width of AMSR-E (1450km, 196 pixels for low-freq. Ch. / 392 for high-freq. Ch.) is extended to be equivalent to that of AMSR2 (1620km, 243 pixels for low-freq. Ch. / 486 for high-freq. Ch.), applying scan bias correction at the scan edges. Also, an improved method to calculate a hot load temperature correction is applied by using two orbit paths to resolve gaps between Ascending and Descending orbit products.

2.2. AMSR2 ON GCOM-W

AMSR2 is a multi-frequency, total-power microwave radiometer system with dual polarization channels for all frequency bands. The instrument is a successor of AMSR and AMSR-E. The frequency bands include 6.925, 7.3, 10.65, 18.7, 23.8, 36.5, and 89.0 GHz.

AMSR2 on board the GCOM-W satellite was launched on 18th May 2012 (JST) and started observation on 3rd July 2012. The GCOM-W satellite was installed in front of the Aqua satellite to keep continuity of AMSR-E observations and provide synergy with the other A-Train instruments for new Earth science researches. Currently, both satellite and instrument are working well. AMSR2 achieved designed mission life of 5 years in May 2017 and continues observation in post-mission phase.

AMSR2 standard products are distributed through the JAXA G-Portal (https://www.gportal.jaxa.jp/gp/) as well as AMSR-E and AMSR standard products. The latest version is version 3 for SST, Sea Surface Wind Speed, Sea Ice Concentration, and Soil Moisture Content, updated on 1st March 2017.

AMSR2 SST Version 3 was validated by comparing with the quality-controlled buoy SST observations of the iQuam V2.1 provided by NOAA/NESDIS; and the root mean square error (RMSE) between AMSR2 and buoy SSTs from 2nd July 2012 to 31st December 2018 is 0.47 °C, which includes both ascending (day) and descending (night).

In addition to eight standard products, currently nine research products were defined, including 10 GHz SST and all-weather sea surface wind speed (ASW). 10 GHz SST (research product) has been included in standard SST product since Version 2 and its accuracy compared with iQuam V2.1 is 0.51 °C for SST higher than 9 °C. ASW product has been released in October 2015 and updated to Version 3 on 11th January 2018. Its accuracy compared with GPS-dropsonde data, which is provided by courtesy of the NOAA/AOML/Hurricane Research Division in Miami, FL (USA), is 4.07 m/s. ASW products are distributed via the GCOM-W Research Product Distribution Service (https://suzaku.eorc.jaxa.jp/GCOM_W/research/resdist.html).

Currently, preparation for AMSR2 follow-on instrument (AMSR3) is underway. AMSR3 will share satellite bus with the GOSAT-2 follow-on mission (greenhouse-gas observation mission), led by the Japanese Ministry of Environment. The Mission Definition Review and project readiness reviews were completed in June 2018, and project preparation phase (Phase-A) activities has been started since September 2018. We expect to complete System Definition Review in autumn 2019 and start Phase-B in winter 2019.

2.3. GMI ON GPM CORE OBSERVATORY

The GPM Core Observatory, a joint mission between JAXA and NASA, was launched on 28th February 2014 (JST). GMI was developed by NASA as a successor of the Tropical Rainfall Measurement Mission (TRMM) Microwave Imager (GMI) on board the TRMM satellite. The GPM Core Observatory achieved designed mission life in 2017 and continues observation in post-mission phase.

The latest product version (V06A) was released in October 2018. Standard products are available from JAXA G-Portal (https://www.gportal.jaxa.jp/gp/) and also from NASA PPS.

JAXA has developed the GMI 10GHz SST, GMI sea ice concentration (SIC), and DPR SIC products as JAXA's GPM research products. The latest GMI 10GHz SST version is Version 3 and data in GDS 2.0 format is available at the JAXA GHRSST server (https://suzaku.eorc.jaxa.jp/GHRSST/).

2.4. SGLI ON GCOM-C

SGLI is a versatile, general purpose optical and infrared radiometer system covering the wavelength region from near ultraviolet to infrared. The SGLI system consists of two components; SGLI-VNR (Visible & Near infrared push-broom Radiometer); and SGLI-IRS (shortwave & thermal InfraRed Scanner) to optimize optics for each wavelength range. Two major new features are added to SGLI, they are 250 m spatial resolution for 11 channels and polarization/multidirectional observation capabilities. The GCOM-C satellite was launched in December 2017. Also, SGLI standard products have been released to the public since December 2018 via the JAXA G-Portal (https://www.gportal.jaxa.jp/gp/).

The 250m resolution data of SGLI-VNR will enable detection of more fine structure in the coastal area such as river outflows, regional blooms, and small currents. SST and ocean colour products derived from SGLI will provide additional information to AMSR2 SST. We are currently preparing SGLI SST in GDS 2.0 format to be distributed via the GHRSST server.

2.5. AHI ON HIMAWARI-8 AND -9

JMA's geostationary satellite Himawari-8 (means sunflower) was launched in October 2014 and has replaced observation by MTSAT-2 since 7th July 2015. The Himawari-9 satellite was also launched in November 2016 and is in stand-by mode at present. Both the Himawari-8 and -9 satellites carry the Advanced Himawari Imager (AHI). The functions and specifications are notably improved from those of the imagers on board MTSATs (see more details at JMA's web site: http://www.jma-net.go.jp/msc/en/support/index.html).

JAXA exchanged agreement with JMA to receive the AHI Level 1 products in near-real-time basis in order to distribute them to user communities for non-profit purposes. In addition, JAXA produces AHI geophysical parameters seeking synergy with JAXA's future Earth Observation missions.

JAXA has started operation of the web site "JAXA Himawari Monitor" (https://www.eorc.jaxa.jp/ptree) since 31st August 2015. The web site provides browse images of Himawari-8 RGB and geophysical parameters in 10-minutes intervals and/or 1-hour composites. Users can download both the Level 1 and JAXA-produced geophysical parameter products, including SST in GDS 2.0 format, via FTP after simple registration.

The latest version of AHI SST is Version 1.2, and we are planning to update the algorithm in 2019, reflecting results from SGLI.

2.6. MODEL ASSIMILATED SST

JAXA has been collaborating with the Japan Agency for Marine-Earth Science and Technology (JAMSTEC) and Nagoya University to assimilate satellite-based SST data into a high-resolution regional ocean model to produce satellite-assimilated model gap-free products (Level 4) in high-spatial and temporal resolution. SSTs from AMSR2, AHI, GMI, and WindSat are assimilated into the 3 km spatial resolution tide-resolving ocean general circulation model (JCOPE-T) around Japan toward the Ocean Weather Forecast (Varlamov *et al.*, 2015; Miyazawa *et al.*, 2017).

Figure 1 is a comparison of the Himawari SST and model SST at 07:00 UTC on 2nd September 2018. SST decrease due to the Super Typhoon "JEBI" (No.21), whose centre was located south-east of Okinawa, was clearly seen in model SST while Himawari SST were widely missing because of typhoon clouds. SST decrease during the typhoon passing was previously observed only by passive microwave imagers that can penetrate clouds, but this information may contribute to studies to simulate development/decay of typhoons.

Hourly model output of SST products with two-week forecasts have been distributed through the JAXA Himawari Monitor (https://www.eorc.jaxa.jp/ptree) since October 2018. Data is in netCDF format but not in GDS 2.0. We plan to improve spatial resolution of the ocean model to 1 km and to introduce SGLI SST to the data assimilation in 2019.

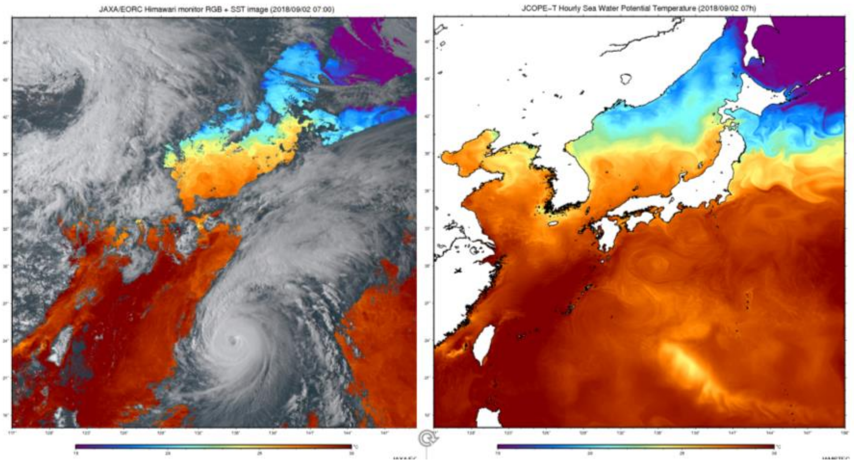

Figure 1: Himawari-8/AHI SST with RGB composite (left) and model SST (right) at 07:00 UTC on 2nd September 2018. Images are also available at "JAXA Himawari Monitor: Ocean Weather Forecast" web site (https://www.eorc.jaxa.jp/ptree/ocean_model/)

3. CURRENT STATUS OF JAXA GHRSST SERVER

The JAXA has two servers to distribute SSTs in GDS 2.0 format. One is the JAXA GHRSST server (https://suzaku.eorc.jaxa.jp/GHRSST/) used to distribute all JAXA-produced SSTs except Himawari-8/AHI. This web site shows information on available SST products produced by JAXA, the registration form for data download, and a near-real-time monitor of products. Simple registration is needed for access to the password protected ftp site in order to download data. Several passive microwave imagers, such as AMSR2, AMSR-E, GMI, NOAA's WindSat onboard the Coriolis, and the Visible Infrared Scanner (VIRS) on board the Tropical Rainfall Measuring Mission (TRMM) satellite are available. L2P and L3C SST products from those instruments will be available in GDS 2.0 format. AMSR2, GMI and WindSat SSTs are provided in near-real-time basis.

The other server is the JAXA Himawari Monitor/P-Tree system, which distributes Himawari-8 SSTs (https://www.eorc.jaxa.jp/ptree/) along with the other Himawari-8 products, mainly due to file size. However, the Himawari-8 SST products are in GDS2.0 format and in 2km resolution for the Full Disk area. Day/night SST has both L2P (10 minute intervals) and L3C (1 hour average, daily minimum, and monthly average) products. Nighttime SST has only a L3C (1 hour average) product. Utilization of Himawari-8 products including SSTs are limited to non-profit purposes only due to the JMA's data policy.

4. CONCLUSION

The current status and future plan of JAXA SST missions and GHRSST server are described. The JAXA GHRSST server currently distributes SST data from AMSR2, WindSat, VIRS and GMI in GDS 2.0 format.

AMSR-E reprocessing with the latest AMSR2 algorithm is implemented. We have started to distribute the new AMSR-E L1 Version 4 and L2 Version 8 products through the G-Portal system.

Both of GCOM-W satellite and AMSR2 instruments are in good condition after the launch in May 2012 and continues observation in post-mission phase. Some of AMSR2 standard products including SST were updated to Version 3 in March 2017 and distributed through the JAXA G-Portal in HDF5 format. AMSR2 10 GHz SST research product, which is included in the AMSR2 standard SST product as complementary information, is also updated to Version 3 in March 2017.

The GPM Core Observatory and its instruments are also in good condition after the launch in February 2014 and continues observation in the post-mission phase. GPM standard products were updated to Version 6A in

October 2018. JAXA has developed the GMI SST algorithm, applied the AMSR2 10 GHz SST algorithm, and distributed data through the JAXA GHRSST server.

The GCOM-C satellite was launched in December 2017 and its SGLI data including SST has been distributed to public through the G-Portal system since December 2018. We are preparing SGLI SST in GDS 2.0 format for distribution from our GHRSST server.

Himawari-8 SST products are produced by JAXA and distributed from the JAXA Himawari Monitor/P-Tree system, also distributed from this system are JMA's Himawari-8 L1 products and other JAXA-produced L2 products. Himawari-8 SST products are distributed in GDS2.0 format with 2km resolution and 10 minute, hourly, daily and monthly intervals. We also produce 1 hour average nighttime SST in GDS2.0 format. We recently started to distribute high-resolution model SST produced by data assimilation of satellite SST. Model SST in netCDF (not GDS2.0) and its two-week forecasts are distributed through the JAXA P-Tree system.

5. REFERENCES

Varlamov, S. M., X. Guo, T. Miyama, K. Ichikawa, T. Waseda, and Y. Miyazawa, M2 baroclinic tide variability modulated by the ocean circulation south of Japan, *J. Geophys. Res. Oceans*, **120**, 3681-3710, doi:10.1002/2015JC010739, 2015.

Miyazawa, Y., S. M. Varlamov, T. Miyama, X. Guo, T. Hihara, K. Kiyomatsu, M. Kachi, Y. Kurihara, H. Murakami, Assimilation of high-resolution sea surface temperature data into an operational nowcast/forecast system around Japan using a multi-scale three-dimensional variational scheme, *Ocean Dyn.*, **67**, 713-728, doi:10.1007/s10236-017-1056-1, 2017.

REPORT TO GHRSST XX FROM JMA

Toshiyuki Sakurai, Hiromu Kobayashi and Ayako Yamane

Office of Marine Prediction, Japan Meteorological Agency, Tokyo (Japan),
Email: tsakurai@met.kishou.go.jp

ABSTRACT

The Japan Meteorological Agency (JMA) produces and maintains two SST analysis products: (1) a daily global SST analysis with 0.25° grid resolution (MGDSST) and (2) a daily SST analysis with 0.1° grid resolution for the western North Pacific (HIMSST). JMA has operated a series of geostationary meteorological satellites (Himawari-8 and -9), and produces HIMAWARI L3 SST with 0.02° grid resolution. This report describes an overview of these SST products and recent activities related to them.

1. INTRODUCTION

JMA has operated an SST analysis system to generate global daily SST data (Merged satellite and in-situ data Global Daily Sea Surface Temperature: MGDSST) on a routine basis since 2005. The system adopts an optimal interpolation (OI) method which considers not only spatial correlation but also temporal correlation. It produces a 0.25° resolution, daily global SST analysis, using both satellite and in-situ SST observation. The satellite data currently ingested to MGDSST are: AVHRR SST (NOAA-18, NOAA-19 and Metop-A), WindSat SST and AMSR2 SST. Prompt analysis of MGDSST is running within JMA'S NWP System on an operational basis, and delayed analysis is conducted five-months later in principle. Since a long term, consistent time series of the SST analysis is needed for climate research, JMA also conducted the reanalysis of MGDSST for the 1982 – 2006 period using AVHRR Pathfinder Version 5.0/5.1 SST and AMSR-E SST. MGDSST analysis contributes to the GHRSST Multi-Product Ensemble (GMPE) system (Martin et al, 2012) as one of the input data streams.

Another SST analysis product is a regional daily high resolution (0.1°) analysis for the western North Pacific. This regional product was named HIMSST (HIgh resolution Merged satellite and in-situ data Sea Surface Temperature) and has been in operation since November 2016. The analysis framework is based on that of MGDSST. In addition to the satellite data used in MGDSST, the components of smaller spatial-temporal scale derived from Himawari-8 L3 SST are ingested to HIMSST.

JMA has operated a series of geostationary meteorological satellites (Himawari-8 and -9) that observe the East Asia and Western Pacific Region, contributing to the space-based global observation system.

JMA's Office of Meteorological Analysis and Application Development has routinely produced Himawari-8 L3 SST. The L3 SST is produced with 0.02° horizontal grid resolution and the coverage of 60°S – 60°N, 80°E – 160°W. The time interval of the product has changed from every one hour to every 10 minutes since late March 2019. JMA adopts the same SST retrieval algorithm as used by JAXA based on a quasi-physical algorithm (Kurihara et al. 2016). One of the main differences between JMA's and JAXA's product is the method of cloud masking. For cloud screening of Himawari-8 L3 SST, JMA uses the Fundamental Cloud Product for Himawari-8 (Imai and Yoshida, 2016) and JAXA adopts the Bayesian inference method (Kurihara et al. 2016).

2. MAIN ACTIVITIES SINCE GHRSST XIX

2.1. IMPACT TEST OF VIIRS DATA FOR PROMPT MGDSST AND HIMSST ANALYSIS

We investigated the impact of assimilating NOAA ACSPO VIIRS L3U SST (version 2.40 and version 2.41) for the prompt MGDSST and HIMSST analysis. The configuration of the test run was the same as the control run (*i.e.* routine analysis), except that VIIRS SSTs are used in place of NOAA18/AVHRR data. The SSES bias was removed from the VIIRS L3U SSTs. Comparison against buoy observation shows that the RMSE for the test run was reduced by 0.02 K in the global area (Fig. 1). The improvement was relatively large in the mid-and high- latitudes. The test run data will be validated in the context of NWP system, and then VIIRS SST will be introduced to the operational analysis.

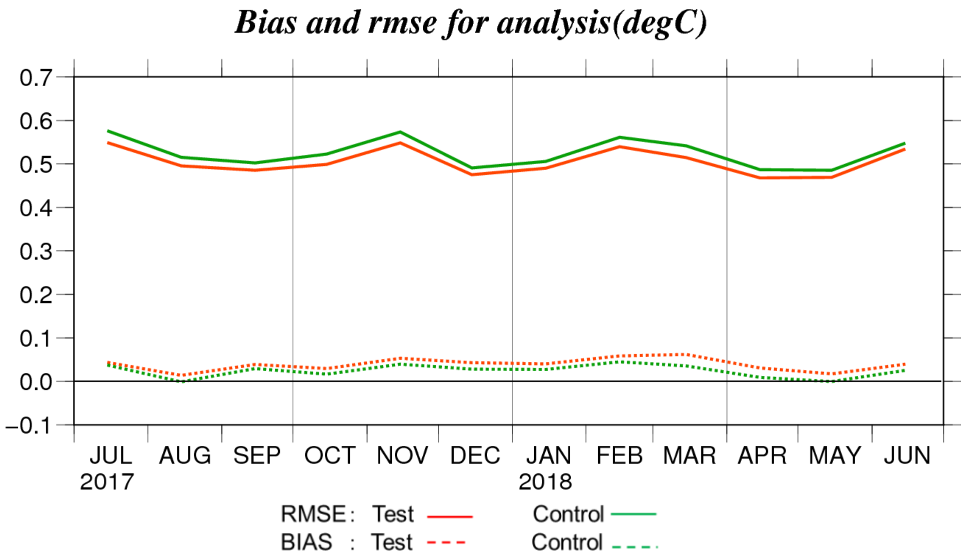

Figure 1: Monthly validation statistics for prompt MGDSST from Jul. 2017 to Jun. 2018. RMSE (°C, solid lines) and bias (dashed lines) for the control run (operational analysis) are shown in green, those of the test run are shown in red. The statistics are calculated using buoy SSTs as the truth.

2.2. NEW SATELLITE SST DATA ACQUISITION

2.2.1. Polar Orbiting Satellites

JMA has begun to acquire NOAA20/VIIRS SST L3U (ACSPO version 2.60) data provided by NOAA/NESDIS/OSPO through PDA system since December 2018. Data are gridded at 0.02° x 0.02° resolution for the global ocean in GDS2.0 netCDF format. JAXA/EORC has provided GCOM-C/SGLI near-real time L2P SST (official data) to JMA since December 2018. L2P SST of SGLI data for global ocean are produced with a spatial resolution of 1km in HDF format. These data will be used for MGDSST and HIMSST analysis.

2.2.2. Geostationary satellites

JMA has a plan to develop a 0.1° daily global SST analysis as a natural extension of HIMSST (a regional high resolution SST analysis for the western North Pacific). The analysis method will be almost the same as for HIMSST, however, SST data of additional geostationary satellites, such as GOES-16, GOES-17 and Meteosat are essential for the new analysis. JMA has begun to acquire GOES-16/ABI L3C SST in GDS2.0 netCDF format provided by NOAA/NESDIS/OSPO through PDA system since April 2019.

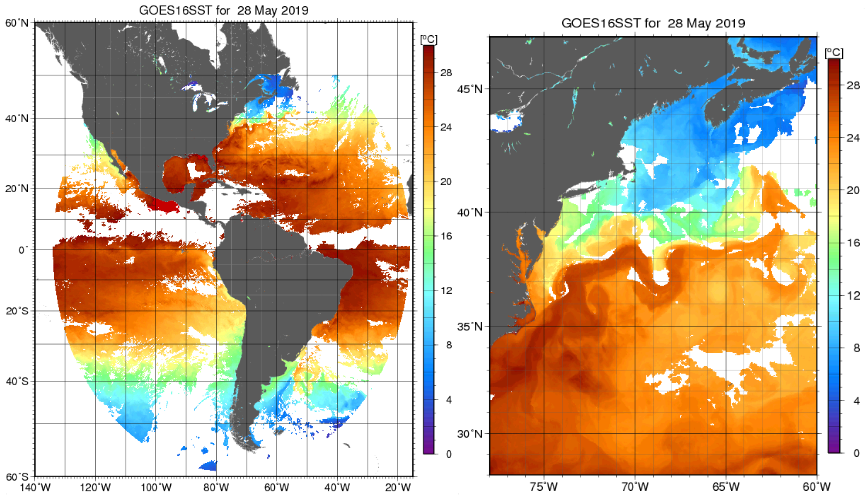

Figure 2: Example of NOAA ACSPO GOES-16 SST for 28 May 2019.

3. DATA AVAILABILITY

MGDSSTs are available from January 1982 via NEAR-GOOS Regional Real Time Database (RRTDB) in text format. HIMSST data are available from February 2017 in text format. We are preparing the GDS 2.0 implementation of MGDSST to facilitate the use of JMA's SST products in GHRSST activities.

4. REFERENCES

Imai T and Yoshida R., Algorithm theoretical basis for Himawari-8 Cloud Mask Product, Meteorological Satellite Center Technical Note, **61**,1-7, 2016.

Kurihara Y, Murakami H and Kachi M., Sea surface temperature from the new Japanese geostationary meteorological Himawari-8 satellite, Geophysical Research Letters, **43(3)**, 1234-40, 2016.

Martin, M., P. Dash, A. Ignatov, V. Banzon, H. Beggs, B. Brasnett, JF Cayula, J. Cummings, C. Donlon, C. Gentemann, R. Grumbine, S. Ishizaki, E. Maturi, R. Reynolds and J. Roberts-Jones, Group for High Resolution Sea Surface temperature (GHRSST) analysis fields inter-comparisons. Part 1: A GHRSST multi-product ensemble (GMPE), Deep Sea Research Part II: Topical Studies in Oceanography, 77–80, 21–30, doi:10.1016/j.dsr2.2012.04.013. 2012.

RDAC UPDATE: MET OFFICE

Chongyuan Mao[(1)] and Simon Good[(1)]

(1) Met Office, FitzRoy Road, Exeter, Devon EX1 3PB, United Kingdom, Email: chongyuan.mao@metofice.gov.uk

1. INTRODUCTION

The Met Office provides two kinds of GHRSST products: near real time products and reprocessed products. This talk introduces the products, including data availability, and updates the science team on major activities at the Met Office since the last science meeting.

2. MET OFFICE GHRSST PRODUCTS

2.1. NEAR REAL TIME DATASETS

The Met Office produces three near real time (NRT) GHRSST products: the Operational Sea Surface Temperature and Ice Analysis (OSTIA), the GHRSST Multi-Product Ensemble (GMPE), and diurnal skin SST. More specifically, the OSTIA dataset is a L4, global and daily foundation SST product, which ingests GHRSST L2/L3 and in situ observations. The system estimates biases for all satellite input data against a reference dataset. The product also includes seasonal and monthly means.

The GMPE is a daily ensemble of global L4 SST analyses. The product includes the median and standard deviation of the ensemble, as well as the anomaly relative to the median and gradients of each participating analysis.

The diurnal skin SST product is a globally complete and daily product containing hourly average skin SST. GHRSST L2/L3 satellite data are used to generate the product.

All products are available from CMEMS (http://marine.copernicus.eu/) in GDS v2 format. OSTIA L4 foundation analyses are also available from PO.DAAC (https://podaac.jpl.nasa.gov/) in both GDS v1 and v2 formats.

2.2. REPROCESSED DATASETS

Two reprocessed datasets are produced using OSTIA configuration, one as part of the ESA SST CCI/C3S project (http://cci.esa.int/) and the other one is a CMEMS long data record that is equivalent to the OSTIA NRT products. The CCI product represents daily average SST at 20 cm depth, which also includes a reprocessed GMPE product. The CMEMS dataset produces foundation SST and the current version covering 1985 – 2007 is available from CMEMS. An updated version covering 1982 – 2018 and onwards is currently in production and will be available in early 2020.

The Met Office also provides three climate datasets: Hadley Centre Sea Ice and Sea Surface Temperature dataset (HadISST), Hadley Centre SST dataset (HadSST) and Hadley Centre Integrated Ocean Database (HadIOD). Note, these three datasets are not in GDS format. All products are available through the Met Office Hadley Centre Observations websites (https://www.metoffice.gov.uk/hadobs/). Some of the data require users to contact the Met Office Hadley Centre prior to accessing the data.

3. MAIN ACTIVITIES SINCE GHRSST XIX SCIENCE MEETING

The NRT OSTIA configuration was upgraded to improve feature resolution and incorporated Sentinel-3A SLSTR SST data in March 2019. The improved feature resolution is illustrated in Figure 1 (from Figure I.1, p8, CMEMS user manual http://resources.marine.copernicus.eu/documents/PUM/CMEMS-SST-PUM-010-001.pdf). The methods used to improve feature resolution were developed as part of the ESA SST CCI project. Further details of the updated OSTIA configuration and assessment of the improved feature resolution are published in Fiedler et al. (2019).

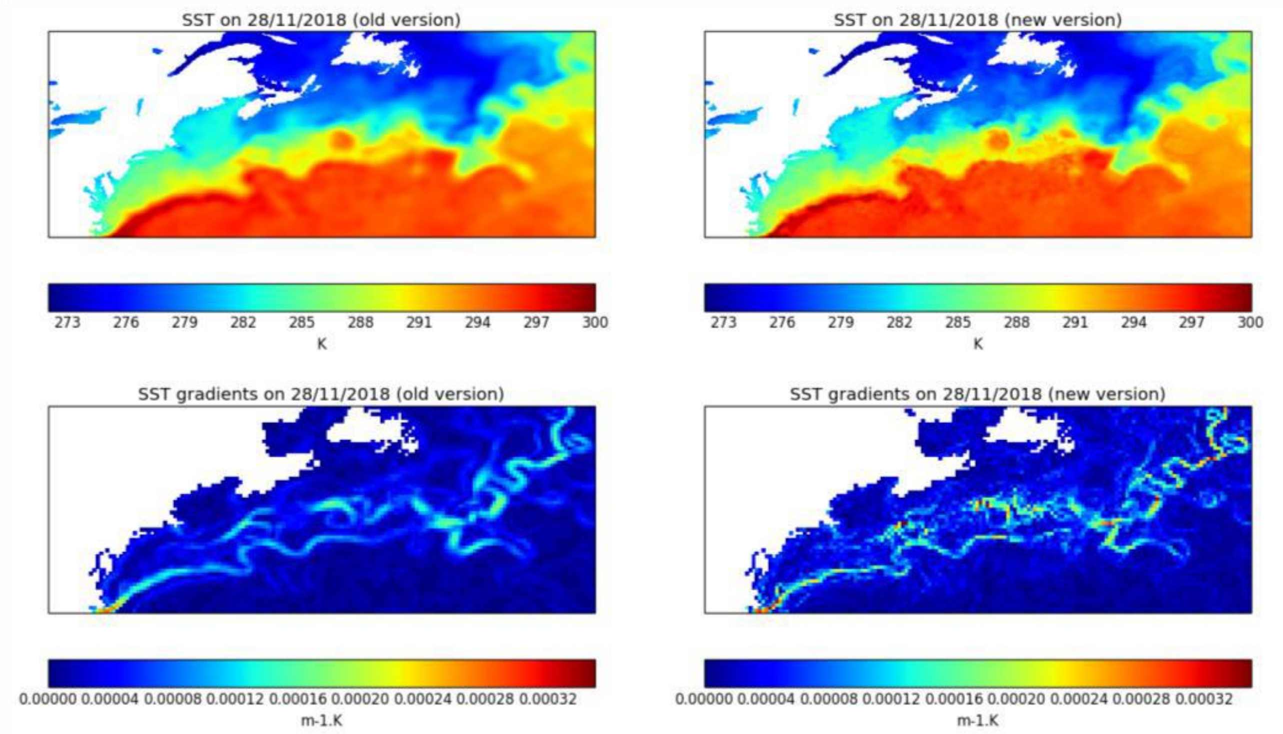

Figure 1: Illustration of the change in sharpness in features and increase in the strength of SST gradients due to the 12th March 2019 update. Figure included as Figure I.1 in CMEMS user manual: http://resources.marine.copernicus.eu/documents/PUM/CMEMS-SST-PUM-010-001.pdf

Preliminary investigation into the use of SLSTR data as a reference sensor was completed, including testing different methods for skin-to-bulk adjustment. The results indicate neutral impact with substituting the current L3U VIIRS data with Sentinel-3A SLSTR as a reference sensor globally, with improvements seen in the tropics and degradation in the high latitudes. Main results are presented in a poster by Mao and Good (2019). Further work includes testing the combination of L3U VIIRS, Sentinel-3A and -3B SLSTR as reference sensors.

We tested the inclusion of NOAA-20 VIIRS and Sentinel-3B SLSTR data in OSTIA in a pre-operational suite. The two datasets will be ingested in OSTIA operationally at the next system upgrade.

The work on a reprocessed OSTIA dataset for CMEMS and on the climate datasets for ESA SST CCI/C3S projects are still ongoing. Some results on the assessment of impact of passive microwave observation on L4 analysis are presented in Worsfold et al. (2019).

4. REFERENCES

Fiedler, E. K, C. Mao, S. A. Good, J. Waters and M. J. Martin, Improvements to feature resolution in the OSTIA sea surface temperature analysis using the NEMOVAR assimilation scheme, *Accepted by Quart. J. Roy. Met. Soc.*, doi: 10.1002/qj.3644, 2019.

Mao, C. and S. A. Good, Assessment of the impact of Sentinel-3A and -3B SLSTR L2P sea surface temperature data on OSTIA, *Proceeding at GHRSST XX Science Meeting, ESA ESRIN, Italy*, 2019.

Worsfold, M., S. A. Good, J. Høyer and E. Alerskans, Impact of passive microwave SST on level 4 analysis, *Proceeding at GHRSST XX Science Meeting, ESA ESRIN, Italy*, 2019.

NASA (RDAC) REPORT TO THE GHRSST SCIENCE TEAM

Edward Armstrong[(1)], Jorge Vazquez[(1)], Wen-Hao Li[(2)], Toshio Chin[(1)], Vardis Tsontos[(1)], Zhijin Li[(1)]

Jet Propulsion Laboratory, California Institute of Technology, Pasadena, CA, USA
Raytheon, 300 N Lake Ave, Pasadena, CA 91101
Email: edward.m.armstrong@jpl.nasa.gov

ABSTRACT

The NASA JPL and JPL_OUROCEAN RDACs continued their scientific dataset contributions to the GHRSST community by providing valuable Level-2 and Level-4 products, of which the MUR and G1SST have been listed as amongst the top 10 most active PO.DAAC datasets in 2019 (See GDAC Report in these proceedings). The JPL RDAC has continually produced the MODIS Aqua/Terra L2P, VIIRS L2P and MUR L4 datasets, while JPL_OUROCEAN RDAC has produced and supported the G1SST L4 dataset.

The report will also discuss updated NASA contributions to the COVERAGE project and the US GHRSST community in general.

1. INTRODUCTION

The summary and future accomplishments performed by the two RDACs are noted below:

1.1. GHRSST DATASETS PROVIDED BY JPL RDAC

1.1.1. Aqua and Terra L2P, v2014.0

- https://podaac.jpl.nasa.gov/dataset/MODIS_T-JPL-L2P-v2014.0
- https://podaac.jpl.nasa.gov/dataset/MODIS_A-JPL-L2P-v2014.0
- MODIS and VIIRS reprocessing's proposed in 2019 or 2020
- Used as input layer in State Of The Ocean (SOTO) visualization tool

1.1.2. VIIRS L2P, v2016.0

- https://podaac.jpl.nasa.gov/dataset/VIIRS_NPP-JPL-L2P-v2016.0

1.1.3. MUR L4 version 4.1

- New 25 km grid global MUR (by-)product
- Addition of anomaly SST (forward stream in version 4.1)
- Addition of VIIRS L2P SST (for version 5)
- Addition of RAN NOAA-17 L2P (for version 5)
- Migration to new JPL hardware
- Used as input layer in State Of The Ocean (SOTO) visualization tool
- Interpolation parameters based on dynamics (see Chin poster)

1.2. GHRSST DATASETS PROVIDED BY JPL_OUROCEAN RDAC

1.2.1. G1SST Level 4

- Upgrade the 2DVAR algorithm for more accurately accounting of observational errors and time difference of measurements
- GDS2 implementation

2. COVERAGE (CEOS OCEAN VARIABLES ENABLING RESEARCH AND APPLICATIONS FOR GEO)

COVERAGE is a collaborative effort within CEOS and 3-year NASA project involving the 4 Ocean VCs (SST, OST, OCR, OSVW) and GEO projects (MBON, Blue Planet) to enable more widespread use of ocean satellite data in support of applications. Recent progress includes the completion of Phase A and planning for Phase B:

2.1. PHASE A (COMPLETED)

a. Inventory/review of target Interagency datasets
b. Design of prototype COVERAGE technical system architecture for implementation in Phase B
c. Specification of a focal COVERAGE pilot application in support of GEO-MBON for implementation in Phase B
d. Processing of MUR-SST product at 0.25 degrees for inclusion in COVERAGE
e. Initial work addressing identified L4 ocean color product gap in coordination with OCR-VC that will be further developed during Phase B.

2.2. PHASE B (IN PROGRESS):

a. Phase B task plan formulated and proposal submitted to NASA. The aim is to implement a demonstration COVERAGE system for community comment within a year.

3. NASA PHYSICAL OCEANOGRAPHY PROGRAM

The activities of the NASA Physical Oceanography Program has supported GHRSST in a number of ways:

3.1. NATIONAL OCEAN PARTNERSHIP PROGRAM (NOPP), MISST: CONTINUING THE GHRSST PARTNERSHIP AND ARCTIC DATA (CHELLE GENTEMANN, EARTH SPACE RESEARCH)

a. Collaboration with Saildrone Project to support future deployments in the Arctic. Current Arctic deployment (began May 1) including 5 Saildrones has already begun. Plans for archiving data at the PO.DAAC.
b. Saildrone Alta California/Baja California Deployment archived at the PO.DAAC. Includes SST data from in-situ radiometer and CTD.

3.2. ONGOING SUPPORT FOR CEOS SST VIRTUAL CONSTELLATION NOTED IN THE PREVIOUS SECTION

3.3. PUBLICATIONS (WITH CONTRIBUTIONS FROM JPL AUTHORS)

a. Sea Surface Temperature Retrievals from Remote Sensing, 2018, Editors Vazquez-Cuervo, J. and X. Li, 2018, Topical Collection for Special Remote Sensing Issue on Sea Surface Temperature, MDPI.

b. SST White Paper (submitted to Frontiers) in support of OceanObs 2019.

c. P. J. Minnett, A. Alvera-Azcárate, T. M. Chin, G. K. Corlett, C. L. Gentemann, I. Karagali, X. Li, A. Marsouin, S. Marullo, E. Maturi, R. Santoleri, S. Saux Picart, M. Steele, and J. Vazquez-Cuervo, 2018, Half a Century of Satellite Remote Sensing of Sea Surface Temperature, under review Remote Sensing of the Environment.

d. J. Salat, J. Pascual, M. Flexas, T. M. Chin, J. Vazquez-Cuervo, 2018, 45 years of oceanographic and meteorological observations at a coastal station in the NW Mediterranean: A ground truth for satellite observations, accepted Ocean Dynamics, Ref.:Ms. No. ODYN-D-18-00177R1

Acknowledgements

This work was carried out at the NASA Jet Propulsion Laboratory, California Institute of Technology. Government sponsorship acknowledged. Government sponsorship acknowledged. URS284471.

SESSION II REPORT (PART 2)

Chair: Charlie Barron[(1)] – Rapporteur: Ioanna Karagali[(2)]

(1) U.S. Naval Research Laboratory, USA Email: charlie.barron@nrlssc.navy.mil
(2) DTU – Technical University of Denmark, Denmark Email: ioka@dtu.dk

ABSTRACT

The session featured eight presentations by seven speakers offering a review of activities of their organizations or projects since GHRSST XIX.

Summary of Speakers and Organizations

1. RDAC update from NAVOCEANO (10min) – Bruce McKenzie
2. RDAC update from NOAA/NESDIS/STAR 1 (10min) – Alexander Ignatov
3. RDAC update from NOAA/NESDIS/STAR 2 (10min) – Eileen Maturi
4. RDAC update from NOAA/NCEI (10min) – Kenneth Casey (given by Huai-Min Zhang)
5. RDAC update from OSI-SAF (10min) – Stéphane Saux Picart
6. RDAC update from RSS (10min) – Chelle Gentemann
7. Report from MISST (10min) – Chelle Gentemann
8. Report from NSOAS (10min) – Qimao Wang

1. SUMMARY OF PRESENTATIONS

The highlights for each talk and floor discussion are given below.

1.1. RDAC UPDATE FROM NAVOCEANO – BRUCE MCKENZIE

Summary of GHRSST products sent to JPL PODAAC

Main activities:

- Updated VIIRS SST
- L4 data updated to GDS v4 on January 2019
- SST match-ups (Day-time stats for L2P: no bias corrections, no skin/subskin corrections)
    - NAVOCEANO Metop-A,-B, NPP VIIRS, NOAA-19
    - MSG SEVIRI L3C from OSISAF
    - GCOM AMSR2 from JAXA
    - Sentinel 3A/B from EUMETSAT
- Plans:
    - Metop-A L2P production to stop later in 2019 when the AVHRR data flow from NOAA is discontinued after the Metop-C data flow becomes operational.
    - VIIRS NOAA20 available August 2019
    - Metop-C L2P available 2020

- K-T high speed, high resolution temperature sensor (1 kHz, 0.001 C) has been developed by Will Hou (NRL) suitable for placement on airborne drones and in-water floats, buoys.

Discussion:

Helen Beggs, BoM: Switching off Metop-A GAC will have a huge impact on the BoM and a number of other users, so a few months' notice would be useful, also because it will require some time to bring Metop-C to operation.

Bruce McKenzie: NAVOCEANO will request that NOAA continue its feed of Metop-A AVHRR observations be continued to overlap for some period after the NOAA Metop-C data feed becomes operational.

(Update on Tuesday) Bruce McKenzie has requested and received confirmation from the NOAA producers of the Metop AVHRR L1B data that they can continue providing Metop-A AVHRR GAC 1B in addition to Metop-B and Metop-C. Present hardware has sufficient margins to support this additional processing.

Action items/questions to GHRSST:

None

1.2. DAC UPDATE FROM NOAA/NESDIS/STAR 1 – ALEXANDER IGNATOV

- Acknowledge support from PO-DAAC serving data.
- Seven year development has led to full constellation of JPSS satellites in orbit with JPSS VIIRS and GOES ABI
- Instruments are performing well, with additional work to address challenges on GOES-17
- Superior spatial and temporal resolution of JPSS/GOES-R (VIIRS/ABI), more and better positioned SST bands, improved radiometric performance
- Data products and volumes:
    - All ACSPO products available in L2P and L2 (.02)
        - Polar L3U: Uncollated in time
        - GEO L3C: Collated in time (1-hour files by collating 10-min data)
    - L3 preferred by many users due to lower bandwidth requirements
    - Sensor-Agnostic, super collated, gridded product (L3S) requested by many users. Present bandwidth savings is more significant for GEO data than for Polar. Additional work underway.
- Major Accomplishments:
    - NOAA produces VIIRS RAN2 and ABI RAN L2/L3 products (working with PODAAC partners to archive)
    - VIIRS ReAnalysis-2: residual striping amplified, Bouali and Ignatov (2014) algorithm applied, BTs are resampled using Gladkova et al. (2016) algorithm.
        - Night-time does not show seasonal cycle, day-time does
        - Resampling and registration improves recognition of thermal front evolution
        - Data archived in PO-DAAC
    - Processing of GAC data discontinued
    - Production of L2P/L3U from Metop-A/B commenced with ACSPO 2.7
- Priorities

  - Complete NPP VIIRS RAN2
  - Complete ABI RAN1
  - Produce AHI RAN1
- Suggested topics for discussion
  - Propose storing the dt_analysis and satellite_zenith_angle as 16bit
  - Efforts to reduce size of polar data sets from present L2P sizes

No time for further questions/discussion.

1.3. RDAC UPDATE FROM NOAA/NESDIS/STAR 2 – EILEEN MATURI

Products:

- Global 5km SST analysis (L4): day/night, night-only, diurnally-corrected
- Geostationary L2 SSTs: Meteosat-8, Meteosat-11, GOES 15
- Reprocessed Blended SST Analysis (2002 to 2013, reprocessing 2002 to 1995)
- Fully operational uses of these data include Coral-Temp and upper ocean heat content products
- Blended SST combines data using the physical retrieval algorithm (Meteosat-8, Meteosat-11 & GOES-15) and ACSPO regression (GOES-16, H-8, VIIRS, Metop)
  - Geostationary (GOES-16, Himawari 8/9, Meteosat-8, Meteosat-11, GOES-15)
  - Polar Orbiters (S-NPP VIIRS, JPSS-1 VIIRS, Metop-B)
  - Thinned OSTIA
- Main Activities:
  - GHRSST products from satellites listed above
  - Data distributed via PO-DAAC
- Issues to be raised
  - Bias correction procedures
- Future: Coral Temp continuation

Craig Steinberg: Some of your processes are using two different retrieval algorithms; are there any issues on how the data are matching?

Eileen Maturi: NOAA NESDIS is moving to a common method for the processing; differences can also arise due to different clod masks, differences in coverage of in-water measurements from buoys for regression-based retrievals, use of physical SST retrievals.

Craig Steinberg: Please clarify your reasons for “thinning OSTIA” as an input to the processing.

Eileen Maturi refers question to Andy Harris: The processing uses a quad-tree approach to calculate the multi-scale OI efficiently. However, slight rounding errors propagating down the quad-tree produce artifacts if there is no data. Including a sparse sample of OSTIA ensures that all quad-tree tiles have a sufficient number of observations for the processing; in most of the ocean the number of OSTIA samples is insignificant relative to data from the satellite sources.

Action items/questions to GHRSST:

None

1.4. RDAC UPDATE FROM NOAA/NCEI – KENNETH CASEY GIVEN BY HUAI-MIN ZHANG

NCEI merged from NCDC, NGDC, NODC

- NCEI responsibilities include data associated with marine surface meteorology and oceanography, with scope from foundational data to analysed products, roles from long term data stewardship to national services and international leadership
- ICOADS updates: Blending TAC and BUFR Marine In Situ data for ICOADS Near Real Time Updates
- Thermosalinograph DataBase (TSG): 1989 to present
- Extended Reconstructed SST (ERSST): 1854 to present
  - New bias corrections → no recent warming hiatus
  - V5 in 2017 (J Climate)
  - ERSST uncertainty representation is based on 1000-member ensemble with variations among 28 control variables (under review, J Climate)
- AVHRR PFSST:
  - Reprocessing of v5.3.1 (improved binning at high latitudes) for production of L2P, L3U, L3C CDR is ongoing
  - Thermal stress anomalies CoRTAD revived and upgraded to v6
- Daily OI SST at .25 degrees: Most notable improvement over the Arctic region
- Expanded GHRSST collection and services

Xu Li: Clarification on the purpose of uncertainty estimates, informative or correction?

Huai-Min Zhang: The uncertainty estimates are intended to be informative at the grid level.

Helen Beggs: When are the buoy data reported with a 7-digit platform id to be ingested? Without this capability, only about 10% of the buoy SST are being ingested.

Huai-Min Zhang: Since ERSST is based on observations from the Argo floats, this product has net been impacted by the ids from the surface buoys. ICOADS will make a beta release of reprocessed data in late summer or early fall.

Helen Beggs: I would like to see evaluation of these products relative to the full set of surface buoys.

Action items/questions to GHRSST:

None

1.5. RDAC UPDATE FROM OSI-SAF – STÉPHANE SAUX PICART

Description of the OSI-SAF: meteorological sat data for comprehensive information on ocean-atmosphere interface (METNO, DMI, KNMI, Météo-France, Ifremer)

- Scatterometer winds

- SST
  - Metop-B, NPP VIIRS and L2P, L3 L2 global and regional products
  - Meteosat-11, GOES 16, Meteosat-8 all L3C at 0.05 degrees, hourly
  - Reprocessed MSG SEVIRI 2004-2012, L3C at 0.05
- Ice Surface Temperature (IST)
- Radiative fluxes: Surface Solar Irradiance and Downward Longwave I
- Sea Ice Concentration, edge, type, emissivity and drift
- Main activities
  - Operational processing of GOES16, Meteosat-11
  - Metop-C in test processing: L2P, L3C SST
  - Metop-B and NPP high latitude IST/SST
  - Probabilistic classifier in addition to the PPS cloud mask for high latitude SST and IST
  - Developing New GEO SST processing chain
  - Arctic and Antarctic Ice Surface temp from AVHRR (1982-2015) from METNO and DMI
- Data access: EUMETCast, PODAAC, Naiad, FTP servers
- User survey: https://framaforms. Org/how-do-you-use-osi-saf-products-1559035861

Pallavi Govekar: Are there validation reports available for the SST products?

Stéphane Saux Picart: Yes, validation reports on OSISAF website and pages showing basic statistics.

Action items/questions to GHRSST:

None

1.6. RDAC UPDATE FROM RSS – CHELLE GENTEMANN

- RSS RDAC produces AMSR2, GMI, WindSat SST
- NRT Status: AMSR2 L2P, GMI L3P, WindSat L3P
- Reprocessing status: occurs regularly

No time for further questions/discussion

Action items/questions to GHRSST:

None

1.7. REPORT FROM MISST – CHELLE GENTEMANN

- MISST projects have been contributing to GHRSST since 2002-2003
- Latest MISST project 2018-2023:
  - Coordinate and integrate new SST observations (GOES-R, VIIRS)

  - Improve data access
  - 5 Arctic Saildrone Cruises: 90days, additional SST profile obs, Improved SST skin, all data on GTS.
    - Open data policy, encourage open software policy
    - OSS netCDF in situ to ICOADS format converter
    - New Arctic data (2015-
  - Request that others providing data sources of Arctic in situ SST measurements send call signs or other access info so this data can be added to the community data resource
- Issues to be raised:
  - Reduce redundancy on algorithm development
  - NetCDF4 has metadata throughout the file which does not fit when working with large datasets. NetCDF5 will be released soon. What about Zarr, another format with a good deal of popularity among communities working with large datasets?
  - Analysis Ready Datasets (ARD) for GHRSST
  - Compliance: CD compliancy checker is not enough to ensure that different large data sets can be consistently and reliably used in combination by generic access capabilities across cloud resources. Maybe develop an open source format checker using Xarray (python) that checks different parts of the actual data format.
- Future of GHRSST:
  - GHRSST embraces open source software and cloud computing
  - How do we reduce redundancy and do new science…set the standard again.

Helen Beggs: Question on Saildrone-what is used to measure SSTskin?

Chelle Gentemann: Downward looking radiometer without no-sky correction. NASA missions have upward looking radiometer for correction. Bias of around 0.5 degrees. Older cruises have 2 CTDs at 0.6 meters depths. Arctic cruises have 3 CTDs. There is a poster on this. This is part of a large issue of communications between engineering capabilities to make a measurement and science teams that understand some of the nuances and ancillary information that would enable the measurements to provide useful information for science associated with different aspects of the environment.

Huai-Min Zhang: Is there a larger problem of data discovery? Some of the saildrone data are on the GTS feed and getting into ICOADS.

Jorge Vazquez: As we think about formatting among other issues to make large and mixed sst data sets more accessible to non-expert users, we need to better communicate guidance that will help them identify which data sets will better address their needs, helping them understand differences in results and communicate how the differences in processing lead to data sets with different error and representativeness characteristics.

Ed Armstrong/Chelle Gentemann discussion on formats for large data sets. We need broader understanding among the community with differences between NetCDF4, HDF5, NetCDF5 (is it not yet fully defined, is it really HDF5 optimized for the cloud), Zarr, potentially others. There are developments in other communities that will make large data sets increasingly accessible to non-expert users, and the GHRSST community is better positioned than many to establish standards for format and metadata that can facilitate this use in terms of both accessibility and understanding. A key development will be the deprecation of the file or granule concept once data is moved to the cloud. Data will be broken into smaller segments and sharded, and stored in databases or similar data objects. In this model metadata does not reside in a file but is dynamically accessible like the data. Metadata is a key issue, with both a need for more metadata to better inform and less metadata to reduce sizes of data transfer. Moving processing to the location of the data can reduce issues of file transfer. Isolating metadata or reducing redundant metadata can reduce data transfer costs at the risk of having users become less informed by accessing data in isolation from the metadata. Are there differences among file formats that comply with GDS2.0 standards but may allow compatibility issues for uninformed users attempting to combine and use the data as a multi-product/long duration source. If there are differences, do these differences pose challenges that reach a level of significance that would suggest revisiting data standards and/or methods to assess compliance with these standards?

Prasanjit Dash: VIIRS day/night band

The Saildrone team uses OLCI images for a background context. It's probably worth exploring the VIIRS day night band as well.

The VIIRS DNB and the corresponding Near Constant Contrast NCC imagery is a KPP of the JPSS for Poleward of 60N. It can be used alongside RADAR data because of its coverage (limited for RADARs due to power requirement). And is useful for sea ice studies, such as freeboard, leads, *etc*.

Action items/questions to GHRSST:
None

1.8. REPORT FROM NSOAS – QIMAO WANG

Introduction:

- National Ocean Satellite Application Center, NSOAS founded in 2000
- Responsibilities:

Support three series of ocean-focused satellites

- HY-1 Ocean colour:
    - A launched in 2002, B in 2007 and C in 2018 (5 payloads).
    - COCTS Optical radiometer for Ocean Colour and SST with 8 channels in visible and near-infrared, 2 channels in thermal infrared. Spatial resolution 1100 m.
    - CZI optical sensor for coastal zones. 4 spectral bands with 250 m spatial resolution.
    - Producing more than 42 products: water leaving radiance, Chl-A, SST (5km)
- HY-2 Ocean dynamic environment satellite:
    - A launched in 2011, B launched in 2018.
    - Scatterometer, altimeter, microwave radiometer and correction microwave radiometer for sea surface winds, heights, currents and SST (25km).
    - More than 20 types of products.
- HY-3 A: SAR (C-band) to be launched in 2020.

- Data applications: Marine environmental monitoring, ecological monitoring, ocean acidification, ocean disaster monitoring, sea ice, green tide monitoring, ocean fisheries.
- Future: HY-1 D and HY-2 C to be launched in 2019.

Charlie Barron: What are the spatial resolution and temporal coverage of your SST products?

Response referred to Lijian Shi:

HY-1C satellite SST has 1km pixel resolution and supports 2 products, a 4km analysis and a 9km analysis, both starting 7 October 2018.

HY-2b satellite SST has 25 km resolution and supports a 1/4° SST product starting 7 October 2018.

Action items/questions to GHRSST:
None

NAVAL OCEANOGRAPHIC OFFICE (NAVOCEANO) REGIONAL DATA ASSEMBLY CENTER (RDAC) UPDATE

Bruce McKenzie, **Doug May, Dan Olszewski, Valinda Kirkland, Michelle Little**

Naval Oceanographic Office, Stennis Space Center, MS (US)

ABSTRACT

NAVOCEANO) is a GHRSST RDAC providing operational near real time L2P and L4 products that are served to the global application community by the Physical Oceanography Distributed Active Archive Center at NASA's Jet Propulsion Laboratory in Pasadena, CA.

1. INTRODUCTION

Details on the GHRSST products generated and acquired by NAVOCEANO are presented along with SST matchup statistics that are calculated using satellite specific drifting buoy matchup databases.

2. L2P AND L4 PRODUCTS PRODUCED

The current set of NAVOCEANO L2P GDSV2.0 products are NOAA-19 AVHRR GAC and LAC, Metop-A and Metop-B AVHRR GAC, and S-NPP VIIRS. Figures 1 and 2 are plots of the daytime and nighttime buoy SST matchup statistics. The NAVOCEANO L4 product is a 1/10th degree composite updated daily from operational SST retrievals generated by NAVOCEANO (Metop-A FRAC, Metop-B FRAC, S-NPP VIIRS) and OSI-SAF (MSG1 and MSG4), along with JPL PENTAD Climatology and the National Ice Center's daily ice edge.

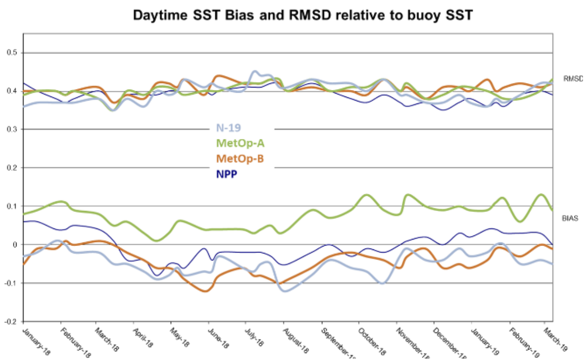

Figure 1. NAVO L2P Daytime buoy matchup statistics

3. PLANS

Plans for 2019 are to provide a NOAA-20 VIIRS L2P and a Metop-C GAC L2P. In 2021, NAVOCEANO will implement high latitude SST processing improvements developed by the Naval Research Lab at Stennis Space Center under the ONR MISST project.

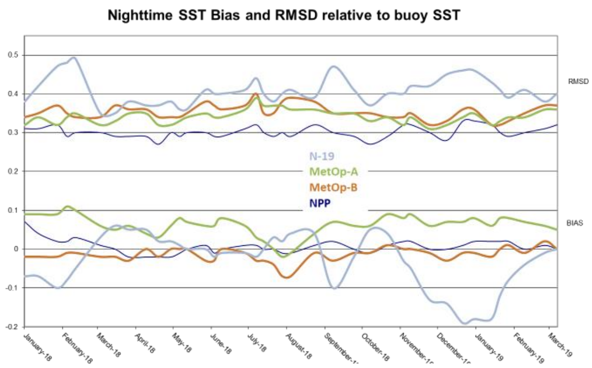

Figure 2. NAVO L2P Nighttime buoy matchup statistics

4. GHRSST PRODUCTS USED BY NAVO

NAVOCEANO operationally retrieves OSI-SAF MSG1 and MSG4 SEVIRI L3C data from the JPL PO.DAAC, GCOM-W AMSR2_NRT from JAXA, and EUMETSAT Sentinel-3A/B SLSTR L2P from NOAA/NESDIS Center for Satellite Applications and Research (STAR), which has a terrestrial EUMETCAST feed of Sentinel-3 data. Figure 3 is a plot of the buoy matchup statistics for these GHRSST products.

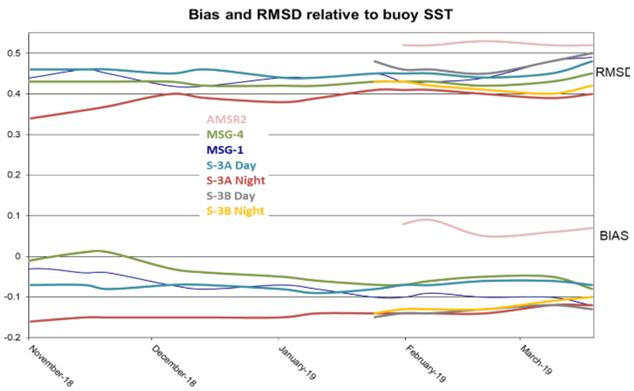

Figure 3. GHRSST buoy matchup statistics

5. CONCLUSION

The GHRSST project is a valuable source of SST data for NAVOCEANO, and a collaborative group to work on issues that affect all aspects of SST.

ACSPO SST PRODUCTS AT NOAA: UPDATE FOR GHRSST-XX

Alexander Ignatov(1), Matthew Pennybacker(2), Olafur Jonasson(3), Yury Kihai(4), Irina Gladkova(5), Boris Petrenko(6), Victor Pryamitsyn(7), John Sapper(8)

(1) NOAA STAR, USA, Email: Alex.Ignatov@noaa.gov
(2) NOAA STAR and GST Inc., USA, Email: Matthew.Pennybacker@noaa.gov
(3) NOAA STAR and GST Inc., USA, Email: Olafur.Jonason@noaa.gov
(4) NOAA STAR and GST Inc., USA, Email: Yury.Kihai@noaa.gov
(5) NOAA STAR, CUNY and GST Inc., USA, Email: Irina.Gladkova@gmail.com
(6) NOAA STAR and GST Inc., USA, Email: Boris.Petrenko@noaa.gov
(7) NOAA STAR and GST Inc., USA, Email: Victor.Pryamitsyn@noaa.gov
(8) NOAA OSPO, USA, Email: John.Sapper@noaa.gov

1. INTRODUCTION

The Advanced Clear Sky Processor for Ocean (ACSPO) is the NOAA enterprise SST retrieval system, which employs consistent cloud masking, SST retrieval and SSES algorithms (Petrenko et al, 2010, 2014, 2016) to generate a uniform line of L2/3 SST products from polar and geostationary sensors: JPSS VIIRS (NPP, N20), AVHRR GAC (N07 – N19), FRAC (Metop-A, B, and C), MODIS (Terra, Aqua), GOES-R ABI (G16, G17) and Himawari-8 AHI (H08). ACSPO products are used by NOAA fisheries and coastal management, assimilated in several ocean forecast systems and L4 SST analyses, and some other applications.

2. ACSPO SST PRODUCTS

ACSPO products in GDS2 format are available in 2 flavors: L2P (original swath projection), and their gridded counterpart, L3 (0.02° grid). L2P products from VIIRS/MODIS-like sensors are de-striped (Bouali, Ignatov, 2014; Mikelsons et al, 2015) and resampled (Gladkova et al., 2016). The gridded, smaller-size L3 products (cf. Tables 1-2) are preferred by many users (Ignatov et al., 2017). All polar data are reported in 10-min granules, 144/day. Polar L3U products are "uncollated" (*i.e.*, L2P data from different overpasses and sensors are mapped independently). All geostationary products are organized into hourly Full Disk (FD; view zenith angle not exceeding 68°) granules and reported hourly, 24/day. Both L2P and L3C data are collated, in which native-temporal resolution 10-min granules are "collated" together using an algorithm which analyzes temporal information, to suppress noise in imagery and reduce residual cloud and reported at 1hr increments (Gladkova et al., 2019). Operational 24/7 processing is performed at the Office of Satellite Products and Operations (OSPO; NPP/N20 VIIRS; Metop-A/B AVHRR FRAC) and at the Center for Satellite Applications and Research (STAR), in a best-effort mode (G16/17 ABI; H08 AHI; Metop-C AVHRR FRAC). Terra/Aqua MODIS and AVHRR GAC "Reanalyses" (RANs) are performed in STAR in a time-delayed mode. OSPO and STAR are two ACSPO Regional Data Assembly Centers (RDACs). Typical file names are 20190301001000-STAR-L3U_GHRSST-SST$_{subskin}$-VIIRS_NPP-ACSPO_V2.61-v02.0-fv01.0.nc or 20120301001000-OSPO-L3U_GHRSST-SST$_{subskin}$-VIIRS_NPP-ACSPO_V2.61-v02.0-fv01.0.nc

The files are 10min L3U VIIRS granules produced by ACSPO v2.61 at STAR and OSPO, respectively.

The following polar and geostationary ACSPO products are currently produced at either OSPO or STAR.

Polar Sensor	L2P	L3U (0.02°)
VIIRS (NPP/N20)	26.0	0.5 (×58)
AVHRR FRAC (Metop-A/B/C)	8.0	0.5 (×16)
AVHRR GAC (N07 – N19)	0.7	0.5 (×1½)

MODIS (Terra, Aqua)	7.5	0.5 (×16)

Table 1: ACSPO polar L2P and L3U products and daily sizes (GB/day).

Geostationary Sensor	L2P	L3U (0.02°)
ABI (G16/17)	1.0	0.6 (×1½)
AHI (H08)	1.0	0.6 (×1½)

Table 2: ACSPO geostationary L2P and L3C products and daily sizes (GB/day).

Global monitoring of data quality/validation against *in situ* data is performed in SST Quality Monitor (SQUAM; www.star.nesdis.noaa.gov/sod/sst/squam/; Dash et al., 2010). QC'ed *in situ* data used for validation in SQUAM come from *in situ* SST Quality Monitor (*i*Quam; www.star.nesdis.noaa.gov/sod/sst/iquam/; Xu and Ignatov, 2014). Imagery is monitored in the ACSPO Regional Monitor for SST (ARMS; www.star.nesdis.noaa.gov/sod/sst/arms/). Stability and cross-platform consistency of BTs used for SST retrievals, is monitored in the Monitoring IR Clear-sky Radiances over Ocean for SST (MICROS; www.star.nesdis.noaa.gov/sod/sst/micros/) system.

3. JPSS VIIRS

Suomi NPP with the first VIIRS instrument on-board was launched on 28 October 2011. Following the opening of its cryoradiator door on 19 January 2012, and thermal stabilization of the sensor, ACSPO SST production at NOAA commenced. Over the period of several years, ACSPO VIIRS SST products have been produced with evolving ACSPO versions (beginning from v2.30, up to the current 2.61). On 18 November 2017, N20 was launched. Following the opening of its cryoradiator door on 3 January 2018, SST production commenced. A consistent reanalysis (RAN) of complete VIIRS records from both NPP and N20 using ACSPO v2.61 has been completed at NOAA STAR. Archival with NASA PO.DAAC and NOAA NCEI is currently underway, which will replace the current incomplete and inconsistent holdings produced by various ACSPO versions. The "regression SST" layer reports SST, retrieved using global regression (GR) equations, separated by day and night (Petrenko et al., 2014). The SSES bias and SSES SD, also reported in ACSPO files, are produced using the Piece-Wise Regression (PWR) algorithm, proposed by Petrenko et al. (2016a). The GR and PWR SSTs are representative of "subskin" and "depth" (the latter representative of drifter/tropical moored depths, from ~0.2-1m) SSTs, respectively. For all data assimilation analyses (including L4 production, especially for those involving blending with *in situ* data) use of "depth" PWR SST is recommended (calculated as PWR SST = GR SST minus SSES bias). Fig. 1 shows time series of validation statistics (satellite L2P SST minus *i*Quam *in situ* SST, from drifters and tropical moorings), including bias and SD, for both GR and PWR SSTs. Statistics for corresponding L3U SST are similar and not shown.

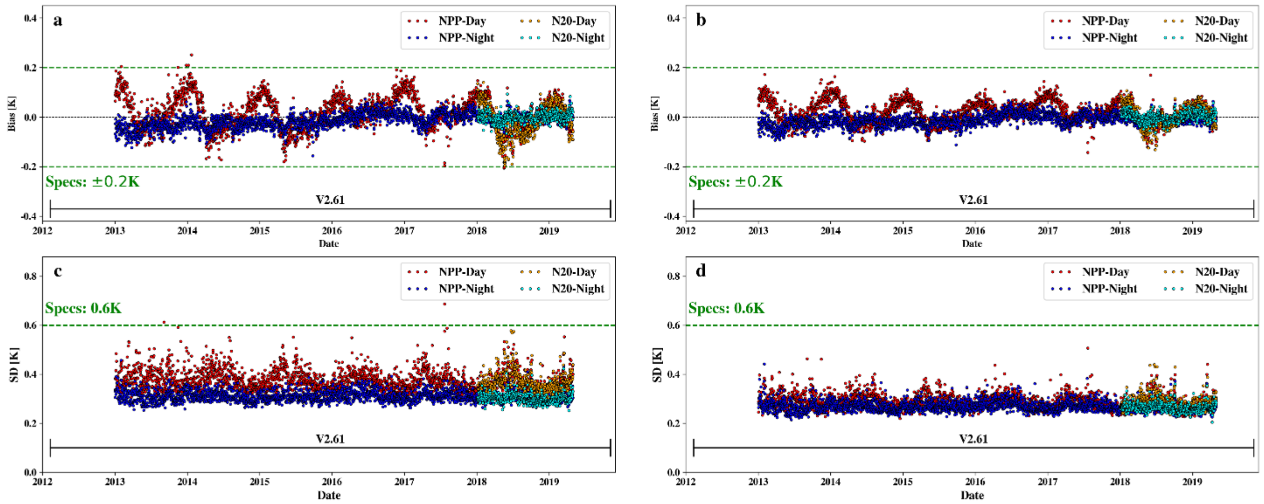

Figure 1: Time series of validation statistics "ACSPO VIIRS L2 SST minus iQuam drifters and tropical moorings", stratified by day and night. Each data point represents corresponding 24-hr global statistics, calculated from match-ups with QC'ed iQuam data (each supported by ~150,000 "one-in-situ to many-satellite-pixels matchups, within 30min and 10km). (a,c) GR SST; (b,d) PWR SST. (a,b) mean biases; (c,d) corresponding SDs.

Both GR and PWR are well within the NOAA SST specs (±0.2K for bias, 0.6K for SD). The daytime statistics are degraded compared to the nighttime, especially for the GR SST. This is because the diurnal thermocline contributes to "subskin" satellite vs. "depth" *in situ* SST comparisons more during the daytime. As expected, the differences are reduced at night, and for the "depth" PWR SST.

The RAN2 ACSPO v2.61 data are available from CW web page https://coastwatch.noaa.gov/cw/satellite-data-products/sea-surface-temperature/acspo-viirs.html and the following URLs

PO.DAAC

NPP ACSPO v2.61 L2P (Feb 2012 – pr) https://doi.org/10.5067/GHVRS-2PO61

NPP ACSPO v2.61 L3U (Feb 2012 – pr) https://doi.org/10.5067/GHVRS-3UO61

N20 ACSPO v2.61 L2P (Jan 2018 – pr) https://doi.org/10.5067/GHV20-2PO61

N20 ACSPO v2.61 L3U (Jan 2018 – pr) https://doi.org/10.5067/GHV20-3UO61

NCEI

NPP ACSPO v2.61 L2P (Feb 2012 – pr) https://doi.org/10.7289/v5pr7sx5

NPP ACSPO v2.61 L3U (Feb 2012 – pr) https://doi.org/10.7289/v5kk98s8

N20 ACSPO v2.61 L2P (Jan 2018 – pr) https://doi.org/10.25921/sfs7-9688

N20 ACSPO v2.61 L3U (Jan 2018 – pr) https://doi.org/10.25921/7c1m-rw73

4. GOES-R ABI

The first two US next-generation geostationary weather satellites, GOES-R and -S, were successfully launched in Nov'2016 and Mar'2018, and renamed GOES-16 (G16) and -17 (G17), after performing required on-orbit tests. Since Dec'2017 and Dec'2018, they have been operating at ~75.2°W (GOES-East) and ~137.2°W (GOES-West) positions, respectively. The primary GOES-R sensor, ABI, provides improved imaging of the Earth full disk (FD) with spatial resolution of 2 km at nadir in the IR bands, and temporal sampling of 10-min for each FD. ABI has more spectral bands, with better radiometric performance, navigation and co-registration than any imager on any previous geostationary platform (Schmit et al., 2017; Kalluri et al., 2018). ACSPO geostationary processing employs the standard masking and SST retrievals, for each 10-min FD. Subsequently, a unique collation-in-time post-processing is run on a sequence of 25 FD images, constructing an "upper-envelope" fit curve in each pixel. The collation algorithm suppresses noise and minimizes residual cloud leakages in the data, while fully preserving its spatial resolution and increasing coverage (Gladkova et al., 2019). The fit curve is subsequently digitized at 1-hr increments, and 24 1-hr FD granules are output as ACSPO product. An example of collated product SST is shown in Fig. 1.

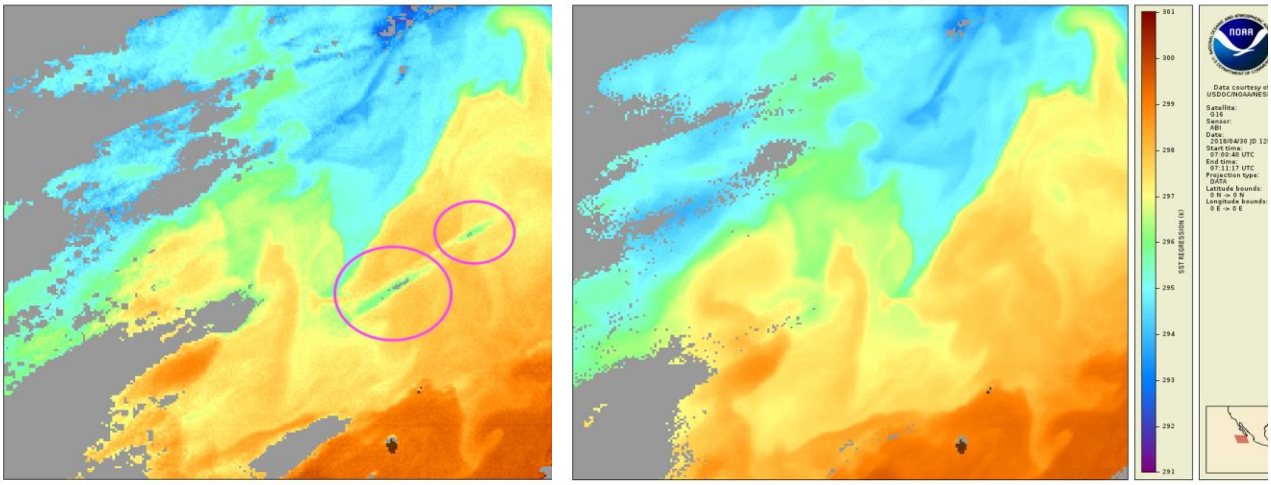

Fig. 2. (Left) uncollated & (right) collated ACSPO GOES-R ABI images (south-west of California on 30 Apr 2018 at 07:00 UTC). Note reduced residual cloud (magenta circles) & increased coverage in collated SST (Gladkova et al., 2019).

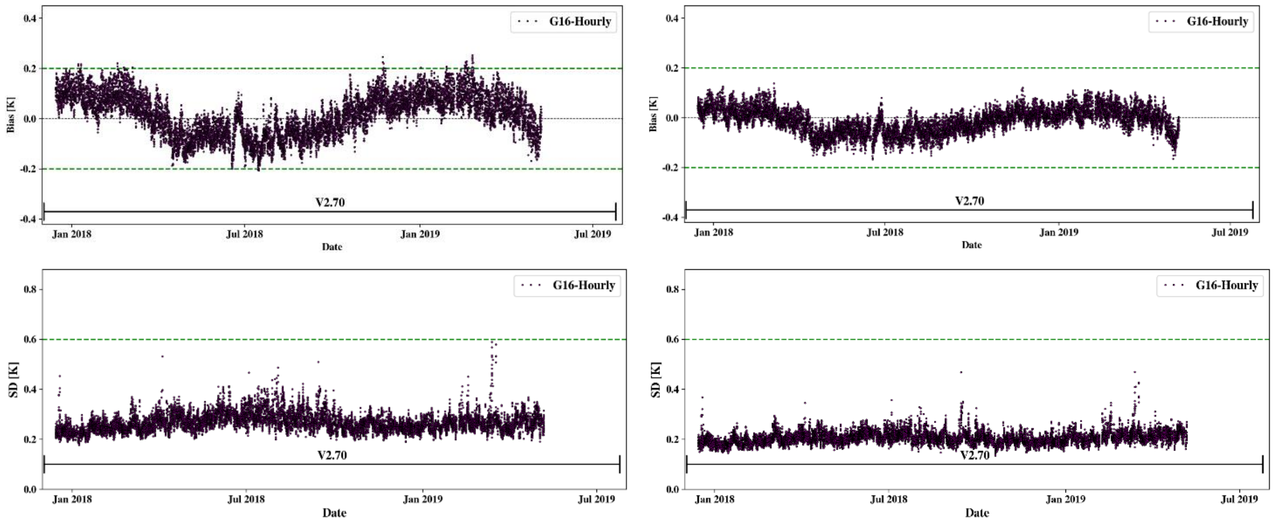

Fig. 3: Same as in Fig. 1 but for G16 ABI SST RAN1 produced with ACSPO v2.70. Each data point represents 1-hr FD statistics (calculated from ~7,000 matchups within 30min and 10km).

As of this writing, reanalysis-1 (RAN1) of G16 SST from 15 Dec 2017 – present has been completed from mid-Dec 2017 till present. Performance statistics are shown in Fig.3. Data are archived in PO.DAAC & NCEI.

PO.DAAC

G16 ACSPO v2.70 L2P (Dec 2017 – pr) https://doi.org/10.5067/GHG16-2PO27

G16 ACSPO v2.70 L3C (Dec 2017 – pr) https://doi.org/10.5067/GHG16-3UO27

NCEI (currently being populated as of this writing)

G16 ACSPO v2.70 L2P (Dec 2017 – pr) https://accession.nodc.noaa.gov/GHRSST-ABI_G16-STAR-L2P

G16 ACSPO v2.70 L3C (Dec 2017 – pr) https://accession.nodc.noaa.gov/GHRSST-ABI_G16-STAR-L3C

G17 ABI experiences performance issues. Following its launch, its Loop Heat Pipe (LHP; responsible for maintaining the temperature of the ABI IR Focal Plane Modules, FPMs) was found to operate at a reduced capacity (Pennybacker et al., 2019). As a result, G17/ABI nominal FPM temperature is kept at ~81K (compared to ~62K for G16), and elevated further during the night, in some seasons to a daily maximum of up to ~107K, when more sunlight impinges on the instrument. The elevated and time-varying FPM temperature causes a number of issues, requiring mitigation with the ACSPO SST retrieval, clear-sky mask, and collation algorithms. Elevated sensor noise and striping are partially mitigated by the collation algorithm. Currently, ACSPO produces SST imagery for 13hrs each day (2000 to 0800 UTC), with quality comparable to G16 (*e.g.* Fig. 4). Various mitigation strategies are currently being tested to increase the period of usable G17 SST data, after which time the full G17 record will be reprocessed and archived with PO.DAAC & NCEI. G16 and G16 operational moderate assurance data are available via CW web page at https://coastwatch.noaa.gov/cw/satellite-data-products/sea-surface-temperature/acspo-abi.html.

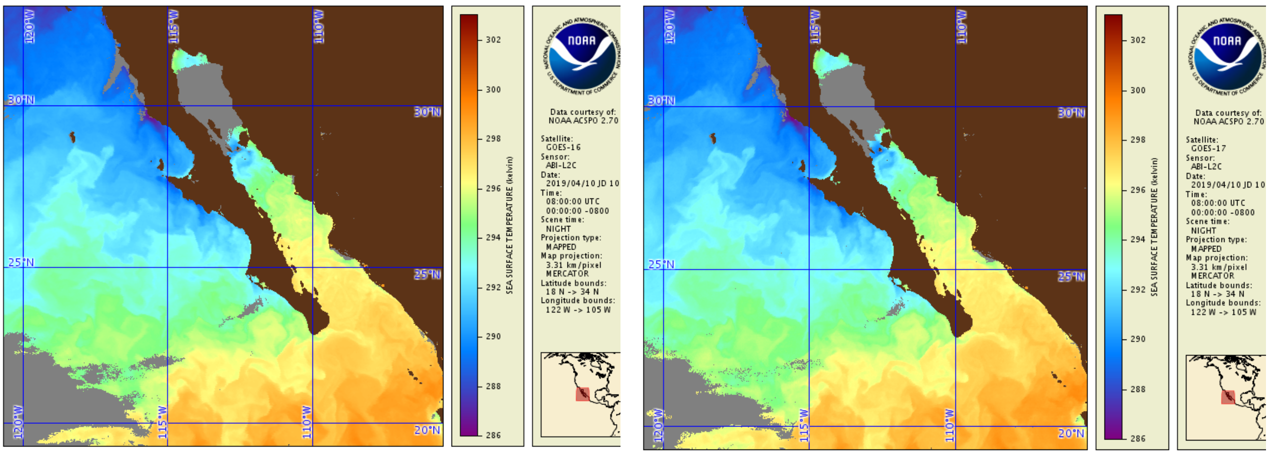

Fig. 4. ACSPO collated L2P images of the Gulf of California from G16 (left) and G17 (right) on 10 April 2019 at 0800 UTC. Note comparable SST image quality (Pennybacker et al., 2019).

5. METOP AVHRR FRAC

NOAA currently operationally produces ACSPO SST products from three Metops: Metop-A and -B are processed in OSPO, and Metop-C in STAR in a best effort mode. Processing of Metop-C commenced in STAR on 20 Dec 2018. ACSPO v2.70 was implemented in OSPO in Jun 2019. The data of three Metops are highly consistent. Validation statistics of Global Regression (GR) SST are shown in Fig. 5. The PWR SST (GR SST minus SSES bias) improves the validation statistics and cross-platform consistency.

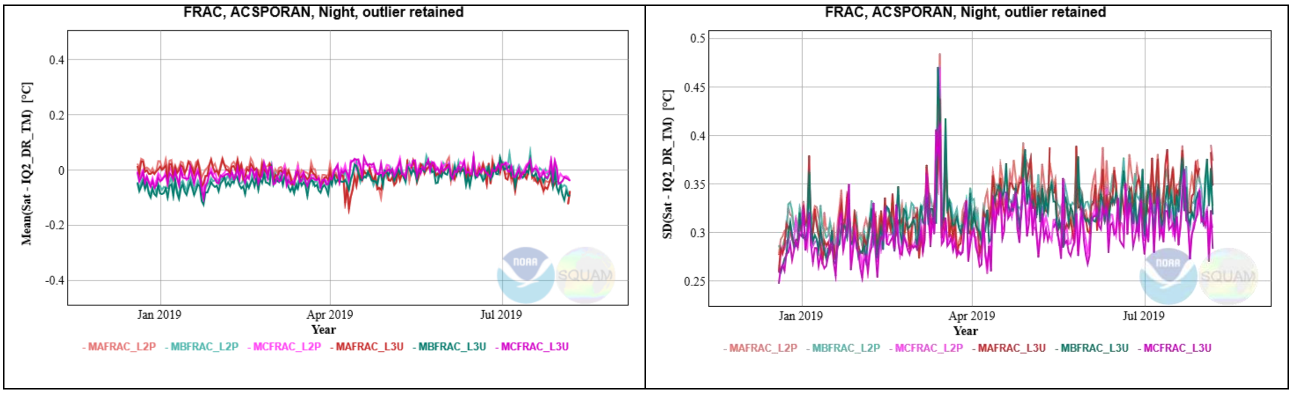

Figure 5: Time series of preliminary Metop night time SST validation statistics: (left) biases; (right) standard deviations.

Currently the Metop-A and -B data are available via NOAA Product Access and Distribution (PDA; email John Sapper if interested) and via CoastWatch web page https://coastwatch.noaa.gov/cw/satellite-data-products/sea-surface-temperature/acspo-avhrr-frac.html. Work is underway to consistently reprocess all Metop-A data from 2006-pr; Metop-B from 2012-pr; and Metop-C from 2018-pr, and discuss with the data archives their interest in ACSPO Metop data distribution to users.

6. NOAA AVHRR GAC

In June 2019, NOAA has terminated operational processing of AVHRR GAC data on-board N18 and N19, whose orbital evolution resulted in significantly degraded calibration in the IR bands used for SST retrievals. Previous reanalysis-1 (RAN1) of GAC data, performed in 2015 with data of AVHRR/3 sensors from 4 NOAA satellites (N16, 17, 18, 19) and one Metop (-A), covered a period Aug'2002-Nov'2018 (Ignatov et al., 2016). The new RAN2 is underway, to include data from older AVHRR/s (on-board N07, 09, 11, 12, and 14), and to extend the RAN2 record back to 1981, which covers the full period of the satellite SST era. An example of preliminary time series of validation bias with respect to *i*Quam buoys, obtained from N14, is shown in Fig.6.

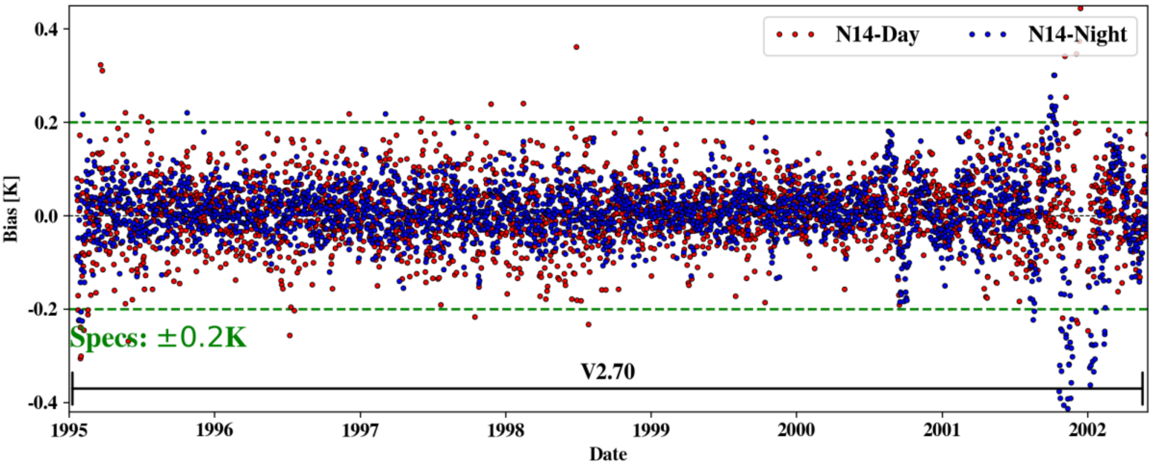

Figure 6: Preliminary nighttime ACSPO Beta-RAN2 SST validation biases produced with variable regression coefficients.

Tweaking/testing RAN2 data, including extensive QC, validation against *in situ* data, and comparisons with Pathfinder and newly released CCI L2/3/4 data, are currently underway and will be presented at the next GHRSST meeting(s). In the meantime, RAN1 data are available from the CW web page https://coastwatch.noaa.gov/cw/satellite-data-products/sea-surface-temperature/acspo-avhrr-gac.html.

7. HIMAWARI-8 AHI

ACSPO L2P/L3C SST products continue being produced at STAR in a best effort mode. The data are available from OSPO PDA and NOAA CW https://coastwatch.noaa.gov/cw/satellite-data-products/sea-surface-temperature/acspo-ahi.html (3-day and 14-day rotated buffers, respectively). Effort is underway to reprocess the full AHI record (going back to mid-2015), and archive with NASA PO.DAAC and NOAA NCEI.

8. TERRA/AQUA MODIS

ACSPO L2P/L3U SST products are produced in STAR from Terra and Aqua MODIS in an experimental mode, with a ~3 day latency. A 2-week rotated buffer is available via NOAA CW page https://coastwatch.noaa.gov/cw/satellite-data-products/sea-surface-temperature/acspo-modis.html. The data may be made available on OSPO PDA, and reprocessed by users' request.

9. CONCLUSION AND FUTURE WORK

There are several major current priorities with ACSPO, including development of improved SST and clear-sky mask algorithms; mitigation of G17 anomalies; consistent reprocessing and archival of all individual sensor products, for easy access by users. Data fusion is being explored, to generate high-quality, global collated and super-collated (L3C/S) gridded products from multiple polar platforms and sensors.

10. REFERENCES

Bouali, M., Ignatov, A., “Adaptive reduction of striping for improved sea surface temperature imagery from Suomi National Polar-Orbiting Partnership (S-NPP) Visible Infrared Imaging Radiometer Suite (VIIRS)”. JTech, 31 (1), 150-163 (2014).

Dash, P., Ignatov, A., Kihai, Y., Sapper, J., "The SST Quality Monitor (SQUAM)". *JTech*, **27**, 1899-1917, doi: 10.1175/2010JTECHO756.1 (2010).

Gladkova, I., Kihai, Y., Ignatov, A., Shahriar, F., Petrenko, B., “SST Pattern Test in ACSPO clear-sky mask for VIIRS,” *Remote Sens. Environ.*, 160, 87–98, doi: 10.1016/j.rse.2015.01.003 (2015).

Gladkova, I., Ignatov, A., Shahriar F., Kihai, Y., Hillger D., Petrenko, B., “Improved VIIRS and MODIS SST Imagery”. *Remote Sensing*, **8**(*1*), 79, doi: 10.3390/rs8010079 (2016).

Gladkova, I., Ignatov, A., Pennybacker, M., Jonasson, O., Kihai, Y. “Collated-in-time SST algorithm for GOES-R/ABI & Himawari-8/AHI,” *Remote Sens. Environ*. (2019; in review).

Gladkova, I., O., Ignatov, A., Pennybacker, M., Kihai, Y., “Towards high-resolution multi-sensor gridded ACSPO SST product: Reducing residual cloud contamination”. *Proc. SPIE 11014*, Ocean Sensing and Monitoring XI, 110140L-1; doi: 10.1117/12.2518462 (2019).

Ignatov, A., Gladkova, I., Ding, Y., Shahriar, F., Kihai, Y., Zhou, X., “JPSS VIIRS level 3 uncollated SST Product at NOAA”. *J. Appl. Remote Sens.*, **11**(*3*), 032405, doi: 10.1117/1.JRS.11.032405 (2017).

Ignatov, A., Zhou, X., Petrenko, B., Liang, X., Kihai, Y., Dash, P., Stroup, J., Sapper, J., DiGiacomo, P., "AVHRR GAC SST Reanalysis Version 1 (RAN1)". *Remote Sens.*, **8**(*315*), doi: 10.3390/rs8040315 (2016).

Jonasson, O., Ignatov, A., “Status of Second VIIRS Reanalysis (RAN2)”. *Proc. SPIE 11014*, Ocean Sensing and Monitoring XI, 110140O; doi: 10.1117/12.2518908 (2019).

Kalluri, S., Alcala, C., Carr, J., Griffith, P., Lebair, W., Lindsey, D., Race, R., Wu, X., & Zierk, S., “From Photons to Pixels: Processing Data from the Advanced Baseline Imager.” *Remote Sens.*, **10(***177*), doi: 10.3390/rs10020177 (2018).

Liang, X., Ignatov, A., “Monitoring of IR Clear-Sky Radiances over Oceans for SST (MICROS)”. JTECH, 28, 1228-1242, doi: 10.1175/JTECH-D-10-05023.1 (2011).

Mikelsons, K., Ignatov, A., Bouali, M., Kihai, Y., "A fast and robust implementation of the adaptive destriping algorithm for SNPP VIIRS and Terra/Aqua MODIS SST". *Proc. SPIE 9459*, Ocean Sensing and Monitoring VII, 94590R; doi: 10.1117/12.2177036 (2015).

Pennybacker, M., Ignatov, A., Jonasson, O., Gladkova, I., Petrenko, B., Kihai, Y., "Mitigation of the GOES-17 ABI performance issues in the NOAA ACSPO SST products". *Proc. SPIE 11014*, Ocean Sensing and Monitoring XI, 110140Q; doi: 10.1117/12.2521051 (2019).

Petrenko, B., Ignatov, A., Kihai, Y., Heidinger, A., "Clear-sky mask for the advanced clear-sky processor for oceans". *JTech*, **27**, 1609–1623, doi: 10.1175/2010JTECHA1413.1 (2010).

Petrenko, B., Ignatov, A., Kihai, Y., Stroup, J., Dash, P., "Evaluation and selection of SST regression algorithms for JPSS VIIRS". *JGR*, **119**, 4580-4599, doi: 10.1002/2013JD020637 (2014).

Petrenko, B., Ignatov, A., Kihai, Y., Dash, P., "Sensor-Specific Error Statistics for SST in the Advanced Clear-Sky Processor for Oceans". *JTech*, doi: 10.1175/JTECH-D-15-0166.1 (2016a).

Petrenko, B., Ignatov, A., Kramar, M., & Kihai, Y., "Exploring new bands in multichannel regression SST algorithms for the next generation infrared sensors at NOAA." *Proc. SPIE*, **9827**, 98270N, 12pp, doi: 10.1117/12.2229578 (2016b).

Petrenko, B, Ignatov, A., Kihai, Y., Pennybacker, M., "Optimization of sensitivity of GOES-16 ABI SST by matching satellite observations with L4 analysis." *Remote Sens., 11*(2), 206; doi: 10.3390/rs11020206 (2019).

Schmit, T.J., Griffith, P., Gunshor, M.M., Daniels, J.M., Goodman, S.J., & Lebair, W.J., "A closer look at the ABI on the GOES-R series." *BAMS*, 681-698, doi: 10.1175/BAMS-D-15-00230.1 (2017).

Xu, F., Ignatov, A., "*In situ* SST Quality Monitor (*i*Quam)". *JTech,* doi: 10.1175/JTECH-D-13-00121.1 (2014).

RDAC REPORT - NOAA/NESDIS/STAR2

Eileen Maturi[1], **Andy Harris**[2], **Gary Wick**[3] , **William Skirving**[4], **John Sapper**[5], **Robert Potash**[6]

(1) NOAA/NESDIS/STAR College Park, MD, USA, Email: Eileen.Maturi@noaa.gov
(2) University of Maryland, CISESS, College Park, MD, Email: Andy.Harris@noaa.gov
(3) NOAA/OAR/ESRL, Boulder, CO, USA, Email: Gary.Wick@noaa.gov
(4) NOAA/NESDIS/STAR College Park, MD, Email: William.Skirving@noaa.gov
(5) NOAA/NESDIS/OSPO College Park, MD, Email: John.Sapper@noaa.gov
(6) Contractor, MAXIMUS, College Park, MD, Email: Robert Potash@noaa.gov

ABSTRACT

The National Oceanic and Atmospheric Administration's (NOAA) office of the National Environmental Satellite, Data, and Information Service (NESDIS) generates operational geostationary Level-2P (L2P) Sea Surface Temperature (SST) products in GHRSST GDS2.0 format from GOES-15, Meteosat-8 and Meteosat-11 and three blended Level-4 (L4) SST analyses to satisfy the requirements of the GHRSST users.

1. INTRODUCTION

NESDIS generates SST products from Geostationary West (GOES-W) satellites on an operational basis in GHRSST format. This capability was extended to permit the generation of operational SST retrievals from the European Meteosat Second Generation (MSG) satellite; MSG-1 and 4. The five geostationary satellites (longitudes 75°W, 135°W, 140°E, 0° and 41.5°E) provide high temporal SST retrievals for most of the tropics and mid-latitudes. The goal is to improve SST product accuracy. The implementation of the physical retrieval algorithm based on a Modified Total Least Squares algorithm (*Koner et al. 2015*) generates GOES-W(15), MSG-1 and MSG-4. Because the H-8 Advanced Himawari Imager (AHI) is similar to the GOES-R Advanced Baseline Imager (ABI), the GOES R SST algorithm generates the H-8. These operational geostationary SST products are blended with the polar operational SSTs to produce daily global, high resolution SST analyses in GHRSST L4 format.

2. GEOSTATIONARY SEA SURFACE TEMPERATURE

Products GHRSST L2P SST

NOAA provides full L2P SST products for GOES W (15) as part of its operational processing. The L2P products come from ½-hourly GOES- West, North & South sectors in native satellite projection and include the full L2P ancillary fields. NOAA provides full L2P SST products for GOES W (15), MSG-1 and MSG-4 as part of routine operations. It produces the L2P product for MSG-1 and MSG-4 every 15 minutes. GOES-15 and MSG-1 and MSG-4 L2P products contain the full L2P ancillary fields as required by the GHRSST Data Specification GSD2.0 format. MSG-1 and MSG-4 include diurnal warming estimates as part of the ancillary field but not Himawari-8. Table 1 lists the NOAA GHRSST operational geostationary SST L2P products with their area of coverage and frequency.

Table 1 - NOAA GHRSST Operational Geostationary SST L2P data for GOES-15, MSG-1 and MSG- 4.

SATELLITE	AGENCY	AREA	FREQUENCY
GOES-15	NOAA	N-HEM Sector S-HEM Sector	Every 30 min Every 30 min
MSG-1	Indian Ocean (EUMETSAT)	Full Disk	Every 15 min
MSG-4	EUROPE (EUMETSAT)	Full Disk	Every 15 min

3. BLENDED SST ANALYSES

Operational SST retrievals from both NOAA and non-NOAA geostationary and polar-orbiting satellites produce an operational daily global, high resolution 5km blended SST analyses and a global, high resolution 5km SST Nighttime Only Analysis and a Diurnally Corrected Analysis (*Maturi, et al 2017*). These analyses are both generated in GHRSST L4 in GSD2.0 format. Figures 1 shows the global 5km Geo-polar GHRSST L4 analysis product for day and night. Night time only and diurnally corrected analyses are also available and will show no difference in coverage. Figure 2. The analysis employs a rigorous multiscale optimum interpolation (OI) methodology that approximates the Kalman filter, together with a data-adaptive correlation length scale, to ensure a good balance between detail preservation and noise reduction. Quad-tree downscaling for efficiency is performed in the analysis.

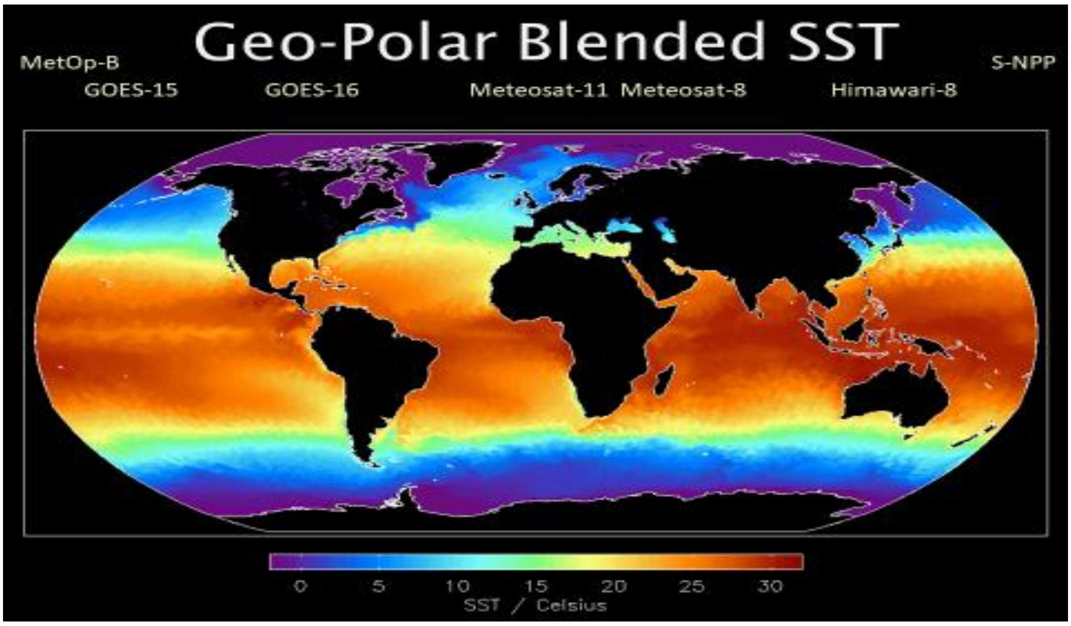

Figure 1: the daily 5 km global Geo-polar SST analysis for day and night.

Data from 24 hours of geostationary and polar-orbiting sea surface temperature satellite retrievals (Metop-B, GOES-E/W, Himawari-8 and Meteosat-11 and Meteosat-8) produce these daily global 5km Geo-polar SST analyses. These analyses do not use surface measurements and buoy data.

The blended SST analysis takes in the level 2 data processed using two different algorithms.

- Geostationary
- -------------------
- GOES-16: 24 images (1 per hour) ACSPO regression algorithm
- Himawari-8/9: 24 images (1 per hour) ACSPO regression algorithm
- Meteosat-11: 96 images (4 per hour) physical retrieval algorithm
- Meteosat-8: 96 images (4 per hour) physical retrieval algorithm
- GOES-15: 96 sectors (4 per hour) physical retrieval algorithm
-
- Polar-Orbiter (ACSPO regression algorithm)

- -----------------
- S-NPP VIIRS: ~14 orbits (24 hours' worth)
- JPSS-1 VIIRS: ~14 orbits (24 hours' worth)
- Metop-B: ~14 orbits (24 hours' worth)
-
- Other
- --------
- Thinned OSTIA (1 in 5 samples, 1 in 5 rows)

- Notes:
- 1) For the geostationary data, very few images are entirely day or night, and the fraction of nighttime data varies with local time
- 2) For the geostationary data, the number ingested is a maximum (there are often a few missing images each day)
- 3) For the GOES-15 data, there are North & South sectors, so the effective coverage is 2 images per hour
- 4) GOES-15 is currently used because of the problems with GOES-17
- 5) Meteosat-8 is at 41.5 E, and covers much of the Indian Ocean
- 6) The polar-orbiting data are more cleanly split between day & night, so the ~14 orbits are more like half-orbits
- 7) The thinned OSTIA do have AMSR-2 MW data, but are generally swamped by the other data sources, except in regions of persistent cloud cover

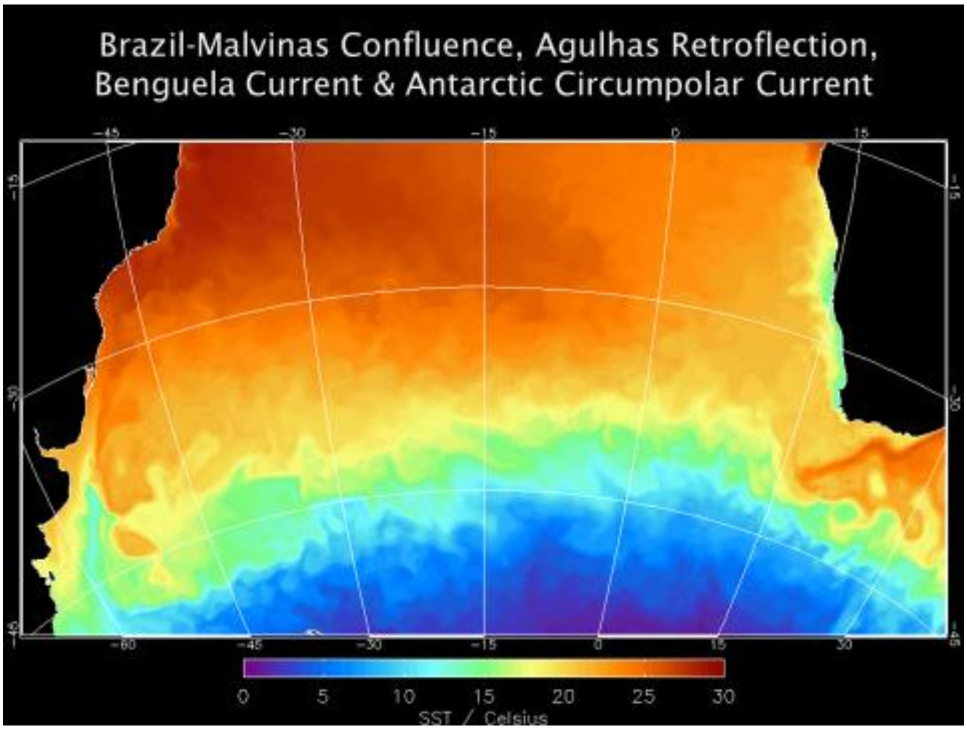

Figure 2: the geo-polar blended 5km SST Analysis for the Brazil-Malvinas Confluence, the Agulhas Retroflection, and the Benguela Current & Antarctic Circumpolar Current.

4. MAIN ACTIVITIES

The main activities for the STAR2 SST team include the operational implementation of the following products: 1) GHRSST L2P AMSR-2 SSTs; 2) the Global 5km Geo-polar diurnally corrected SST analysis; 3) generation of Meteosat-11 and Meteosat-8; 4) Inclusion of Meteosat-8 and Meteosat-11 SST into the SST Analysis; 5) inclusion of S-NPP VIIRS and JPSS-1 VIIRS into the SST analysis and; 6) Reprocessing of the SST Analysis

Reprocessed GHRSST L4 products

Geostationary SST and polar-orbiting SST data have been reprocessed for 2002-2016.

The global 5km day/night Geo-polar SST analyses (using the reprocessed geostationary and polar-orbiting data) were reprocessed in GHRSST L4 format for the years 2002-2016. This requires reprocessed geostationary data (GOES-E/W, MSG, MTSAT) (MTLS + Bayesian) using ACSPO reprocessed AVHRR GAS-resolution (NOAA and Metop) OSTIA bias correction reference (OSTIA RAN + Operational).

We currently reprocess 1995 to 2002 (GOES-E/W) data for reprocessing of the SST Analysis.

Other Systems and Services

The blended SST Analysis provides a 0.5 degree, daily, gap-free SST product for day/night, night-only and diurnally corrected products.

CoralTemp and the Ocean Heat Content (OHC) products use this blended SST analysis. CoralTemp forms the basis of the Coral Reef Watch heat stress product suite which NOAA provides as an operational product.

The OHC is fully operational. Figures 3 through 7 show the suite of OHC products for the North Atlantic Basin. NOAA also generates a suite of ocean heat products for the North Pacific and South Pacific.

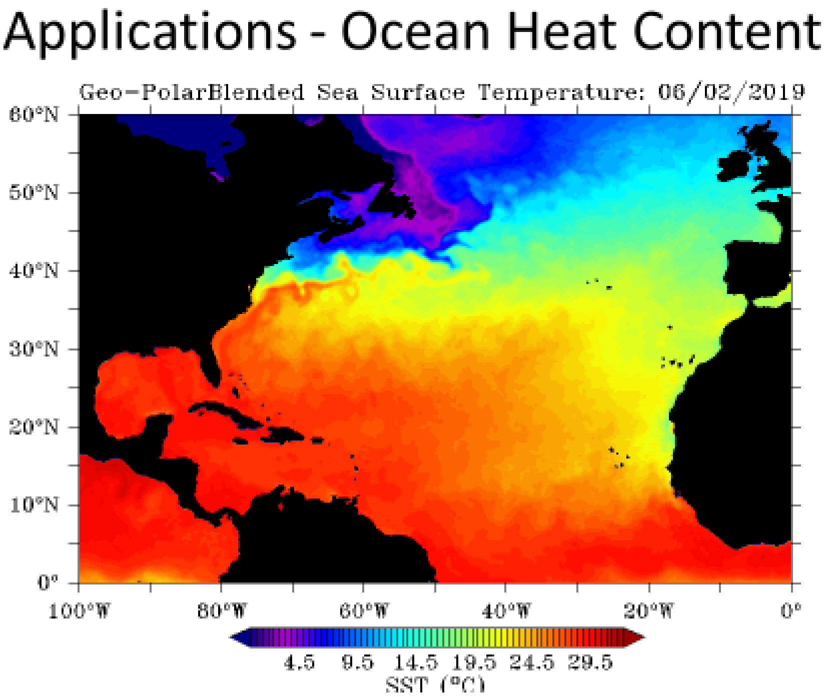

Figure 3: the Geo-Polar Blended SST used to generate the Ocean Heat Content product for the North Atlantic Basin

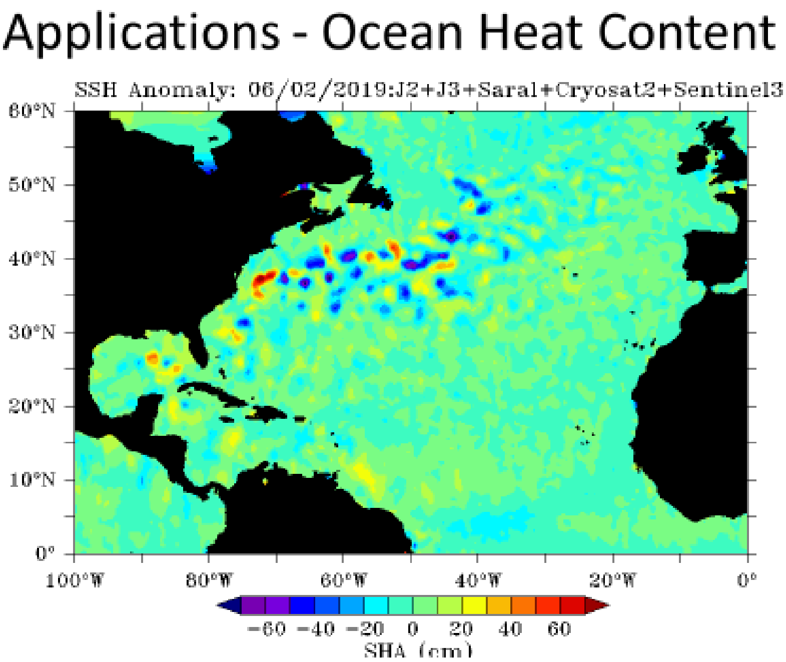

Figure 4: Sea Surface Height (SSH) generated from the altimeters Jason 2 and 3, Saral, Cryosat-2 and Sentinel-3 for the North Atlantic Basin.

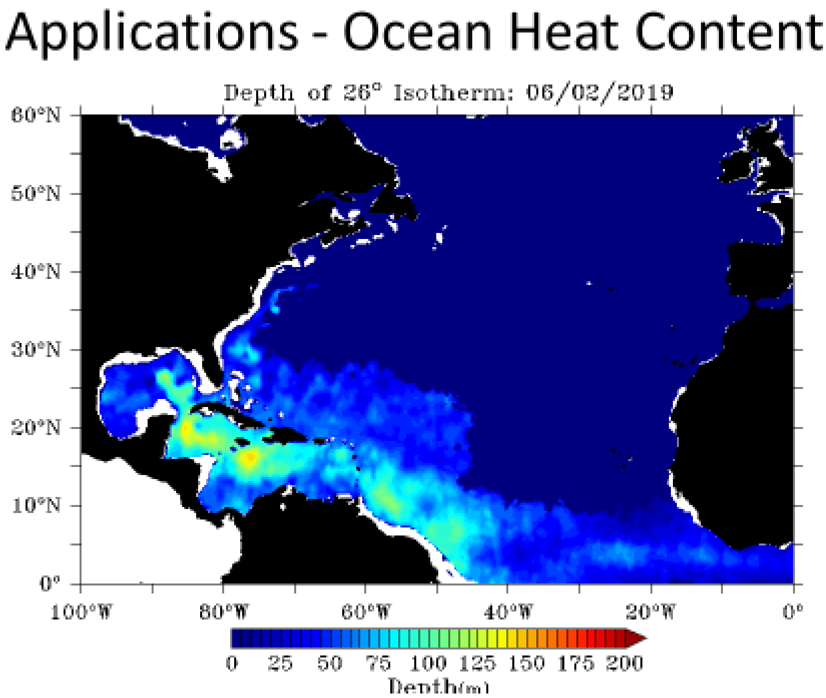

Figure 5: The depth of the 26 degree isotherm for the North Atlantic Basin.

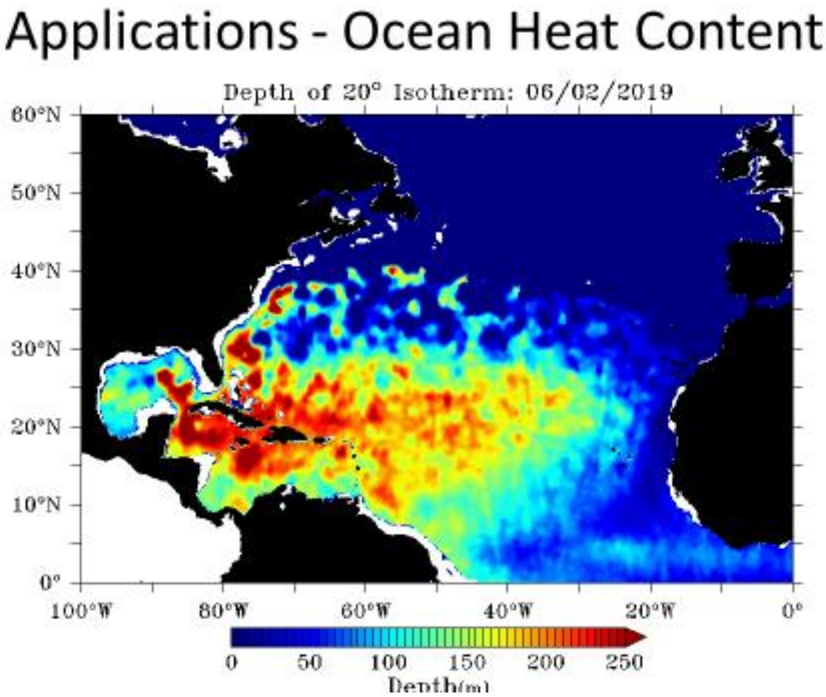

Figure 6: The depth of the 20 degree isotherm for the North Atlantic Basin.

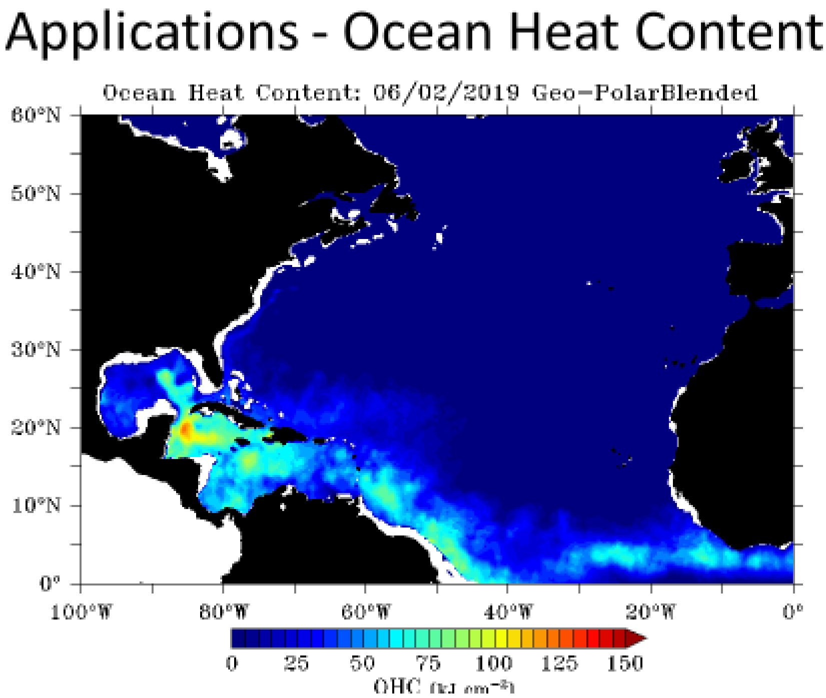

Figure 7: The Ocean Heat Content Product for the North Atlantic Basin.

5. DATA AVAILABILITY

All the GHRSST L2P and L4 SST products are currently produced operationally at NOAA/NESDIS and are pulled by NASA's Jet Propulsion Laboratory (JPL) Physical Oceanography (PO): Distributed Active Archive Center (DAAC) in real time. After thirty days, the National Centers for Environmental Information (NCEI) in Silver Spring, Maryland pulls the data from NASA JPL PO: DAAC into their stewardship archive where it is archived and set up for user data access.

6. CONCLUSION

The GHRSST geostationary SST and blended SST Analyses products provide to the GHRSST user community a uniquely powerful data set for studying SST making it possible to study such effects as diurnal warming of the ocean surface and the evolution of mesoscale features such as fronts and eddies. The temporal and increased data coverage of the geostationary satellites and the gap free SST analyses provides reliable, accurate data coverage in important oceanographic,meteorological, and climactic regions.

Currently we bias-correct the Geo-Polar Blended 5km SST Analysis using every 5th row and every 5th line from the Non-Real Time (NRT) Operational Sea Surface Temperature and Sea Ice Analysis (OSTIA) Level 4 SST. Coral Reef Watch has suggested the possibility of creating inaccuracies over coral reefs due to use of interpolated values. They consider the L2 product as better for bias correction. We are currently investigating this issue and will continue to work with Coral Reef Watch to improve the CoralTemp product.

7. FUTURE WORK

We plan to do the following: (1) perform regional bias corrections using Sentinel 3; (2) generate ~1km regional Geo-polar SST analysis for specified regions; (3) generate Lake SSTs in GHRSST L2P format; and 4) generate Geostationary Frontal SST product in GHRSST format.

8. REFERENCES

Koner, P., A. Harris, and E. Maturi, "A physical deterministic inverse method for operational satellite remote sensing: an application for SST retrievals," IEEE Transactions on Geoscience and Remote Sensing, Volume 53, Issue 11, pages 1-17, NOVEMBER, 2015.

Maturi E, Harris A, Mittaz J, Sapper J, Wick G, Zhu X, Dash P, Koner P (2017), "A New High-Resolution Sea Surface Temperature Blended Analysis," Bull Amer Meteor Soc 98(5): 1015-1026 [doi: 10.1175/BAMS-D-15-00002.1]

RDAC UPDATE: NOAA/NCEI

H-M Zhang

THE SATELLITE APPLICATION FACILITY ON OCEAN AND SEA ICE (OSI SAF)

S. Saux Picart[1] & OSI SAF team

(1) Météo-France, Lannion, France, Email: stephane.sauxpicart@meteo.fr

1. INTRODUCTION

The EUMETSAT Satellite Application Facilities (SAFs) are dedicated centres of excellence for processing satellite data. They form an integral part of the distributed EUMETSAT Application Ground Segment. The Ocean and Sea Ice SAF has the responsibility of developing, validating and distributing near real time products of Sea Surface Temperature (SST), radiative fluxes, wind and Sea Ice for a variety of platforms/sensors.

The OSI SAF consortium includes Meteo-France, as leading institute, and the following co-operating institutes : MET Norway (Norway), DMI (Denmark), Ifremer (France), KNMI (Netherlands).

The OSI SAF production is divided between three subsystems:

- Low and Mid latitude (LML) Centre, under Météo-France responsibility, processes and distributes the SST and Radiative Fluxes products covering LML, North Atlantic Regional (NAR) and Global areas. Ifremer contributes to the products distribution and archiving,
- High Latitude (HL) Centre, under MET Norway responsibility with the co-operation of DMI, processes and distributes the Global Sea Ice products, the High Latitude SST and the High Latitude Radiative Fluxes,
- Wind (WIND) Centre, under KNMI responsibility, processes and distributes the Wind products.

2. OSI SAF PRODUCTS

The OSI SAF develops, processes and distributes, in near real-time, products related to key parameters of the ocean-atmosphere interface: sea-ice concentration, edge, type, emissivity, drift, surface temperature, radiative fluxes, wind speed and direction, and sea surface temperature.

2.1. OPERATIONAL SST PRODUCTS

OSI SAF operational SST production is using data from meteorological satellites of the EUMETSAT polar orbiting program Meteorological Operational (Metop) and geostationary program Meteosat Second Generation (MSG), and on satellite from the American NOAA polar orbiting program and geostationary program.

2.1.1. Low Earth orbiting satellites production

Currently OSI SAF is processing data from the Advanced Very High Resolution Radiometer (AVHRR), the Infrared Atmospheric Sounding Interferometer (*IASI*) on-board Metop-B and from the Visible Infrared Imaging Radiometer Suite (VIIRS) on-board Suomi-NPP. SST and Ice Surface Temperature products are listed in the table below.

Product ID	Instrument	Coverage
OSI-201-b	METOP-B/AVHRR	L3 global on a 0.05 ◦ grid/12 hourly
OSI-202-b	METOP-B/AVHRR and SNPP/VIIRS	L3 North Atlantic Region/6 hourly
OSI-203	METOP/AVHRR, NOAA/AVHRR	L3 poleward of 50N/12 hourly
OSI-203-a	METOP-B/AVHRR	L3 poleward of 50N/12 hourly (SST + IST)
OSI-203-b	NPP/VIIRS	L3 poleward of 50N/12 hourly (SST + IST)
OSI-204-b	Metop-B/AVHRR	L2P global 1km
OSI-205-a	METOP-B/AVHRR	L2 poleward of 50N/50S (SST + IST)
OSI-205-b	NPP/VIIRS	L2 poleward of 50N/50S (SST + IST)
OSI-208-b	METOP-B/IASI	L2P global 12 to 40km

2.1.2. From geostationary satellites

OSI SAF is currently processing data from three geostationary satellites: GOES-16 which is in East position (75W), Meteosat-11 (MSG4) in 0E position and Meteosat-8 (MSG1) over Indian Ocean in 41.5E. Note that the Indian Ocean products is currently produced on best effort basis (this means that production may stop if the server is down – no backup).

Products are Level-3 one hourly composites mapped onto regular latitude-longitude 0.05° grids.

Product ID	Instrument	Coverage
OSI-206-a	Meteosat-11/SEVIRI	L3C 0.05° grid/hourly
OSI-207-a	GOES-16/ABI	L3C 0.05° grid/hourly
OSI-IO-SST	Meteosat-8/SEVIRI	L3C 0.05° grid/hourly

2.1.3. Quality assessment

SST products are quality assessed using in situ data, mostly coming from drifting buoys measurements and collected through the Global Telecommunication System (GTS). For each sensor a Match up Data Set (MDS) is assembled. It contains satellite and in situ observation collocated in time and space as well as some intermediate variables of the processing and brightness temperature simulations.

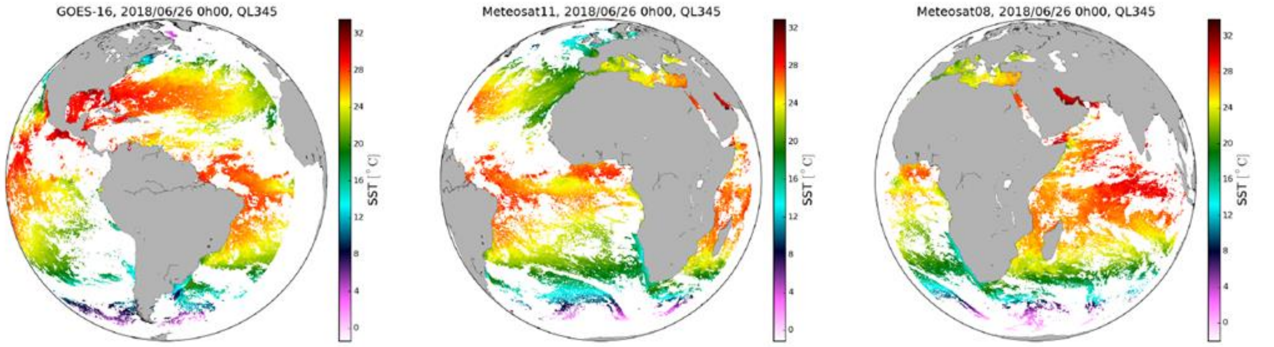

Figure 1: SST from GOES-16, Meteosat-11 and Meteosat-8 at 0h00 on 2018/6/26

Validation is routinely performed using MDS with a five days delay with respect to near real time data production to ensure most in situ data are captured. Monthly operational validation results are accessible through the OSI SAF website (http://osi-saf.eumetsat.int) as well as validation reports which are updated every time a major change occurs in the processing (new sensor, change in the retrieval methodologies or input data).

2.2. SST REPROCESSING ACTIVITIES

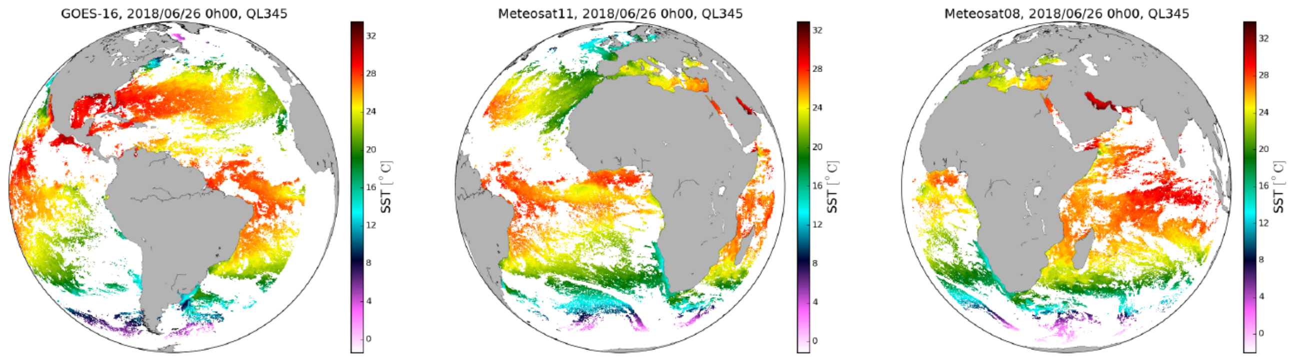

Figure 2: SST from GOES-16, Meteosat-11 and Meteosat-8 at 0h00 on 2018/6/26

OSI SAF has achieved a consistent reprocessing of SST from the MSG/SEVIRI archive from 2004 to 2012 (corresponding to operational phases of Meteosat-8 and Meteosat-9). The dataset is available to user via means described in the Data access section.

3. MAIN ACTIVITIES SINCE G-XIX

Since GHRSST XIX several activities have been carried out according to OSI SAF project plan. This include:

- New operational SST products based on GOES-16 and Meteosat-11. These should become operational by the end of 2019.
- New operational SST and IST products for high latitudes: now include Metop-B and NPP.
- Processing Metop-C/AVHRR: global L2P and L3C SST are produces but not distributed. Operational dissemination of these is expected at the end of 2019.
- Introduced probabilistic classifier in addition to the PPS for high latitude SST and IST processing.

- Development of new GEO SST processing chain

Some activities related to OSI SAF products have also taken place:

- Production of data record of the Arctic and Antarctic Ice Surface Temperatures from AVHRR thermal Infrared satellite sensors (AASTI), 1982-2015
- Produced IST monthly climatology.

4. DATA ACCESS

OSI SAF data are freely accessible to anyone via several means (ftp, EUMETCast, thread server,…). Data are also available through the Physical Oceanography Distributed Active Archive Center (PODAAC) at http://podaac.jpl.nasa.gov, and the data discovery tool exists: Naiad (http://naiad.ifremer.fr).

More information on data access can be found on the OSI SAF website: http://osi-saf.eumetsat.int

5. CONCLUSION

OSI SAF production is in constant evolution due to the changing satellite capabilities, in particular new satellite missions. The major changes in the coming decade are related to the launch of EUMETSAT new generation sensors such as METImage on-board Metop-Second Generation platforms, and the Flexible Combined Imager (FCI) on the third generation of geostationary satellites of the program Meteosat Third Generation (MTG). These new generation sensors will be launch by 2022 and it is expected that they will allow for better SST products with for instance higher spatial resolution.

RDAC UPDATE: RSS

Chelle Gentemann

REPORT FROM MISST

Chelle Gentemann

CHINA OCEAN SATELLITE AND APPLICATION SERVICE

Qimao Wang[(1)], Lijian Shi[(1)], Xiaomin Ye[(1)]

(1) National Satellite Ocean Application Service, Beijing, China, Email: qmwang@mail.nsoas.org.cn

1. INTRODUCTION OF NSOAS

National Ocean Satellite Application Center (NSOAS) is a public-interested institutional organization under the jurisdiction of Ministry of Natural Resources of the People's Republic of China, mainly responsible for development of ocean satellite series and satellite ocean applications. NSOAS provides public services for ocean economy, ocean management, ocean safety. Established in 1996, the predecessor of NSOAS was State Oceanic Administration ocean satellite integrative system design department. In September 2000, approved by State Commission Office for Public Sector Reform China, NSOAS was officially founded.

The main responsibilities of NSOAS includes: to make strategy and development program for Chinese oceanic satellites, to build up ground segment for Chinese oceanic satellites, to fulfill scientific researches on oceanic satellite and satellite oceanic application, to be responsible for receiving, processing, distributing and application of oceanic satellite data.

2. CHINA OCEAN SATELLITE

The ocean satellite planning of China is developing Chinese ocean satellite in three series, they are the ocean colour environment satellite (HY-1), ocean power ocean dynamic environment satellite (HY-2) and ocean radar satellite (HY-3), making these three series satellites regular, long-time and continuously operation, meeting ocean monitoring modernization, scientific, informational globalization requirement, proving service to ocean environment monitoring, maritime rights safeguarding and disaster prevention and mitigation, national economy and national defence construction.

HY-1 Satellite is ocean colour satellite, it is used for obtaining offshore and global ocean colour and temperature and coastal zone dynamic change. Its main remote sensing loads are ocean colour scanner and coastal zone imager. This series satellite is used to observe sea optical characteristics, chlorophyll concentration, sea surface temperature, river estuarial coastline and sediment source evolvement. China's first ocean satellite HY-1A was launched on 15 May 2002 and stopped working on 2004. China's second ocean satellite HY-1B was launch on Apr. 11, 2007 and stopped working on 2016, almost 9 years. The third ocean satellite HY-1C was launch on Sept. 7, 2018. It is equipped with the China Ocean Colour and Temperature Scanner (COCTS) and Coastal Zone Imager (CZI), as well as an ultraviolet imager, spectrometer and a satellite-based automatic identification system (AIS) receiver payload for receiving transmissions from AIS-equipped vessels for ship tracking.

Table1 Detailed information of sensors of HY-1C

Sensor	band	Resolution	Swath
COCTS	10	1100 m	≥2900km
CZI	4	50 m	≥950km
UVI (Ultraviolet imager)	2	550/1100 m	
SCS (Satellite calibration spectrometer)	10	550/1100 m	≥11 km
AIS	4	——	950 km

HY-2 Satellite is marine dynamic environment satellite, it is used for all-weather, all-aerospace obtaining the information of Chinese offshore and global sea surface wind field, sea surface height, significant wave heights and sea surface temperature. Its remote sensing payloads include microwave scatterometer, radar altimeter, scanning microwave radiometer, calibration microwave radiometer and *etc.* China’s first ocean dynamic satellite, HY-2A was launched on August 16, 2011. The second ocean dynamic satellite, HY-2B was launched on Oct. 25, 2018. The satellite is expected to remain operational for five years.

HY-3 carried C band SAR (synthetic aperture radar) and it is used to observe the sea ice, oil spill, wind field, wave information, internal wave, *etc.* The first satellite of HY-3 will be launched in 2020.

3. DATA AND ITS APPLICATION

3.1. APPLICATION IN OCEAN DISASTER PREVENTION AND REDUCTION

HY-2 satellite has the abilities of identifying marine storm strength and location, direction and structure, can observe 90% of the global region every day. It also can nearly capture all global cyclones.

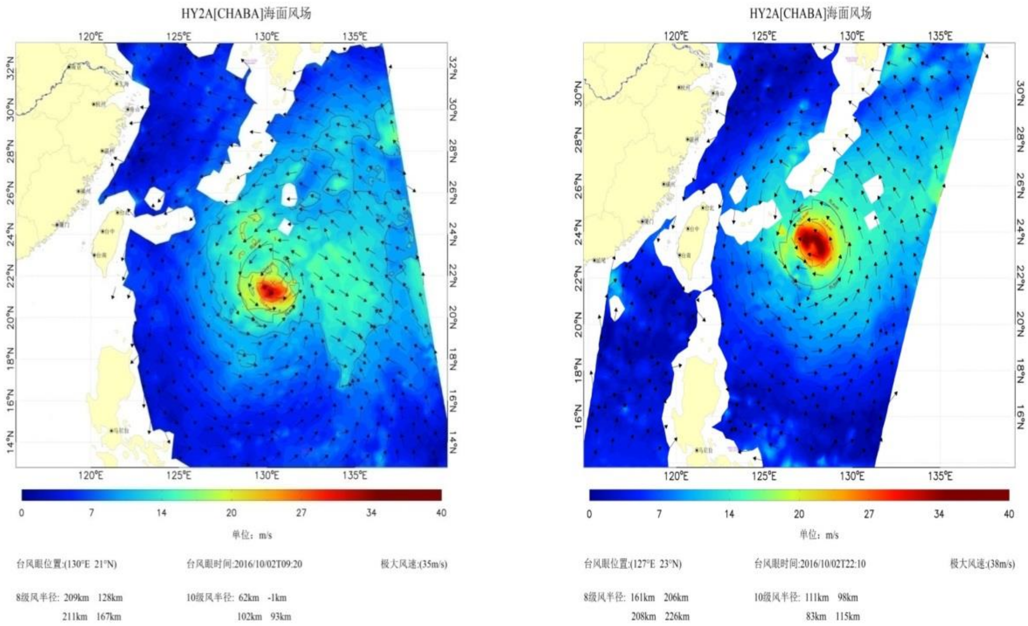

Figure 1: Sea surface wind of the super typhoon Chaba, the 18th typhoon in 2016

3.2. MARINE ENVIRONMENT MONITORING AND FORECAST

The Northwest Pacific sea surface temperature data captured by scanning microwave radiometer has been brought into the ocean environment information broadcast system of National Oceanic Environment Prediction Center. It provides the important sensing observation data for CCTV13 ocean environment broadcast. Meanwhile, Northwest Pacific wind field data captured by microwave scatterometer will be brought into broadcast system and public. In addition, the wave height and wind speed captured by radar altimeter will be brought into ocean environment broadcast system.

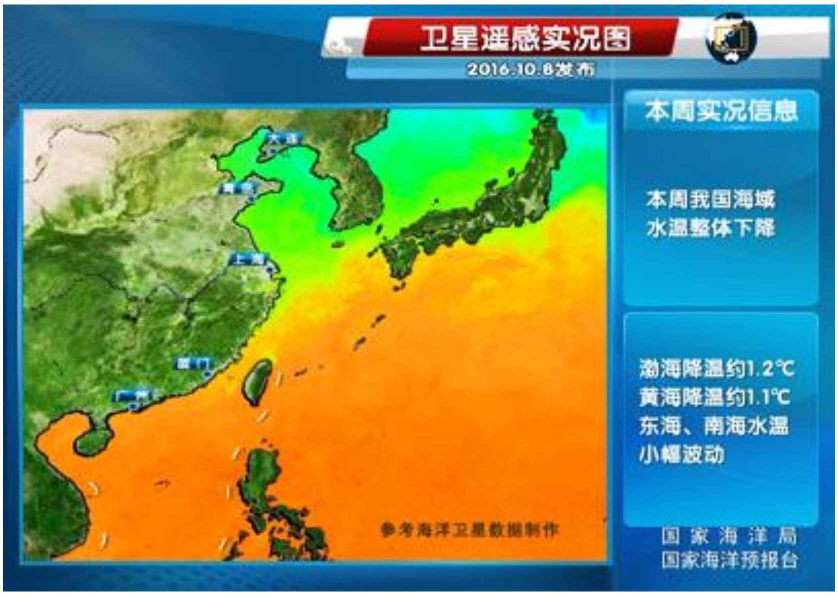

Figure 2: Sea surface temperature over northwest Pacific

3.3. OCEANIC FISHERY

Hy-2 radar altimeter and scanning microwave radiometer can identify oceanic front and meso-scale eddy, to detect the fishery. The radar altimeter, microwave scatterometer and microwave radiometer can provide meteorological support to the oceanic fishery.

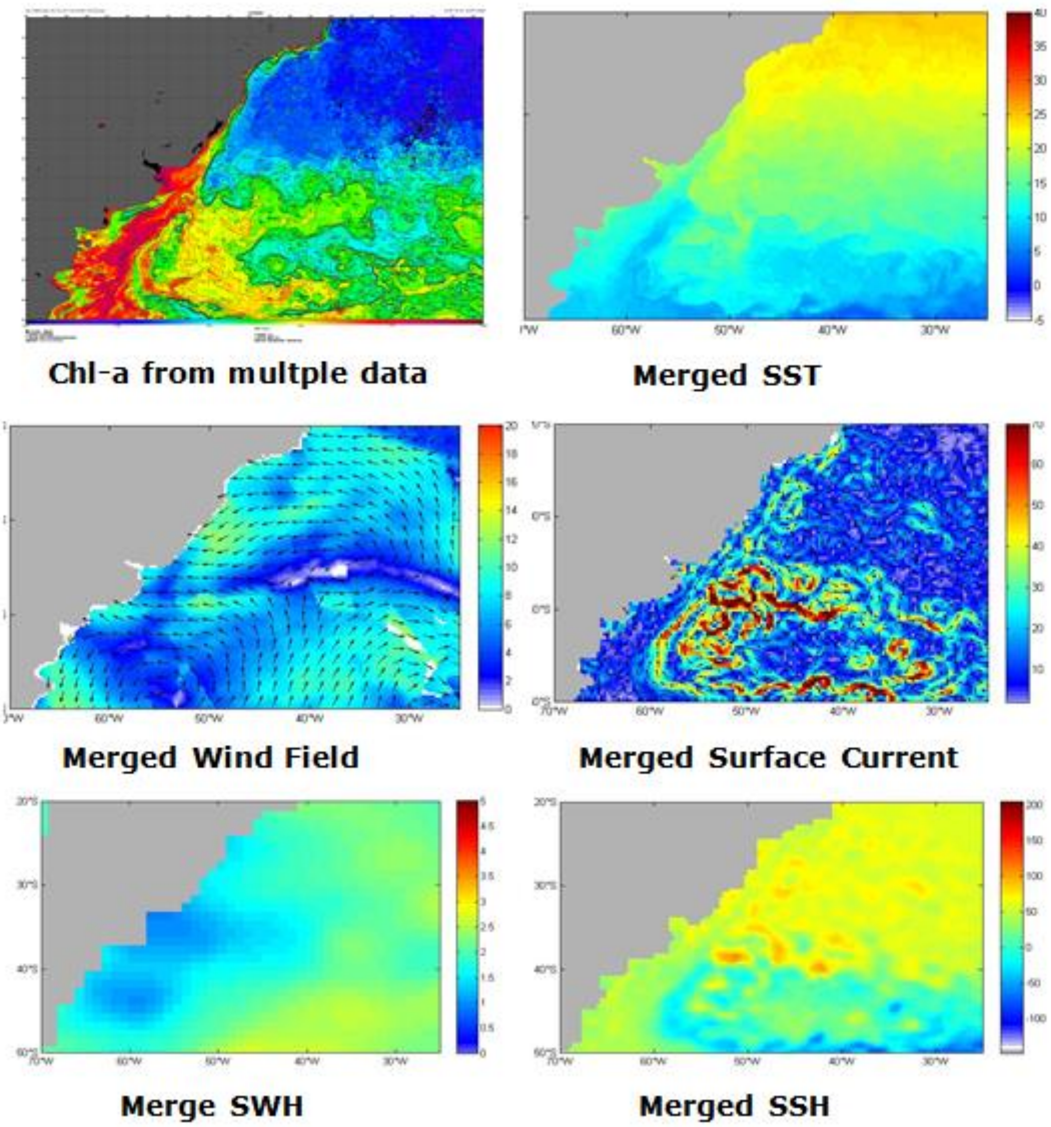

Figure 3: Ocean environmental information for oceanic fishery

PLENARY SESSION III: PASSIVE MICROWAVE MEASUREMENTS

SESSION III REPORT

Chair: Chelle Gentemann [(1)]; Rapporteur: Craig Donlon [(2)]

(1) Earth and Space Research, USA, Email: cgentemann@esr.org
(2) European Space Agency/ESTEC, The Netherlands, craig.donlon@esa.int

1. INTRODUCTION

This is a short summary of session III which featured three oral presentations and an open discussion.

- Recent Improvements in AMSR2 Sea Surface Temperature Products -- Misako Kachi, Hideyuki Fujii, Akira Shibata, and Yukio Kurihara, JAXA/EORC
- Determining the AMSR-E SST Footprint from Co-Located MODIS SSTs – Brahim Boussidi, Peter Cornillon, Gavino Puggioni, and Chelle Gentemann, U. Rhode Island, USA
- Use of Copernicus Imaging Microwave Radiometer (CIMR) in the Baltic Sea -- Jacob Høyer, Mads Hvid Ribergaard and Emy Alerskans, Danish Meteorological Institute Denmark
- Open discussion

2. RECENT IMPROVEMENTS IN AMSR2 SEA SURFACE TEMPERATURE PRODUCTS - MISAKO KACHI, HIDEYUKI FUJII, AKIRA SHIBATA, AND YUKIO KURIHARA, JAXA/EORC

- AMSR3 expected to complete System Definition Review (SDR) in mid-JFY2019.
- AMSR3 like AMSR2 design with possible addition of 166 GHz and 183 GHz
- Orbit 666 km altitude and 13:30 LT in ascending node
- AMSR2 status – small trend in bias since 2018 due to TB drifts possible aging of sensor linearity
- Evaluating 3-frequency channel to retrieve SST closer to coastline

3. DETERMINING THE AMSR-E SST FOOTPRINT FROM CO-LOCATED MODIS SSTS - BRAHIM BOUSSIDI, PETER CORNILLON, GAVINO PUGGIONI, AND CHELLE GENTEMANN, U. RHODE ISLAND, USA

- Aqua satellite carries both AMSR-E with a 56x56 km^2 footprint sampled every 10 km and MODIS with a 1 km^2 footprint
- Objective: to deconvolve the AMSR-E field to obtain a true 10km^2 resolution SST from AMSR-E using coincident MODIS SSTs in cloud-free areas
- Correct footprint valuable for comparisons with other SST fields

4. USE OF COPERNICUS IMAGING MICROWAVE RADIOMETER (CIMR) IN THE BALTIC SEA - JACOB HØYER, MADS HVID RIBERGAARD AND EMY ALERSKANS, DANISH METEOROLOGICAL INSTITUTE DENMARK

- CIMR ~95% global coverage in 1 day and no 'hole at the pole'
- Sea ice concentration, SST (15 km), SSS, wind, soil moisture, terrestrial snow extent

- Improved spatial resolution will substantially improve the number of retrievals near coastlines, especially in regions with complex coastlines (*e.g.* Baltic Sea)
- CIMR will improve the use of PMW SSTs for coastal and shelf seas
-

5. DISCUSSION

RECENT IMPROVEMENTS IN AMSR2 SEA SURFACE TEMPERATURE PRODUCTS

Misako Kachi[(1)], Hideyuki Fujii[(2)], Akira Shibata[(3)], and Yukio Kurihara[(4)]

(1) Japan Aerospace Exploration Agency, Tsukuba, Japan, Email: kachi.misako@jaxa.jp
(2) Japan Aerospace Exploration Agency, Tsukuba, Japan, Email: fujii.hideyuki@jaxa.jp
(3) Remote Sensing Technology Center of Japan, Tsukuba, Japan, E-mail: shibata_akira@restec.or.jp
(4) Japan Aerospace Exploration Agency, Tsukuba, Japan, Email: kurihara.yukio@jaxa.jp

1. INTRODUCTION

Passive microwave imager has great advantages in its all-weather and day-and-night observation capabilities compared to infra-red imager, while its spatial resolution is coarse – several tens of kilometres. Sea surface temperature (SST) retrievals in passive microwave imager uses C-band (around 7 GHz) or X-band (around 10 GHz), which are sensitive to subskin SST. The Advanced Microwave Scanning Radiometer 2 (AMSR2) on board the Global Change Observation Mission – Water (GCOM-W) has a bigger antenna, size of 2.0 m and has both 6.9 GHz and 10.65 GHz channels among other passive microwave imagers. JAXA produces several sea surface temperature (SST) products from AMSR2 and applied those algorithms to other passive microwave imagers such as the Global Precipitation Measurement (GPM) Microwave Imager (GMI), WindSat and AMSR-E (AMSR for EOS). The current version of AMSR2 SST is Version 3, which was released in March 2017. Although the current AMSR2 6.9 GHz and 10.65 GHz SSTs achieved the required standard for accuracy when compared with in-situ data, they still have some issues to be solved in future version updates.

In this paper, recent improvements in AMSR2 SST retrievals for future Version 4 are introduced.

2. GCOM-W AND AMSR2

The Global Change Observation Mission (GCOM) provided by the Japan Aerospace Exploration Agency (JAXA) consists of two satellite missions: GCOM-W (Water) and GCOM-C (Climate).

The GCOM-W (or "SHIZUKU") satellite was launched in May 2012 and carries the Advanced Microwave Scanning Radiometer 2 (AMSR2). AMSR2 is a multi-frequency, total-power microwave radiometer system with dual polarization channels for all frequency bands (Imaoka *et al.*, 2010). AMSR2 is a successor of JAXA's Advanced Microwave Scanning Radiometer for EOS (AMSR-E) on NASA's Aqua satellite, which was launched in May 2002. The basic concept of AMSR2 is almost identical to that of AMSR-E. The GCOM-W1 satellite was launched from JAXA Tanegashima Space Center on 18th May 2012 (JST) and has started scientific observation since 3rd July 2012. The GCOM-W satellite has joined A-train orbit since 29 June 2012 (Kasahara *et al.*, 2012).

The GCOM-C (or "SHIKISAI") satellite was launched in December 2017 and carries the Second-generation Global Imager (SGLI). SGLI is a versatile, general purpose optical and infrared radiometer system covering the wavelength region from near ultraviolet to infrared.

Both GCOM satellites aim to provide comprehensive information of the Climate Change Observing System (GCOS) Essential Climate Variables (ECVs) of atmosphere, ocean, land, cryosphere and ecosystem to contribute water cycle and climate change studies as well as operational applications, such as weather services and fisheries.

Table 1 is the specification of the GCOM-W and GCOM-C satellites. The GCOM-W satellite was injected in front of the Aqua satellite to keep continuity of AMSR-E observations and provide synergy with the other A-Train instruments and satellites, such as Aqua and CloudSat, for new Earth science researches. Table 2 shows the instrument characteristics of AMSR2, and Table 3 is a list of the channel set of AMSR2. AMSR2 has almost identical frequency channel set to that of AMSR-E except for the additional 7.3 GHz channel to help Radio Frequency Interference (RFI) mitigation. In addition, AMSR2 has a deployable main reflector system with 2.0 m diameter while AMSR-E has that with 1.6 m diameter. Two-point external calibration with the improved hot-load are introduced to AMSR2, and a redundant momentum wheel is added to increase reliability.

Satellite	GCOM-W	GCOM-C
On-board instrument	Advanced Microwave Scanning Radiometer-2 (AMSR2)	Second generation Global Imager (SGLI)
Orbit	Sun Synchronous orbit	Sun Synchronous orbit
Altitude	699.6 km (on Equator)	798 km (on Equator)
Inclination	98.2 degrees	98.6 degrees
Local Time	13:30 +/- 15 min (at ascending node)	10:30 +/- 15 min (at descending node)
Launch	18 May 2012 by H-IIA Rocket	23 December 2017 by H-IIA Rocket
Design Life	5-years	5-years

Table 1: Satellite Specification of GCOM-W and GCOM-C

Scan and rate	Conical scan at 40 rpm
Antenna	Offset parabola with 2.0 m diameter
Swath width	1450 km (nominal) 1617 km (effective)
Incidence angle	Nominal 55 degrees
Polarization	Vertical and horizontal

Table 2: AMSR2 Instrument Characteristics

Centre Frequency [GHz]	Band width [MHz]	Pol.	Beam width [deg] (Ground resolution [km])	Sampling interval [km]
6.925/7.3	350	V/ H	1.8 (35 x 62)	10
10.65	100		1.2 (24 x 42)	
18.7	200		0.65 (14 x 22)	

23.8	400		0.75 (15 x 26)	
36.5	1000		0.35 (7 x 12)	
89.0	3000		0.15 (3 x 5)	5

Table 3: AMSR2 Channel Set

3. IMPROVEMENTS IN SST RETRIEVALS

3.1. CURRENT ACCURACY AND REMAINED ISSUES

AMSR2 standard SST product uses 6.9 GHz brightness temperature for SST retrieval, and AMSR2 research SST product uses 10.65 GHz brightness temperature. Major differences between standard and research SSTs are; 1) spatial resolution (50 km for standard and 30 km for research); 2) retrieval accuracy of 10.65 GHz SST is worse than that of 6.9 GHz SST in low temperature range (less than about 10 °C); and 3) random noise in the SST retrieval is larger in 10.65 GHz SST.

The latest AMSR2 SST algorithm version is Version 3, released in March 2017. Figure 1 is scatter diagram of AMSR2 SST compared to buoy observation for both ascending (daytime) and descending (nighttime) paths. We used NOAA's iQuam V2.1 data as quality-controlled buoy data. Left figure shows results for 6.9 GHz (standard) SST and the figure on the right is for 10.65 GHz (research) SST above 9 °C. Root Mean Square Error (RMSE) of 6.9 GHz SST is 0.46 °C, and that of 10.65 GHz SST is 0.51 °C. Figure 2 is daily variation of RMSE and bias of 6.9 GHz SST compared with iQuam V2.1. Small increasing trends in bias since 2018 are found in the variation of the ascending paths (not shown). The cause of these increasing trends is assumed to be some drift of brightness temperature of AMSR2, and its possible cause may be aging of sensor linearity. We need to check further.

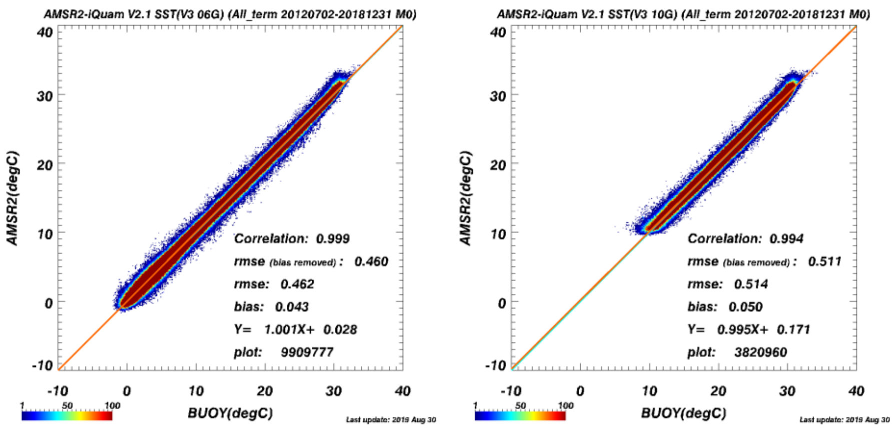

Figure 1: Comparison of AMSR2 6.9 GHz SST (left) and 10.65 GHz SST (right) with in-situ buoy observation (NOAA iQuam V2.1) during 2nd July 2012 and 31st December 2018 for both Ascending and Descending paths.

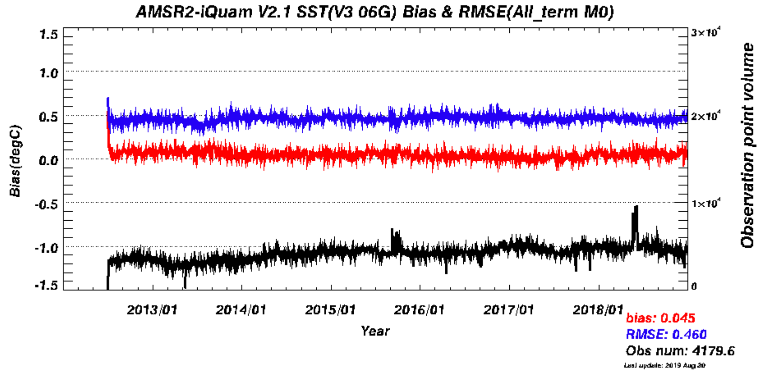

Figure 2: Daily variation of RMSE (blue), bias (red), and observation number (black) of 6.9 GHz SST and iQuam V2.1 (Figure 1 left) for both Ascending and Descending paths.

Whilst the accuracy of AMSR2 SSTs show good performance, three major issues are noticed in current AMSR2 SST Version 3; 1) recent increasing trends in biases; 2) users request higher spatial resolution SST, to estimate SST closer to the coast line – while 10.65 GHz SST has finer spatial resolution than 6.9 GHz SST, it has poor sensitivity to SST less than 10-12 °C; and 3) more random noise is found in 10.65 GHz SST than 6.9 GHz SST since 6.9 GHz SST uses a simple spatial filter.

3.2. DEVELOPMENT OF 3-CHANNEL SST

For future AMSR2 SST Version 4, we examined two possible improvements. One is the development of a new SST product by combining information from AMSR2's three frequencies, 6.9, 7.3 and 10.65 GHz. The 7.3 GHz channel was newly introduced in AMSR2 to reduce influences by Radio Frequency Interference (RFI) mainly over land areas. Using both 6.9 and 7.3 GHz channels, we can estimate SST even if one of the channels is affected by RFI. In addition, 10.65 GHz SST is combined with 6.9 and/or 7.3 GHz SSTs to improve spatial resolution. While current standard (6.9 GHz) SST product can estimate SST whose distance from the coast is more than about 80 km, new three-frequency SST can retrieve SST whose distance from the coast is more than about 45 km and accuracy of low SST range is almost equivalent to current standard SST.

Figure 3 shows example of current AMSR2 6.9 GHz SST (current Version 3) and newly-developing three-frequency SST. SSTs in coastal area and small ocean eddies are sharpened in three-frequency SST. In our preliminary analysis, new 10.65 GHz may estimate SST about 30 km offshore from the coast line around Japan, while current 6.9 GHz SST can estimate SST about 80 km offshore (not shown).

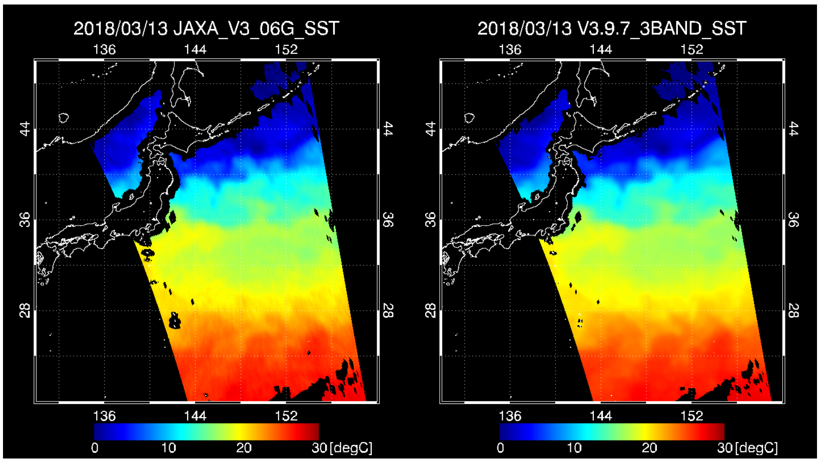

Figure 3: Example of AMSR2 6.9 GHz SST Version 3 (left) and newly developing three-frequency AMSR2 SST (right) on 13th March 2018 around Japan.

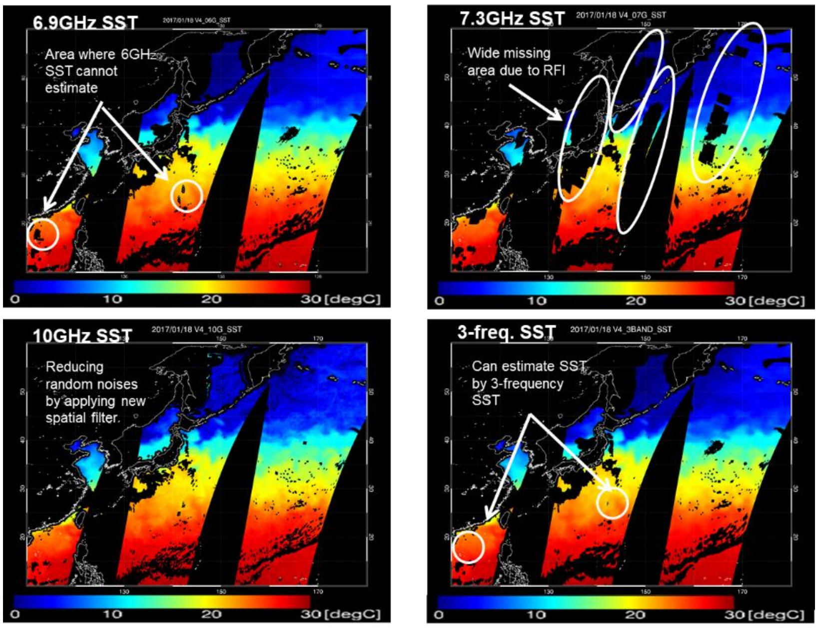

Figure 4: Comparison of SSTs by 6.9 GHz (upper left), 7.3 GHz (upper right), 10.65 GHz (lower left) and three-frequency (lower right) SSTs in 18th January 2016 (Descending paths) around Japan by new algorithm.

Figure 4 is comparison of SSTs estimated by using a single frequency algorithm (6.9 GHz, 7.3 GHz, and 10.65 GHz) and by the new three frequency SST algorithm around Japan in descending node on 18th January 2017. Around Japan and US, 7.3 GHz SST has been affected by more RFIs than other SSTs. In the other area, such as Europe and Asia, RFI impacts to 6.9 GHz SST is dominant. By combining SSTs from separate frequency channel, missing areas are reduced. Figure 5 shows scatter diagrams of AMSR2 SSTs and buoy SST by iQuam V2.1 for new algorithm. RMSE of 6.9 GHz SST is 0.46 °C, that of 10.65 GHz for all SST range is 0.62 °C (0.46 °C if using only SSTs higher than 9 °C, not shown), and that of three-frequency SST is 0.47 °C. Performance of the three-frequency SST is almost equivalent to 6.9 GHz SST.

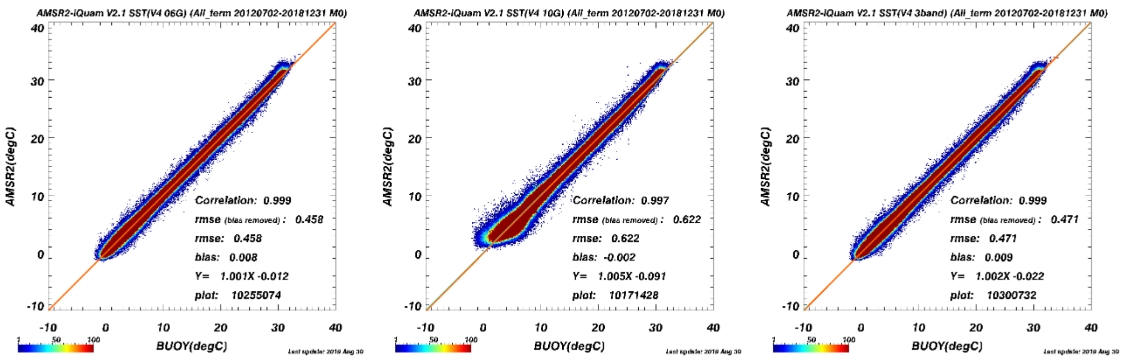

Figure 5: Comparison of 6.9 GHz (left), 10.65 GHz (middle), and three-frequency (right) SSTs with in-situ observation (iQuam V2.1) from 12th July to 31st December 2018 for both ascending and descending paths.

3.3. IMPROVEMENT OF SPATIAL FILTER

The other improvement is improvement of spatial filter to reduce random noise found in 10.65 GHz SST. Applying the improved spatial filter significantly reduced random noise in 10.65 GHz SST, and we are also examining to apply same filter to 6.9 GHz or three-channel SSTs to reduce scan biases and some random noises remained.

Figure 6 is comparison of 6.9 GHz and 10.65 GHz SST without spatial filtering and Figure 7 is the same as Figure 6 but for SSTs applying a Kolmogorov-Zurbenko (KZ) spatial filter. Improvement of SST estimates is found (Figure 7); reduction of smaller random noise, which is apparent in Figure 6. Figure 8 shows scatter diagrams of AMSR2 10.65 GHz SST with and without KZ filter and the Advanced Himawari Imager (AHI) on board the geostationary meteorological satellite Himawari-8 at around 03:00 UTC on 12th July 2017, and SST with KZ filter shows better agreement with Himawari-8 SST spatially. Figure 9 is a comparison of AMSR2 10.65 GHz SST with in-situ data for 1 year period of 2017, the KZ filter largely improves RMSE from 0.68 °C to 0.54 °C while there are no changes in biases (-0.08). It indicates no difference in average fields before and after applying KZ filter.

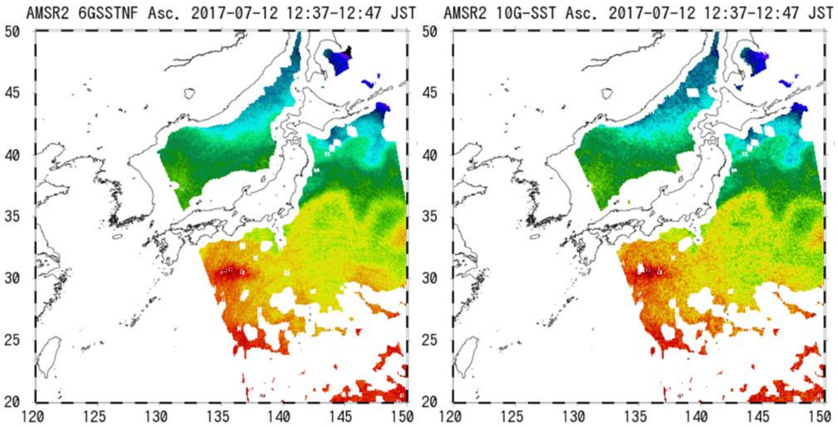

Figure 6: Example of AMSR2 6.9 GHz SST (left) and 10.65 GHz (right) SSTs without spatial filter around Japan at 03:00 UTC in 12th July 2017.

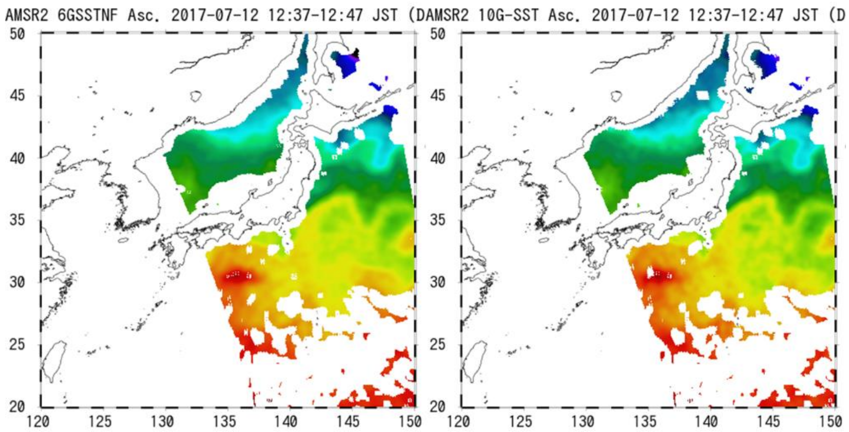

Figure 7: Same as Figure 6 but for SSTs with KZ filter.

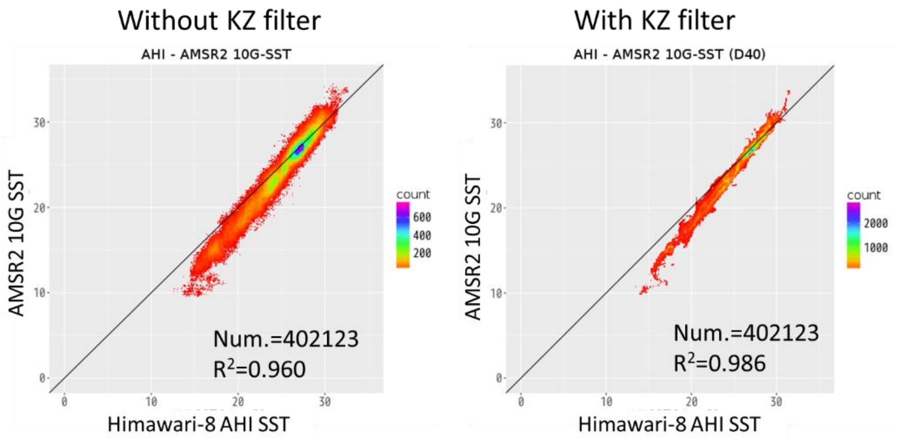

Figure 8: Comparison of AMSR2 10.65 GHz SST with (right) and without (left) KZ filter and Himawari-8 AHI SST at around 03:00 UTC on 12th July 2017.

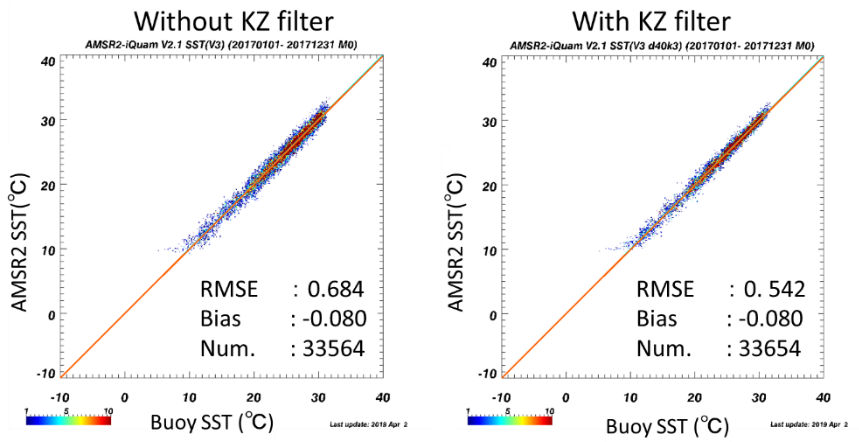

Figure 9: Comparison of AMSR2 10.65 GHz SST with in-situ buoys (iQuam V2.1) from 1st January to 31st December 2017.

4. SUMMARY

AMSR2 on board the GCOM-W satellite is in post-mission phase since 2017 and is working in healthy condition. JAXA has started preparation of AMSR2 follow-on sensor (AMSR3) which is now in the pre-project phase and expected to become project in winter 2019.

Although current AMSR2 SST (Version 3) has achieved standard accuracy as defined in the mission requirement, some issues remained to be solved in future algorithm updates. We are preparing and testing a new algorithm for AMSR2 SST (Version 4) and planning to introduce two major improvements.

One is to develop a new SST product using three-frequency channels (6.9, 7.3, and 10.65 GHz) to reduce missing area due to RFI and other reasons. RMSE of new three-frequency SST is almost equivalent to current AMSR2 6.9 GHz SST Version 3. The three-frequency SST is planning to be defined as research product.

The other one is improvement of a spatial filter used to reduce random noise in SST retrievals which are especially noticeable in 10.65 GHz SST due to the worse NEDT in 10.6 GHz brightness temperature compared to that of 6.9 GHz (Kasahara *et al.*, 2015). We tested a KZ filter to be applied to both AMSR2 6.9 GHz and 10.65 GHz SSTs. Validation of 10.65 GHz SST with in-situ buoy observation shows improvement of RMSE from 0.68 to 0.54 °C and no bias changes before and after filter (-0.08) and no changes in averaged field. We also found some SST dependencies on water vapour and wind direction in current AMSR2 SST Version 3 (not shown) and it is currently under investigation. Release of AMSR2 SST Version 4 is planned in early 2020.

5. REFERENCES

Imaoka, K., M. Kachi, H. Fujii, H. Murakami, M. Hori, A. Ono, T. Igarashi, K. Nakagawa, T. Oki, Y. Honda, and H. Shimoda, Global Change Observation Mission (GCOM) for monitoring carbon, water cycles, and climate change, *Proc. of the IEEE*, **98**, 717-734, 2010.

Kasahara, M., K. Imaoka, M. Kachi, H. Fujii, K. Naoki, T. Maeda, N. Ito, K. Nakagawa, and T. Oki, Status of AMSR2 on GCOM-W1, *Proc. of the SPIE*, **8533**, doi:10.1117/12.975810, 2012.

Kasahara, M., N. Ito, and K. Imaoka, Status of GCOM-W1/AMSR2 Operation and Calibration, *Proc. of the 30th ISTS*, 2015.

DETERMINING THE AMSR-E SST FOOTPRINT FROM CO-LOCATED MODIS SSTS

Brahim Boussidi[(1)], **Peter Cornillon**[(1)], **Gavino Puggioni**[(1)] **and Chelle Gentemann**[(2)]

(1) U. Rhode Island, RI, USA, Email: brahim.boussidi@gmail.com, pcornillon@uri.edu and gpuggioni@uri.edu
(2) Earth and Space Research, Seattle, WA USA, Email: cgentemann@esr.org

1. INTRODUCTION

The overall objective of this project was to take advantage of the oversampling of the Remote Sensing System's (RSS) Level 2 (L2) AMSR-E sea surface temperature (SST) product to create a product closer to the actual sampling resolution of the AMSR-E instrument (10x10 km). In order to accomplish this we found that we needed a better characterization of the footprint of the RSS L2 product than existed at the time as well as an estimate of the noise in the field based on this footprint. In this presentation, we detail the approach we used to obtain the footprint and an early attempt at the deconvolution of the SST field based on a simple neural network. The uncertainty of the RSS L2 retrievals is presented in a poster at this meeting prepared by Boussidi: *AMSR-E, MODIS, In Situ Three-Way Analysis of SST Error Variance.*

2. THE FOOTPRINT

We elected to use the full resolution (~1 km) SST fields from MODIS (on the same satellite) together with the AMSR SST fields to determine the footprint. The MODIS SST fields were averaged in non-overlapping 4x4 pixel squares to reduce the volume of data. Only cloud-free MODIS values were used in the averages. A matchup was defined for each L2 AMSR-E SST pixel for which at least 90% of the averaged MODIS pixels in a 25x31 pixel rectangle centred on the AMSR-E pixel were clear. The four million element matchup dataset was used to determine the footprint by regressing the 775 4x4 pixel MODIS averages on the AMSR-E values:

$$\mathbf{A}_{\mathbf{N}\mathbf{x}1} = \mathbf{M}_{775\mathbf{x}\mathbf{N}}\,\mathbf{H}_{775\mathbf{x}1} + \varepsilon_{\mathbf{N}\mathbf{x}1}$$

where **A** are the AMSR-E values, **M** the MODIS values, **H** the footprint vector containing the weighting elements and **ε** instrument and retrieval noise. **N** is the number of matchups and there are (25x31=) 775 4x4 MODIS averages for each matchup.

Given the large number of matchups, this is an over constrained problem hence readily solved via regression. We used the bootstrap method for the regression. Figure 1 shows the resulting mean footprint. We also obtained the footprint by year, by cell position on the scan-line and by latitude. The footprint only showed a dependence on cell position and that quite weak. The reason for this is not clear. These results have been published (Boussidi et al., 2019).

3. NEURAL-NETWORK DECONVOLUTION OF RSS L2 SST FIELDS.

With the footprint in hand we were ready to experiment with different methods to deconvolve the RSS L2 SST fields. We examined both conventional approaches and approaches based on machine learning. For the latter, we considered two approaches: (1) used AMSR-E fields together with higher resolution MODIS fields to train and test the neural networks and (2) used simulated versions of the MODIS and AMSR-E fields derived from the output of the 2 km llc run of the MIT General Circulation Model (MITgcm) to train and then the true AMSR-E and MODIS fields to test. We started with a Multilayer Perceptron (MLP) feedforward Artificial Neural Network (ANN) with three layers: an input layer (54 nodes), a hidden layer (10 neurons) and an output layer (one node). The inputs consisted of the directional derivatives of a 3x3 AMSR-E patch plus the similar directional derivatives of the median filtered image. The total number of variables input into the network was fifty-four (9 x 3 x 2). The trained neural net was then applied to several AMSR-E fields and the output compared with the coincident MODIS fields – the test set. We selected a pass showing the Loop Current in the Gulf of Mexico (Figure 2).

Next, we simulated the AMSR-E field by taking the weighted average of the 2x2 km^2 MITgcm SST fields over the AMSR-E footprint described in Section 1 and added zero mean, 0.28K standard deviation Gaussian noise to this field (the standard deviation is that determined based on the poster by Boussidi). The target field was determined by averaging the MITgcm SST field over 5x5 pixel squares aligned with the simulated AMSR-E field. Figure 3 shows the original AMSR-E field; the original MODIS field - the target of the deconvolution effort; the deconvolved field using the ANN trained with real data, and; the deconvolved field using the ANN trained with simulated match-ups. Visually, the deconvolution, although not perfect, shows significant improvement when compared with the input AMSR-E field as well as when compared with conventional approaches (not shown).

4. FIGURES AND TABLES

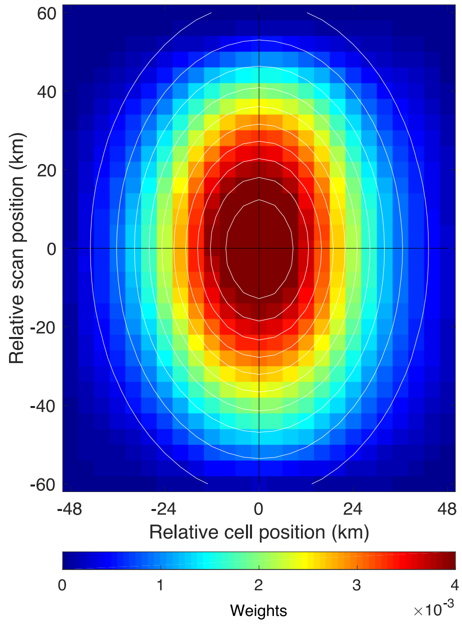

Figure 1: Mean AMSR-E footprint. Contour-lines in white from a fitted analytic model. The standard error of the mean of the weights does not exceed 9 x 10^{-5}.

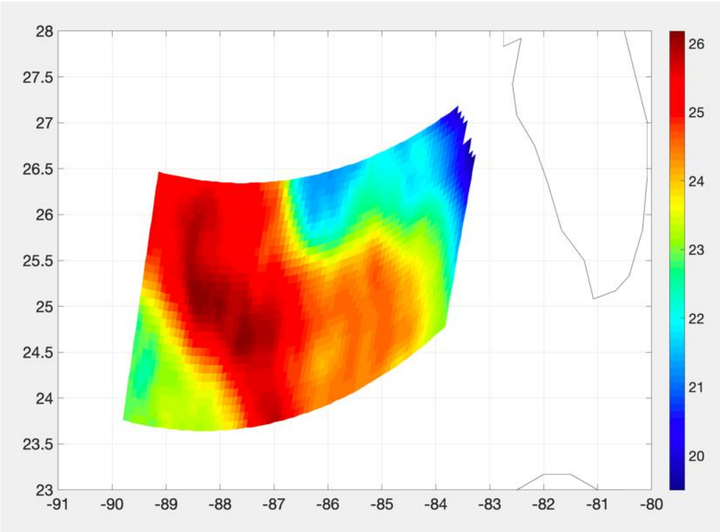

Figure 2: AMSR-E test field.

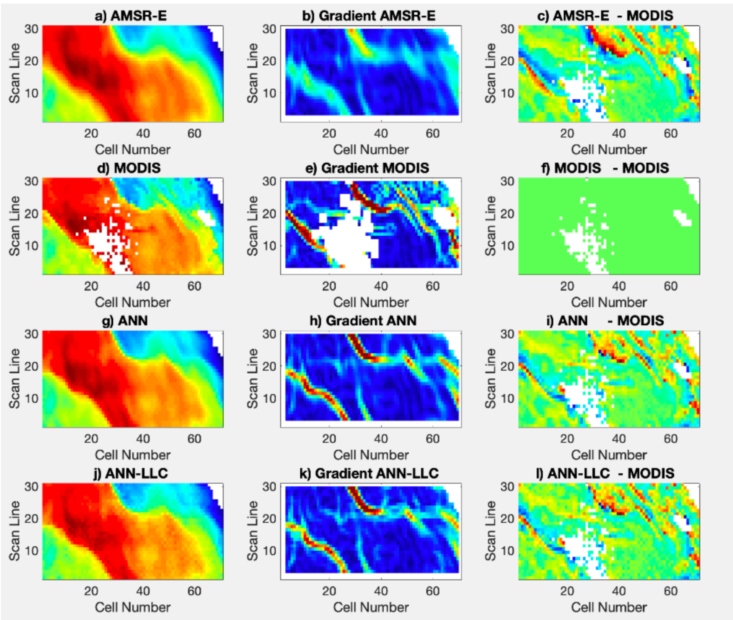

Figure 3: 1st row: AMSR-E SST field, its gradient and the difference between this field and the coincident MODIS SST field. 2nd row: same for the coincident MODIS field. 3rd row: ANN deconvolution trained with true MODIS/AMSR-E matchups. 4th row: ANN deconvolution trained with simulated MODIS/AMSR-E matchups.

5. CONCLUSION

We have developed an accurate characterization of the RSS L2 SST footprint. We have also shown that deconvolution with a simple neural network shows promise and, more importantly, that we can train the neural network with simulated match-ups based on the output of an ocean general circulation model. This means that we do not need the MODIS data to train the neural networks, which, in turn, means that we have an almost unlimited training set. This will allow us to experiment with other neural networks as well as with different SST configurations.

6. REFERENCES

Boussidi, B., Peter Cornillon, Puggioni, G. and Gentemann, C. (2019). Determining the AMSR-E SST Footprint from Co-Located MODIS SSTs. Remote Sensing 11, 715–21.

IMPACT OF CIMR MICROWAVE OBSERVATIONS ON THE CMEMS SST PRODUCT IN THE NORTH SEA/BALTIC SEA

Jacob L. Høyer, Mads Hvid Ribergaard and Emy Alerskans

Danish Meteorological Institute, Email: jlh@dmi.dk

1. ABSTRACT

The use of passive microwave (PMW) observations for sea surface temperature (SST) and sea ice is presently very limited in the Baltic Sea due to the contamination from land and from sea ice during winter. At the same time, persistent cloud cover can exist for weeks, preventing SST observations to being by the Infrared (IR) satellites.

This paper discusses the challenges in the present day satellite observing system from the perspective of the operational Copernicus Marine Environment Service (CMEMS) SST product for the Baltic Sea. The cloud and coastal limitations in the current IR and PMW satellites are presented and the impact of using SST observations from the Copernicus Imaging Microwave Radiometer (CIMR) high priority candidate mission is demonstrated here.

The CIMR satellite mission will provide daily coverage, sea ice concentration with a spatial resolution better than 5 km and SST better than 15 km. In addition, reduced side lobe contamination will facilitate the use of these observations in coastal regions and in regions close to sea ice. For more information on the CIMR, see CIMR MRD, 2019 and http://cimr.eu. The CIMR characteristics will make these PMW SST observations very suitable for a coastal region like the Baltic Sea and this study discusses the benefits of the CIMR observations to the CMEMS L4 SST analysis through the use of realistic IR observations and simulated CIMR SST observations. The impact has been determined through an analysis of the expected coverage of the CIMR observations relative to the current satellite constellation. In addition, the improvements in the CMEMS SST analysis have been determined through an experiment with simulated CIMR observations. The results clearly demonstrate the benefits of CIMR that could make a unique contribution to the existing satellite SST constellation in order to get an improved CMEMS SST analysis for the Baltic Sea.

2. INTRODUCTION

The objectives of this study are to present the challenges in the present day satellite IR and PMW observing systems and to demonstrate how the improved coverage of the CIMR mission will have a significant impact on the operational Copernicus Marine Environment Monitoring Service (CMEMS) SST products in the North Sea/Baltic Sea, which is a key region for several of the operational northern European Copernicus users

3. RESULTS

3.1. AVAILABILITY OF IR AND PMW SSTS IN THE BALTIC SEA

To present the coverage of the existing satellite IR products in the Baltic Sea, the CMEMS Baltic Sea SST super-collated level 3 (L3S) product (Høyer, 2018) was used to estimate the availability of IR SST during a year (13 February 2017 – 12 February 2018) (Figure 1). Pixels were classified as either SST (green), missing (red), ice (cyan) or land (not included in results). Pixels with a sea ice concentration of 30% or more were classified as “ice”. The SST category includes pixels with a valid SST value that were not classified as land or ice pixels. Pixels classified as sea (*i.e.* not as land or ice pixels) with a missing SST value were classified as “missing”. The total number of pixels in the Baltic Sea (excluding pixels classified as land) was used as a reference when calculating the percentages of the three categories of data. The percentages were then averaged over 5-day intervals for visualization purposes.

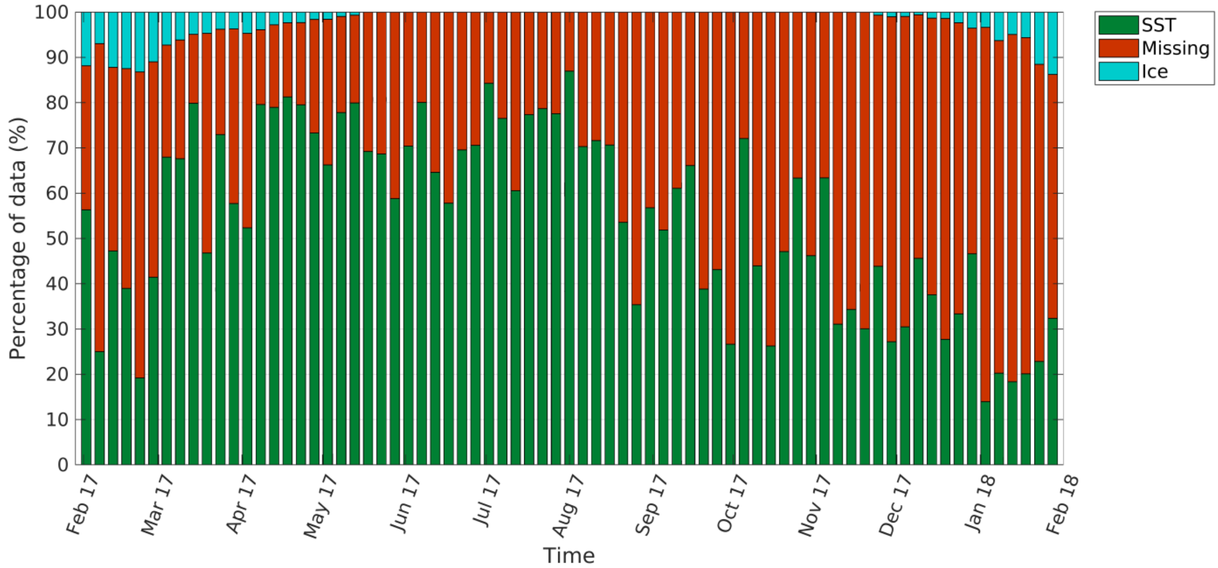

Figure 1: Percentage of pixels in the Baltic Sea that contains a valid SST value (green), sea ice (cyan) and missing data, due to e.g. clouds (red) for 13 February 2017 to 12 February 2018. The percentages have been averaged over 5-day intervals.

IR satellite SSTs cannot be retrieved in cloudy conditions and persistent cloud cover will therefore lead to periods with large areas of missing-value pixels. The annual mean percentage of pixels classified as SST, missing and ice is 54%, 43% and 2%, respectively. However, Figure 1 shows that the availability of IR SST varies over time, with highest availability during summer months (on average 72%) and lowest availability during autumn and winter months (on average 47% and 32%, respectively). The availability of IR SST for the Baltic Sea area even reaches below 10% on individual days, demonstrating the need for an all-weather SST product from *e.g.* CIMR.

Figure 2 shows the SST for the Baltic Sea area for three different SST products; the combined coverage of the operational IR SST products ingested in the CMEMS processing, RSS AMSR2 SST product version 8 and simulated CIMR SSTs for 20th February 2017. The grey areas denote regions of missing data. The simulated CIMR SSTs were derived from subsampled fields in the CMEMS L4 SST product. The L4 SSTs were smoothed to obtain a resolution representative of CIMR (15 km). A land and sea ice mask was constructed to mask out data within one CIMR 6.9 GHz footprint (15 km) of sea ice and land to simulate sea and ice contamination.

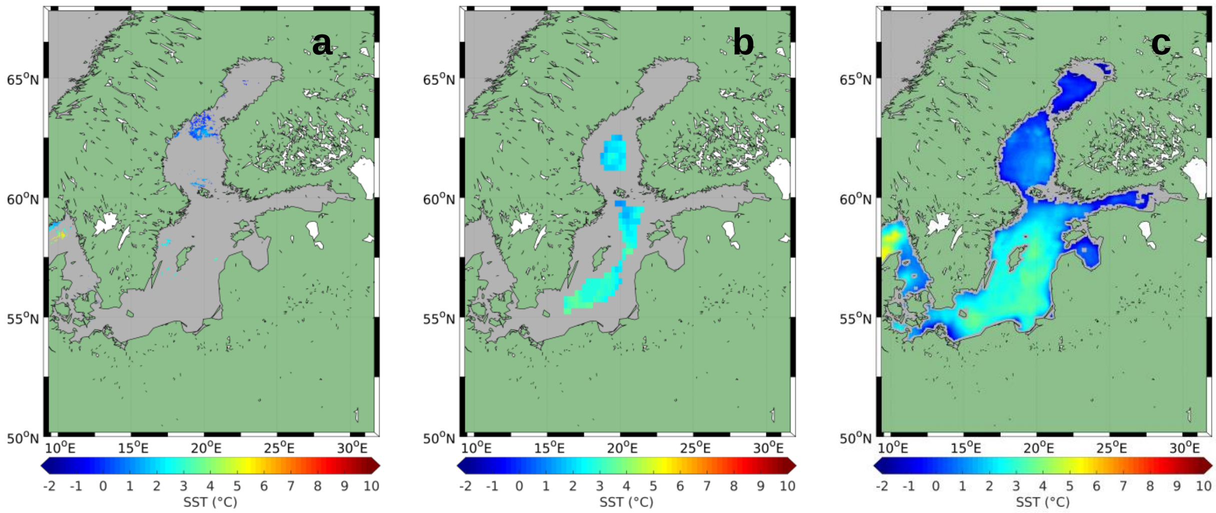

Figure 2:.Sea surface temperature in the Baltic Sea for 20th February 2017 for a) IR L3S SST product; b) RSS AMSR2 SST product; and c) simulated CIMR SSTs. Grey areas indicate regions of missing data.

The Baltic Sea is an area with a persistent cloud cover during the winter months (December – February). This is reflected in Figure 2a, which shows the very low availability of IR SSTs for a selected day in the winter season (20th February 2017). In comparison, PMW SSTs from AMSR2 show a better coverage (Figure 2b). However, the large land and sea ice mask needed to exclude coastal and sea ice contamination significantly decreases the availability of PMW SSTs and therefore limits the use of passive microwave observations in coastal and shelf seas. The simulated CIMR SSTs have a significantly improved coverage compared to both the combined IR SST product and the RSS AMSR2 SST product (Figure 2c). Because CIMR is a passive microwave sensor, it is able to retrieve satellite observations during cloudy conditions and is therefore a valuable complement to existing IR satellite observations. Contaminations due to coastal and sea ice side-lobe effects are diminished with CIMR due to the improvement in resolution compared to AMSR2.

3.2. SIMULATION EXPERIMENT SETUP

The graphics shows the logic behind the simulation experiments, where simulated CIMR observations are added to the existing L4 operational data streams using the DMI Optimal interpolation scheme. The DMI OI produces an SST value and an estimate of the uncertainty, which is based upon the data coverage, the uncertainties of the observations and the first guess error (Høyer and She, 2007; Høyer et al., 2014). The impact of the CIMR observations is assessed through an evaluation of the differences in SST uncertainty between the reference (IR only) and test (IR + CIMR) run.

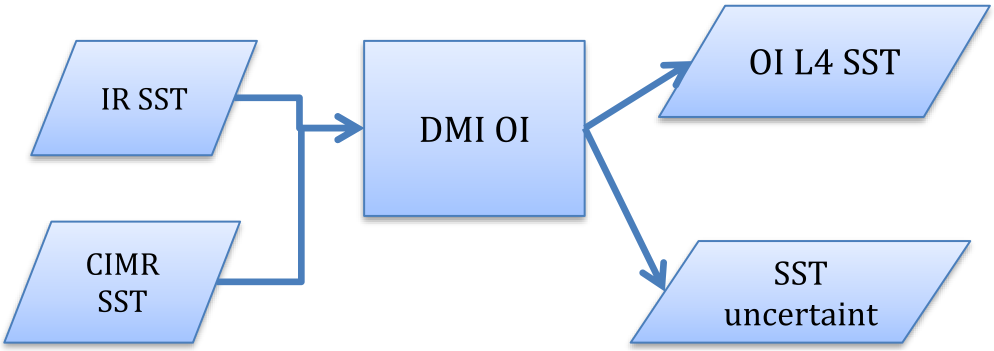

Figure 3: Diagram of the CIMR simulation experiment.

The figure outlines that using CIMR observations can easily be added to the operational data stream and thus can be ingested in the production of the CMEMS operational product for the Baltic Sea.

To obtain the one year of simulated CIMR observations, the DMI HBM ocean hydrodynamic model was subsampled to represent a 15 km spatial resolution SST product, given on a 5 km grid. Observations are taken from the model fields at 6 am and 6 pm every day, to combine into a daily product. Observations in conditions of precipitating clouds have been filtered out, using a threshold rain rate of 2mm/hour on the NWP observations. A mask of 15 km has been applied to remove observations in the vicinity of land and sea ice and spatial smoothing has been applied to simulate the 15 km footprint. The uncertainty on the CIMR SST observations has been set to 0.3 degrees, in agreement with CIMR MRD v2.0.

3.3. IMPACT OF CIMR OBSERVATIONS

Figure 4 shows the spatial DMI OI L4 uncertainties, averaged over the full year. The left and middle panel are the reference run with IR only, whereas the middle panel shows the uncertainty, when the CIMR simulated observations have been added to the IR observations. The right panel shows the improvements in percent, relative to the reference run.

It is evident from the figure that improvements are seen throughout the domain, when CIMR SST observations are included. The largest impacts are seen in the Danish Straits (Kattegat), the Bay of Bothnia and the Gulf of Finland with a reduction of more than 25% in the uncertainties. The central Baltic Sea shows improvements of 15-20% and the coastal band with no CIMR observations show about 5 % improvements. The regions with largest improvements are to some extent similar to the regions with poor IR data coverage.

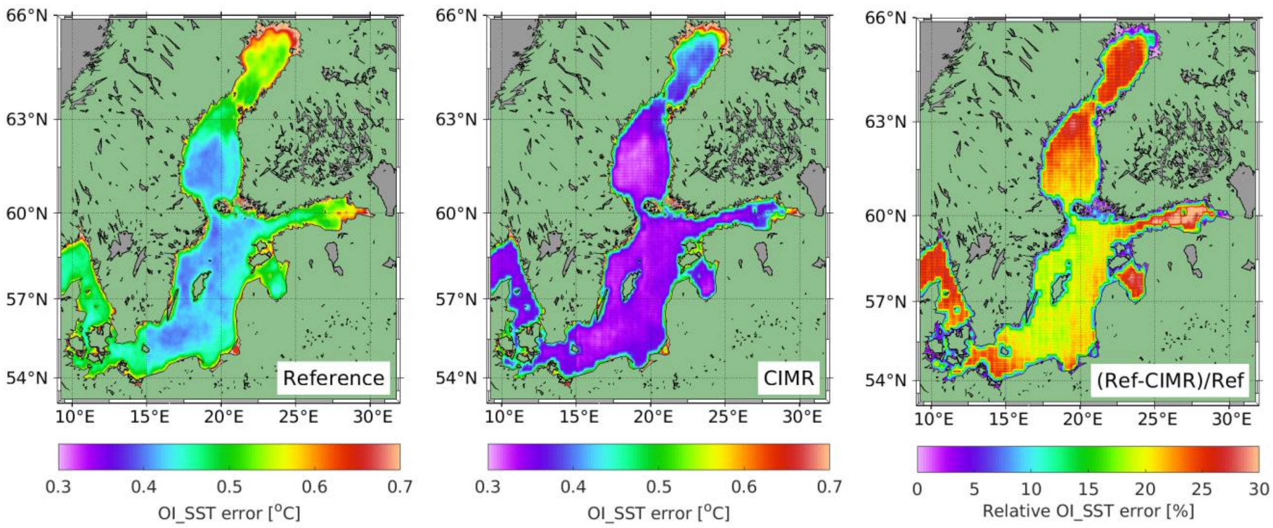

Figure 4: DMI OI L4 uncertainty in °C for the IR only reference run (left), for the test run including CIMR observations (middle) and improvements in percent (right)

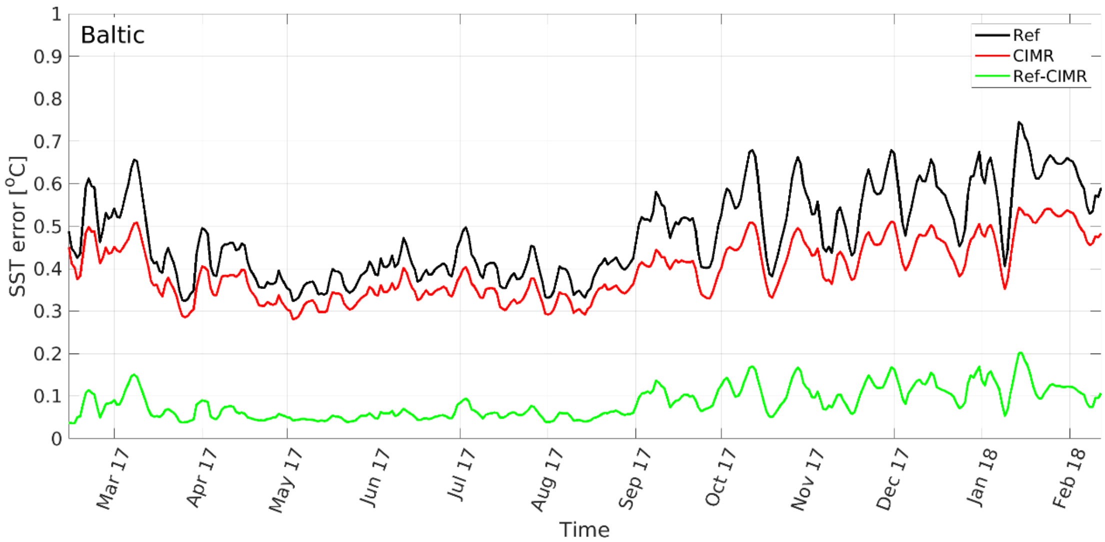

Figure 5: 5 days Baltic Sea averages of the DMI OI uncertainty for the reference (black), the test run with CIMR (red) and the differences between the two runs (green).

Uncertainties have been averaged for 5 days for all grid points in the Baltic Sea. The temporal evolution in the uncertainties has been calculated for the reference run and the CIMR run. The difference between the reference run and the CIMR run is also shown and the overall numbers are shown in Table 1.

Region	Improvements
Danish waters	15 %
Eastern Baltic Sea	18 %
Danish waters+Baltic Sea	17 %

Table 1: Overall improvement in the uncertainties between the reference run and the CIMR run.

Figure 5 shows that the overall uncertainty in the DMI OI L4 product is larger during winter than summer, due to the poorer IR data coverage. The CIMR run shows consistent improvement in the uncertainties at all times throughout all the year. The impact of the CIMR observations is larger in the winter time than during summer.

As the DMI OI L4 is used as input to *e.g.* the operational NWP model at DMI, the improvements in winter are very interesting as this is the time of the year, where the extreme weather events, such as hurricanes and storm surges, occur in the Baltic Sea region. The atmospheric low pressure systems are typically driven by the warmer ocean and improvement in the DMI OI L4 SST product during winter will thus potentially lead to an improved forecasting of the extreme events.

4. CONCLUSIONS

The results obtained in this study show that the Infrared observations of SST have limitations in the Baltic Sea due to persistent cloud cover. The cloud cover has a seasonal cycle with maximum cloud cover during winter. Microwave observations can be obtained in cloudy, non-precipitating conditions, but the coverage of the existing product is very limited in this coastal sea due to land contamination and it is thus not feasible to use the existing products in this region. The Copernicus Imaging Microwave Radiometer (CIMR) has the potential for improving upon the existing CMEMS products and it is demonstrated, through the use of the DMI-OI processing chain and simulated CIMR data, that including CIMR observations could lead to significant improvements in the uncertainties on the L4 SST product. The largest improvements will be during winter, which is the peak season for extreme weather events. Improvements in the SST field during this time could thus have a direct impact on the quality of the forecasting of extreme events, as the SST field is being used for boundary conditions in the NWP models.

To conclude, the CIMR observations will be an important component in the future evolutions of the Copernicus CMEMS satellite SST products in the coastal and Shelf seas.

5. REFERENCES

CIMR MRD (2019) Mission Requirements Document v2, https://cimr.eu/sites/cimr.met.no/files/documents/CIMR-MRD-v2.0-20190305-ISSUED_0.pdf

Høyer, J. L. and She, J., (2007) Optimal interpolation of sea surface temperature for the North Sea and Baltic Sea, J. Mar. Sys., Vol 65, 1-4, pp. 176-189.

Høyer, J. L., Le Borgne, P., & Eastwood, S. (2014). A bias correction method for Arctic satellite sea surface temperature observations. *Remote Sensing of Environment*, *146*, 201-213.

Høyer, Jacob. (2018) Quality Information Document (QUID) For SST TAC product 010-007_b Issue: 1.7, http://marine.copernicus.eu/documents/QUID/CMEMS-SST-QUID-010-003-007.pdf.

PLENARY SESSION IV: FEATURE RESOLUTION

SESSION IV REPORT

Chair: Alexander Ignatov[(1)] – Rapporteur: Dorina Surcel Colan[(2)]

(1) NOAA STAR, USA, Email: alex.ignatov@noaa.gov:
(2) Numerical Environmental Prediction Section, National Prediction Development Division, Meteorological Service of Canada, Dorval, QC, Canada, Email: dorina.surcel-colan@canada.ca

ABSTRACT

The session included three speakers representing three organizations, and an open floor discussion.

Summary of Speakers

On the Importance of the Spectral Phase on the Upper Ocean Studies: from Geophysical Fluid Dynamics to Statistical Mechanics (20 min) – Jordi Isern-Fontanet

Towards High-Resolution Multi-Sensor gridded ACSPO SST Product at NOAA (20 min) – Irina Gladkova

A Comparative Study of Ocean Thermal Gradients from GHRSST Level 4 SST Products (20 min) – Marouan Bouali

Open floor discussion (30 min)

In the introduction to the session, the chair spoke about the "High-Resolution" term in the GHRSST name. This term was initially introduced some 20 years ago, in the era when low-resolution satellite data (such as AVHRR GAC) were the main source of satellite SST, and first MODIS was just launched. Today, the meaning has shifted towards high feature resolution in SST products. The evolution naturally occurred over the past 20 years and the importance of feature resolution in GHRSST products is now clearly recognized, hence this session.

1. ON THE IMPORTANCE OF THE SPECTRAL PHASE ON THE UPPER OCEAN STUDIES: FROM GEOPHYSICAL FLUID DYNAMICS TO STATISTICAL MECHANICS - JORDI ISERN-FONTANET, INSTITUT DE CIENCIES DEL MAR (CSIC), BARCELONA, CATALONIA, SPAIN

This presentation exposes the idea of a modern view of SST by looking at the dynamics and the turbulent layer. It focuses on the information that could be retrieved from observations, and at what spatial and temporal scales. An example of spectral analysis was presented but mentioned that the method leads to losing the phase information. The second part of the talk focused on presenting a method to quantify the phase and its application to improve the cloud masking.

Questions:

Chis Merchant: In your method, you don't care about the specific functional form of the spectra, do you?

Response by the speaker: Correct, we don't.

Charlie Barron: The model should represent non-geostrophic solution going to higher resolution, or shouldn't it?

Response by the speaker: We lose the inertial range. That means we don't care about geostrophic versus non-geostrophic field.

2. TOWARDS HIGH-RESOLUTION MULTI-SENSOR GRIDDED ACSPO SST PRODUCT AT NOAA – IRINA GLADKOVA, NOAA STAR AND CUNY, CITY COLLEGE OF NEW YORK, USA

In the introduction the speaker presented the current ACSPO SST products, swath L2P and equal-grid 0.02° L3U (Uncollated), and mentioned a significant reduction in volume for L3U products compared to L2P, without losing the quality. However, users find it challenging to use even the much smaller L3U products, due to multiple passes from multiple platforms and sensors, and are requesting collated (multiple passes from the same sensor) and super-collated (multiple passes and sensors) products. Although users want high-resolution, satellite-based (not interpolated or artificially created), and gap-free products, at this moment, only two out of these tree requirements can be satisfied.

The presenter continued with the challenges of collation and super-collation algorithms, and focused on cloud screening. The proposed algorithm employs a modified image pyramid, to aggregate SST images from various sensor-specific spatial resolutions. The algorithm contains a decision step, based on SSIM index (Structural Similarity Index).

In conclusion remaining challenges were discussed, including minimising sensor-specific residual biases, proper handling of the effect of different spatial resolutions in original L2P data, and mitigating the varying acquisition time for different satellites.

Questions:

Helen Beggs: Nice presentation, clear. Have you considered comparison with buoy data?

Response by the speaker: Yes, I considered and compared. The cloud mask looks cleaner in the collated product. The problem with residual cloud leakages is present in some regions, especially when thin cirrus clouds are present, which affect data from all satellites and passes.

Jorge Vazquez commented that in the future, GHRSST might consider focusing on coastal regions, where challenges are largest and therefore collation most beneficial.

3. A COMPARATIVE STUDY OF OCEAN THERMAL GRADIENTS FROM GHRSST LEVEL 4 SST PRODUCTS - MAROUAN BOUALI, INSTITUTE OF OCEANOGRAPHY OF THE UNIVERSITY OF SAO PAULO, BRAZIL

In the beginning, the speaker mentioned the ongoing collaboration with Jorge Vazquez for this work. The presentation focused on the importance of fronts and inter-comparisons of fronts derived from various L4 products.

Presented were: the necessity of detecting fronts (for fisheries, characterization of ocean-atmosphere interaction, *etc.*); the different characteristics of fronts (spatial and time scales); and the multitude of available L4 products. The author pointed out that the standard evaluation metrics of L4 products to evaluate their quality is based on comparisons with in situ measurements. This is necessary but may not be sufficient, and gradients must be analyzed to evaluate the feature resolution of various L4 products.

A comparison of six L4 SST products was done over 5 regions. The conclusion was that despite the consistency of L4 SST products in terms of their validation statistics against in situ data, there are many differences in the magnitudes of SST gradients. These differences come from L2 data ingested in the analysis, but also from the SST analyses themselves. The existing metrics based on validation against in situ data, are not thus appropriate for quantifying the fronts. At the end, it was highlighted that validation of SST gradients requires new metrics and new methods.

Questions: none

4. OPEN FLOOR DISCUSSION LED BY THE CHAIR

The discussions opened with a few slides presented by Sasha Ignatov about feature resolution in NOAA products from VIIRS onboard SNPP and NOAA20 in Chesapeake Bay at 1km resolution. Comparing with Metop-A and L4 MUR products suggests that their feature resolutions are visually all different. He reiterated the point made in the Bouali's presentation, that there is the need to find a metric for feature resolution in different products.

Other points raised for discussion:

- How do we measure feature resolution?
- Feature resolution should be more than just one number, *e.g.* distribution (maps, time series, etc.).
- How can we validate it, against what data? And using what metrics?
- Improvements to spatial resolution should go hand-in-hand with improvements in temporal resolution.
- Grid size of L3/4 product and their feature resolution are not synonymous.

Jorge Vazquez agreed that we need better information about SST accuracy and precision, but also about feature resolution.

Peter Cornillon commented about the metrics for feature resolution, and referred to the poster he presented. They have done a study about white noise or pixel to pixel noise applying this for Aqua MODIS.

Chris Merchant said that GHRSST decided not to use ARGO and keep them for validation. He also said that if we want to validate gradients then we need to find some equivalent data which are not assimilated, *e.g.* images from independent sensors.

Helen Beggs proposed to use S3A or S3B data as at this moment the data are not assimilated. She commented also on "ship data", *e.g.* IMOS but Charles Barron replied that calibration of IMOS data needs to be independently verified.

Chelle Gentemann added that looking at ship data for validation is a good idea.

Helen Beggs said that 1-minute temporal resolution ship data, could capture spatial features and fronts.

Marouan Bouali commented about the "atmospheric smoothing" applied by some retrievals algorithms (OSI SAF, NOAA) and questioned whether such smoothing can remove trends in SST gradients associated to stripe noise in individual channels used for SST retrieval.

ON THE IMPORTANCE OF THE SPECTRAL PHASE FOR UPPER OCEAN STUDIES: FROM GEOPHYSICAL FLUID DYNAMICS TO STATISTICAL MECHANICS

Jordi Isern-Fontanet[1,2], Antonio Turiel[1,2], Cristina Gonzalez-Haro[1,2], Estrella Olmedo[1,2]

[1]Institut de Ciencies del Mar (CSIC), Spain; [2]Barcelona Expert Centre in Remote Sensing

Satellite infrared radiometers have provided high resolution (~1 km) measurements of the ocean surface during the last forty years. The existence of such time series enables us to investigate different dynamical regimes of the upper ocean and monitor potential changes related to global warming. The main problem, however, is to extract the dynamical characteristics of the upper ocean. To overcome this difficulty, we have approached the problem focusing on the phase of thermal images, *i.e.* the relative position and geometry of oceanic structures, from two complementary perspectives: Geophysical Fluid Dynamics and Statistical Mechanics. On one side, we have exploited the Surface Quasi-Geostrophic (SQG) framework to derive high resolution currents from Sea Surface Temperature (SST) alone or combined with along-track altimetric measurements of Sea Surface Heights (SSH). Our results showed that we are able to reconstruct the velocity field of small (~ 10 km) coastal eddies from SST. At present, we are developing a preoperational system based on AVHRR images, which we plan to extend to Sentinel-3. On the other side, we have used the multifractal interpretation of turbulence to develop descriptors of the different oceanic regimes in order to classify SST images and better understand the energy cascade in the ocean. In both approaches to the problem, the methodologies we have developed are first tested in numerical models and, then, applied to real data from (A)ATSR AVHRR and MODIS; and compared to in situ data. In addition to the insight on upper ocean dynamics, our research demonstrates the importance of precisely locating oceanic fronts and provides new directions to develop new methods for improving cloud masks as it will be shown.

TOWARDS HIGH-RESOLUTION MULTI-SENSOR GRIDDED ACSPO SST PRODUCT AT NOAA

Irina Gladkova[1,2,3], Alexander Ignatov[2], Matthew Pennybacker[2,3], Yury Kihai[2,3]

[1]CUNY, City College of New York, USA; [2]STAR, NOAA Center for Weather and Climate Prediction, USA; [3]Global Science and Technology, Inc., USA

NOAA started development of multi-sensor, high-resolution, gridded (Level 3 collated and super-collated, L3C/S) ACSPO SST products from available polar platforms and sensors (initially from NPP and N20 VIIRS; Terra/Aqua MODIS, and Metop-A/B/C AVHRR FRAC will be included later). The L3C/S products will have larger coverage, reconciled inter-satellite biases and reduced image noise.

Averaging of SSTs from multiple sensors and overpasses appears to be a simple and intuitive way to collate multiple observations, but it may result in large image artefacts, as the retrieved temperatures may have biases, cloud-contaminated pixels, and are taken at different times, leading to the shift in oceanic features. The burden of dealing with these residual data artefacts and complexities should not be left to the user, but is better done by the data producers (*i.e.* the NOAA ACSPO team). Data producers know the peculiarities of individual sensors and potential remaining issues with the swath L2P products and their gridded L3U counterparts, and therefore are best positioned to remove the root causes of those and/or mitigate their impact on the collated product.

The main challenges of the multi-sensor aggregation are sensor-specific residual angular and regional biases, cross-sensor biases, different spatial resolutions and noise levels in the original L2P data gridded into uncollated L3Us, the varying time of acquisition, and cloud leakages present in the data. Small, opaque clouds and cloud boundaries are very difficult, if at all possible, to detect without temporal context. We show how multiple looks can be used to mitigate residual cloud leakages in individual overpasses. With respect to spatial resolution, the main challenge is related to capturing the middle position of fronts, which can move between subsequent overpasses, rather than averaging SSTs which can degrade the details in dynamic regions and may even result in “ghost” fronts. We give an update on the progress with an ACSPO thermal fronts product, and show how the information about fronts’ locations and local rate of change can be used to aggregate multiple observations, without degrading their original spatial resolution. The main idea is similar to what is known in the image processing community as the “image pyramid”, which has been successfully used for decades for image morphing, blending and stitching into a seamless image mosaic. Image pyramids can be employed to extract spatial features with multiple scales from different overpasses, and then create a high fidelity composite image from a set of intermediate pyramid layers, some of which may have different scales.

We will present the current status of the ACSPO L3C/S algorithm development, testing and validation, and compare the proposed products with existing L4 analyses, including high-resolution 1km L4 MUR. We discuss the users’ need for, and fundamental difference between, the L4 and L3C/S products.

A COMPARATIVE STUDY OF OCEAN THERMAL GRADIENTS FROM GHRSST LEVEL 4 SST PRODUCTS

Marouan Bouali[1], **Jorge Vazquez-Cuervo**[2], **Paulo Polito**[1] **and Olga Sato**[1]

(1) Institute of Oceanography of the University of Sao Paulo, Brazil, Email: marouan.bouali@usp.br
(2) NASA/Jet Propulsion Laboratory, Pasadena, California, USA, Email: jorge.vazquez@jpl.nasa.gov

1. INTRODUCTION

High resolution imagery of ocean biophysical parameters such as chlorophyll-a concentration and Sea Surface Temperature (SST) from satellite sensors have become a pivotal tool for the analysis of ocean fronts given the increasing evidence of their impact on climate and weather patterns. In addition to many applications such as the detection of fishing spots and marine ecosystem boundaries, ocean fronts affect the interaction between ocean and atmosphere (via transfer of heat and gas in the mixed layer) and provide information on the ocean 2D and 3D dynamics. When it comes to the study of thermal fronts, most data users rely on Level 4 SST due to persistent cloud coverage in Level 2 infrared observations and other practical considerations such as data volume and manipulation. Currently, the PODAAC systems contains 25 different Level 4 SST datasets. Therefore, which Level 4 SST is best suited for the investigation of spatial and temporal characteristics of thermal gradients is a common question among the user community.

Although SST fields (from Level 2 to Level 4) are statistically validated against *in situ* measurements using bias and standard deviation, these metrics provide little information on the geometrical quality of Level 4 SST products, *i.e.*, their ability to preserve small scale structures present in Level 2 SST while displaying minimum processing artefacts.

Further, the selection of an appropriate Level 4 SST depends on the application, *i.e.* whether a given user is interested in the detection of fronts in synoptic/daily data, the analysis of the seasonal variability of coastal upwelling or the investigation of long term changes in frontal activity.

The goal of this study is to compare SST fields derived from various GHRSST Level 4 SST datasets and determine how consistent they are with respect to the spatial distribution and temporal variability of SST gradients.

2. DATA AND METHODOLOGY

Six different GHRSST Level 4 (daily) SST datasets have been selected for the period from 2016-2018 and include:

- Canadian Meteorological Center (CMC) (0.1°)
- Naval Oceanographic Office (NAVOCEANO) K10 (0.1°)
- Remote Sensing Systems Microwave and Infrared (0.09°)
- UK MetOffice OSTIA (0.05°)
- Danish Meteorological Institute (DMI) (0.05°)
- Jet Propulsion Laboratory Multiscale Ultrahigh Resolution (MUR) (0.01)

Most of these Level 4 products are based on the Optimal Interpolation (OI) method with the exceptions of K10 which uses a weighted average scheme and MUR which uses a wavelet decomposition to account for the scale of data ingested in the SST analysis. All these datasets have been reprojected/downsampled to a latitude-longitude grid of 0.1° and the comparison was conducted over 5 different regions with strong frontal activity that results from either the interaction of mesoscale currents or coastal upwelling. Selected regions include the Brazil-Malvinas confluence region, the Agulhas retroflection zone, the California Current System, the Gulf Stream and the Peruvian Upwelling System (Figure 1).

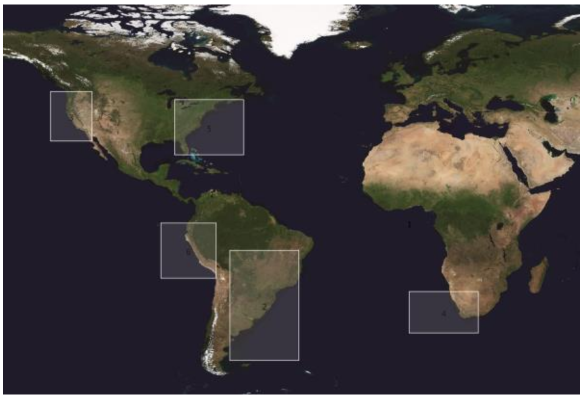

Figure 1: Regions with strong frontal activity selected for the comparison of GHRSST Level 4 SST gradients.

2.1. FEATURE RESOLUTION

A major requirement for a SST analysis method is the preservation of small scale features observed in the ingested Level 2 data. A common practice to compare the feature resolution of Level 4 products is to analyse wavenumber spectra, *i.e.* the amount of small scale features preserved is reflected in the power of high frequencies. However, such approach may not be fully reliable. In fact, high frequencies in wavenumber spectra may be associated mostly with sensor noise (Gaussian and stripe noise) in the Level 2 data. Further, depending on the time window used in the SST analysis, frontal features may be resolved at a different location and with different geometrical properties, which cannot be seen in the frequency domain. An alternative approach to quantify feature resolution is to use in the spatial domain a geometry-based metric such as the Structural Similarity index (SSIM) instead of statistical metrics such as the Mean Squared Error (the reference being a Level 3U dataset with the same resolution). Illustration of feature resolution from the six GHRSST products and corresponding MSE and SSIM are provided in Figure 2 and Table 1.

	MSE	SSIM
CMC	0.46	0.59
K10	0.22	0.79
REMS	0.17	0.76
OSTIA	0.35	0.66
DMI	0.39	0.72
MUR	0.47	0.91

Table 1: Mean Squared Error (MSE) and Structural Similarity Index (SSIM) between Level 4 and a Level 3U SST fields (Figure2). Note how CMC and MUR have similar performance in MSE but different feature resolution capability when analysing SSIM.

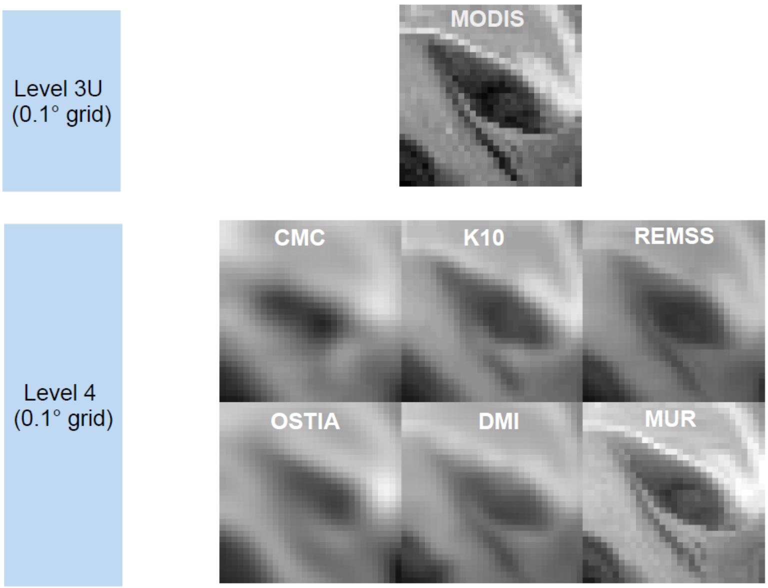

Figure 2: Feature resolution in the spatial domain for six GHRSST level 4 datatsets.

2.2. TEMPORAL VARIABILITY

Feature resolution provides only partial information on the performance of a given SST analysis as most users are also interested in the temporal variability of frontal activity. As a preliminary step we analysed the consistency between time series of SST from various GHRSST Level 4 for all selected regions. Figure 3 shows that very small differences exist in the temporal variability of selected Level 4 SST datasets.

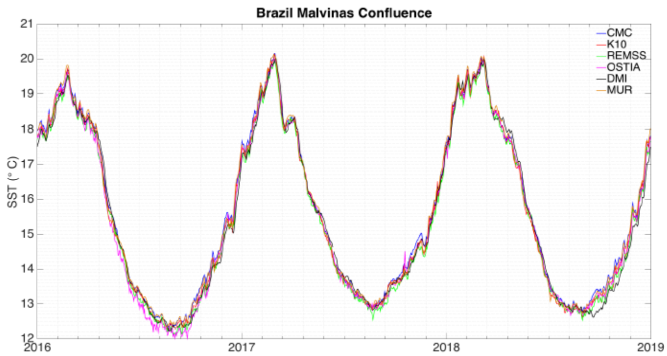

Figure 3: Time series (2016-2018) of SST from various GHRSST Level 4 products in the Brazil-Malvinas Confluence region

However, a similar analysis conducted on SST gradients indicates major discrepancies between Level 4 SST products in both the magnitude and temporal variability of frontal activity (Figure 4).

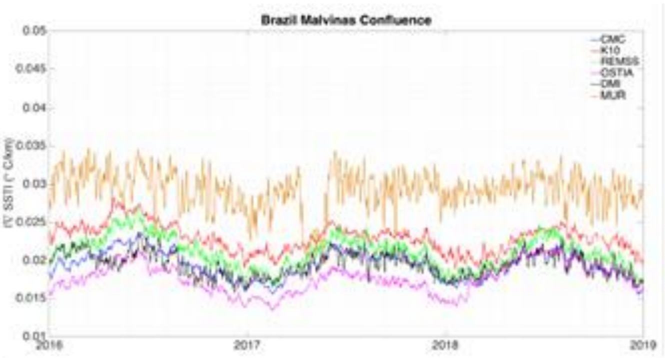

Figure 4: Time series (2016-2018) of SST gradient magnitudes from various GHRSST Level 4 products in the Brazil-Malvinas Confluence region

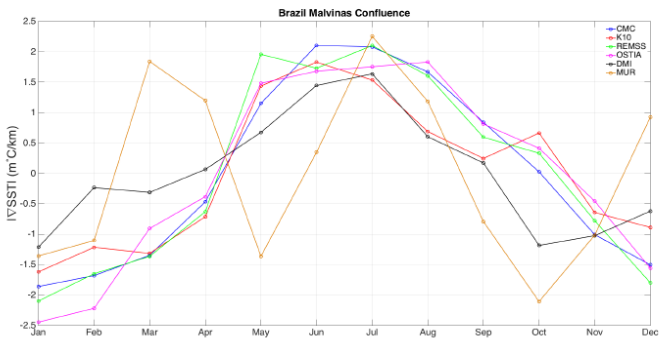

Figure 5: Annual cycle (averaged to 0 for display) of SST gradient magnitude in the Brazil-Malvinas confluence region.

As expected, MUR SST displays the highest magnitude of SST gradients. This is due to the fact that the wavelet analysis does not smooth the high resolution infrared data ingested as much as products based on OI. A drawback to this is the strong temporal variability associated with cloud coverage (*i.e.* more cloud coverage leads to more data from microwave sensors and thus lower gradients) which hinders the analysis of the temporal variability related to ocean submesoscale processes. Another important observation is that Level 4 products derived from the same SST analysis method (*i.e.* OI) also display discrepancies. This can be clearly seen in the annual cycle of SST gradient magnitude where the month of maximum frontal activity in the Brazil-Malvinas confluence region is June in CMC, July in REMSS and August in OSTIA (Figure 5).

3. CONCLUSION AND FUTURE WORK

Although Level 4 SST datasets are highly consistent when comparing statistical metrics in space and time, significant differences are observed in the corresponding gradients.

These can be attributed not only to the SST analysis method used to generate Level 4 products but also to the Level 2 data ingested in the analysis. In fact, many issues in Level 2 SST, affect mainly the geometrical properties of SST fields and can contribute to differences in Level 4 SST gradient magnitudes. These include Gaussian noise, striping, undetected clouds and fronts misclassified as clouds to cite a few. Spatio-temporal differences observed in gradients from GHRSST Level 4 datasets constitute a major incentive to develop new metrics and methodologies for the validation of SST gradients from satellite observations.

PLENARY SESSION V: APPLICATIONS

SESSION V REPORT

Chair: Prasanjit Dash(1) – Rapporteur: Rosalia Santoleri (2)

(1) NOAA NESDIS STAR, USA, Email: prasanjit.dash@noaa.gov
(2) Institute of Marine Sciences of the National Research Council, Italy, Email: rosalia.santoleri@cnr.it

1. INTRODUCTION

Application of satellite-based SST data ranges from scientific use for understanding the ocean phenomena to use by governmental bodies for reporting the status of the ocean as well as end-user applications. The session featured three presentations offering an overview of different applications:

- Senyang Xie- Satellite-observed Spatial and Temporal Evolution of The East Australian Current Encroachment from Himawari-8 SST Data: Implications for Upwelling and Shelf Circulation.
- Giulio Ceriola - From SST Measurements to Actionable Information for Public and Private Users: Rheticus© Services.
- Hiroyuki Tomita - SSTs Over and Around Reefs (SOAR) Workshop Outcomes.

Short summaries and outcome from these presentations are given in the following sections and additional research was reported in the interactive sessions.

2. SATELLITE-OBSERVED SPATIAL AND TEMPORAL EVOLUTION OF THE EAST AUSTRALIAN CURRENT ENCROACHMENT FROM HIMAWARI-8 SST DATA: IMPLICATIONS FOR UPWELLING AND SHELF CIRCULATION

Dr. Xie opened the session with a presentation on use of SST to study the East Australian Current (EAC). This is a complex system which exhibits significant variability ranging from eddies to decadal timescales. He used 6-day composite Himawari-8 SST images covering the period of July 2015 and Sep 2017 to map EAC's spatial structure. He defined a Topographic Position Index to capture the SST difference between the centre pixel and its neighbours. As a result, areas of positive TPI indicate positive SST spatial anomalies which are usually associated with warm ocean currents. A TPI threshold indicating middle-upper slope and ridge locations along a cross-current SST profile was used to separate the potential EAC from the background. The analysis indicated that the variation of the EAC encroachment is primarily dominated by eddy timescale (60 ~ 100 days), but it also exhibits a seasonal cycle. The results demonstrated that Himawari-8 SST product, thanks to its geostationary characteristic and the very high temporal resolution, provided unprecedented opportunity for investigating the variability of the vast and dynamic system as EAC.

3. FROM SST MEASUREMENTS TO ACTIONABLE INFORMATION FOR PUBLIC AND PRIVATE USERS: RHETICUS© SERVICES.

Dr. Ceriola from Planetek, an Italian SME, presented the Rheticus® Marine system. This is an innovative, high-performing geo-information service for monitoring coastal water quality and eutrophication status. The service provides key parameters of water quality retrieved from satellite products available to the public, and generates thematic maps, dynamic geo-analytics and pre-set reports. Rheticus® Marine has been designed to satisfy the requirements for different types of customers, such as a) National and Regional Governmental Institutions in charge of environmental monitoring and reporting; b) Policy and Decision Makers, from international to local level; c) Private sector such as industries involved in offshore drilling, wind plants, and d) Wastewater services, desalination, *etc.*). The inputs to Rheticus® Marine are SST and Chlorophyll data acquired from CMEMS together with other CMEMS model products and geographical information recovered by Planetek, such as historical catching reports from professional fishermen in case of fishery applications. The outputs are added value products and indicators accessible also *via* web or mobile phones to public authorities and users of private sectors. The results showed that Rheticus is able to provide customized information on water quality that can be useful to respond to the requirements of the environmental directives like the MSFD (Marine Strategy Framework Directive) and for aquaculture as well as for fishing tourism. The recommendation was to provide open and free access to satellite SST products and to improve the spatial and temporal resolutions of SST to meet the requirements for coastal applications.

4. SSTS OVER AND AROUND REEFS (SOAR) WORKSHOP OUTCOMES

Dr. Steinberg reported the results of the SOAR workshop carried out in 27-31 August 2018, Townsville, Queensland, Australia. The objective of the workshop was to discuss ways to improve SST products in complex shallow-water coastal and coral reef regions. In fact, the global bleaching event that occurred in 2014-2017 highlighted the need to understand and improve SST data products. The goals were to facilitate an understanding of end-user problems and requirements by the product and algorithm developers so that these requirements could be used to improve SST products and meet the needs of the coral reef scientific and management communities. One of the conclusions was that most of the L4 products, such as OSTIA largely used by the community, are optimized for numerical weather prediction, oceanography and/or climate – 'large-scale applications' and therefore are not able to resolve the spatial variability required by coral reef applications. The influence of SST on coral physiology and bleaching tolerance were also reviewed along with the key questions such as: a) temperature influences on physiology; b) potential adaptation of corals to water warming; c) bleaching event predictions for Survey Response. The outcomes were a series of recommendations to the users in selecting the products and requirements to the SST products developers.

5. CONCLUSION

The conclusion of the session was that the SST products are crucial for many applications and a large availability of historical and newer measurements from satellites provides great opportunities, but also poses a challenge for their effective exploitation. The following comments and recommendations were made:

- Promote an open and free access data policy for all SST products
- Easy and automated access
- Sensors inter-calibration is crucial for many applications requiring the study of SST variability in long time scales
- Standardized climatology
- Increased spatial and temporal resolutions for coastal applications
- Estimates of diurnal and vertical temperature variations
- Uncertainty information

SATELLITE-OBSERVED SPATIAL AND TEMPORAL EVOLUTION OF THE EAST AUSTRALIAN CURRENT ENCROACHMENT FROM HIMAWARI-8 SST DATA: IMPLICATIONS FOR UPWELLING AND SHELF CIRCULATION

Senyang Xie[1,2], Zhi Huang[3], Xiao Hua Wang[1,2] Aero Leplastrier[3]

(1) The Sino-Australian Research Centre for Coastal Management, University of New South Wales, Canberra, Australia, Email: senyang.xie@student.adfa.edu.au
(2) School of Science, University of New South Wales, Canberra, Australia
(3) National Earth and Marine Observations Branch, Geoscience Australia, Canberra, Australia

1. INTRODUCTION

The East Australian Current (EAC) is a complex and highly dynamic western boundary current (WBC) component of the South Pacific Gyre, which exhibits significant variability ranging from eddy to decadal timescales. The interaction between the EAC and the continental shelf, for example, the EAC encroachment, exerts significant influence on the ocean dynamics (*e.g.* upwelling) and hence the marine ecosystem off the south-east coast of Australia. The EAC's temporal variability has been examined at some locations (*e.g.* Cape Byron, Coffs Harbour, Smoky Cape and Sydney) through in-situ observations and modelling studies (Roughan and Middleton, 2002; Roughan and Middleton, 2004; Schaeffer et al., 2013; Schaeffer et al., 2014; Archer et al., 2017). However, the systematic investigation of the spatial and temporal variability of the entire EAC system received little attention. This study, by using time-series of remotely sensed SST data, aimed to map the spatial structures of the entire EAC and investigate the spatial and temporal evolution of the EAC encroachment from July 2015 to September 2017. The results were then used to discuss the impacts of the EAC encroachment on the coastal upwelling and shelf circulation.

2. MATERIALS AND METHODS

In this study, 6-day composite Himawari-8 SST images (Fig. 1a) between July 2015 and September 2017 were used to map the EAC's spatial structure. The observation frequency of Himawari-8 is every 10 minutes for the study domain with a spatial resolution of ~2 km. The Himawari-8 SST product, with the geostationary characteristic and the very high temporal resolution, therefore provides unprecedented opportunity of investigating the variability of the vast and dynamic EAC system. We calculated the Topographic Position Index (TPI) from the SST data to identify EAC's SST signatures (Fig.1 b). TPI captures the SST difference between the centre pixel and its neighbours. As a result, areas of positive TPI indicate positive SST spatial anomalies which are usually associated with warm ocean currents. A TPI threshold indicating middle-upper slope and ridge locations along a cross-current SST profile, was deemed appropriate to separate the potential EAC from the background. The raster cells with TPI value above the threshold value were then classified as EAC's SST signatures.

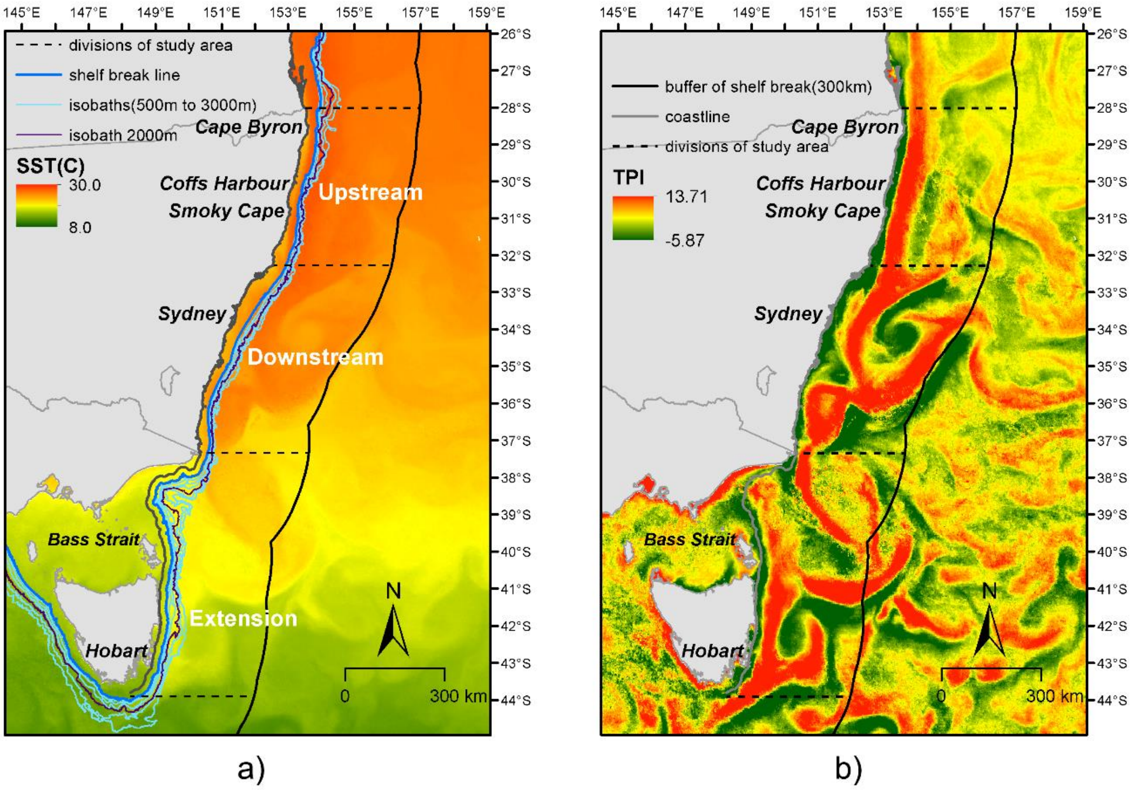

Figure 1. The study area off the coast of southeast Australia with a) 6-day composite (13 to 18 January 2017, summertime) Himawari-8 SST image as background. The total study area is enclosed by the coastline (dark grey line) and the 300 km offshore buffer of shelf break (bold black line), from 28 ºS to 44 ºS, and is divided into three focused sub-regions (meridional dash lines): upstream and downstream of the EAC separation, and the EAC extension zone off the coast of eastern Tasmania. The isobaths at water depth from 500 m to 3000 m with 500 m interval are depicted in light blue, with the 2000 m isobath highlighted in purple; b) the Topographic Position Index (TPI) derived from the SST image shown in a), with 2-D spatial standard deviation = 0.28 and the TPI threshold value = 0.5×0.28 = 0.14; the locations above the threshold are classified as the EAC's SST signature.

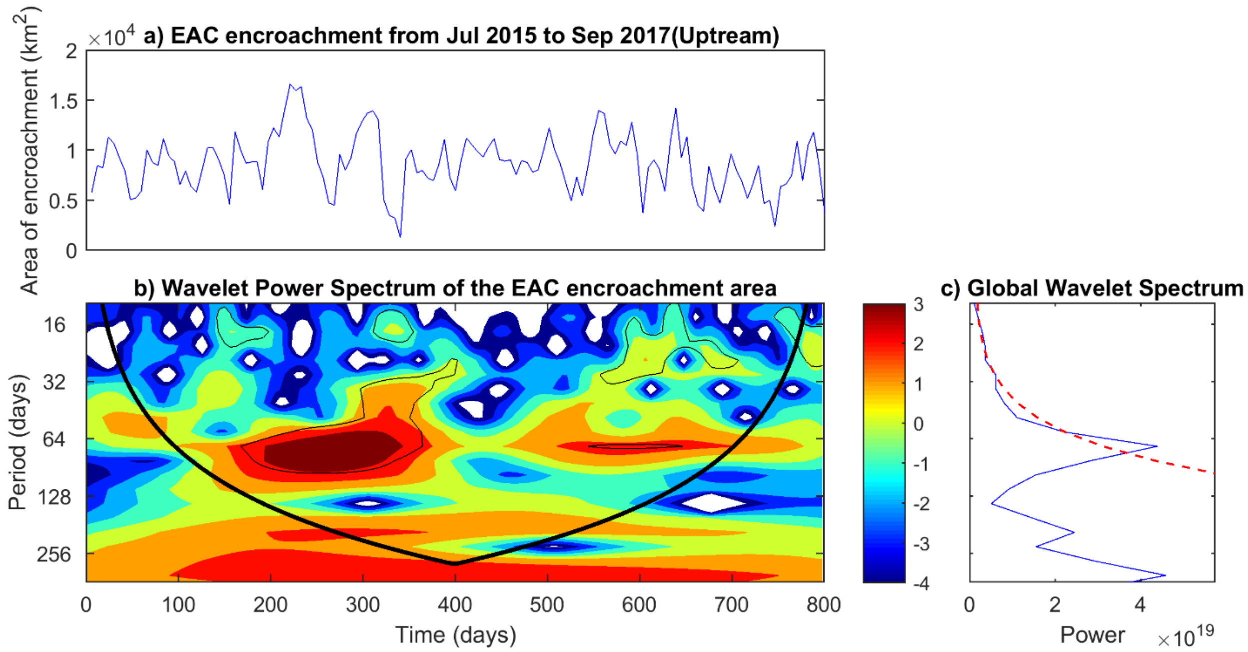

Fig. 2. Morlet wavelet power spectrum of the EAC encroachment time series (upstream), normalized (minus the mean and divided by the standard deviation) prior to wavelet analyses: (a) the EAC encroachment time series (upstream) from July 2015 to September 2017; (b) local spectrum and (c) global spectrum (average in time of local power outside the cone of influence (bold black line in b)), for the EAC encroachment in the upstream shown in (a). The 95% confidence lines are indicated (black contours on left plot (b) and dashed red line on right plot (c)), based on a chi-squared test.

The mapped EAC SST signatures were used in the spatial analysis of the EAC encroachment. In this study, the 2000 m isobath was defined as the "starting line" of the EAC encroachment onto the shelf. On this basis, the areal extent of the EAC's signature between the coast and the 2000 m isobath was calculated and then used as an index to evaluate the EAC encroachment (Figure 2a). To examine how close the EAC approaches the coast, we also calculate the distance between the coast and the inshore edge of the EAC.

3. CONCLUSION

The results indicate that the variation of the EAC encroachment is primarily dominated by eddy timescale (60 ~ 100 days), both in the upstream (60 ~ 80 days) and the downstream (70 ~ 100 days) (Figure 2). The distance between the coast and the inshore edge of the EAC also fluctuates in this "eddy period", ranging from 10 to 70 km offshore in the upstream, and 5 to 200 km offshore in the downstream. This eddy timescale variation of the EAC encroachment is consistent with the findings of previous studies inferred from the Ekman transport in the bottom boundary layer, using mooring array data at Coffs Harbour and Sydney. Based on this, we suggest that the EAC driven upwelling and the associated coastal nutrient bloom off the south-east coast of Australia exhibits an eddy-timescale frequency and can occur all year round.

Despite the frequent EAC encroachment onto the shelf, its influence on the coastal upwelling may differ between the upstream and the downstream. Combined with the BRAN 3.5 ocean current data, we found that, in the upstream, during the summer season of 2016/2017, the EAC encroachment was associated with the EAC's acceleration, a key process that induces coastal upwelling (Oke and Middleton, 2000; Roughan et al., 2003; Roughan and Middleton, 2002; 2004); however, in the downstream, the encroachment was actually associated with the EAC's deceleration, which was therefore less likely to induce upwelling.

The EAC encroachment also exhibits a seasonal cycle. In the upstream, the encroachment peaked in summer (2015/2016; 2016/2017) and reached the lowest in winter (2015; 2016; 2017). Accordingly, although the EAC driven upwelling may occur all year round at an eddy frequency, it is inferred to be strongest and most massive in summer seasons. The seasonality of the EAC encroachment also provides further explanation for the seasonal current sheer previously found on the continental shelf upstream of the EAC separation. We suggest that the seasonality of shelf circulation in this area is affected by both the EAC encroachment and the associated thermal wind effect, though the time series used in this study is relatively short.

4. REFERENCES

Archer, M.R., Roughan, M., Keating, S.R. and Schaeffer, A., 2017. On the variability of the East Australian Current: Jet structure, meandering, and influence on shelf circulation. Journal of Geophysical Research: Oceans, 122(11), pp.8464-8481.

Oke, P.R. and Middleton, J.H., 2000. Topographically induced upwelling off eastern Australia. Journal of Physical Oceanography, 30(3), pp.512-531.

Roughan, M. and Middleton, J.H., 2002. A comparison of observed upwelling mechanisms off the east coast of Australia. Continental Shelf Research, 22(17), pp.2551-2572.

Roughan, M. and Middleton, J.H., 2004. On the East Australian Current: variability, encroachment, and upwelling. Journal of Geophysical Research: Oceans, 109(C7).

Roughan, M., Oke, P.R. and Middleton, J.H., 2003. A modeling study of the climatological current field and the trajectories of upwelled particles in the East Australian Current. Journal of Physical Oceanography, 33(12), pp.2551-2564.

Schaeffer, A., Roughan, M. and Morris, B.D., 2013. Cross-shelf dynamics in a western boundary current regime: Implications for upwelling. Journal of Physical Oceanography, 43(5), pp.1042-1059.

Schaeffer, A., Roughan, M. and Wood, J.E., 2014. Observed bottom boundary layer transport and uplift on the continental shelf adjacent to a western boundary current. Journal of Geophysical Research: Oceans, 119(8), pp.4922-4939.

FROM SST MEASUREMENTS TO ACTIONABLE INFORMATION FOR PUBLIC AND PRIVATE USERS: RHETICUS© SERVICES

Giulio Ceriola[(1)], D. Drimaco[(2)], A. Aiello[(3)], Stelios Bollanos[(4)]

(4) Planetek Italia, via Massaua, 12 - 70132 - Italy, Email: ceriola@planetek.it, Phone: +390809644200
(5) Planetek Italia, Italy, Email: drimaco@planetek.it
(6) Planetek Italia, Italy, Email: aiello@planetek.it
(7) Planetek Hellas, Greece, Email: bollanos@planetek.gr

1. INTRODUCTION

A definition of Sea Surface Temperature (SST) can be "the water temperature close to the ocean's surface", however we have to keep in mind that different complementary SST measurements at the upper 10m of the ocean can be measured from Earth Observation (EO) satellites.

Measurement of SST from satellite can be considered a solid asset in the remote sensing applications over sea areas based on consolidated algorithms and methodologies. SST has been measured for over 30 years and nowadays with new EO satellite constellations (like the Copernicus Sentinel-3 or Suomi NPP missions) whose availability is guaranteed at least for the next decade. Furthermore there are several platforms which provide SST measurements in a routine way, including Near Real Time (NRT) and Forecast, accessible with free and open policies and through web services which allow automatic access. Examples are GHRSST or the Copernicus Marine Environment Monitoring Service (CMEMS).

Temperature is one key factor in the biological and physical processes that occur at sea, in particular SST is influenced by and influences many related phenomena *e.g.* to Ocean heat content, Coastal areas, Upwelling, Air masses in the Earth's atmosphere, *etc.* For this reason SST is a key parameter as input and/or output to many algorithms and models to assess and predict the status of sea areas from off shore to coastal zones. Typical applications can be the assessment of historical behaviour/evolution/trend or the provision of real and near real time information.

Building of such scenarios, in the last years Planetek has been putting on the market two commercial services (Rheticus® Marine and Rheticus® Aquaculture) on the basis of which it has been implementing a new third service that answers to specific needs of public authorities and private companies operating in the field of environmental protection and sea resources' sustainability. Rheticus® is an automatic cloud-based geo-information service platform, designed to provide fresh and accurate data and information on our changing world. It provides as a service timely information that fits the needs of a growing number of applications and includes maps, reports and geospatial indexes, designed to monitor several phenomena.

The approach to building a Rheticus® service starts from customers who have a problem to solve ("pain") and at a certain moment is addressed by Research and Development actors (*e.g.* scientists, research institutions, private companies, *etc.*) which define an innovative EO based solution. Then it comes Rheticus® which, by accessing directly to open data images (*i.e.* Copernicus Sentinel, Landsat8 satellites, *etc.*), cartographic data and environmental information, engineers the innovative solution and designs a service application to provide tailored and actionable *Information as a service*. In this way the customers receive concrete support to solve their problem ("gain").

2. APPLICATION CASE 1: RHETICUS® MARINE SERVICE

Rheticus® Marine is an innovative, high-performing geo-information service for monitoring coastal water quality and eutrophication status. The service provides key parameters of water quality retrieved from satellite open data through extensively tested models and algorithms and generates thematic maps, dynamic geo-analytics and pre-set reports. Rheticus® Marine is useful to different customers: from National and Regional Governmental Institutions in charge of environmental monitoring and reporting (*e.g.* for the European Marine

Strategy Framework Directive) to Policy and Decision Makers (from international to local level), including the Private sector (*e.g.* industries involved in offshore drilling, wind plants, wastewater services, desalination, *etc.*)

Rheticus® Marine takes as input satellite measurement of SST, chlorophyll and water leaving radiances from various sources (*e.g.* CMEMS) and ancillary data provided by the customer. Then it provides tailored information though a traditional GIS-like Web application (Figure 1) including near real time maps (locally re-calibrated: SST, Chlorophyll, Water Transparency and Turbidity) and temporally and/or spatially aggregated maps. Furthermore Rheticus® Marine provides also a Smart web application (Figure 2) providing dynamic geo-analytics and is able to automatically generate pre-set reports.

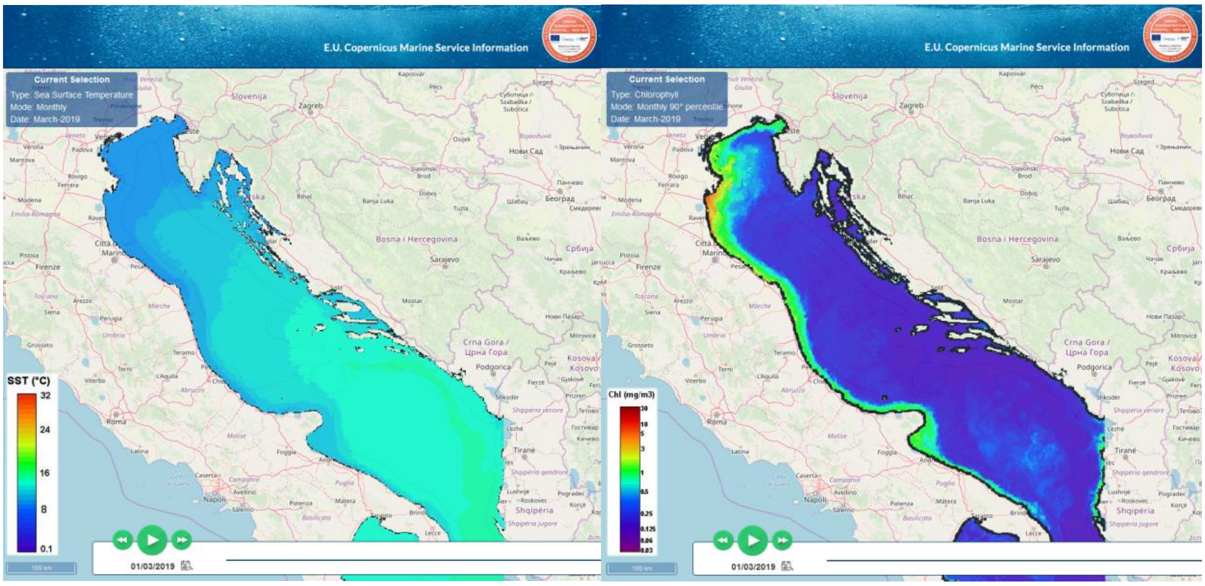

Figure 1: Rheticus® Marine Web Application

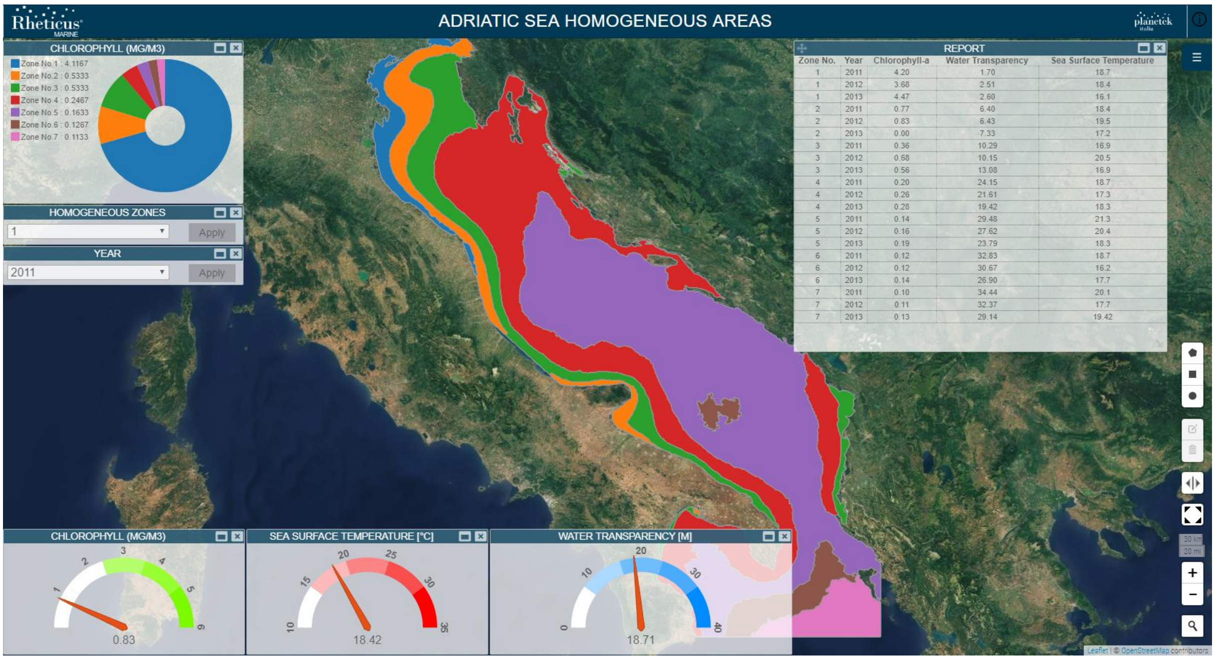

Figure 2: Rheticus® Marine Smart web application, with dynamic geo-analytics and report tailored for the European Marine Strategy Framework Directive.

3. APPLICATION CASE 2: RHETICUS® AQUACULTURE SERVICE

The aquaculture sector in Europe is highly competitive. Companies face many costs and challenges that represent a great effort for them as the sector is mainly dominated by small enterprises. To this regards, aquaculture activities need to be optimised in order to maximise the profitability, fulfil constraints set by environmental legislation and avoid risky situations for the production activities and the marine environment as well. In this framework, Rheticus® Aquaculture supports aquaculture activities. It provides farmers with daily information designed for the optimal management of their farming activities in marine waters, aimed at increasing production and profitability, and monitoring environmental conditions nearby farms.

Rheticus® Aquaculture is based on a model – developed and owned by a spin-off of the Venice University – which provides hind cast and forecast of shellfish length, weight, *etc.* starting from Rheticus® Marine's historical and near real time water quality measurements (Baldan et al., 2018). User data are integrated as well. The information generated are supplied through a Smart Web application (Figure 3) which allows an immediate overview about the percentage of current product lengths and current product dry weights vs. the optimal market sizes. Also more specific dynamic geo-analytics, which give valuable information about product length and dry weight trends over time, easily highlight anomalies. Going further nearer to the operative needs of the customers, Rheticus® Aquaculture can also provide user-tailored reports, by means of key information that the farmers can use to take decisions for increasing production and profitability.

Figure 3: Rheticus® Aquaculture Smart web application, with dynamic geo-analytics

4. APPLICATION CASE 3: MAP2FISH PILOT SERVICE

Map2Fish is a pilot service which addresses the fishing tourism sector, an increasing segment of maritime tourism industry and also a way being more and more adopted to match the need of maintaining work level among fishermen and of reaching a sustainable exploitation of marine resources in particular related to fishing. Map2Fish pilot service is based on Rheticus® and implements an innovative model – developed and owned by a spin-off of Bari University – which provides pelagic fish concentration, based on detection of SST and chlorophyll fronts trained and validated with historical catching reports from associations of fishermen (Tijani et al., 2016). The model takes as input measurements of SST, Chlorophyll and Water Transparency from Rheticus® Marine and of dissolved oxygen, waves and currents from CMEMS. Near real time and forecast of probability of pelagic fish concentration – together with other key sea parameters – are then provided through being-designed web and mobile applications and also merged with crowdsourcing information. Map2Fish pilot involves an association of former fishermen now providing fishing tourism services which will use such information to plan their trips and increase their customers' experience and satisfaction.

Figure 4: Rheticus® Aquaculture: example of user-tailored report

5. CONCLUSIONS AND RECOMMENDATIONS

In all mentioned applications, SST played a key role in providing actionable information to customers and so it can be considered a consolidated asset for building marine services. However from the experience gained and in order to increase the impact and utility towards the real needs of the customers, a set of recommendations of improvements on SST measurements from satellite have been identified:

- Increase of spatial details (*i.e.* resolution) in particular for applications related to coastal areas;
- Improvement of temporal factor: usually SST is provided as daily night mean (foundation SST), but reliable and comparable SST measurements near shore in some cases are needed at different daytimes (*e.g.* diurnal cycle for supporting shellfish growing models)
- The large availability of historical and new measurements from satellite provides great opportunities, but also poses a challenge for their effective exploitation. So key elements to reach for the near future are inter-sensor comparability and unified point of access.

6. REFERENCES

Baldan D, Porporato EMD, Pastres R, Brigolin D (2018), "An R package for simulating growth and organic wastage in aquaculture farms in response to environmental conditions and husbandry practices". *PLoS ONE 13(5): e0195732*. 10.1371/journal.pone.0195732

Tijani K, Morea A, Chiaradia M T, Nutricato R, Guerriero L, "Prototype of a multi-platform remote sensing service for fishing forecasting", *Environmental Energy and Structural Monitoring Systems (EESMS) 2016 IEEE Workshop on*, pp. 1-6, 2016.

SSTS OVER AND AROUND REEFS (SOSR) – WORKSHOP OUTCOMES

Craig Steinberg[1], William Skirving[2]

[1]Australian Institute of Marine Science, Australia; [2]National Oceanic and Atmospheric Administration, Coral Reef Watch

With the recent 2014-2017 global bleaching events, the need for improved Sea Surface Temperature (SST) data products has never been greater to better understand, predict and respond to these threats. Complex shallow-water coastal and coral reef regions pose unique challenges to the development and application of satellite SST products. A workshop entitled SSTs Over and Around Reefs (SOAR), was held in August 2018 to discuss the development of improved methodologies for satellite SST retrieval algorithms that will meet the needs of coral reef scientific and management communities. The workshop gathered international experts from the fields of coral reef ecology, coral reef management, oceanography, modelling and satellite SST algorithm development to specifically discuss the use and development of algorithms for satellite SST. Users explained their needs and use of existing products, while the satellite algorithm developers provided an overview of the current set of solutions available, as well as their applicability, limitations and potential. The increased mutual understanding stimulated group and panel discussions on how to improve algorithms and generate more suitable SST products.

The most urgent unmet requirements and potential improvements to cater for them were identified:

1. Compatibility between multiple sources of data, *e.g.* standard climatologies
2. Higher temporal and spatial resolution of data
3. Estimates of diurnal and vertical temperature variations
4. Uncertainty information

The workshop was held jointly by the Australian Institute of Marine Science and the National Oceanic and Atmospheric Administration Coral Reef Watch and endorsed by IMOS and GHRSST.

PLENARY SESSION VI: RETRIEVAL

SESSION VI REPORT

Chair: Peter Cornillon [(1)] - Rapporteur: Misako Kachi [(2)]

(1) University of Rhode Island, USA, Email: pcornillon@gso.uri.edu
(2) Japan Aerospace Exploration Agency, Japan, Email: kachi.misako@jaxa.jp

1. INTRODUCTION

Plenary Session VI "Retrieval" was held from 9:00 to 10:30 on Thursday, 6 June 2019. Peter Cornillon chaired the session and Misako Kachi acted as rapporteur. The session consisted of three oral presentations and an open discussion led by the session chair.

2. PRESENTATIONS

2.1. EXPLORATION OF RETRIEVAL APPROACHES FOR SLSTR BY ANDY HARRIS

Andy Harris presented different approaches for the retrieval of SST from SLSTR carried on Sentinel-3. Its dual-view provides robust and accurate SSTs, and stability of the system promises trends of less than 0.04 K/decade exceeding the requirements for most climate studies. Validation of product accuracy is performed with ARGO drifters adjusted for the depth of the measurements. A variety of algorithms were considered, including the operational algorithms based on radiative-transfer based regression, direct regression against in situ matches, and two physical retrieval methods (Optimal Estimation, OE, and Modified Total Least Squares, MTLS). The retrievals based on conventional OE were better than the results for 2 variants of MTLS, and with better sensitivity. The "optimized" OE approach (which is only possible if matchup data are available), uses the magnitude of the actual initial guess error for each point in the background error covariance matrix and produced the best results in terms of RMS, although with sensitivity that decreases to zero when the initial guess is "perfect". This raises some interesting questions regarding the trade-off between sensitivity and accuracy.

A question was asked regarding the variation in emissivity. Harris answered that there is no dependence in the algorithms, either for the operational or experimental algorithms, although the facility is there in the CRTM. However, the effect is actually very slight in the thermal-IR, especially for nadir-only algorithms

A second question related to possible improvements of sensitivity. Specifically, C. Merchant pointed out that having a high sensitivity is important for some applications, even if the initial guess is close to truth, because it will affect the strength of small retrieved gradients. Harris agreed, but noted that it means the trade-off between sensitivity and accuracy needs to be thought about carefully.

2.2. SATELLITE INFRARED RETRIEVALS OF SEA-SURFACE TEMPERATURE AT HIGH LATITUDES BY PETER MINNETT

Peter Minnett's presentation, given on behalf of a graduate student, Chong Jia, addressed Aqua/MODIS SST retrievals at high-latitudes (>60°N) for climate studies related to the MISST3 project focussed on the Arctic. SST retrievals were compared with in situ match-ups with drifting buoy measurements taken from iQuam for 2013-2018, but the distribution of in-situ values is concentrated between 30W and 30E, in the Greenland and Norwegian Seas. MODIS SST minus buoy SSTs show a cold tail with negative biases. Problems in cloud screening and atmospheric correction were presented as possible causes for the differences. The MODIS data will soon be reprocessed, and a new AI-based cloud screening algorithm will be applied to MODIS data in place of the current decision tree approach. Minnett's group also experimented with a single channel retrieval approach using separately the 11 and 12 µm channels, but, in both cases, the median is improved but standard deviations are worse than the split window approach. Future work will investigate the use of the Radiative Transfer for TOVS (RTTOV) code for improving the atmospheric correction.

During question and discussion time, the match-up accuracy when the in situ measurement was cloud covered but the match-up still met the distance requirements was discussed as a function of distance between the in situ value and the cloud edge. Exploration of variability within 1 km pixels and the 10 km spatial separation window of the matchups is possible using high-resolution ship and Saildrone data.

2.3. DETERMINING COVARIANCE PARAMETERS FOR OPTIMAL ESTIMATION OF SEA SURFACE TEMPERATURE BY EXPLOITING MATCHED IN-SITU REFERENCES BY CHRISTOPHER MERCHANT

Chris Merchant discussed issues associated with satellite/radiative-transfer-model biases and error covariance parameters in the context of optimal estimation of SST from brightness temperatures obtained from space-borne instruments. The optimality of OE depends on the underlying assumptions (bias free, known error covariances), which are usually not met in OE implementations to date. To determine the bias and error covariance parameters of OE, a match-up dataset of SEVIRI and drifting buoys was used. OE retrievals were based on 8.7, 10.8 and 12.0 micron channels. 2011 data was used for training and 2012 data for validation. Biases in brightness temperature were effectively retrieved in conjunction with SST, and the “Desroziers equation” method, which is used in data assimilation, was introduced to estimate error covariances. Validation results with match-up buoys show good estimation of prior SST bias, increased sensitivity to SST, and more realistic uncertainty estimates. New insights into the relative errors between observations and forward modelling are also obtained.

The only question was whether or not the OE (physical) retrieval uses a radiative transfer model to calculate the atmospheric profile. The response was that they use physical retrieval to simulate whole profile.

3. OPEN DISCUSSION

The focus of the open discussion related to the relative uncertainty of in-situ data, such as drifting buoys, and their depth (*e.g.*, skin-effect, vertical profile, *etc.*) used in validation. Although observation uncertainty of drifting buoys is lower, quantifying and separating the effects by element should be addressed carefully. This discussion resumed in the next session “In-situ measurements”.

EXPLORATION OF RETRIEVAL APPROACHES FOR SLSTR

Andrew Harris

University of Maryland, United States of America

The Sea and Land Surface Temperature Radiometer (SLSTR) series represents the next generation of dual-view infrared radiometers designed for temperature retrieval primarily for the purposes of climate monitoring. Following on from the (A)ATSR series, one long-established tenet of the program has been to preserve, as best as possible, the independence of the observations. The main approach to achieving this has been to employ radiative transfer modelling in the development of the retrieval algorithms. Such methods are dependent on getting everything right, including prelaunch characterization of the instrument, inflight calibration, selection of representative atmospheric states for the radiative transfer modelling, and so on.

This presentation will firstly evaluate the success of the approach, using comparisons of the reprocessed Sentinel-3 SLSTR sea surface temperature matchup database with high-quality Argo near-surface temperature measurements, in combination with a state-of-the-art model of the vertical temperature profile of the upper ocean. The diurnal model is used to adjust the SLSTR skin temperatures to the depth of the Argo measurements. The key aspect of this work is the independence and accuracy of Argo data, and the ability to adjust to the depth of the in situ measurement is critical to facilitate this. Assessment of the residual biases between depth-adjusted SLSTR temperatures and the extremely high-quality and well-distributed Argo *in situ* measurements provides a valuable indication of the quality and accuracy of the SLSTR SST record with respect to mission goals. Possible causes of any residual bias, including algorithm sensitivity to SST (the diurnal adjustment assumes 1:1 relation between the geophysical and retrieved anomalies), geophysical dependencies, and RTM spectroscopy, are also considered.

In the light of the findings, the feasibility of alternative SST retrieval algorithm approaches are discussed, along with possible benefits and potential drawbacks. In particular, the use of fast-forward RTM in physical retrieval is explored. In such methods, an initial guess state is required, top-of-atmosphere brightness temperatures (BTs) are modelled, and the initial guess then adjusted based on the difference between observed and modelled BTs. Such schemes have the advantage of minimizing geographic biases, but are similarly dependent on accurate calibration, *etc.* It will be shown that the result can be more tolerant of unknown errors, if an appropriate inverse method is chosen.

SATELLITE INFRARED RETRIEVALS OF SEA-SURFACE TEMPERATURE AT HIGH LATITUDES

Chong Jia [1], Peter J. Minnett [2]

(1) Rosenstiel School of Marine and Atmospheric Science, University of Miami, USA,
Email: chong.jia@rsmas.miami.edu
(2) Rosenstiel School of Marine and Atmospheric Science, University of Miami, USA,
Email: pminnett@rsmas.miami.edu

1. INTRODUCTION

Climate change is amplified in the Arctic region relative to elsewhere. This Arctic amplification has also been found in past changes in warm and glacial climates, as well as in historical simulations. The phenomenon is often explained by retreating snow and ice leading to more solar surface warming (surface albedo feedback). However, by analysing climate model simulations Pithan and Mauritsen (2014) found that the largest contribution to Arctic amplification comes from temperature feedbacks, due to the smaller increase in heat loss by longwave emission per unit of warming at colder temperatures compared to tropical conditions.

Satellite remote sensing offers the best way of deriving surface temperatures in the Arctic, but there are significant issues with deriving sea-surface temperature (SST) from measurements of infrared (IR) radiometers on satellites.

2. BACKGROUND

There are two major steps to deriving SST from calibrated on-orbit IR radiance measurements: 1) identifying pixels that are clear of clouds and aerosols, and 2) correcting the effects of the clear atmosphere on the IR propagation. In general, IR SST retrieval algorithms are designed to compensate for the effects of the atmosphere, mainly water vapour, satellite-derived surface temperatures have larger errors and uncertainties at high latitudes because the atmosphere is very dry and cold. When the water vapour concentrations are low, the correction algorithms tend to over-compensate leading to warm biases. The motivation of the study is to improve the algorithms to obtain more accurate SST which can be used to research feedback mechanisms.

3. DATA AND OBJECTIVES

To undertake the study, we use satellite measurements of brightness temperature at the top of atmosphere taken by MODIS on the NASA satellites Terra and Aqua (Kilpatrick et al., 2015) and collocated, near-simultaneous in situ measurements of surface temperature from drifting buoys (Xu and Ignatov, 2014). The matchups between satellite and buoy measurements are within 10 km and taken within 30 minutes, and data from the years 2013 to 2018 taken north of 60 °N were selected for this analysis to characterize the differences between satellite retrieved temperatures and in-situ measurements, and to identify the main causes of the discrepancies. This involves regional optimization of the SST retrievals with the expectation that the near two-decadal time series of MODIS surface temperature fields will contribute to studying climate change in the Arctic.

4. RESULTS

The MODIS data are those from the 5th reprocessing available from the NASA PO.DAAC. The atmospheric correction algorithm is based on the Non-Linear SST formulation (Walton et al., 1998), with some additional terms that are specific to MODIS:

$$SST = a_0 + a_1{*}T_{11} + a_2{*}\,(T_{11}-T_{12}){*}T_{sfc} + a_3{*}(\sec(\theta)){*}(T_{11}-T_{12}) + a_4{*}(mirror) + a_5{*}(\theta) + a_6{*}(\theta^2)$$

where T_{11} and T_{12} are brightness temperatures in the MODIS channels 31 and 32 (λ ~11 µm and ~12 µm), T_{sfc} is a reference SST (taken from the NOAA Optimum Interpolation SST analysis (Banzon et al., 2014)), θ is the satellite zenith angle, and a_n are statistically determined coefficients. The MODIS-specific terms are those with coefficients numbered 4, 5, and 6. The a_4 term is a correction for the slightly different spectral reflectivities of the two sides of the MODIS scan mirror (ref) and the a_5 and a_6 terms account for the angular dependences of the mirror reflectivities and the non-linear effects of the increased path length towards the edges of the swath. The coefficients are derived by a statistical analysis of the large matchup data sets divided into calendar months and latitude bands. The high latitude bands are poleward of 40º latitude in each hemisphere.

The seasonal distributions of the MODIS-derived SST_{skin} for latitudes north of 60 °N are shown in Figure 1. The great majority of matchups are in the Atlantic Ocean sector and the seasonal progression of SST_{skin} is clearly apparent. The absence of matchups in the Arctic Ocean is due to the paucity of in situ measurements in areas covered by sea ice. The warmest SST_{skin} are in the Norwegian Current which feeds warm North Atlantic surface water into the Arctic Ocean. The coldest SST_{skin} are in the Greenland Sea, close to the East Greenland Current bringing Arctic Ocean surface water and ice southwards, and in the northern part of the Barents Sea. The time series of MODIS SST_{skin} retrievals is displayed in Figure 2 and the differences between the MODIS-derived SST_{skin} and the subsurface buoy measurements (ΔSST) in Figure 3. There is a distinct seasonality in the SST_{skin} time series, as is expected, but also in ΔSST, which, while not unexpected, is undesirable. Figure 4 shows the distributions of the derived SST_{skin} and ΔSST. The ΔSST distribution departs from Gaussian, being more "peaky" (kurtosis = 6) and has a cold tail which is usually found in such distribution, not only at high-latitudes, and is attributed to imperfect cloud screening.

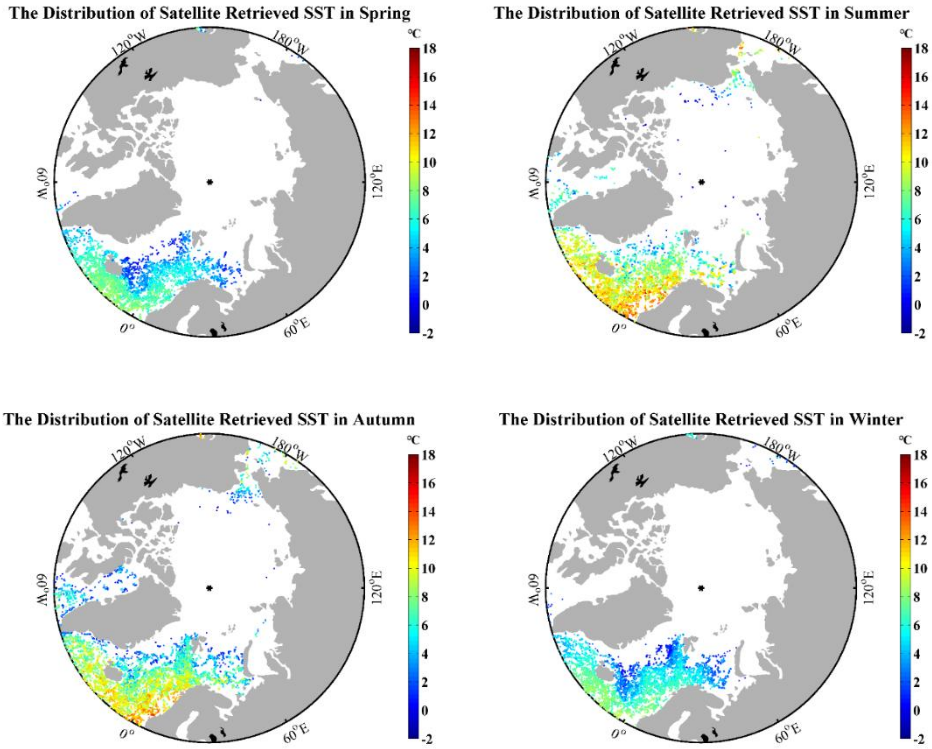

Figure 1. SST_{skin} derived from MODIS measurements latitudes north of 60 °N for Spring (March, April, May), Summer (June, July, August), Autumn (September October, November), and Winter (December, January, February).

Following the results of Vincent et al. (2008), who found a single-channel algorithm improved the accuracy of AVHRR SST retrievals in the north Water Polynya, when compared to a standard multi-channel atmospheric correction algorithm, we derived algorithms using only T_{11} or T_{12} measurements, but these did not improve the MODIS SST_{skin} accuracy when derived with the NLSST algorithm (Table 1).

Improvements to the formulation of the atmospheric correction algorithms are currently being developed.

Single	**11µm**			**12µm**			**Dual Channel NLSST**		
Channel	Mean	Median	Std	Mean	Median	Std	Mean	Median	Std
Aqua	-0.170	-0.012	0.922	-0.170	0.013	1.099	-0.535	-0.475	0.603
Terra	-0.170	-0.009	0.931	-0.170	0.025	1.090	-0.513	-0.455	0.647

Table 1: Statistics of the differences between MODIS-derived SST_{skin} and corresponding sub-surface temperatures measured from drifting buoys, using single channel atmospheric correction (left columns) and the standard NLSST (right)

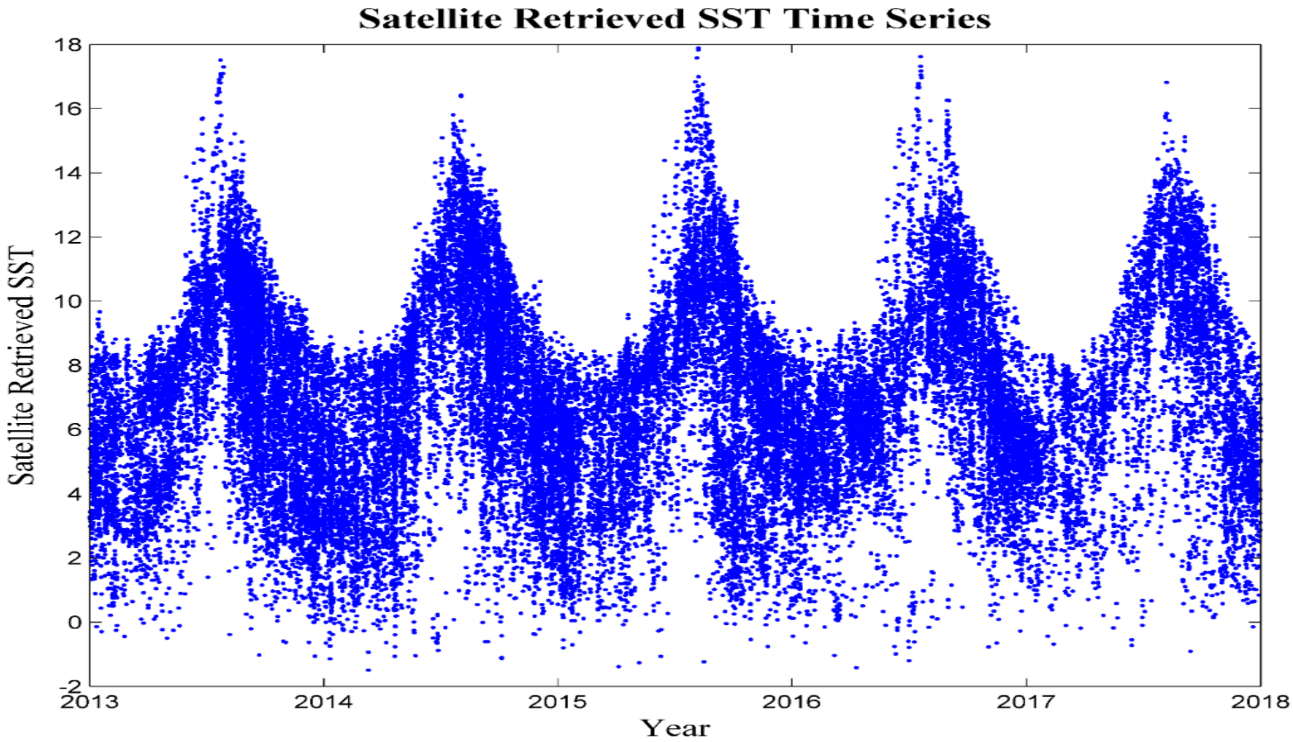

Figure 2: Time series of SST_{skin} derived from MODIS measurements at latitudes north of 60 °N

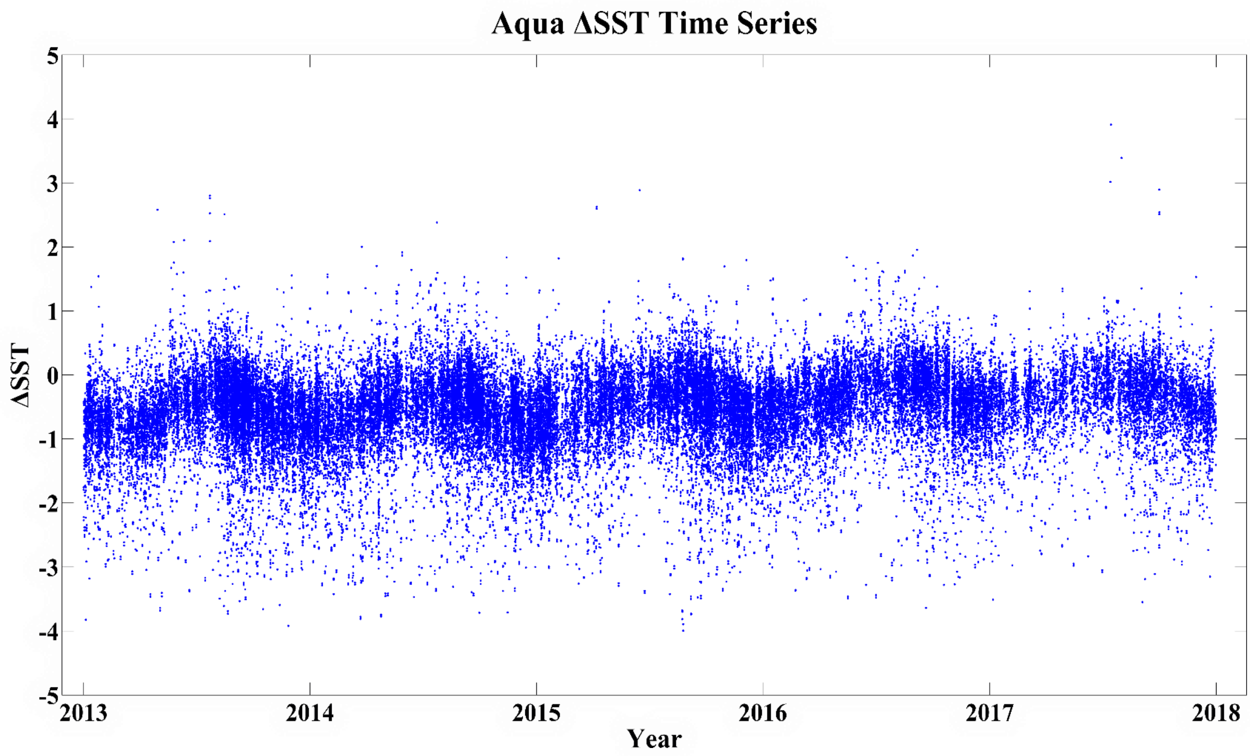

Figure 3: Time series of SST_{skin} derived from MODIS measurements in Figure 2, minus subsurface buoy measurements (ΔSST).

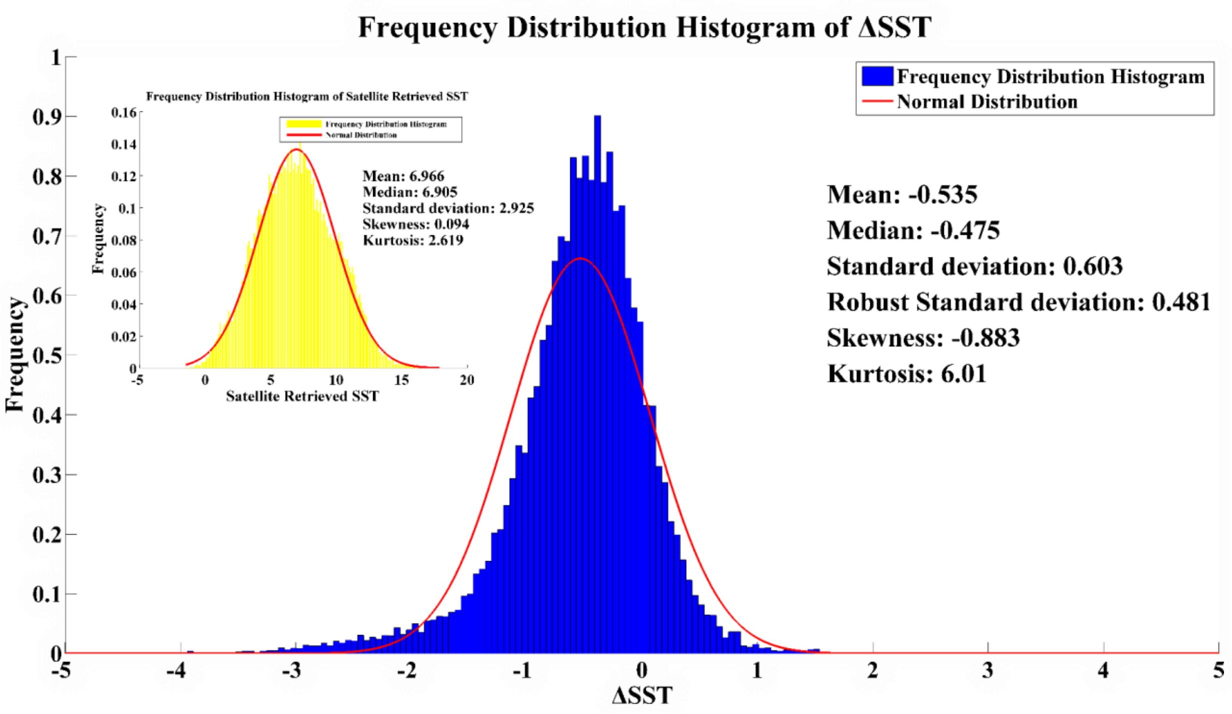

Figure 4: Histograms of MODIS-derived SST_{skin} show in Figure 2, and ΔSST shown in Figure 3.

5. CONCLUSION

There is a clear requirement to improve the accuracy of satellite-derived SST_{skin} at high latitudes to support research into feedback mechanisms that control the response of the Arctic to climate change. We are studying the effects of the very low atmospheric water vapour concentrations found in the Arctic, especially in winter, and the consequences of surface emissivity variations that become more important when the atmospheric effect is reduced.

6. REFERENCES

Banzon, V.F., Reynolds, R.W., Stokes, D., & Xue, Y. (2014). A 1/4°-Spatial-Resolution Daily Sea Surface Temperature Climatology Based on a Blended Satellite and in situ Analysis. *Journal of Climate 27*, 8221-8228. 10.1175/JCLI-D-14-00293.1

Kilpatrick, K.A., Podestá, G., Walsh, S., Williams, E., Halliwell, V., Szczodrak, M., Brown, O.B., Minnett, P.J., & Evans, R. (2015). A decade of sea surface temperature from MODIS. *Remote Sensing of Environment 165*, 27-41. http://dx.doi.org/10.1016/j.rse.2015.04.023

Pithan, F., & Mauritsen, T. (2014). Arctic amplification dominated by temperature feedbacks in contemporary climate models. *Nature Geosci 7*, 181-184. 10.1038/ngeo2071

Vincent, R.F., Marsden, R.F., Minnett, P.J., Creber, K.A.M., & Buckley, J.R. (2008). Arctic Waters and Marginal Ice Zones: A Composite Arctic Sea Surface Temperature Algorithm using Satellite Thermal Data. *Journal of Geophysical Research 113*, C04021. 10.1029/2007JC004353

Walton, C.C., Pichel, W.G., Sapper, J.F., & May, D.A. (1998). The development and operational application of nonlinear algorithms for the measurement of sea surface temperatures with the NOAA polar-orbiting environmental satellites. *Journal of Geophysical Research 103*, 27,999-928,012.

Xu, F., & Ignatov, A. (2014). In situ SST Quality Monitor (iQuam). *Journal of Atmospheric and Oceanic Technology 31*, 164-180. 10.1175/JTECH-D-13-00121.1

DETERMINING PARAMETERS FOR OPTIMAL ESTIMATION BY EXPLOITING MATCHED REFERENCES

Christopher J Merchant[1], Stéphane Saux Picart[2] and Joanne Waller[1]

(1) Department of Meteorology, University of Reading, Email: c.j.merchant@reading.ac.uk
(2) Meteo-France, Lannion, Email: stephane.sauxpicart@meteo.fr

1. THE PROBLEM WITH OPTIMAL ESTIMATION

Optimal estimation is a powerful retrieval technique, essentially consisting of an application of Bayes' theorem in which explicit prior knowledge is adjusted in the light of new measurements (the satellite brightness temperatures). The results are optimal in a well-defined sense (maximising the posterior probability) under certain assumptions. The problem with OE is that usually the assumptions are only approximately met, and we have lacked an objective means of making the retrieval closely optimal.

OE is only actually optimal if all error distributions are zero mean (prior, satellite observation and radiative transfer modelling [RTM]), and two error covariance matrices well estimated (describing the errors in the prior information and simulation-observation difference). In general, satellite calibration and RTM are biased, the prior is biased and the error covariance matrices are expert estimates.

2. SOLVING THIS PROBLEM

To solve this problem requires estimating OE parameters to rectify the biases and quantify the error covariances. Since parameters and covariances are functions of circumstances such as satellite zenith angle, many values need to be estimated. This can be done iteratively, according to the sequence in Figure 1.

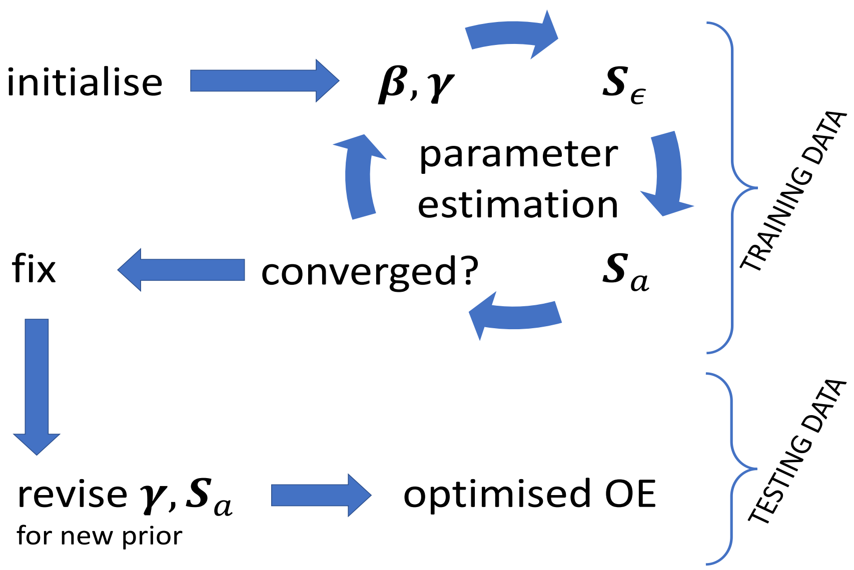

Figure 1. Sequence for OE parameter estimation.

In this figure, β represents observation biases, γ represents prior biases and the matrices S_ϵ and S_a are the error covariance matrices used in the OE retrieval. The bias estimates are obtained as follows:

- Simulate matches, using buoy SST as a reference in the RTM (meaning, the drifting buoys are assumed to be uncertain but unbiased)

- Iteratively apply parameter estimation by Kalman filtering across random draws from the match-up dataset
- The error covariance estimates are improved by using the relationships from the paper of Desroziers et al. (2005).

3. APPLICATION AND CONCLUSIONS

We applied these ideas to a SEVIRI matchup dataset, using 2011 and for training and 2012 for testing.

Marginal improvements in SST retrieval statistics were obtained, but more important was the insight gained into the retrieval system:

- All-sky NWP atmospheric humidity needs to be bias corrected to be drier to apply to clear-sky retrieval situations
- The RTM (here RTTOV) errors have inter-channel correlations that increase to ~0.5 at satellite zenith angles ~60 degrees.
- The calibration of 2011 was successfully carried forward to the SEVIRI observations of 2012 (shown by the bias in the test dataset being about 0.01 K.
- Prior bias can be estimated even where there are no in situ observations available, which matters in the early part of the satellite SST climate records, when drifting buoy distributions were sparser.

Additionally, the uncertainty estimate associated with the retrieval is more realistic.

We conclude that the approach may be relevant to a number of needs:

- SST constellation consistency (inter-sensor bias correction)
- Optimum exploitation of fiducial reference measurements
- Improving the wide-swath SSTs of SLSTR (by using OE tuned to the coefficient-based dual view retrievals
- Experiments to extend the state vector used for SST retrieval by OE

4. REFERENCES

Desroziers G, Berre L, Chapnik B, Poli P. Diagnosis of observation, background and analysis-error statistics in observation space. Quarterly Journal of the Royal Meteorological Society 2005; 131: 3385-3396.

PLENARY SESSION VII: IN SITU MEASUREMENTS

SESSION VII REPORT

Chair: Lei Guan [(1)]; Rapporteur: Werenfrid Wimmer [(2)]

(1) Ocean University of China, China, Email: leiguan@ouc.edu.cn
(2) University of Southampton, UK, Email: W.Wimmer@soton.ac.uk

1. INTRODUCTION

This is a short summary of Session VII which featured three oral presentations and an open discussion.

- Accurate Temperature Measurements of GHRSST Quality from Global Drifter Program Drifters – Luca Centurioni, Scripps Institution of Oceanography, US
- Using Saildrone Autonomous In Situ Data for Satellite Validation and Research into Upper Ocean Physics and Ecology – Chelle Gentemann, Earth and Space Research, US
- Sea Surface Temperature and Air-Sea Interaction in The Mediterranean Region – Salvatore Marullo, ENEA, Italy
- Open discussion

2. ACCURATE TEMPERATURE MEASUREMENTS OF GHRSST QUALITY FROM GLOBAL DRIFTER PROGRAM DRIFTERS – LUCA CENTURIONI

- With in-tank calibration, SVP drifters provide GHRSST quality SST data.
- NIST certified and traceable components need to be used. Alternatives to in-tank calibration can be used. Protocols/assurance certificates should be discussed and agreed upon (the FRM angle).
- The SVP drifter design does not introduce a temperature measurement bias when the drifter's hull overheats.
- The observed RMS temperature errors between two sensors scale with wind speed, over 20 cm vertical scale. A depth sensor, may be useful in calm seas, may not be needed for wind speeds greater than 5-6 m/s. The use of match ups at large wind speeds is recommended for now

Q Sasha: Good to have communication with drifter data provider, NOAA has questioned the need for it in the past. GHRSST should keep in mind that balance between other needs and SST needs. Manage vertical profiles and high accuracy measurements.

A: It should be possible to have those requirements concurrently at sensible cost.

Q Anne: Interesting talk and nice to see improvements. Good to work together, EUMETSAT project meeting towards the end of next year, invitation to come to the meeting.

A: Thank you.

3. USING SAILDRONE AUTONOMOUS IN SITU DATA FOR SATELLITE VALIDATION AND RESEARCH INTO UPPER OCEAN PHYSICS AND ECOLOGY – CHELLE GENTEMANN

- 2018 Baja Cruise observations by the Saildrone Unmanned Surface Vehicle.
- Satellite validation results using Saildrone data. Results are good for all except skin (physics) and pressure (sensor).

- Upper ocean physics and ecology results on SF bay plume, diurnal warming and air-sea fluxes.
- Next steps - Organize research / publications on topics: coastal front analysis, offshore front analysis, across / along winds front differences, circulation in frontal regions, baroclinic instability waves along fronts, diurnal warming in surface layer.

Q Ken: data volume.

A: Low, most sensors are 1 minute data, ADCP is 10min data but get turned off if power is low. 2 months of data for Baja is 100 MB, netcdf4.

Q Jorge: is there any discussion of putting echosounders on the Saildrone.

A: Yes, some cruises have ek80, NOAA has done some cruises to estimate fish. Comparison with research vessel, shows lower fish count for vessel than the Saildrone.

Q: How many drones?

A: NOAA Saildrone in every 10 degree box, at the moment 20 deployed. It's commercial, people have to pay for data, but data can be released by the project paying for it. Goal to build one a week, including sensors.

Q Peter: correction on the 10 degree box claim

A: Yes, and a more targeted approach, like front research.

Q Ken: free data, license is CC BY.

A: For the ice NASA project licenses intention is CC BY, the NOAA ones different policy. More talk offline.

4. SEA SURFACE TEMPERATURE AND AIR-SEA INTERACTION IN THE MEDITERRANEAN REGION – SALVATORE MARULLO

- Recent re-analysis (ERA5) have made an excellent work in reproducing essential meteorological variables for air sea heat flux estimate.
- The inclusion of hourly time resolution had contributed to ameliorate the products, including a better description of the diurnal cycle.
- Radiative heat fluxes estimates either from satellite or from model are good but can be ameliorate.
- The study of the aerosols effect on radiative components of the heat fluxes is promising and the Lampedusa station is certainly an interesting site for these study considering the variety of atmospheric conditions experienced by the island.

Q: No questions.

5. DISCUSSION

Helen: High resolution drifting buoys, not sure if they go into the BOM systems. How do you distinguish between normal and high resolution on the GTS. Especially Platform ID?

A: Luca, not sure but there is a specific format and it is in the metadata.

Gary: There is a list of buoys available on GDCBP, E-SURFMAR.

Not just GDP drifters, all data on GTS but no constant list at the moment, needs addressing.

Viva: Argo for validation, Luca has some high quality drifter data. Should we have a separate set to inter calibrate?

Sasha: High resolution drifter not yet globally representative?

Helen: which operational systems are able to ingest high resolution drifting buoys?

Chris: At present they are exactly the same.

Gary: The only change in ID is from 6 to 7 digits, no specific change for high resolution data.

Lei: Data on GTS is mostly in BUFR (new data) and high resolution.

Chris: About depth, doesn't think a depth sensor on drifting buoys is needed, just a characterization in relation to wind speed. Drogue on or off is the main change. Pressure sensor not needed.

Craig: We need pressure sensor for a number of uses.

Anne: Pressure sensor on the EUMETSAT NKE buoys.

Chris: We want to use all the data, but at low wind speed we like to understand the structure, but not a requirement for all buoys.

Q: How is deployment location determined? Where would we like more with respect to GHRSST?

Luca: Methodology to generate a requirement map, not exclusive of SST. Years of experience to understand operational needs. But could be room for improvement.

Can we do lakes? Yes.

ACCURATE TEMPERATURE MEASUREMENTS OF GHRSST QUALITY FROM GLOBAL DRIFTER PROGRAM DRIFTERS

Luca Centurioni[1], Lancelot Braasch[1], Verena Hormann[1], Sidney Thurtston[2]

[1]Lagrangian Drifter Laboratory, Scripps Institution of Oceanography, La Jolla, California, United States of America; [2]Global Ocean Monitoring and Observing, NOAA Climate Program Office, Silver Spring, Maryland, United States of America

The NOAA funded Global Drifter Program (GDP), the principal component of the Global Surface Drifting Buoy Array (GSDA) of the Data Buoy Cooperation Panel (DBCP), maintains an array of over 1,250 water following drifting buoys, reporting their observations in near real-time and designed to measure 15 m depth currents, sea-level atmospheric pressure and sea surface temperature (SST). The drifters from the GSDA provide more in-situ SST observations than any other source, including ships, coastal moorings, tropical moorings and Argo floats. GDP drifter data are widely used for validation of satellite SST retrievals algorithms and to characterize their uncertainty and the long-term stability of satellite SST products.

Given their use as reference measurements, it is crucial that the accuracy of drifter-derived in-situ SST observations is carefully quantified and understood. The nominal accuracy and digitization of the temperature probes used to measure SST from GDP drifters deployed before 2014, was O(0.1 °C). The use of more accurate temperature sensors, with smaller drift, improved accuracy (0.05 °C or better) and digitization (0.01 °C or better), and more accurate geolocation from GPS chipset has become the new standard, due to more stringent accuracy requirements from the Group for High Resolution Sea Surface Temperature (GHRSST) and to the rapid improvement of the drifter technology.

81 drifters co-funded by NOAA, NASA and the US Office of Naval Research as part of the SPURS-2 and ASIRI experiments were deployed in the tropical eastern Pacific Ocean and in the Bay of Bengal in the 2015-2018 period. Such drifters, fabricated by the Lagrangian Drifter Laboratory at the Scripps Institution of Oceanography, were fitted with two independent temperature sensors: an accurate, self-contained and externally mounted SBE-37 SI sensor, with an accuracy of ± 0.002 °C (-5 to +35 °C) and the standard, fully integrated GDP temperature sensor, with an accuracy of ± 0.05 °C (-5 to +40 °C). Both sensors have very low drifts, of the order of 1 x 10^{-4}°C per month. A careful comparison of the two concurrently sampled time series of SST obtained from two independent thermometers showed a temperature difference between the two sensors of the order of 2-3 x 10^{-2}°C with a 99.7% confidence level, and a drift comparable to their nominal specifications. Furthermore, the temperature difference between the two sensors decreases with increasing wind speed, suggesting that upper-ocean stratification contributes significantly to the measured temperature differences. For both experiments, the observed temperature differences suggest a very small bias which can be explained by the depth separation between the two sensors, which is of the order of 0.25 m, and the ocean's stratification. This analysis also suggests that direct solar heating of the drifter's hulls, which is also measured with a third internal thermometer, does not introduce any significant bias to the SST observations obtained with the standard GDP temperature sensor.

EVALUATION AND INITIAL RESULTS FROM THE 2018 SAN FRANCISCO TO BAJA CRUISE OF THE SAILDRONE UNMANNED SURFACE VEHICLE

Chelle Gentemann[1], Peter Minnett[2], Peter Cornillon[3], Piero Mazzini[4], Cassia Pianca[4], Ivona Cetinic[5], Joel Scott[5], Jose Gomez-Valdes[6], Jorge Vazquez[7], Vardis Tsontos[7], Santha Akella[5], Mike Chin[7], John Largier[8], Richard Jenkins[9], Sebastien De Halleux[9], Dave Peacock[9], Nora Cohen[9], Thomas Mattias[9]

[1]Earth and Space Research; [2]University of Miami; [3]University of Rhode Island; [4]San Francisco State University; [5]GSFC NASA; [6]CICESE; [7]JPL NASA; [8]University of California, Davis; [9]Saildrone

In the California Current region, the air-land-sea interface is complex, characterized by coastal promontories, upwelling jets and shadows, river plumes, and narrow continental shelves that affect coastal dynamics producing highly variable oceanographic features affecting air-sea interactions and feedbacks. A new type of observation platform, the Saildrone unmanned surface vehicle (USV), collected data on a 60-day cruise from San Francisco Bay, down along the US/Mexico coast to Guadalupe Island and back, during 11 April 2018 to 11 June 2018. The cruise track was selected to optimize both the science and validation objectives of the project. The scientific objectives include studies of upwelling dynamics, river plumes, air-sea interactions including frontal regions, and diurnal warming regions. The validation objectives include establishing the utility of Saildrone measurements for inclusion into ocean models and validation of satellite-derived fluxes, sea surface temperatures, ocean currents, and wind vectors. The Saildrone USV carried its normal suite of instruments plus 4 additional temperature loggers which were added to provide information on thermal variability in the upper ocean. There are 5 more Saildrone cruises planned for 2019 - 2022 to provide additional high latitude sea surface temperature (SST) data for satellite SST algorithm development and improve our understanding of air-sea fluxes in the highly stratified Arctic Ocean.

SEA SURFACE TEMPERATURE AND AIR-SEA INTERACTION IN THE MEDITERRANEAN REGION

Salvatore Marullo[1], Alcide Di Sarra[1], Chunxue Yang[2], Vincenzo Artale[1], Fabrizio Anello[1], Carlo Bommarito[1], Tatiana Di Iorio[1], Daniela Meloni[1], Francesco Monteleone[1], Giandomenico Pace[1], Salvatore Piacentino[1], Damiano Sferlazzo[1], Marco Bellacicco[1], Rosalia Santoleri[2]

[1]Italian National Agency for New Technologies, Energy and Sustainable Economic Development, ENEA, Italy; [2]CNR, Institute of Marine Sciences, Roma, Italy

The interactions between atmosphere and ocean largely affect regional and global climate, as well as weather evolution at both local and global scales. These interaction processes are essentially governed by heat, momentum, freshwater and gas exchange at the air-sea interface. Thanks to the data acquired at the climatic station of Lampedusa, in the central Mediterranean Sea, a research effort aimed at assessing the capability of reproducing the air-sea interaction processes was started from the comparison of directly measured radiative budget components with satellite and model derived estimates. Lampedusa is an integrated atmospheric/oceanic observatory composed of two sections: a ground-based laboratory, operating since 1997, dedicated to the investigation of changes in atmospheric composition and structure and their effects on the surface radiation, and an oceanographic buoy operating since 2015, dedicated to the investigation of air-sea interactions and to ground-truth of satellite observations. The instruments installed on the buoy include a Vaisala MAWS401 meteorological station, Kipp and Zonen CMP21 and CGR4 radiometers for shortwave and longwave irradiances, and a Gill Windsonic anemometer. Among other measurements, water temperature is measured at 1 and 2 m depth using two SeaBird SBE39_Plus sensors acquired with a frequency of 1 minute, and at 18 m depth using a SBE 37 temperature and salinity sensor (foundation temperature). The data collected at Lampedusa constitute a unique dataset to continuously evaluate the accuracy of turbulent and radiative heat fluxes derived from satellites, models, and bulk formulae, and to develop new parameterizations of fluxes.

Our analysis, based on 1 year of acquisitions of radiative components with sampling frequency of 1 second, reveals that satellite estimates of the downwelling radiation components overestimate the surface solar and longwave irradiances. The SEVIRI MSG4 observations overestimate the short-wave irradiance by 5 W/m^2 with a RMS deviation of 22 W m^{-2} and the downward atmospheric longwave irradiance by 7 W m^{-2} with a RMS deviation of 12 W m^{-2}.

Similarly, based on ECMWF ERA5 re-analysis, the shortwave incoming radiation shows a very small bias of 1.2 W m^{-2} and a RMS deviation of 32 W m^{-2}, while the longwave irradiance is underestimated by 17 W m^{-2} with a an RMS deviation of 12 W m^{-2}.

The impact of these determinations was also investigated by using a 1D numerical model, the General Ocean Turbulence Model, for the evolution of the upper ocean temperature profile. The model simulations have been compared with water temperatures recorded at 1 and 2 m depth. The mean bias is 0.02 °C and -0.01 °C respectively, and the RMSE is 0.5 °C when the model is forced using measured radiative fluxes at the mooring and turbulent fluxes estimated from in situ observations. When the model, instead, is forced by satellite based radiative fluxes the bias increases to 1.5 °C with a RMSE of about 1°C. These results confirm the importance of reducing uncertainties in satellite estimates of radiative fluxes including effects of atmospheric aerosols. Reduced uncertainties and increased space and time resolutions, thanks to a multi-satellite approach, will be essential to resolve the closure problem of the Mediterranean heat budget.

PLENARY SESSION VIII: DIURNAL VARIABILITY

SESSION VIII REPORT

Chair: Andrew Harris[1] – Rapporteur: Sandra Castro[2]

(1) University of Maryland, USA, Email: aharris2@umd.edu
(2) University of Colorado, USA, Email: sandrac@colorado.edu

1. INTRODUCTION

Relating the skin (or subskin) temperature to the ocean temperature at depth continues to be one of the key scientific challenges for the use of remotely-sensed SST. In particular, under conditions of high insolation and persistent low wind speed, a warm layer builds up at the surface, leading to temperatures that may be several kelvin warmer than that of the oceanic mixed layer (a.k.a. "foundation" temperature). This year's plenary session illustrates the ongoing effort being directed towards practical solutions for addressing the aforementioned challenge. Unfortunately, one of the scheduled presenters was unable to attend, but the two presentations stimulated lively discussion, which continued into the open forum period at the end of the session.

2. ORAL PRESENTATIONS

Pimentel *et al*., "*Results from the SOSSTA project on developing a statistical-dynamical observation operator for SST data assimilation*"

Ocean models do not resolve within the upper ~metre, thus an observation operator (OO) is required in order to assimilate diurnally-resolved satellite skin SST observations into such models. The authors chose to develop a fast coefficient-based model by running configurations of GOTM, forced with ERA-Interim fluxes of heat & momentum. A variety of chlorophyll-dependent insolation parameterizations were also tested. Canonical Correlation Analysis (CCA) is used to develop the statistical model, and the GOTM simulations were matched against SEVIRI skin SST observations. Since the interest was only in the evolution of the diurnal layer, the model simulations were initialized to uniform profiles of salinity & temperature each dawn.

Results show that the statistical operator can reproduce the GOTM temperatures reasonably well and can resolve the diurnal warming (DW) signal at low winds and high insolation. The performance of the operator is evaluated via two different skill scores: in one the mean square error (MSE) between the SEVIRI subskin SST and the subskin obtained from the CCA OO is standardized by using the temperature at 1.47m-depth from the MED MFC profiles and in the other by using the Bernie *et al*. 2007 DW parameterization. Preliminary results from POSEIDON Aegean Sea model runs show an 11% improvement in RMSE when using the CCA OO for assimilation of satellite SSTs.

Points raised during the subsequent discussion include clarification of the analysis variable being the first level of the ocean model, and possible reasons for the existence of a 2nd peak in the diurnal signal of $T_{subskin} – T_{skin}$ for the GOTM model training runs. In the case of the latter, the presenter thought it might be due to the local time of initialization. However, this session chair is of the opinion that it is merely an artefact of including insolation absorption within the laminar skin layer, which depresses the skin effect. The maximum depression will be around noon, reducing to ~zero at sunrise/sunset, and this corresponds to the figure shown in the presentation.

Karagali et al., "*DIVOST-COM: Improved Diurnal Variability "Forecast" Of Ocean Surface Temperature through Community Model development*"

The goal of the work is to develop and integrate a diurnal variability model with the Baltic MFC 3-D physical-biological model and the SST TAC L4 analysis to improve the CMEMS satellite products for the Baltic Sea.

Currently, the DMI Baltic MFC operational models (HBM/NEMO) produce good bulk temperature estimates but don't resolve the diurnal cycle. CMEMS would like to improve the SST representation in the upper few meters by using GOTM operationally within the MFC PHY-BIO forecasting system. GOTM SST forecasts are required to have similar quality to the bulk SSTs from HBM or NEMO.

The authors propose to use κ-ε TKE mixing scheme – various turbulent diffusion schemes have already been tested (see Karagali *et al*., 2017, JGR). Initialization & forcing has temperature and salinity profiles from DMI's HBM 3-hourly forecast system, while atmospheric forcing comes from HIRLAM (High-Resolution Limited Area Model). The top GOTM level is 2.5 mm thick. There are various test/validation sites, including 6 profiling stations and 9 surface stations, while SEVIRI hourly L3C SSTs are also available for comparison.

The analysis consists of 4 months (Apr-Aug, 2018) of GOTM simulations with and without daily initialization. During the simulation period, 4 instances were identified in which SEVIRI shows DW events with large amplitude (>0.5 and up to 1.2 °C). In those instances, however, the SEVIRI DW exceeds the modelled DW from both GOTM and HDM by at least 1 °C. In general, GOTM gives slightly better results (bias and RMS) relative to SEVIRI than does the HBM model relative to SEVIRI. Maps (2D analyses) of differences (SEVIRI-2D GOTM, SEVIRI-HBM) over the entire Baltic domain for those dates show SEVIRI-GOTM differences having consistently smaller biases than HBM-GOTM by about 0.5 degree C. Next steps include finalizing the GOTM setup, and extending the 2D simulations to cover the entire 4-month period.

The audience about various aspects of the study raised a number of questions. Have amplitudes of 2-3 degrees been produced by GOTM, since such excursions are often seen in SEVIRI day – night observations for the Baltic (Ioanna recalled that such magnitudes have been reproduced in the past). Has precipitation information been included (possible, but has not been tried yet). What are the significant changes in the latest GOTM release (mostly insolation parameterization, which now includes Pimentel's model)? This requires further study, as extreme chlorophyll values in the Baltic are problematic. They have made a switch from ECMWF to DMI forcing fluxes (not GOTM-specific, but it has improved results and therefore presumably influenced model tuning). This session chair anticipates the underlying reason is higher resolution, especially for the wind field. It was noted that there is a need to undertake a sensitivity study for GOTM w.r.t. forcing fluxes.

Another question was raised as to whether or not RMSE is the best metric for modelled diurnal warming, especially if there are location mismatches (*e.g.* due to phase errors in NWP forcing fields). The Science Team discussed the possibility of isolating the DW events themselves, rather than considering the entire basin. Note in passing that it is better, in an RMSE sense, to simply predict zero warming everywhere than to have predicted warming with a location error. This topic served as a segue into the Open Discussion.

3. OPEN DISCUSSION

This section was primarily focused on identifying the leading issues arising from the presentations. First off, we are better at observing DW than modelling it. Phase errors: there are large differences for 1 or 2 m s^{-1} winds. NSST from NCEP has the model adjoint in it, so it has the potential to influence the wind field. Even if it is a very simplified model, by introducing a structure field; it can compute a consistent Jacobian, therefore observations of DW can influence the NWP wind field. It is also important to note that that warming is not just a function of instant wind speed, but persistent winds – we really need history of wind, which makes for a very difficult adjoint.

DW statistical distribution type studies were being performed by some groups ~10 years ago, primarily in deriving scale-to-amplitude relationships. We could revisit those distributions now with improved data from the new geostationary satellites (Himawari-8 and GOES-16). Might be able to do better job now with the new generation of geostationary satellites; much more data.

Regarding the effect of wind on the assimilations: what should the wind speed be given the simulations? What wind speed in GOTM could give the best match for the locations of the observed DW and the simulated DW? It was suggested to do an ensemble of GOTM runs with a distribution of wind speeds to get a distribution of

DW. It is not realistic to do this at the data assimilation stage, but it might be possible to build a multidimensional LUT based on an ensemble of GOTM runs.

There remains a need to validate the models, especially over the basin scale. SST algorithm sensitivity is very important (many SST products don't report sensitivity), but we need to factor sensitivity into the validation.

Model validation leads to the question about adding additional sensors to drifting buoys – what depths, and how often to sample? How easy would it be to have 3 temperatures from the buoys? Apparently it is very feasible and should not be expensive. What depths? Do we (GHRSST *et al*.) need this as a community? It has long been argued that drifter data with depth information would be highly valuable. The Science Team encourages outreach to all the Met communities represented at GHRSST – do they have a need? There should be a recommendation on this from the DW group.

However, it may be hard to justify a large program for the context of this community, but there is interest. Important to hear from modellers on what is needed with respect to having multiple temperatures from drifters; would be good to entrain (pun intended) the coupled ocean community; which is a much bigger group.

The UK Met Office has combined observations and modelling with assimilation (James While presented in 2015). There was a request for certain details of their model (skin effect in particular, the diurnal parameterization is an adaptation of Zeng & Beljaars), and has the scheme made an impact on data assimilation (or fluxes)? At the meeting, the answers were not to hand, so the Met Office may provide a briefing on their skin analysis at the next ST meeting.

RESULTS FROM THE SOSSTA PROJECT ON DEVELOPING A STATISTICAL-DYNAMICAL OBSERVATION OPERATOR FOR SST DATA ASSIMILATION

Sam Pimentel[(1)], Dimitra Denaxa[(2)], Eric Jansen[(3)], Gerasimos Korres[(2)], Isabelle Mirouze[(3)], Andrea Storto[(3)], and Wang-Hung Tse[(1)]

(1) Trinity Western University, Langley, BC, Canada, Email: sam.pimentel@twu.ca
(2) Hellenic Centre for Marine Research (HCMR), Athens, Greece
(3) Centro Euro-Mediterraneo sui Cambiamenti Climatici (CMCC), Italy

1. INTRODUCTION

We present results from the completed CMEMS funded SOSSTA project. This project developed a dynamical-statistical observation operator for satellite SST observations that accounts for the diurnal variability of the skin and subskin SST layers. We present an overview of the main achievements of the project. This includes (1) a modelled data set of fine-scale diurnal SSTs for the Mediterranean Sea, (2) the use of canonical correlation analysis (CCA) to develop a highly-efficient observation operator to parametrize the diurnal cycle, and (3) the implementation of this observation operator into an ocean data assimilation system.

2. GOTM MODELLING

We have used an ocean column model (GOTM) to simulate diurnal SST variability across the Mediterranean Sea with fine vertical resolution (*e.g.* 21 levels in the top 1 m). GOTM is run on a ¾-degree grid (391 locations with a depth of 75 m or greater) for 2013 - 2014. The model is initialized at sunrise each day using MED-MFC temperature and salinity profiles, and forced using 3-hourly ERA-Interim atmospheric data. GOTM models the near-surface ocean thermodynamics, including dynamically computing the skin SST using the Fairall parameterization which has been adapted to take into account the fraction of solar radiation absorbed in the cool-skin layer. We explore the influence of several solar absorption parameterizations including those that use MODIS chlorophyll data and MODIS IOP data. We present results showing the number of intense diurnal warming events and highlight the non-uniform cool-skin effect, as well as compare the influence of various solar absorption parameterizations on the modelled near-surface temperatures. Our simulated results for the Mediterranean Sea allow us to contrast skin SST, subskin SST, SST at depth, and foundation SST. The GOTM SSTs are validated against SEVIRI L2C observations from OSI-SAF. Further details and the full set of results are published in Pimentel et al., 2019. In addition to these published results we also explored other configurations of the experiment, including running GOTM over a 1/16-degree grid and using ECMWF forecast data for forcing and MED-MFC forecast data for profile initialization.

3. DEVELOPING AN OBSERVATION OPERATOR

The GOTM data is used as a training set for performing a canonical correlation analysis (CCA). The CCA extracts the maximally correlated modes of variability between temperatures at depth and skin/subskin SST. CCA finds joint structures between two data sets, in our case profile temperatures and skin and subskin SSTs. The CCA is a linear method, however, to handle the non-linearity of the diurnal variability problem we perform the CCA in different categories of atmospheric state (daily mean insolation and daily mean wind speed) and hour of day. These canonical correlations are then used to formulate an observation operator that is designed to project OGCM temperature profiles onto a skin or subskin SST for computing the innovation (y-Hx) in the assimilation of satellite SST data. These low-dimension projections are highly efficient and are shown to effectively capture the diurnal variability and cool-skin effect without having to use a dynamical model. We examine the performance of the CCA observation operator by comparing skill-scores using L3C SEVIRI subskin SST observations from OSI-SAF. The observation operator is shown to provide significant improvements over simply using the SST from the top model level of an OGCM or using the diurnal parameterization of Bernie (which is implemented as an option in NEMO). Further details on the theoretical development of this new operator and its performance are found in Jansen et al., 2019. The statistical-dynamical observation operator was implemented for testing in the POSEIDON model forecasting system

(Aegean Sea). Offline results using the new operator as opposed to the top model level when comparing to L2P SEVIRI skin SST observations show an improvement of 11% in RMSE. An online assimilation run for a full year is performed where the new operator is used to assimilate L2P SEVIRI skin SSTs at 12:00 UTC. The results show the benefits of daytime SST assimilation in the forecast and analysis system. These results are being finalized and prepared for publication.

4. CONCLUSION

GOTM is used to produce a high-resolution data set of diurnal SSTs in the Mediterranean Sea which can be used to compare skin SST, subskin SST, SST at depth, and foundation SST (see Pimentel et al, 2019). This training data set was used to produce canonical correlations, which we found to be a simple and efficient means to provide good estimates of the skin and subskin SST. The CCA is used to create a low computational cost observation operator for assimilating SST (see Jansen et al., 2019). The CCA observation operator has been tried in the POSIEDON Aegean Sea model and initial results look promising. This low computational method has potential for use in a wide array of SST applications including computing diurnal skin SST for air-sea flux calculations, as a means of comparing different in-situ observations at various depths to satellite observations, including diurnal SSTs in climate models, *etc.*

5. REFERENCES

Pimentel, S., W.-H. Tse, H. Xu, D. Denaxa, E. Jansen, G. Korres, I. Mirouze, and A. Storto, Modeling the near-surface diurnal cycle of sea surface temperatures in the Mediterranean Sea, *J. Geophys. Res. Oceans,* https://doi.org/10.1029/2018JC014289, 2019.

Jansen, E., S. Pimentel, W.-H. Tse, D. Denaxa, G. Korres, I. Mirouze, and A. Storto, Using Canonical Correlation Analysis to produce dynamically-based highly-efficient statistical observation operators, *Ocean Sci. Discuss.,* https://doi.org/10.5194/os-2018-166, in review, 2019.

IMPROVED DIURNAL VARIABILITY FORECAST OF OCEAN SURFACE TEMPERATURE THROUGH COMMUNITY MODEL DEVELOPMENT

Ioanna Karagali[(1)], Jun She[(2)], Jens Murawski[(2)], Jacob Høyer[(2)]

(1) DTU Wind Energy, Technical University of Denmark, Roskilde, Denmark, Email: ioka@dtu.dk
(2) Danish Meteorological Institute, Copenhagen Ø, Denmark, Email: js@dmi.dk, jmu@dmi.dk, jlh@dmi.dk

1. INTRODUCTION

The diurnal variability of SST, driven by the coincident occurrence of moderately low winds and solar heating, is currently not properly understood and resolved in models and products from the Copernicus Marine Environment Monitoring Service (CMEMS) of high spatial resolution. This results in erroneous estimation of air-sea interactions and heat budget, which causes demised model accuracies. In addition, diurnal SST variability complicates merging of SSTs from different satellite sensors thus having a direct impact on efforts to create climate records. Finally, a misrepresentation of the diurnal variability of the upper ocean temperature may result in large errors when modelling harmful algal blooms. The “Improved Diurnal Variability Forecast of Ocean Surface Temperature through Community Model development (DIVOST-COM)” project aims at developing and integrating a diurnal variability model with the Baltic Modelling & Forecasting Center (MFC) 3D physical-biological model and the SST Technical Advisory Council (TAC) Level 4 analysis to improve existing products and services for the Baltic Sea. To achieve this, the existing 1-dimensional General Ocean Turbulence Model (GOTM) will be developed to a common modelling tool, which uses the MFC PHY-BIO forecast and SST Thematic Assembly Centre (TAC) products as input to resolve and forecast the vertical temperature structure of the upper ocean with very high resolution. The aim is to assess the ability of the operational HBM model to reproduce the variability of the upper ocean temperature and evaluate the magnitude of the simulated and observed diurnal variability in the Baltic Sea. Preliminary results indicate similar biases and root-mean-square-errors when compared to in situ measurements and an overall reduction of bias and RMSE with SEVIRI, for some of the GOTM simulations.

2. DATA AND METHODS

2.1. HBM AND HIRLAM

The operational BAL MFC model, *i.e.* currently the HIROMB-BOOS Model (HBM), temperature and salinity profiles are used as initial conditions. The state of the lower atmosphere, *i.e.* 2 m air temperature, wind components at 10 m above the ocean surface, mean sea level pressure, cloud cover and specific humidity, is retrieved from DMI’s operational modelling chain (DMI-HARMONIE 54h forecast). All input variables were available at hourly intervals. The Baltic (BAL) Monitoring & Forecasting Centre (MFC) domain is used as an example for the implementation and experiments.

2.2. SEVIRI

The O&SI SAF L3C, hourly subskin SST retrievals derived from Meteosat-11 SEVIRI brightness temperature data on a 0.05º regular grid (DOI 10.15770/EUM_SAF_OSI_0004) were obtained for the period April to August 2018 from the LML FTP server, hosted by IFREMER.

2.3. IN SITU MEASUREMENTS

In situ measurements from fifteen stations in the Baltic Sea were collected, through CMEMS, for the period April - August 2018 (see Figure). The water depth at the sites ranges from 20 m to 100 m. Six stations have available temperature measurements at various depths while the remaining nine stations have only surface measurements, typically at 0.5 m or 1 m.

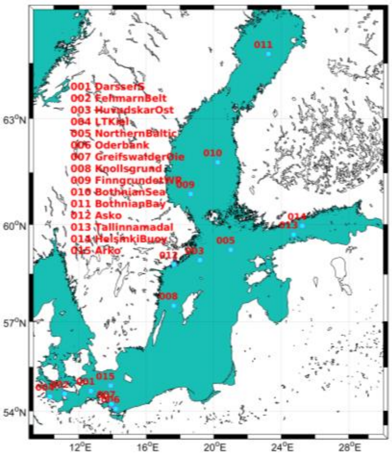

Figure 1: Locations of in-situ measurement stations.

2.4. GOTM

The 1-dimensional General Ocean Turbulence Model (GOTM) [1] was used; building on previous sensitivity experiments from [3], surface fluxes and short-wave radiation were calculated from input meteorological data using the Fairall algorithm. The turbulence method was selected to be the turbulence model calculating TKE and length scale using a dynamic Kε equation and the dynamic dissipation rate for the length scale. For the stability, the Kantha-Clayson quasi-equilibrium method was used. The long wave radiation calculation was performed using a Brunt type formula with coefficients from [3]. For the attenuation of light in the water column a 9-band model with attenuation lengths from [5] and proportional coefficients from MODTRAN was used.

2.5. DV ANALYSIS

Using SEVIRI from April to August 2018, dates with significant diurnal warming were identified. The criteria for selection were based on the "dt_analysis" field included in the SEVIRI files, defined as the deviation from SST analysis or reference climatology – OSTIA [1] was used as a reference. Requirements were set such that for the domain of interest, defined as 53 °N – 60 °N and 6° E - 24.5 °E, at least 5 % of the grid points included in the domain with quality of the SST retrieval of 3 or more, showed a deviation from the reference of at least 1 °C. From a total of 115 days identified, four were selected for more specific analysis, *i.e.* detailed GOTM simulations and comparisons with SEVIRI and HBM. In order to allow direct comparisons between the models and SEVIRI, the former have been re-gridded to match the SEVIRI grid, which is coarser than the simulations; approximately 5.5 x 3.5 km for the domain of interest.

Furthermore and for the test sites (see Figure) located below the latitude of 60 °N, *i.e.* the upper boundary of the SEVIRI disc, mean diurnal variability was computed by estimating the nighttime foundation temperature between midnight and 04:00 and extracting it from the daytime hourly SST. The diurnal amplitude, δSST, was defined as the mean of hourly day-time SST from 07:00 to 19:00 minus the foundation temperature, defined as the mean of night-time values from 00:00 to 04:00.

3. RESULTS

The mean δSST for SEVIRI, GOTM and HBM at some of the test sites from Figure 1 is shown in the left panel of Figure 2, with its variance on the right panel. SEVIRI shows mean diurnal amplitudes ranging from 0.4 °C to 1.2 °C with a variance ranging from almost 0 °C and up to 1.6 °C, depending on the location. Lowest variances, lower than 0.05 °C were identified for the Northern Baltic (station 005 in Figure) and Greifswalder Oie (station 007), where the mean diurnal amplitude was relatively low, *i.e.* between 0.4 °C and 0.6 °C. To the contrary, stations Fehmarn Belt (002) and Asko (012) showed the highest mean amplitude (1 - 1.2 °C) and variance (1.5 - 1.6 °C).

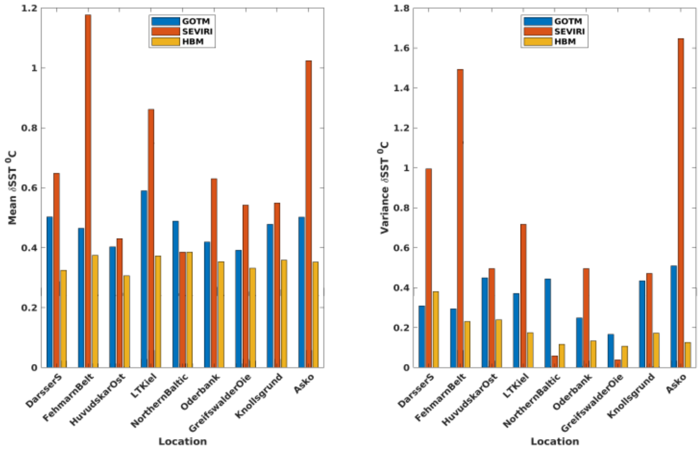

Figure 2: Statistics of mean diurnal variability (left) and its variance (right) from 4 months of SEVIRI SST (red), GOTM (blue) and HBM (yellow) at selected test sites.

Overall comparisons from the 2D simulations of GOTM, SEVIRI SST and HBM and for selected dates identified through the DV analysis of SEVIRI SST, are shown in Figure 3. The mean bias between SEVIRI and GOTM ranges between 0.2 °C and 0.85 °C, depending on the date. The mean bias between SEVIRI and HBM ranges between 0.6 °C and 1.25 °C; it is 0.4 °C and up to 0.6 °C higher than between GOTM and SEVIRI. When looking at the RMSE (right panel of Figure 3), values range between 1 °C and 1.4 °C for GOTM, while for HBM they are much higher, *i.e.* 1.2 °C to 2.0 °C.

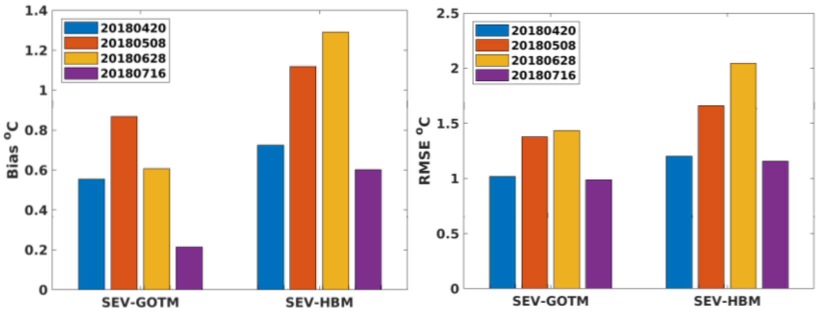

Figure 3: Mean bias (left) and its standard deviation (right) for SEVIRI, GOTM, HBM comparisons from 07:00 - 19:00 on each of the 4 identified dates (different colours).

During the event of May 8, warming exceeding 1 °C in more than 5 % of the SEVIRI grid points covering the domain was maintained during the whole day, *i.e.* for 24 hours. The differences between SEVIRI and the models at 13:00 are presented at the top row of Figure, while the differences at 16:00 at the bottom row. Areas of significant SEVIRI warming that are misrepresented in the models appear as very bright and their extent is significantly larger at HBM compared to GOTM for both time instances considered.

Figure 4 shows differences between GOTM and HBM at 13:00 (*a*, *b*) and 16:00 (*c*, *d*). As expected, significant deviations of up to 2°C are identified for the same areas where SEVIRI indicated strong warming patterns, especially for the GOTM 2.5 mm layer (*a*, *c*) consistent with the results from Figure 4. Note how the differences become significantly smaller in amplitude and area at 16:00 compared to 13:00. Panels *b* and *d* of Figure 5 show the same differences as described above but calculated using the 1.5 m GOTM layer. Differences between the two models are significantly lower in amplitude and spatial extent when the same depth is considered and for the simulation at 13:00, while they become almost zero at 16:00.

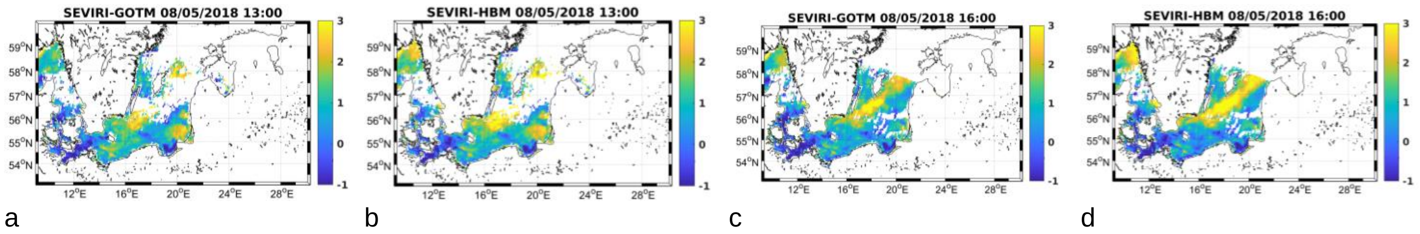

Figure 4: SEVIRI-GOTM temperature (0.2 cm vs 9 cm) and SEVIRI-HBM temperature (0.2 cm vs 1 m) for the grid points with SEVIRI quality flag >=3. Panels a and b show comparisons at 13:00 while the panels c and d at 16:00.

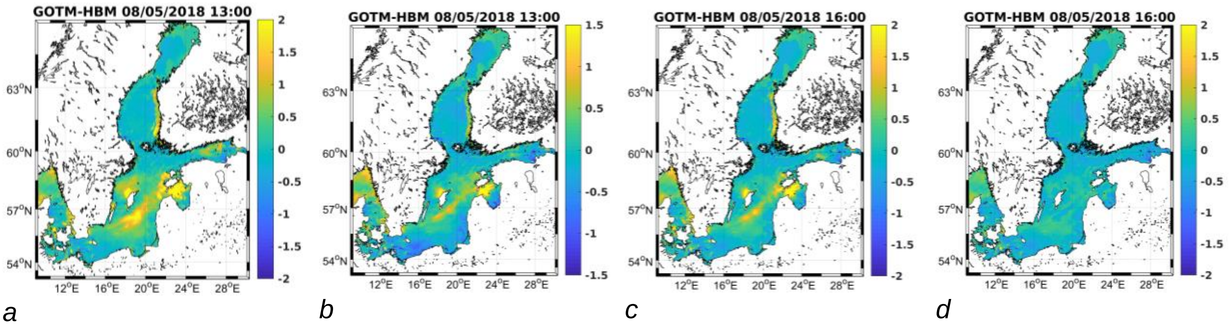

Figure 5: GOTM temperature at 2.5 mm minus HBM 1.5 m (a,c) and GOTM-HBM at 1.5 m (b,d), at 13:00 (a,b) and 16:00 (c,d) on 8th May 2018.

4. CONCLUSION

Mean δSST from SEVIRI exceeding 1 degree at test locations in the Baltic, where mean DV amplitudes from GOTM were found to approximate SEVIRI better compared to HBM. Individual diurnal warming cases simulated over the entire domain indicated that GOTM was able to resolve warming not present in HBM, with mean biases SEVIRI minus GOTM being 0.5 °C lower compared to SEVIRI minus HBM. For extended diurnal warming events, GOTM reduced biases with SEVIRI by 1°C or more compared to HBM.

5. REFERENCES

[1] Burchard, H., Bolding, K., and Villarreal, M.R., GOTM - A general ocean turbulence model. Theory, applications and test cases, Tech.Rep. EUR 18745 EN, 1999, Eur. Comm. Brussels, Belgium.

[2] Donlon, C. J., Martin, M., Stark, J., Roberts-Jones, J., Fiedler, E., & Wimmer, W. (2012). The Operational Sea Surface Temperature and Sea Ice Analysis (OSTIA) system. Remote Sensing of Environment, 116(Sp. Iss. SI), 140–158. https://doi.org/10.1016/j.rse.2010.10.017

[3] Grant, A.L.M., & Hignett, P. (1998). Aircraft observations of the surface energy balance in TOGA-COARE, Q. J. R. Meteorol. Soc., 124, 101–122.

[4] Karagali, I., Høyer, J.L., & Donlon, C.J. (2017). Using a 1-D model to reproduce the diurnal variability of SST. Journal of Geophysical Research: Oceans, 122(4), 2945–2959.

[5] Paulson, C.A., & Simpson, J.J. (1981). The temperature difference across the cool skin of the ocean, J. Geophys. Res., 86, 11044–11054

PLENARY SESSION IX: CLIMATE DATA RECORDS

SESSION IX REPORT

Chair: Helen Beggs(1) – Rapporteur: Christopher Merchant(2)

(1) Bureau of Meteorology, Melbourne, Australia, Email: helen.beggs@bom.gov.au
(2) University of Reading, Reading, UK, Email: c.j.merchant@reading.ac.uk)

ABSTRACT

This is a report of the presentations and discussion during the GHRSST-XX Plenary Session IX on Climate Data Records.

1. SUMMARY OF PRESENTATIONS AND ASSOCIATED DISCUSSION

1.1. TITLE: A 35 YEAR SEA SURFACE TEMPERATURE CLIMATE DATA RECORD FROM THE ESA CLIMATE CHANGE INITIATIVE. PRESENTER: OWEN EMBURY

The ESA SST CCI Phase II products were described – L2P from ATSR-1, ATSR-2, AATSR and AVHRR (from NOAA-7, 9, 11, 12, 14, 15, 16, 17, 18, 19, Metop-A) and Daily 5 km L4 SST(0.2m) analysis based on the OSTIA system. The files are available from 1981 to 2016 from http://cci.esa.int/data via the FTP method only at this stage. NOAA-7 to NOAA-11 AVHRR SSTs are referenced to in situ data, while NOAA-12 AVHRR SSTs onwards are referenced to A(A)TSR. The CCI v2 L4 is formed only from CCI v2 satellite SST inputs.

New Copernicus Climate Change Service (C3S) L2P, L3C and daily 5 km L4 SST(0.2m) products, designed to extend the SST CCI v2 SST products for climate applications, were also described. Inputs are currently Sentinel-3A SLSTR L2P and Metop-A FRAC AVHRR L2P, processed using the CCI method. The C3S SST products are available from http://data.ceda.ac.uk/neodc/c3s_sst/data/ICDR_v2 from 1 Jan 2017 up to 9 months behind real-time.

Future work will include adding Sentinel-3B SLSTR and Metop-B data.

Comments/Questions:

- Ken Casey asked about whether the products were GHRSST compliant and Owen confirmed that they are, with additional fields. Regarding the updates, the plan is to move towards daily updates of the ICDR within 10 days.
- Andy Harris asked about the causes of residual biases, and Owen gave the view that some arise from instrumental effects.

1.2. TITLE: CCI OSTIA AS THE STANDARD OF TRUTH: DETAILED ERROR MODELS FOR IN SITU SST DATA FROM SHIPS AND OTHER PLATFORMS. PRESENTER: ALEXEY KAPLAN

- Used ICOADS R2.5 (Woodruff et al., 2011) for the in situ SST data, separated by platform type,
- Used ESA SST CCI version 1 SST reanalysis (based on OSTIA method) for the satellite-derived data set. This is a global, daily 0.05 degree x 0.05 degree SST analysis, independent of in situ data, gapless data set (Merchant et al., 2014), with validated error estimates.
- Binned data into 1 degree x 1 degree x 1 month bins.
- Studied sampling error and measurement separately
- Observed large systematic biases between ICOADS ship SST and truth (CCI OSTIA).

- Alexey therefore computed a climatology of ship SST for a period and subtracted the seasonal means, using the Kent and Challenor (2006) Variogram Method for 1970 – 1997.
- Used CCI OSTIA to estimate the sampling error of the ship SST
- However, this method does not work for drifters, since drifters are not truly Lagrangian platforms.

Comments/Questions:

- Helen Beggs asked whether the reporting to only 0.1 °C of traditional drifting buoys is significant to the conclusion that drifting buoys underestimate uncertainty, and Alexey confirmed his view that the Lagrangian nature of the platform is the key here (the multiple measurements of the drifter is of “correlated water” within the area).
- Results appear due to the number of drifter platforms, not number of observations.

1.3. TITLE: USE OF SST FOR MONITORING CORAL STRESS: LOOKING FORWARD WHILE KEEPING AN EYE ON THE PAST. PRESENTER: WILLIAM SKIRVING

In the talk he emphasised that for this application it is of crucial importance that SST specifically at the warmest part of the year is well represented, with low biases. SSTs from satellites cover the entire history of mass coral bleaching events, and are therefore extremely important for Coral Reef management.

NOAA Coral Reef Watch quantify coral bleaching risk using following metrics:

- MMM = Maximum of the Monthly Means (1985 – 2012)
- HotSpot = daily SST – MMM where HotSpot ≥ 0.
- DHW = Sum of HotSpot for HotSpot ≥ 1.

William compared coral bleaching metrics calculated using two long term SST analysis products:

- New ESA SST CCI version 2.0 Daily 0.05 degree SST(0.2m) analysis
- Existing NOAA Coral Reef Watch (CRW) “CoralTemp” Global Daily 0.05 degree SST_{fnd} analysis formed from MyOcean OSTIA Daily 0.05 degree SST_{fnd} reanalysis (1985 – 2001) and NOAA/NESDIS/STAR Geo-Polar Blend Daily 0.05 degree Night-time SST analysis (2002 – present). Real-time UK Met Office OSTIA SST analysis is used to bias-correct the Geo-Polar Blend SST.

Results showed CCI derived percentage of reefs with DHW ≥ 4 significantly less than CoralTemp derived values for recent years (after 2002). Possibly linked to OSTIA reanalysis being cold-biased at beginning of the period.

- For all months, CoralTemp – CCI was cold biased until 2005, and OK after.
- For 1985 to 2012, the average difference was -0.11K
- For February only: 1985 – 2012 average difference was -0.19K.
- The CCI-derived metrics indicate that the relationship between DWH and bleaching is entirely consistent for all three mass bleaching GBR events (1998, 2002, 2016).
- Implies that CCI v2 L4 is very consistent (unbiased) through time for high SST anomalies over Tropical coral reefs – really important.
- New SST products need to be related to historic products or should be able to be reprocessed back through time.
- Suggested that one can use coral bleaching data to check for consistency through time.

Comments/Questions:

- Chelle Gentemann commented that the presentation illustrated the importance of having user perspectives on GHRSST data presented at meetings.
- Chongyuan Mao (Met Office) emphasised that the Met Office does not recommend users blending two OSTIA products together as the real-time OSTIA analysis system has had many changes and is not aiming to stay consistent in time.
- William explained that the idea for Coral Reef Watch is long-term consistency, with one real-time SST product which is linked to the reprocessed product. A latency of 10 days (as planned for C3S SST analysis) is too long. CRW definitely require a near real-time (within 24 hour) product. Considering using NOAA Geo-Polar Blend L4 but “re-jig” at 10 days behind real-time to use C3S L4.
- Chongyuan Mao: It would be interesting to compare C3S L4 with RT OSTIA L4.

2. GENERAL DISCUSSION

- Helen Beggs raised the question of how to maintain long-term records in the face of changing satellite sensors, particularly as Metop-C is the last AVHRR, a series which has been widely used for climatology and climate monitoring.
- Andy Harris noted that new sensors (*e.g.* SLSTR) give opportunities for improvement and understanding the errors of the older sensors (*e.g.* AVHRR).
- Bob Evans: The solution to VIIRS vs AVHRR is to process the raw L0 VIIRS data with the AVHRR processing method. The Cooperative Institute between NOAA and the University of North Carolina is the only group that can input NOAA’s L0 data from all NOAA satellites (VIIRS and AVHRR), and all this data is on the Amazon Cloud. You could spatially sub-set the VIIRS data to GAC AVHRR-like pixels

A 35 YEAR SEA SURFACE TEMPERATURE CLIMATE DATA RECORD FROM THE ESA CLIMATE CHANGE INITIATIVE

Owen Embury[(1)], Christopher J. Merchant[(2)], Claire E. Bulgin[(3)], Thomas Block[(4)], Gary Corlett[(5)], Simon A. Good[(6)], Jonathan Mittaz[(7)], Nick A. Rayner[(8)], David Berry[(9)], Steinar Eastwood[(10)], Kevin Pearson[(11)], Jacob L. Høyer [(12)], Ruth Wilson[(13)], Hugh Kelliher[(14)], and Craig Donlon[(15)]

(1) Department of Meteorology, University of Reading, UK, Email: o.embury@reading.ac.uk
(2) Department of Meteorology, University of Reading, UK, Email: c.j.merchant@reading.ac.uk
(3) Department of Meteorology, University of Reading, UK, Email: c.e.bulgin@reading.ac.uk
(4) Brockmann Consult GmbH, Hamburg, Germany, Email: tom.block@brockmann-consult.de
(5) EUMETSAT, Darmstadt, Germany, Email: Gary.Corlett@eumetsat.int
(6) Met Office, Exeter, UK, Email: simon.good@metoffice.gov.uk
(7) Department of Meteorology, University of Reading, UK, Email: j.mittaz@reading.ac.uk
(8) Met Office, Exeter, UK, Email: nick.rayner@metoffice.gov.uk
(9) National Oceanography Centre, Southampton, UK, Email: dyb@noc.ac.uk
(10) METNO, Oslo, Norway, Email: s.eastwood@met.no
(11) Department of Meteorology, University of Reading, UK, Email: k.j.pearson@reading.ac.uk
(12) Danish Meteorological Institute, Denmark, Email: jlh@dmi.dk
(13) Space Connexions Ltd, Harpenden, UK, Email: ruth.wilson@spaceconnexions.com
(14) Space Connexions Ltd, Harpenden, UK, Email: hugh.kelliher@spaceconnexions.com
(15) European Space Agency, ESTEC, Katwijk, Netherlands, Email: craig.donlon@esa.int

1. INTRODUCTION

Understanding the state of the climate requires long-term, stable observational records of essential climate variables (ECVs) such as sea surface temperature (SST). ESA's Climate Change Initiative (CCI) was set up to exploit the potential of satellite data to produce climate data records (CDRs). The initiative now includes over 20 projects for different ECVs, including SST, which has recently released its second set of CDRs. Complementary to the ESA CCI, the Copernicus Climate Change Service (C3S) is producing an Interim CDR (ICDR) to extend the CCI CDR in short-delay mode. The C3S ICDR is produced using the same software and systems as the CCI CDR. This report will summarise the progress and latest products available from SST-CCI.

The ESA SST CCI CDR v2.1 (Merchant et al. 2019) provides a 35-year global SST record (1982 - 2016) developed from 1.8 x 10^{13} satellite measurements. Products include skin SST and depth-and-time-of-day adjusted SST from both Along Track Scanning Radiometer (ATSR) and Advanced Very High Resolution Radiometer (AVHRR) instruments at GHRSST levels L2P, L3U, and L3C; plus a Level 4 SST analysis based on the Met Office OSTIA system. Complementing this is the C3S ICDR (2017 onwards) which is producing L3C products from the Sea and Land Surface Temperature Radiometer (SLSTR) and AVHRR instruments; along with a L4 analysis. Current data coverage is illustrated in Figure1.

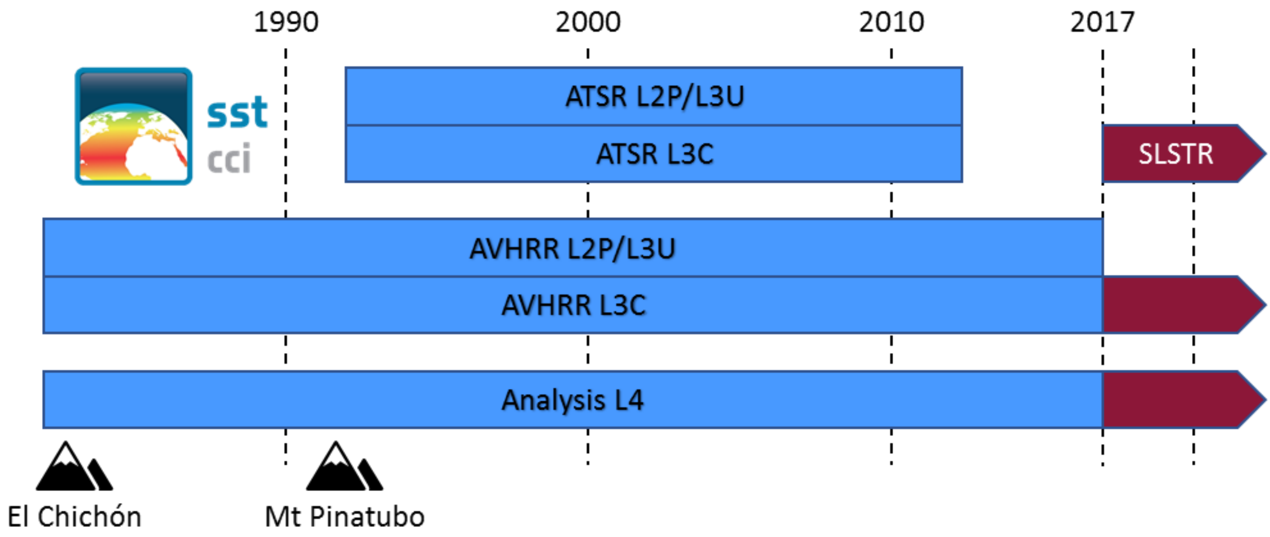

Figure 1: CDR (dark blue) / ICDR (dark red) datasets: temporal coverage and availability. C3S ICDR provides an ongoing extension of the SST daily products (L3C and L4) from 2017 onwards.

2. SENSORS AND METHODS

The satellite datasets used to generate the CDR are considered in two main groups: the dual-view reference sensors (ATSR, SLSTR), and single-view meteorological sensors (AVHRR). The temporal coverage and daytime equator crossing of each instrument is shown in Figure 2.

The ATSR instruments were well calibrated, dual-view radiometers intended to produce long-term, consistent SST observations. Three ATSR instruments have flown on board ESA's two European Remote Sensing (ERS) satellites and Envisat satellite. All three satellites were in stable sun-synchronous orbits with near-constant Local Equator Crossing Times (LECTs) – the ERS-1 and ERS-2 platforms had a LECT of 10:30 and Envisat had a crossing time of 10:00 all of which were maintained within a few minutes. The design of the SLSTR instrument builds on the heritage of the earlier (A)ATSR instruments adding more spectral bands and a wider swath. The first SLSTR instrument is carried on board the Sentinel-3A satellite launched in February 2016, the second Sentinel-3B was launched in April 2018. The SST retrieval algorithm used for the dual-sensors is based on the banded linear coefficients developed for ATSR Reprocessing for Climate (ARC) project (Embury 2012). Due to the dual-view design it is possible to produce coefficients that are robust to the presence of stratospheric aerosol.

The AVHRRs are a series of multipurpose imaging instruments carried on board the National Oceanic and Atmospheric Administration (NOAA) Polar Operational Environmental Satellites (POES) and EUMETSAT Polar System (EPS) Metop satellites. The first AVHRR instrument was carried on board the TIROS-N satellite launched in October 1978. Unlike the ATSR/SLSTR sensors the AVHRRs were not designed for climate observations and must be cross-calibrated against the ATSR record for maximum stability. The SST retrieval for the AVHRR sensors is an Optimal Estimation (OE) based on Merchant et al. (2013). The retrieval is then harmonized against collocated ATSR observations accounting for the different time of observation using a model for diurnal variability. However, prior to 1991 there are no ATSR observations and there is insufficient overlap between AVHRR instruments to propagate the harmonization from one sensor to the next (see Figure 2). Therefore the early AVHRR data (from NOAA-7, -9, and -11) covering the 1980s has been referenced to in situ observations (ships + a subset of drifters excluded from the validation statistics below).

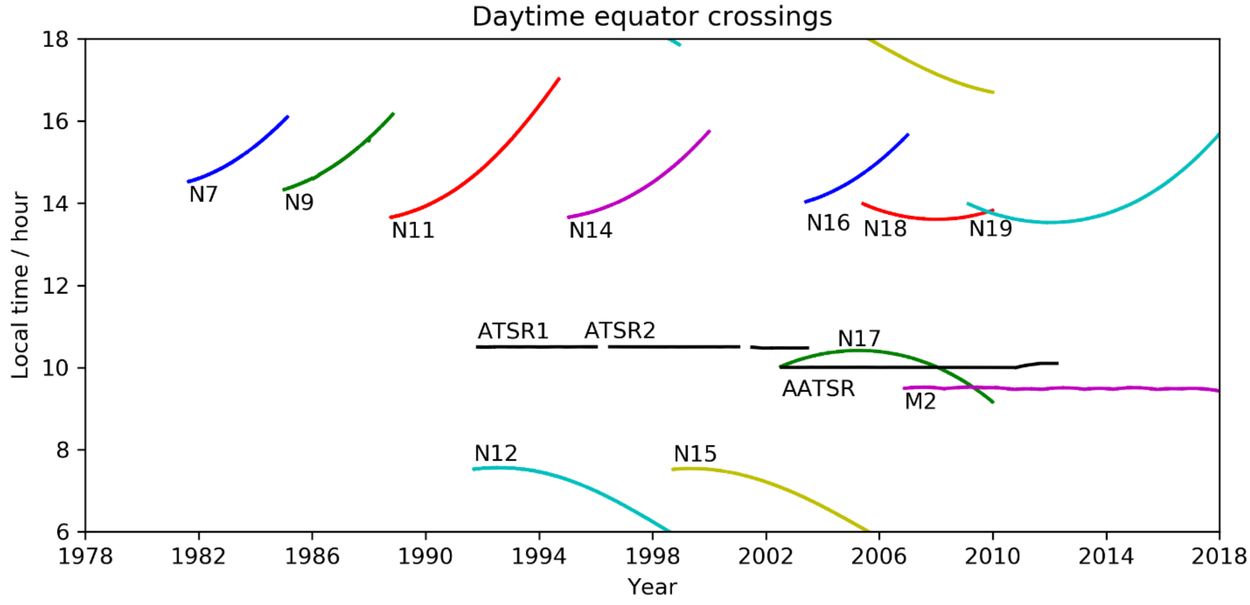

Figure 2: Day-time equator crossings of primary input sensors.

3. VALIDATION

Validation against in situ drifters is shown in Table 1, for the ATSRs the median bias is of order 0.01 K with robust standard deviation (RSD) ~0.2 K for the ATSR2 and AATSR instruments. RSD is higher (0.3 – 0.5 K) for the ATSR1 instrument which was affected by high instrument noise due to operating at a higher than intended temperature. The majority of the AVHRR instruments are also have median biases less than 0.1 K.

	Level 2				Level 3			
	Day		Night		Day		Night	
	Median	RSD	Median	RSD	Median	RSD	Median	RSD
NOAA-07	-0.15	0.56	-0.06	0.66	-0.17	0.55	-0.06	0.68
NOAA-09	-0.07	0.59	+0.02	0.61	-0.10	0.59	-0.02	0.65
NOAA-11	-0.06	0.52	+0.03	0.49	-0.09	0.51	+0.01	0.47
NOAA-12	-0.01	0.51	+0.02	0.44	-0.03	0.50	-0.00	0.45
NOAA-14	-0.03	0.45	-0.00	0.37	-0.05	0.45	+0.01	0.35
NOAA-15	-0.01	0.39	-0.01	0.38	-0.04	0.38	-0.02	0.37
NOAA-16	+0.02	0.36	-0.01	0.33	-0.01	0.37	-0.02	0.32
NOAA-17	+0.01	0.34	+0.02	0.28	-0.02	0.34	+0.00	0.27
NOAA-18	-0.07	0.34	-0.15	0.28	-0.11	0.34	-0.17	0.27
NOAA-19	+0.03	0.34	+0.02	0.29	-0.00	0.33	-0.00	0.27
Metop-A	+0.01	0.33	+0.04	0.27	-0.02	0.33	+0.02	0.26

ATSR-1	+0.03	0.33	+0.01	0.25	+0.02	0.46	-0.00	0.28
ATSR-2	-0.01	0.26	+0.01	0.20	-0.00	0.27	+0.02	0.21
AATSR	+0.01	0.19	+0.01	0.16	+0.01	0.20	+0.01	0.18

Table 1: L2/L3 validation against in situ drifters. Red shading indicates where sensor bias exceeds 0.1 K target. Green shading indicates dual-view reference sensors.

Assessment of the independent uncertainty estimates provided with the products show that the ATSR uncertainties are well estimated, as are the AVHRR nighttime estimates. However, the AVHRR uncertainties are overestimated during the daytime (*i.e.* retrievals are more accurate than indicated by the uncertainty estimates).

The long-term stability of the products is assessed using the method of Berry et al. (2018) against long-term stable moorings in the tropical pacific (1990-2012). The results in Table 2 show that the ATSR and Analysis products have excellent stability with drift relative to the tropical moorings ~2 mK per year (well under the target stability of 10 mK year^{-1} or 0.1 K decade^{-1}). Nighttime AVHRR data is within target, though during the day AVHRR stability is between 3.6 and 15.5 mK year^{-1}.

Data	Trend (mK / year)
ATSR (day)	-2.1 < trend < 2.3
ATSR (night)	-2.6 < trend < 0.4
AVHRR (day)	3.6 < trend < 15.5
AVHRR (night)	-2.1 < trend < 9.8
Analysis	-1.51 < trend < -0.05

Table 2: Stability assessment of SST products. Trend range is the 95% confidence interval for the relative multi-year trend between satellite SSTs and the Global Tropical Moored Buoy Array.

4. SUMMARY

The ESA SST CCI CDR v2.1 is now available and provides a 35-year global SST record (1982-2016) with an ongoing extension available via the C3S SST ICDR. Data from 1991 onwards are referenced to ATSR (independent of in situ SST), while 1980s data is referenced to in situ SST. Validation against in situ show the ATSR2/AATSR sensors with global biases $\lesssim$ 0.01 K; and AVHRR sensors (with the exception of NOAA-7 and NOAA-18) have global biases $\lesssim$ 0.1 K.

5. DATA AVAILABILITY

ESA SST CCI data are currently available from the CCI Open Data Portal (http://cci.esa.int/data), C3S SST ICDR data will be available from the Copernicus Climate Data Store (CDS) (https://cds.climate.copernicus.eu). DOIs for the individual CDR products are shown in Table 3.

.

Dataset Title	DOI
ESA SST CCI ATSR L2P v2.1	https://doi.org/10.5285/916b93aaf1474ce793171a33ca4c5026

ESA SST CCI ATSR L3U v2.1	https://doi.org/10.5285/2282b4aeb9f24bc3a1e0961e4d545427
ESA SST CCI ATSR L3C v2.1	https://doi.org/10.5285/5db2099606b94e63879d841c87e654ae
ESA SST CCI AVHRR L2P v2.1	https://doi.org/10.5285/373638ed9c434e78b521cbe01ace5ef7
ESA SST CCI AVHRR L3U v2.1	https://doi.org/10.5285/42f7230ab55641cdac1bba84eabd446a
ESA SST CCI AVHRR L3C v2.1	https://doi.org/10.5285/7db4459605da4665b6ab9a7102fb4875
ESA SST CCI Analysis v2.1	https://doi.org/10.5285/62c0f97b1eac4e0197a674870afe1ee6
ESA SST CCI Climatology v2.1	http://dx.doi.org/10.5285/83e51cf29821434ea14db56c564946d5

Table 3: Dataset DOIs

6. REFERENCES

Berry, D. I., Corlett, G. K., Embury, O., Merchant, C. J., Stability assessment of the (A)ATSR sea surface temperature climate dataset from the European Space Agency Climate Change Initiative. *Remote Sensing*, **10** (1). 126. 2019, https://doi.org/10.3390/rs10010126

Embury, O., Merchant, C. J., A reprocessing for climate of sea surface temperature from the along-track scanning radiometers: A new retrieval scheme, *Remote Sensing of Environment*, **116**, 47-61, 2012, https://doi.org/10.1016/j.rse.2010.11.020

Merchant, C. J., Le Borgne, P., Roquet, H., Legendre, G., Extended optimal estimation techniques for sea surface temperature from the Spinning Enhanced Visible and Infra-Red Imager (SEVIRI), *Remote Sensing of Environment*, **131**, 287-297, 2013, https://doi.org/10.1016/j.rse.2012.12.019

Merchant, C. J., Embury, O., Bulgin, C. E., Block, T., Corlett, G., Fiedler, E., Good, S. A., Mittaz, J., Rayner, N., Berry, D., Eastwood, S., Taylor, M, Tsushima, T., Waterfall, A., Wilson, R., Donlon, C., Satellite-based time-series of sea-surface temperature since 1981 for climate applications, *Scientific Data*, in review, 2019.

CCI OSTIA AS THE STANDARD OF TRUTH: DETAILED ERROR MODELS FOR IN SITU SST DATA FROM SHIPS AND OTHER PLATFORMS

Alexey Kaplan

Columbia University, United States of America

Small-scale and short-term variability plays an important role for reconstructing gapless gridded fields of climate variables from irregular sets of observations. With regards to the target space-time grid, the small-scale and short-term variability of observations combine to produce "sub-gridbox" variability (SGBV). Estimates σ of SGBV std serve as a scaling factor for the std e of the effective data error of gridded (by binning) observational averages: $e=\sigma/n^{1/2}$, thus influencing both the analysed values of the climate variable and their error estimates. While it has been known that estimates of SGBV and based on them error estimates for bin averages depend on the sampling scheme of the observing system, recently developed by the European Space Agency (ESA) Climate Change Initiative (CCI) satellite sea surface temperature (SST) products that are independent of in situ observations made it possible to bring a particular clarity to the SGBV estimates for SST. The corresponding observational error estimates for ship data from the International Comprehensive Ocean-Atmosphere Data Set (ICOADS) show an excellent consistency with the actual differences between SST from ships and from a high-resolution analysis of satellite data. By contrast, for the SST from drifting buoys (DB), a strong underestimation of error occurs. This surprising finding is tracked to the Lagrangian nature of DB as an observing platform and the near-conservative property of the SST variable, also explaining a slower than expected error reduction rate in the DB SST averages, as well as in the estimates of SST mean from a combined ICOADS database of all in situ sources.

USE OF SST FOR MONITORING CORAL STRESS: LOOKING FORWARD WHILE KEEPING AN EYE ON THE PAST.

William Skirving, Benjamin L. Marsh, Gang Liu, Jacqueline L. De La Cour, Andrew Harris, Eileen Maturi, Christopher Merchant, Jonathan Mittaz, Erick F. Geiger, Craig Steinberg, Roxana Vasile, C. Mark Eakin

The National Oceanic and Atmospheric Administration's (NOAA) Coral Reef Watch (CRW) program relies heavily on satellite-based sea surface temperature (SST) products to provide a wide range of environmental stress metrics for use by coral reef managers and scientists. Its flagship product, Degree Heating Week (DHW), provides a measure of accumulated heat stress, which is a strong predictor of mass coral bleaching. This and most of the other CRW heat stress products rely heavily on climatologies to detect and estimate the accumulated effect of temperature extremes.

Historically, when developing these anomaly products, CRW has been challenged by two separate and thorny issues: having a long enough dataset to create a stable and accurate climatology, and ensuring that the dataset is sufficiently similar to the near-real-time SST data being used to create the anomalies (*i.e.*, creating an anomaly by subtracting apples from apples, rather than apples and pears). These historical data are also invaluable for computation of past heat stress, allowing an understanding of past stress events, which can then influence present management amid rapid and accelerating climate change.

In an attempt to overcome the problem of consistency, prior to the release of the ESA Climate Change Initiative (CCI) SST data set, CRW created a long term data set that used the Operational Sea Surface Temperature and Sea Ice Analysis (OSTIA) as its reference. Called CoralTemp, it is a mixture of three related satellite SST products. 1985 to 2002 used OSTIA Reanalysis, 2002 to 2016 used the NOAA Geo/Polar Blended SST product, which was bias corrected against OSTIA Reanalysis for 2002 to 2007 and against near real-time (NRT) OSTIA for 2007 to 2016. Finally, the NOAA Geo/Polar Blended SST NRT product was used for 2016 onwards and was also bias corrected against NRT OSTIA. CoralTemp thus took advantage of the continuity that OSTIA provided, whilst incorporating the spatial completeness of the NOAA Blended SST product from 2002 onwards.

For the first time in CRW's 21 year history, the climatology used to derive the heat stress products was related to the near real-time SST products. Previously, the climatologies were derived from a historical analysis of satellite SST that was not related to the analysis used for the production of the NRT SST. Although this worked on average, there were a number of regions in the world where the climatology was clearly out of step with the SSTs being used to derive the anomalies.

Although many of these regional problems seemed to be fixed with the use of CoralTemp, a SQUAM comparison using Drifting Buoys and Moored Arrays indicates that there still may be some issues with DHWs derived from CoralTemp (Figure 1). Note that this figure suggests that OSTIA Reanalysis (1985 – 2002) has a cool bias of around 0.1 °C when compared to the Blended SST (2002 – 2018), and since OSTIA Reanalysis dominates the climatology used to derive DHWs (1985 – 2012), this would imply that the DHWs of recent years may be overestimated due to the accumulation of this bias.

Figure 2 is a plot of the percentage of reef-pixels (at 0.05 degrees resolution) with DHW ≥ 4 (indicating significant bleaching-level heat stress) for each year over the period 1982 to 2017. The NOAA Coral Reef Watch DHW methodology was used for each of two data sets, CoralTemp (plotted in red and covering 1986 to 2017) and CCI (plotted in black and covering 1982 to 2016).

The two graphs show a not too dissimilar story up until around 2005, at which point CoralTemp begins to show significantly larger heat stress extent than CCI. Given that we know that CoralTemp is using a cold biased climatology to derive its DHWs, it is reasonable to expect that CoralTemp will produce overestimates of DHW in more recent years due to their improved bias (Figure 1). It therefore follows that the DHW plot from CCI in Figure 2 indicates that the CCI bias is likely to be consistent throughout the dataset since if this were the case and if CoralTemp had a cool biased climatology (derived from 1985 to 2012), then it is reasonable to expect that DHWs from both data sets would roughly agree in the first half of this period and that CoralTemp's DHW values would be overestimated when compared with the CCI-derived DHWs in the second half of the period, both of which seem to be the case in Figure 2.

This observation seems to indicate that there might be an opportunity to use a combination of DHW values and ground-truth coral bleaching surveys to derive a methodology to test the bias consistency of SST products through time.

It also emphasizes the need for consistent SST bias through time if groups like Coral Reef Watch are to be able to utilize satellite SST data for monitoring and understanding the effects of climate change on marine biology. Since marine organisms have adapted to their local climate over many hundreds to thousands of years, the rate of climate change in recent years is such that most are not adapting fast enough, meaning that they are likely to be adapted to pre-industrial climates. Hence there is a need for teams such as Coral Reef Watch to be setting their climatologies as far back in time as possible. It is therefore very important for satellite SST development to keep one eye on the past and ensure that there are near real-time products that are related to historical satellite SST products such that calculations such as DHW remain accurate.

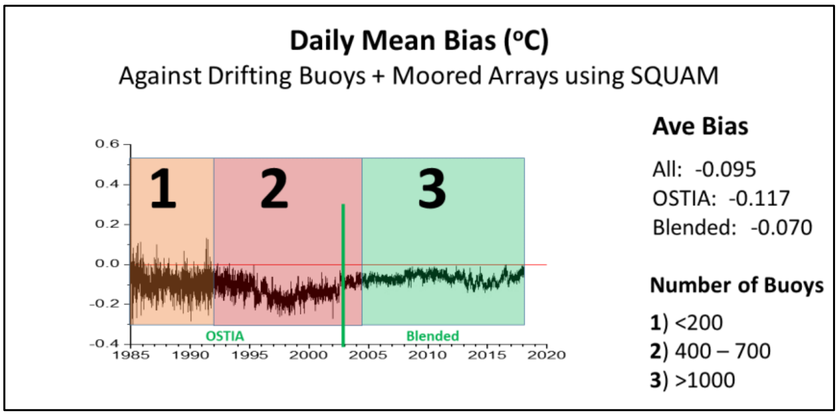

Figure 1: *NOAA SQUAM analysis of daily mean bias (°C) for CoralTemp over the period 1985 to 2018. Note that the number of buoys available for this analysis is correlated with the variance and that OSTIA Reanalysis is on average around 0.1 °C cooler than the Blended SST.*

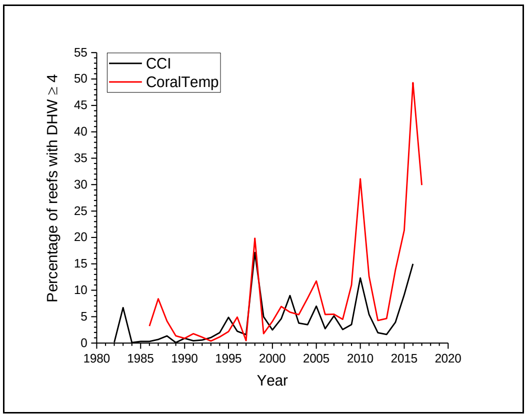

Figure 2: *Extent of global coral reef bleaching-level heat stress through time using Coral Temp and CCI.*

CLOSING SESSION

CLOSING SESSION REPORT

Chair: Anne O'Carroll[(1)] – Rapporteur: Karen Veal[(2)]

(1) EUMETSAT, Darmstadt, Germany, Email: Anne.Ocarroll@eumetsat.int
(2) NCEO, University of Leicester, United Kingdom, Email: klv3@le.ac.uk

1. INTRODUCTION

The closing session was held on 7th June 2019 and included a report from the GHRSST Advisory Council presented by Jean-François Piollé, a session on Task Team planning for the next year, a review of actions, AOB and closing remarks from the Science Team Chair, Anne O'Carroll.

2. 11:00 – 11:15 REPORT FROM ADVISORY COUNCIL MEETING - JEAN-FRANÇOIS PIOLLÉ

Jean-François Piollé reported on the GHRSST Advisory Council (AC) Meeting that took place on the 6th June 2019. There are two new members of the AC: Chongyuan Mao (Met Office, UK) and Karen Veal (GHRSST Project Office Coordinator). The AC proposed that an early career scientist should be added to the AC membership. The discussions of the AC will be reported in the minutes of the meeting.

3. 11:15 – 12:00 TASK TEAM PLANNING FOR NEXT YEAR

Two new task teams were set up:

Shipborne Radiometry, chair: Werenfrid Wimmer

Coral heat stress – gathering user needs, chair William Skirving

The Climatology and Intercomparison of L4 task teams will be merged into the Intercomparison Task Team. Helen Beggs is currently chair but will seek an early career scientist to mentor in the position.

4. 12:15 – 12:45 REVIEW OF ACTIONS AND AOB

The issue of RFI and 5G was discussed. An action was put on the Science Team to send evidence to Anne O'Carroll for presentation to CEOS at the CEOS SIT Technical Workshop in September 2019.

A suggestion to compile a special issue of Remote Sensing for G-XX was discussed but there was not enough interest to go ahead.

There was one action from the meeting

Action: Science Team to send evidence of RFI to AOC before September 2019

5. 12:45 – 13:00 WRAP UP/CLOSING REMARKS

Anne O'Carroll gave the closing remarks. Once again, the vibrancy and enthusiasm of the community was noted. There were 88 attendees at this year's meeting which discussed a variety of topics such as new results from Passive Microwave instruments, feature resolution, applications, retrievals, in situ measurements, diurnal variability and climate data records. The future of GHRSST, its strengths and weaknesses, opportunities and threats were considered. Anne thanked ESA for hosting this year's meeting and looked forward to next year's meeting which will be hosted by NASA and MISST in Boulder, Colorado, USA on 1st – 5th June 2020.

SECTION 3: POSTERS

POSTER LISTS

Posters are published on the GHRSST website and can be found in the 'Event Resources' of the G-XX meeting page (https://www.ghrsst.org/agenda/g-xx/). They are available - as presented - in the 'Monday 3rd June', 'Tuesday 4th June' and 'Thursday 6th June' sessions, under 'Interactive Presentations'.

Where posters are available, individual links are also provided below.

GHRSST XX -INTERACTIVE PRESENTATIONS – MONDAY 3 JUNE 2019

Nr	Presenter	Title
1	Armstrong, Edward Marcus	In situ Datasets from the PO.DAAC – Saildrone, SPURS and OMG
2	Banzon, Patria Viva	Comparison of Proxy SST Estimation Methods in the Arctic
7	Beggs, Helen Mary	Measuring Coastal Upwelling using Himawari-8, AVHRR and VIIRS SST
8	Bouali, Marouan	15 years of SST Gradients in the California Current System from the MODIS sensor
13	Cornillon, Peter	Pixel-to-Pixel Variability of AVHRR and MODIS L2 SST Fields
14	Dash, Prasanjit	Synergistic Monitoring of Multi-sensor and Multiple Ocean Parameters: SST, Salinity, Height, Wind and Color
19	Govekar, Pallavi	Exploiting Higher Resolution Satellite Sensors To Produce 2 km Multi-sensor Composites Of Sea Surface Temperature
20	Guan, Lei	Prediction of Sea Surface Temperature in the South China Sea by Artificial Neural Networks
25	Kilpatrick, Katherine Ann	Improvements In The NASA MODIS R2019.0 Reprocessed SST Products
26	Kim, JaeGwan	Preparation for Sea Surface Temperature Retrieval Using GK-2A at KMA
31	Liu, Mingkun	Retrieval of Sea Surface Temperature from HY-1B/COCTS
32	Lloyd, David Trevor	Noise and Striping Suppression in Landsat 8 Thermal Infrared Sea Images
37	Mao, Chongyuan	Assessment of the Impact of Sentinel-3A And -3B SLSTR L2P Sea Surface Temperature Data on OSTIA
38	Maturi, Eileen	Lake Water Temperatures for NCEP Regional Modelling
43	Orain, Françoise	Improvement of Trihourly Analysis of CMEMS (Copernicus) satellite SST over European Seas with Dineof method
44	Park, Kyung-Ae	Status of Algorithm Development for Sea Surface Temperature Retrieval of Geo-Kompsat-2A / Advanced Meteorological Imager
50	Shi, Lijian	GHRSST International Science Team (G-XX) meeting: Sea ice thickness retrieval with ice surface temperature data over the Liaodong Bay
55	Wimmer, Werenfrid	Sentinel-3 SLSTR SST Validation using a Fiducial Reference Measurements (FRM) Service
56	Worsfold, Mark	Impact Of PMW Observations On Level 4 Analysis.

Nr	Presenter	Title
61	Zhang, Yongsheng	Scientific Stewardship of GHRSST Products at the NOAA National Centers for Environmental Information (NCEI)

GHRSST XX -INTERACTIVE PRESENTATIONS – TUESDAY 4 JUNE 2019

Nr	Presenter	Title
3	Barron, Charlie N.	Overview of US Navy SST and Ice Products in the Arctic Seas
9	Boussidi, Brahim	AMSR-E, MODIS, In-Situ Three-Way Analysis of SST Error Variance
10	Chin, Toshio Michael	High-Resolution Analysis Parameters from Simulated SST
15	Donlon, Craig	The European Space Agency and GHRSST
16	Donlon, Craig	The Copernicus Imaging Microwave Radiometer (CIMR)
22	Hoeyer, Jacob L	Generation of ESA CCI SST L2 CDRs from Passive Microwave observations and impact on L4 analysis
28	Kurihara, Yukio	Current Status of GCOM-C/SGLI SST
33	Lucas, Marc	Copernicus TRUSTED: HRS-SST in situ datasets
34	Luo, Bingkun	Comparison Of Sentinel-3a/SLSTR Derived SST With MAERI
40	Minnett, Peter James	Improving Accuracy Of Sea Surface Temperature Retrievals By Incorporating Optimal Estimation
45	Park, Kyung-Ae	Status of Algorithm Development for Sea Surface Current Retrieval of Geo-KOMPSAT-2A /Advanced Meteorological Imager
46	Pennybacker, Matthew	ACSPO Collated SST Products from GOES-16/17 and Himawari-8
51	Tomazic, Igor	Sentinel-3 SLSTR ongoing Cal/Val activities for Sea Surface Temperature measurements
52	Tomazic, Igor	Sentinel-3 SLSTR L1 and L2 MARINE product updates
58	Ye, Xiaomin	A Sea Surface Temperature retrieval method of China Ocean Color and Temperature Scanner (COCTS)

GHRSST XX -INTERACTIVE PRESENTATIONS – THURSDAY 6 JUNE 2019

Nr	Presenter	Title
6	Beggs, Helen Mary	Inter-comparison of High-Resolution SST Climatology data sets over the Australian region
11	Ciani, Daniele	Regional to Global Scale Monitoring of the Sea Surface Currents from the Optimal Combination of Sea Surface Temperature and Sea Surface Height Data
12	Corlett, Gary	Independent Validation of Sentinel 3 SLSTR Sea Surface Temperature Products
17	Gangwar, Rishi Kumar	1d-Variational based Retrieval of SST using INSAT-3D Imager
18	Gentemann, Chelle	Diurnal warming observed during the 2018 Saildrone cruise
23	Jonasson, Olafur	VIIRS SST Reanalysis 2 (RAN2)
24	Kachi, Misako	JAXA Satellite Missions and Services for SST
29	Li, Wen-Hao	PO.DAAC Tool and Services Improvements to Support the GHRSST Community
30	Li, Xu	The operational Sea Surface Temperature Analysis within the NCEP GFS
35	Luo, Bingkun	Accuracy Assessment Of ERA5 Sea Surface Skin Temperature And Near-Surface Air Temperature Using MAERI And ISAR Observations
36	Luo, Bingkun	Correcting Satellite Derived Infrared SST Considering Aerosol Vertical Distribution
42	Nielsen-Englyst, Pia	Assessment of Channel Selection for the Copernicus Imaging Microwave Radiometer (CIMR) for Retrieval of Sea Surface Temperature (SST)
48	Pereira, Bruno Gonçalves	Comparison of SST estimates by AVHRR Sensor and PIRATA project buoys in the Equatorial Atlantic Ocean
53	Vazquez, Jorge	Using the Saildrone Unmanned Surface Vehicle For Validation Of Satellite Derived Level 4 Sea Surface Temperature: The California/Baja Coast Deployment
54	Wick, Gary Alan	Characterizing Extreme Diurnal Warming in Satellite-Derived Operational Sea Surface Temperature Products
59	Zhang, Haifeng	On the Differences Between Daytime and Nighttime Ocean Cool Skin Signals under Well Mixed Conditions
60	Zhang, Huai-Min	NOAA NCEI's Global Sea Surface Temperature Datasets and Services

POSTER EXTENDED ABSTRACTS

VIIRS SST REANALYSIS 2 (RAN2)

Olafur Jonasson [(1)], Alexander Ignatov [(2)]

(1) NOAA STAR and GST Inc., USA, Email: olafur.jonasson@noaa.gov
(2) NOAA STAR, USA, Email: Alex.Ignatov@noaa.gov

Visible Infrared Imager Radiometer Suite (VIIRS) is the newest generation NOAA operational sensor, flown on board the polar platforms NPP (launched in October 2011) and N20 (launched in November 2017). The goal of VIIRS SST reanalysis (RAN) is to consistently reprocess all available L0 from both satellites into L1b using up-to-date calibration, and further into L2P and L3U SST products using a consistent version of the NOAA Advanced Clear-Sky Processor for Oceans (ACSPO) enterprise software. SST data is produced in GDS2 compliant L2P (swath) and L3U (0.02º; gridded) formats. Both are reported in 10 minute granules (144/day) and archived at NOAA (CoastWatch/NCEI) and NASA (PO.DAAC). All RAN SST products are quality controlled using match-ups with in situ data from NOAA in situ SST Quality Monitor (*i*Quam; www.star.nesdis.noaa.gov/sod/sst/iquam) as well as with various L4 analysis products. The Quality Control and Cal/Val statistics are published in the NOAA SST Quality Analysis Monitor (SQUAM; www.star.nesdis.noaa.gov/sod/sst/squam). The stability of the corresponding brightness temperatures (BTs) is monitored on the Monitoring of IR Clear-sky Radiances over Ocean for SST website (www.star.nesdis.noaa.gov/sod/sst/micros/; MICROS), where BTs in VIIRS SST bands are compared with simulations using the Community Radiative Transfer Model (CRTM).

RAN1 was performed in 2015 in conjunction with U. Wisconsin CSPP Team, using ACSPO v2.40, and covered a period from March 2012 – December 2015. Period from December 2015 onward is supplemented by NRT processing (ACSPO v2.41, 2.60 and 2.61). RAN1 results are available on the NOAA CoastWatch website (full archive of L3U; the L2P data are also available on request). The goal of RAN2 is to backfill the operational NPP and N20 SST data, from the date of v2.61 implementation (April 2019), back to the beginning of both missions, and provide a complete and uniform-quality time series. As of this writing, RAN2 is completed for 2017 - 2018 for NPP and 2018 for N20. Archival with CoastWatch/PO.DAAC/NCEI is currently in progress. We will continue releasing RAN2 to PO.DAAC and NCEI in increments, 1 - 2 years at a time, stitching RAN2 with the operational implementation of V2.61.

In this poster, we report on the status of VIIRS RAN2 and present analysis of the SST products quality in terms of stability, global statistics, imagery and inter-platform consistency. We discuss various improvements over RAN1, including:

(1) RAN2 provides complete and more stable and consistent time series of NPP and N20 SST. (RAN1 included only NPP.)

(2) For RAN2, we started from L0 data and worked with the NOAA calibration team to minimize the effects of VIIRS warmup cool-down (WUCD) on BTs and SST. (RAN1 suffered from quarterly ~ 0.25K warm biases in daytime SST during WUCD calibration exercises.)

(3) RAN2 is performed using a single ACSPO version (2.61), which includes several improvements over previous versions, such as new SST and SSES algorithms, resampled imagery to fill bow-tie deletion zones, and improved clear-sky mask.

(4) RAN2 employs updated SST look-up tables that take advantage of increased number of available in situ matchups for N20 and mitigates high-latitude positive SST biases observed in v2.60.

ACSPO COLLATED SST PRODUCTS FROM GOES-16/17 AND HIMAWARI-8

Matthew Pennybacker(1), Alexander Ignatov(2), Irina Gladkova(3), Olafur Jonasson(4), Boris Petrenko(5), Yury Kihai(6)

(1) NOAA STAR and GST Inc., USA, Email: Matthew.Pennybacker@noaa.gov
(2) NOAA STAR, USA, Email: Alex.Ignatov@noaa.gov
(3) NOAA STAR, GST Inc., and City College of New York, USA, Email: Irina.Gladkova@gmail.com
(4) NOAA STAR and GST Inc., USA, Email: Olafur.Jonasson@noaa.gov
(5) NOAA STAR and GST Inc., USA, Email: Boris.Petrenko@noaa.gov
(6) NOAA STAR and GST Inc., USA, Email: Yury.Kihai@noaa.gov

Following some operational delays, the NOAA Advanced Clear-Sky Processor for Ocean (ACSPO) system version 2.70, released in April 2019, started operational production of hourly collated L2P and L3C products from the new generation geostationary sensors ABI (onboard GOES-16/17, G16/17) and AHI (on board Himawari-8, H08). The collation algorithm, presented at GHRSST-XIX, explores frequent looks (every 10/15 minutes) of the same geographical region to reduce sensor noise, minimize residual cloud contamination, and improve clear-sky coverage by up to 70% compared to uncollated L2P.

Real-time collated ACSPO L2P/3C products from G16 and H08 are currently operationally produced at NOAA, and distributed via its CoastWatch and Product Distribution and Access (PDA) systems and monitored in the NOAA SQUAM. Moreover, the operational G16 products will be also archived at NASA PO.DAAC and NOAA NCEI. First Reanalysis (RAN1) of G16 SST (going back to mid-December 2017, when it was placed in the operational GOES-East position) is also being produced at STAR, and will be provided to PO.DAAC and NCEI to back-fill their operational holdings. Work is underway to also archive and back-fill H08 SSTs with its RAN1.

Real-time production from G17 has been complicated and delayed by its ABI performance issues. Following the launch of G17, an issue was discovered with its ABI focal plane module (FPM) loop heat pipe, which is used to regulate the temperature of the sensor. As a result, its ABI nominal temperature is elevated compared to GOES-16 ABI. The temperature of its FPM, which strongly affects the performance of the thermal infrared bands, is ~81K compared to ~58K on G16. This leads to elevated radiometric and striping noise in the G17 ABI brightness temperatures being used in SST retrievals. Moreover, in some seasons during nighttime, when more sunlight impinges directly on the instrument, the FPM temperature is elevated even further, causing more noise, unstable and inaccurate calibration, and even saturation of the thermal bands. Some bands are affected more than others. The band centred at 11.2 microns is the most affected and had to be excluded from the retrievals.

In this presentation, we briefly summarize the ACSPO collation algorithm. The focus is on the current status of ACSPO L2P/3C products from G16/17 and H08, including the G16 RAN1, products performance as seen in the NOAA SQUAM and ARMS systems. Ongoing mitigation strategies for G17 ABI SST products, given its inherent limitations, are reviewed and discussed.

ON THE DIFFERENCES BETWEEN DAYTIME AND NIGHTTIME OCEAN COOL SKIN SIGNALS UNDER WELL MIXED CONDITIONS

Haifeng Zhang[1], Alexander V. Babanin[2], Alexander Ignatov[3], Helen Beggs[4]

(1) Department of Infrastructure Engineering, University of Melbourne, Melbourne, Australia; Email: Haifeng.zhang@unimelb.edu.au
(2) Department of Infrastructure Engineering, University of Melbourne, Melbourne, Australia; Email: a.babanin@unimelb.edu.au
(3) NOAA/STAR, College Park, MD 20740, USA; Email: alex.ignatov@noaa.gov
(4) Bureau of Meteorology, Melbourne, Australia; Email: helen.beggs@bom.gov.au

The differences between daytime and nighttime cool skin signals (ΔT, defined as skin sea surface temperature, SST_{skin}, minus depth SST, SST_{depth}) are investigated under well mixed conditions (wind speed > 6 m s^{-1}), using > 150 days of matchups between shipborne ISAR (the Infrared SST Autonomous Radiometer) SST_{skin} and water intake SST_{depth} at ~ 7.1 m to 9.9 m depth, collected by IMOS ships in oceans around Australia. When the wind speed is > 6 m s^{-1}, the average daytime ΔT size (-0.14 ± 0.13 K) is smaller than that at night (-0.20 ± 0.10 K) by ~ 0.06 K. A diurnal pattern is seen in the sample average ΔT values with a minimum of ~-0.21 K occurring at ~ 4 - 5 hr local time (LT), and maximum ~-0.10 K at 15 - 16 hr LT. The ΔT highly correlates with the net heat flux, which includes the shortwave insolation absorbed in the skin layer. Our analyses suggest that the observed diurnal variation of the cool skin effect reaches 0.11 K. A widely used cool skin model (Fairall et al., 1996) is evaluated. It captures well the diurnal pattern of the cool skin, but significantly underestimates the ΔT diurnal cycle range (0.03 K compared to the observed 0.11 K), largely due to an underestimation of nighttime cool skin amplitude. Our results also suggest that the no "warm skin (ΔT > 0 K)" limit in this cool skin model should be revisited. This day-night ΔT difference could be of practical use in satellite SST_{skin} data validation against in situ measurements. In particular, we recommend that different constants should be subtracted from in situ measurements for day (-0.14 K) and night (-0.20 K) when calibrating or validating satellite SST_{skin} data under well mixed conditions.

SECTION 4: APPENDICES

APPENDIX 1 – LIST OF PARTICIPANTS

GHRSST XX SCIENCE TEAM MEETING,
ESA, Frascati, Italy, 3-7 June 2018

Name	Affiliation	Email
Armstrong, Edward Marcus	NASA Jet Propulsion Laboratory, US	edward.m.armstrong@jpl.nasa.gov
Artale, Vincenzo	ENEA, Italy	vincenzo.artale@enea.it
Autret, Emmanuelle	Ifremer, France	emmanuelle.autret@ifremer.fr
Banzon, Patria Viva	NCEI/NOAA, US	viva.banzon@noaa.gov
Barron, Charlie N.	U.S. Naval Research Laboratory, US	charlie.barron@nrlssc.navy.mil
Barton, Ian James	CSIRO, Australia	ian.barton@ozemail.com.au
Beggs, Helen Mary	Bureau of Meteorology, Australia	helen.beggs@bom.gov.au
Bellacicco, Marco	ENEA, Italy	marco.bellacicco@enea.it
Bouali, Marouan	Institute of Oceanography of the University of Sao Paulo, Brazil	marouanbouali@gmail.com
Bragaglia-Pike, Silvia	GHRSST/University of Leicester, UK	sbp9@leicester.ac.uk
Buongiorno Nardelli, Bruno	Consiglio Nazionale delle Ricerche, Italy	bruno.buongiornonardelli@cnr.it
Cagnazzo, Chiara	ISMAR, Italy	chiara.cagnazzo@cnr.it
Casey, Kenneth Scott	NOAA, US	Kenneth.Casey@noaa.gov
Castro, Sandra Liliana	University of Colorado, US	sandrac@colorado.edu
Cayula, Jean-Francois	Perspecta, US	j.cayula@ieee.org
Centurioni, Luca	Scripps Institution of Oceanography, US	lcenturioni@ucsd.edu
Ceriola, Giulio	Planetek Italia	ceriola@planetek.it
Chin, Toshio Michael	JPL/Caltech, US	mike.chin@jpl.nasa.gov
Chung, Chu-Yong	NMSC / KMA, south Korea	cychung@kma.go.kr
Ciani, Daniele	National Research Council of Italy	daniele.ciani@cnr.it
Corlett, Gary	EUMETSAT, Germany	gary.corlett@eumetsat.int
Cornillon, Peter	University of Rhode Island, US	pcornillon@me.com
Dash, Prasanjit	NOAA NESDIS STAR, US	prasanjit.dash@noaa.gov
de Toma, Vincenzo	Tor Vergata Università di Roma, Italy	vincenzo.detoma@students.uniroma2.eu
di Sarra, Alcide Giorgio	ENEA, Italy	alcide.disarra@enea.it

Name	Affiliation	Email
Dionisi, Davide	Institute of Marine Science (ISMAR-CNR)	davide.dionisi@cnr.it
Donlon, Craig	European Space Agency	craig.donlon@esa.int
Dransfeld, Steffen	ESA	steffen.dransfeld@esa.int
Eastwood, Steinar	Norwegian Meteorological Institute	s.eastwood@met.no
Embury, Owen	University of Reading, UK	o.embury@reading.ac.uk
Evans, Robert H	NC State U, US	sst4bob@gmail.com
Farrugia, Reuben	University of Malta	Reuben.farrugia@um.edu.mt
Folco, Sergio	ESA, Netherlands	sergio.folco@esa.int
Gentemann, Chelle	Earth and Space Research, US	cgentemann@esr.org
Gladkova, Irina	CUNY, City College of New York, US	irina.gladkova@gmail.com
Govekar, Pallavi	Bureau of Meteorology, Australia	pallavi.govekar@bom.gov.au
Guan, Lei	Ocean University of China	leiguan@ouc.edu.cn
Harris, Andrew	University of Maryland, US	aharris2@umd.edu
Hoeyer, Jacob L	Danish Meteorological Institute	jlh@dmi.dk
Ignatov, Alexander	NOAA, US	alex.ignatov@noaa.gov
Isern-Fontanet, Jordi	Institut de Ciencies del Mar (CSIC), Spain	jisern@icm.csic.es
Kachi, Misako	Japan Aerospace Exploration Agency (JAXA)	kachi.misako@jaxa.jp
Kaplan, Alexey	Columbia University, US	alexeyk@ldeo.columbia.edu
Karagali, Ioanna	Technical University of Denmark	ioka@dtu.dk
Kim, Hee-Young	Seoul National University, South Korea	heeyoungkim@snu.ac.kr
Kim, JaeGwan	National Meteorological Satellite Center/KMA, south Korea	kimjgwan@korea.kr
Kurihara, Yukio	JAXA, Japan	ykuri.kiyo@gmail.com
Lee, Byung-il	NMSC/KMA, South Korea	bilee01@korea.kr
Li, Wen-Hao	Raytheon, US	whl52059@gmail.com
Li, Xu	EMC/NCEP/NOAA, US	xu.li@noaa.gov
Liu, Mingkun	Ocean University of China	liumingkun_ouc@126.com
Lloyd, David Trevor	University of Malta	david.lloyd@um.edu.mt
Luo, Bingkun	RSMAS / University of Miami, US	lbk@rsmas.miami.edu
Mao, Chongyuan	Met Office, UK	chongyuan.mao@metoffice.gov.uk
Marullo, Salvatore	ENEA, Italy	salvatore.marullo@enea.it

Name	Affiliation	Email
Mastracci, Diana	University of Oxford, UK	diana.mastracci@ouce.ox.ac.uk
Maturi, Eileen	NOAA, Dept of Commerce, US	eileen.maturi@noaa.gov
McKenzie, Bruce	Naval Oceanographic Office, US	bruce.mckenzie@navy.mil
Merchant, Christopher	University of Reading, UK	c.j.merchant@reading.ac.uk
Minnett, Peter James	RSMAS. University of Miami, US	pminnett@rsmas.miami.edu
Nielsen-Englyst, Pia	Technical University of Denmark	pne@dmi.dk
O'Carroll, Anne	EUMETSAT, Germany	Anne.Ocarroll@eumetsat.int
Oliveira, Ana Patricia	Universidade de Lisboa, Portugal	anolive@mail.com
Orain, Françoise	Météo-France	francoise.orain@meteo.fr
Park, Kyung-Ae	Seoul National University, South Korea	kapark@snu.ac.kr
Pennybacker, Matthew	NOAA/STAR and GST, Inc., US	matthew.pennybacker@noaa.gov
Pereira Gonçalves, Bruno	University of Sao Paulo, Brazil	brunoscience@hotmail.com
Pimentel, Sam	Trinity Western University, Canada	sam.pimentel@twu.ca
Piollé, Jean-François	Ifremer, France	jfpiolle@ifremer.fr
Pires, Nelson	University of Porto, Portugal	nelson.pires@fc.up.pt
Sakurai, Toshiyuki	Japan Meteorological Agency	tsakurai@met.kishou.go.jp
Santoleri, Rosalia	CNR, Italy	rosalia.santoleri@cnr.it
Saux Picart, Stéphane	Météo-France	stephane.sauxpicart@meteo.fr
Scifoni, Silvia	Serco c/o ESRIN, Italy	silvia.scifoni@serco.com
Shi, Lijian	National Satellite Ocean Application Service, China	shilj@mail.nsoas.org.cn
Skirving, William John	NOAA, US	william.skirving@noaa.gov
Steinberg, Craig	Australian Institute of Marine Science	c.steinberg@aims.gov.au
Surcel Colan, Dorina	Environment and Climate Change Canada	dorina.surcel-colan@canada.ca
Thapliyal, Pradeep Kumar	Indian Space Research Organisation	pkthapliyal@gmail.com
Tomazic, Igor	EUMETSAT, Germany	igor.tomazic@eumetsat.int
Vazquez, Jorge	JPL/Caltech, US	jorge.vazquez@jpl.nasa.gov
Veal, Karen Louise	University of Leicester, UK	klv3@le.ac.uk
Wang, Qimao	National Satellite Ocean Application Service, China	qimwang@mail.nsoas.org.cn
Wick, Gary Alan	NOAA, US	gary.a.wick@noaa.gov

Name	Affiliation	Email
Wimmer, Werenfrid	University of Southampton, UK	w.wimmer@soton.ac.uk
Worsfold, Mark	Met Office, UK	mark.worsfold@metoffice.gov.uk
Xie, Senyang	The University of New South Wales, Australia	senyang.xie@student.adfa.edu.au
Yang, Chunxue	ISMAR-CNR, Italy	chunxueyang@gmail.com
Ye, Xiaomin	National Satellite Ocean Application Service, China	yexiaomin2011@foxmail.com
Zhang, Haifeng	The University of Melbourne, Australia	haifeng.zhang@unimelb.edu.au
Zhang, Huai-Min	NOAA NCEI, US	huai-min.zhang@noaa.gov
Zhang, Yongsheng	NOAA/NESDIS/NCEI - UMD/ESSIC/CICS, US	yongsheng.zhang@noaa.gov

APPENDIX 2 – GXX - PARTICIPANTS PHOTO

APPENDIX 3 – SCIENCE TEAM MEMBERS 2018-19

Anne O'Carroll (Chair)	EUMETSAT, Darmstadt, Germany
Ed Armstrong	NASA JPL PO.DAAC, USA
Viva Banzon	NOAA/NCDC, USA
Charlie Barron	US Naval Research Laboratory, USA
Helen Beggs	Bureau of Meteorology, Melbourne, Australia
Maouan Bouali	Institute of Oceanography of the University of Sao Paulo, Brazil
Kenneth S Casey	NOAA/NESDIS NODC, USA
Sandra Castro	University of Colorado, Boulder, USA
Jean-François Cayula	Vencore, Inc, Stennis Space Center, Mississippi, USA
Mike Chin	NASA JPL, USA
Carol Anne Clayson	WHOI, USA
Peter Cornillon	University of Rhode Island, USA
Prasanjit Dash	NOAA, USA
Craig J Donlon	European Space Agency, The Netherlands
Steinar Eastwood	Met.no, Norway
Owen Embury	University of Reading, UK
Chelle Gentemann	Earth and Space Research, USA
Simon Good	MetOffice, UK
Lei Guan	Ocean University of China, China
Andrew Harris	NOAA/NESDIS ORA, USA
Jacob Høyer	Danish Meteorological Institute, Denmark
Alexander Ignatov	NOAA/NESDIS/STAR, USA
Misako Kachi	Japan Aerospace Exploration Agency (JAXA), Japan
Alexey Kaplan	Columbia University, USA
Ioanna Karagali	Technical University of Denmark, Denmark
Prabhat Koner	ESSIC, University of Maryland, USA
Yukio Kurihara	Japan Aerospace Exploration Agency (JAXA), Japan
W Timothy Liu	NASA JPL, USA
Yang Liu	RSMAS, University of Miami, USA
Salvatore Marullo	ENEA, Italy
Eileen Maturi	NOAA/NESDIS/STAR/SOCD/MECB, USA

Christopher Merchant	University of Reading, UK
Peter Minnett	RSMAS, University of Miami, USA
Jonathan Mittaz	University of Reading, UK
Tim Nightingale	Rutherford Appleton Laboratory, UK
Kyung-Ae Park	Seoul National University, Korea
Jean–François Piollé	IFREMER, France
Toshiyuki Sakurai	Japan Meteorological Agency (JMA), Japan
Rosalia Santoleri	ARTOV.ISAC.CNR, Italy
Stéphane Saux Picart	Météo-France, France
Dorina Surcel Colan	CMC - Environment Canada
Igor Tomazic	EUMESTAT, Darmstadt, Germany
Jorge Vazquez	NASA JPL PO.DAAC, USA
Sujuan Wang	National Satellite Meteorological Center, Met Administration, China
Christo Whittle	CISR, South Africa
Gary Wick	NOAA ETL, USA
Werenfrid Wimmer	University of Southampton, UK

LAST PAGE